Genetic determinants for virulence and adaptation of avian influenza viruses H9N2 and H5N8 subtypes in poultry and mammals

I n a u g u r a l d i s s e r t a t i o n

zur

Erlangung des akademischen Grades eines

Doktors der Naturwissenschaften (Dr. rer. nat.)

der

Mathematisch-Naturwissenschaftlichen Fakultät

der

Universität Greifswald

vorgelegt von

Claudia Blaurock

Greifswald, April 2021

Dekan:	Prof. Dr. Gerald Kerth
1. Gutachter:	Prof. Dr. Dr. h.c. Thomas C. Mettenleiter
2. Gutachter:	Prof. Dr. Stephan Ludwig
3. Gutachter:	Prof. Dr. Benedikt Kaufer
Tag der Promotion:	29.09.2021

For my family.

Content

List of abbreviations

aa	Amino acid
AIV	Avian influenza virus
AKT	Protein kinase B
ANT3	Adenine nucleotide translocator 3
ATP	Adenosine triphosphate
C	Cysteine
CALCOCO2	Calcium-binding and coiled-coil domain-containing protein 2
CPSF30	Cleavage and polyadenylation specificity factor 30
CRM1	Chromosomal region maintenance 1
cRNA	Complementary RNA
CS	Cleavage site
CTE	C-terminus
DDX21	DExD-Box Helicase 21
DNA	Deoxyribonucleic acid
Dpi	Days post inoculation
dsRNA	Double strand RNA
E	Glutamic acid
ED	Effector domain
EE	Early endosome
elF2	Eukaryotic initiation factor 2
elF4G1	Eukaryotic translation initiation factor 4G1
G	Glycine
GD	Guangdong
GIT	Gastrointestinal tract
Gs	Goose
HA	Hemagglutinin
HACS	Hemagglutinin cleavage site
HAT	Human airway trypsin-like protease
HP	High pathogenic
HPAIV	Highly pathogenic avian influenza virus
IAV	Influenza A virus
IFN	Interferon
IKKα and β	Inhibitor of nuclear factor kappa-B kinase subunits α and β
IL	Interleukin
IRF	Interferon regulatory factor
ISA	Infectious Salmon Anemia
ISG	Interferon-stimulated gene
IVPI	Intravenous pathogenicity index
IκBα	NF κ inhibitor alpha
JAK	Janus kinase
K	Lysine
kDa	Kilo Dalton
LE	Late endosome
LGP2	Laboratory of genetics and physiology 2
LP	Low pathogenic
LPAIV	Low pathogenic avian influenza virus
LPS	Lipopolysaccharides
LR	Linker region
M1	Matrix protein-1
M2	Matrix protein-2
MAVS	Mitochondrial antiviral signaling protein
MDA5	Melanoma differentiation-associated protein 5
mRNA	Messenger RNA

Mx1	Myxoma resistance protein 1
MyD88	Myeloid differentiation factor 88
N	Asparagine
N	Nitrogen
NA	Neuraminidase
NEMO	Nuclear factor-κB essential modulator
NEP	Nuclear export protein
NES	Nuclear export signal
NFκB	Nuclear factor κB
NGS	*N*-glycosidic linkages
NK	Natural killer
NLR	NOD-like receptors
NLS	Nuclear localization signal
NOD	Nucleotide-binding oligomerization domain
NoLS	Nucleolar localization signal
NP	Nucleoprotein
NPC	Nuclear pore complex
NS1	Non-structural protein 1
NS2	Non-structural protein 2
NXF1	Nuclear export factor 1
NXT1	NTF2-related export protein 1
O	Oxygen
OAS	2',5'-oligoadenylate synthetase
OIE	World Organisation for Animal Health
ORF	Open reading frame
P	Proline
PA	Polymerase acidic
PABPII	Polyadenine binding protein II
PAMP	Pathogen associated molecular patterns
PB1	Polymerase basic subunit 1
PB2	Polymerase basic subunit 2
pDC	Plasmacytoid dendritic cells
PI3K	Phosphoinositide 3-kinase
PKR	Protein kinase R
Poly(I:C)	Polyinosinic-polycytidylic acid
PRR	Pattern recognition receptors
R	Arginine
RBD	Receptor binding domain
RBD	RNA binding domain
RdRp	RNA-dependent RNA-polymerase
rER	Rough endoplasmic reticulum
RIG-I	Retinoic acid-inducible gene-I
RLR	RIG-I-like receptors
RNA	Ribonucleic acid
RNaseL	Ribonuclease L
rRNA	Ribosomal ribonucleic acid
S	Serine
SA	Sialic acid
ssRNA	Single stand RNA
STAT	Signal transducer and activator of transcription protein
SUMO	Small ubiquitin-like modifier
T	Threonine
TBK1	TANK-binding kinase 1
TGN	Trans-Golgi-network
TLR	Toll-like receptor
TMD	Transmembrane domain

TMPRSS2	Transmembrane protease serine member 2
TNF	Tumor necrosis factor
TRAF	TNF receptor-associated factor
TRIM	Tripartite Motif
UK	United Kingdom
USA	United States of America
VDAC-1	Voltage-dependent anion channel
vRNA	Viral ribonucleic acid
vRNP	Viral ribonucleoprotein
WHO	World Health Organization
α	Alpha
β	Beta
γ	Gamma
δ	Delta
ε	Epsilon
ζ	Zeta
κ	Kappa
λ	Lambda
τ	Tau
ω	Omega

Figure Legend

Figure 1: Influenza A virion and viral ribonucleoprotein (vRNP) complex.

Figure 2: Replication cycle of influenza A virus.

Figure 3: Antigenic drift of influenza A virus.

Figure 4: Reassortment of influenza A virus.

Figure 5: Structure of NS1 and binding to cellular proteins and factors.

Figure 6: Interaction of NS1 with cellular factors.

Figure 7: HPAIV H5 cases in European domestic (red dot), wild (blue triangle) and zoo birds (red square).

1 Introduction

1.1 General introduction

The family *Orthomyxoviridae* comprises seven genera: Influenza A, B, C, D, Infectious Salmon Anemia (ISA) Virus, Quaranjavirus and Thogotovirus (ICTV, 2019). Influenza A viruses (IAV) can infect birds and mammals including humans (Webster et al., 1992), whereas influenza B viruses have been isolated from humans and seals (Osterhaus et al., 2000) and influenza C viruses have only been isolated from humans (primary reservoir) and swine (Guo et al., 1983; Hause et al., 2013). For influenza D virus, cattle are thought to be the main reservoir, but it was also isolated from swine, sheep and goats (Hause et al., 2014; Kaplan et al., 2020).

Avian influenza viruses (AIV) belong to the genus IAV and can be divided into possible 144 HxNy subtypes due to different antigenic properties of the two major surface glycoproteins hemagglutinin (HA) and neuraminidase (NA). So far, there are 16 HA and 9 NA subtypes known to infect birds (Fouchier et al., 2005; Tong et al., 2012). Recently, two subtypes, H17N10 and H18N11, have been identified in bats (Tong et al., 2012; Tong et al., 2013). Furthermore, the HA and NA can be allocated to two different phylogroups each. HA Group 1 contains H1, H2, H5, H6, H8, H9, H11, H12 (Air, 1981; Tong et al., 2012), H13 (Nobusawa et al., 1991) and H16 (Fouchier et al., 2005), whereas HA Group 2 contains H3, H4, H7, H10, H14 and H15 (Tong et al., 2012). N1, N4, N5 and N8 are allocated to NA Group 1, whereas NA Group 2 includes N2, N3, N6, N7 and N9 (Russell et al., 2006a; Tong et al., 2012).

The natural reservoir of AIV are aquatic birds (e.g. gulls, ducks), but they can also infect e.g. poultry, swine, seals and humans (Gao et al., 2013; Krog et al., 2015; Meseko et al., 2018). According to the World Organization for Animal Health (OIE), AIV can be classified into two pathotypes: Low pathogenic AIV (LPAIV) and highly pathogenic AIV (HPAIV) (OIE, 2008). All AIV subtypes are LP, but H5 and H7 viruses can shift to HP phenotype. Therefore, AIV H5/H7 infections in birds are notifiable animal diseases.

1.2 Nomenclature

The World Health Organization (WHO) established a standard nomenclature for influenza viruses in the 1980s. It has to contain an information about the influenza virus type, the host of origin (for viruses from non-human origin), the geographical origin, as well as the strain number, the year of isolation and the HA/NA subtypes (WHO, 1980). According to the WHO definition, A/turkey/Germany/R1685/2016 (H9N2) is an influenza A virus that was isolated from turkeys in Germany in 2016. The laboratory number is R1685 and H9N2 refers to the HA-H9 and NA-N2 subtypes.

1.3 Influenza A viruses

1.3.1 Virus particle

IAV are mostly pleomorphic in shape, but can also be spherical (diameter about 120 nm) or filamentous (20 µm in length) (Noda, 2011). They possess a host-derived lipid bilayer membrane. Influenza virions are composed of surface and internal proteins. Surface proteins, which are embedded in the viral membrane, are the HA, NA and matrix protein-2 (M2). The HA and NA are present in a ratio between 4:1 to 5:1 (Webster et al., 1968) (Figure 1), while the ion channel M2 protein is less abundant (1:10 compared to HA) (Chlanda and Zimmerberg, 2016; Lamb et al., 1985). The internal proteins are the polymerase basic 2 (PB2) and polymerase basic 1 (PB1), polymerase acidic (PA), nucleoprotein (NP), matrix protein-1 (M1) and the nuclear export protein (NEP). PB2, PB1, PA and NP bind to the viral ribonucleic acid (vRNA) segments to form a viral ribonucleoprotein complex (vRNP) (Figure 1) (see point 1.3.3). M1 is one of the most abundant proteins and resides underneath the viral envelope (Ruigrok et al., 2000). NEP, also known as non-structural protein 2 (NS2) (Bouvier and Palese, 2008), is a low abundant structural protein which probably interacts with M1 in the virion (Figure 1) (Hutchinson et al., 2015).

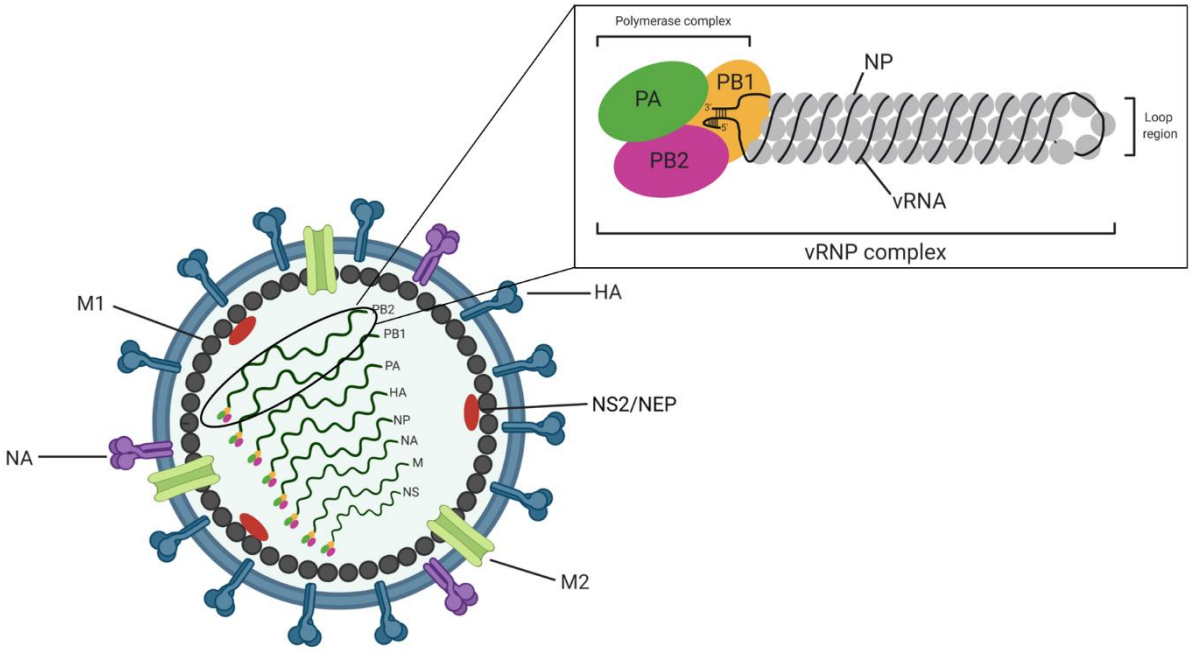

Figure 1: Influenza A virion and viral ribonucleoprotein (vRNP) complex. The two surface glycoproteins hemagglutinin (HA, blue) and neuraminidase (NA, purple) as well as the matrix protein 2 (M2, light green) ion channel are embedded in the viral envelope. Each viral ribonucleoprotein (vRNP) complex contains a viral RNA segment which is encapsidated by many nucleoprotein monomers (NP, grey). The heterotrimeric viral polymerase (PB2 (pink), PB1 (yellow) and PA (green)) is associated with the ends of each viral RNA segment. The matrix protein M1 is associated with both the vRNP complexes and the viral envelope. Created with Biorender.

1.3.2 Genome

The genome of IAV consists of eight single-stranded vRNA segments of negative polarity (~ 13.5 kb) (designated segment 1 to segment 8 for PB2, PB1, PA, HA, NP, NA, M and NS, respectively) (Shaw et al., 2008). Each of the eight segments contains 13 highly conserved nucleotides at the 5´-end (GGAACAAAGAUGA) and 12 highly conserved nucleotides at the 3´-end (AGCAAAAGCAGG). The two termini are complementary and form a double stranded panhandle-like structure which is important for binding the viral RNA-dependent RNA-polymerase (RdRp) to initiate genome transcription and replication (Desselberger et al., 1980; Robertson, 1979). Besides these conserved termini each viral gene segment contains segment-specific nucleotides (non-coding region) and at least one internal coding region (Goto et al., 2013). The segment specific nucleotides at the 5´- and 3´-termini of each vRNA are important for packaging (see below point 1.4.5). The packaging region flanks the coding region in each segment (Takizawa et al., 2019). Each gene segment encodes at least one structural protein, while segment 7 encodes two structural proteins. Some segments encode strain-dependent non-structural proteins (see point 1.3.4).

1.3.3 vRNP complex

Inside the virus particle, the eight vRNAs are found as individual vRNP complexes (Chou et al., 2012; McGeoch et al., 1976). These vRNP complexes are composed of the specific vRNA which is wrapped around many copies of the viral NP and is bound by a single copy of the heterotrimeric vRNA polymerase complex, consisting of PB2, PB1 and PA (Moeller et al., 2012). PB2, PB1 and PA are the three components of the RdRp and act synergistically. PB1 binds the 5´ and 3´ terminal ends of the vRNA and contains the catalytic domain, whereas PB2 and PA contain active sites for priming transcription (Dias et al., 2009).

1.3.4 Non-structural proteins

Non-structural proteins are expressed in the host cell and are not packaged into the virus particle (Vasin et al., 2014). IAV is able to increase the coding capacity of its relatively small genome by encoding more than one protein in each segment through different mechanisms, for instance, via splicing (e.g. M3, M4, M42, NS3, PB2-S1), the use of alternative open reading frames (ORF) (e.g. PB1-F2, PB1-N40, PA-N155, and PA-N182) as well as ribosomal frameshift (e.g. PA-X). All IAV express NS1, while the majority of viruses possess PB1-F2 and other do not have, for example, PA-X or PB1-N40 (Chen et al., 2001; Jagger et al., 2012; Muramoto et al., 2013; Selman et al., 2012; Wise et al., 2009; Wise et al., 2012; Yamayoshi et al., 2016).

1.4 Replication cycle of influenza A virus

1.4.1 Attachment, internalization and uncoating

The replication of IAV takes place in the host cell nucleus (Figure 2), which is exceptional compared to other RNA viruses. The initiation of the infection process starts by the attachment of HA to sialic acid (SA) on the host cell surface. SA is therefore the main receptor for IAV (Connor et al., 1994). The virus is taken up by receptor-mediated endocytosis, mainly by clathrin-dependent endocytosis or macropinocytosis (Dou et al., 2018; Matlin et al., 1981; Yoshimura et al., 1982) into early endosomes (EE). Acidification of the EE and the turnover into a late endosome (LE) is mediated by an adenosine triphosphate (ATP)-dependant proton pump which is located in the endosomal membrane of the EE and decreases the interior pH from 6.0 to 4.8 (Forgac, 2007; Gerlach et al., 2017). The low pH activates the M2 ion channel to pump H^+ into the virus particle. Lowering the pH results in (i) conformational changes in the HA to expose the fusion peptide which subsequently triggers the fusion of viral and endosomal membranes and (ii) dissociation of M1 from the vRNPs (Bui et al., 1996; Skehel and Wiley, 2000). The latter enables the release or "uncoating" of vRNPs into the cytosol (Martin and Helenius, 1991). After the release of the vRNPs into the cytosol, nuclear localization signals (NLS) in the NP (Neumann et al., 1997) are used to translocate the vRNPs into the nucleus via the nuclear pore complex (NPC) (Martin and Helenius, 1991; Wu et al., 2007).

1.4.2 vRNA replication and transcription

Arrival of the vRNPs in the nucleus is followed by replication as well as transcription of the viral genome. The vRdRp has access to the exposed vRNA on the surface of the vRNP (Dou et al., 2018) and transcribes the negative-sense vRNA into complementary positive sense RNA (cRNA). cRNA is used for synthesis of new copies of vRNA for the progeny virus as well as for messenger RNA (mRNA) which is used for translating viral proteins. In general, mRNA is the first to be synthesized, followed by cRNA and vRNA transcription. To produce viral mRNA which can be translated by host ribosomes, a process called "cap-snatching" has to be completed. "Cap-snatching" is a prerequisite for synthesis of viral mRNA. PB2 binds the cap-binding domain of a host pre-mRNA at the 5'-cap, followed by PA, which acts as an endonuclease and cleaves 10 - 13 nucleotides downstream from the 5'-cap (Dias et al., 2009; Shi et al., 1995). The newly capped cellular pre-mRNA fragment subsequently acts as a primer for initiating the transcription of viral mRNA and PB1 elongates these primary strands. Each IAV gene segment contains a conserved stretch of five to seven uracil bases at the 3' end which acts as a signal for polyadenylation (Poon et al., 1999; Robertson et al., 1981). Viral mRNA is capped and polyadenylated like cellular mRNA and is transported back into the cytoplasm mainly by the chromosomal region maintenance 1 (CRM1) export pathway (Eisfeld et al., 2015; Gales et al., 2020).

1.4.3 Translation of viral mRNA

Translation of viral mRNA takes place in the cytoplasm using the host translation machinery. Viral envelope proteins HA, NA and M2 are translated at ribosomes which are fixed in the rough endoplasmic

reticulum (rER), whereas PB2, PB1, PA, NP, NS1, NS2 and M1 are translated at cytosolic ribosomes. After translation, all viral proteins are present as monomers and have to be arranged, depending on their final function, into either di-, tri- or tetramers in the ER. NA (Wrigley et al., 1973) and M2 are homotetramers (Sugrue and Hay, 1991), whereas HA is a homotrimer (DuBois et al., 2011) and NS1 is a homodimer (Marc, 2014). NP is the only protein which forms higher order oligomers (Hu et al., 2017). The newly formed vRNA must be encapsidiated by the polymerase subunits and NP, therefore, after translation, PB2, PB1, PA and NP will return to the nucleus exploiting their NLSs to form the vRNPs (Ozawa et al., 2007; Wu et al., 2007). The RNA binding function of NP is achieved by the interaction of the negatively charged phosphate backbone of the RNA with the positively charged amino acids of NP (Portela and Digard, 2002; Turrell et al., 2013). Furthermore, the new vRNP complexes inside the nucleus are further involved in viral mRNA transcription and vRNA replication. M1 (Cao et al., 2012) and NS2/NEP (Huang et al., 2013; Yu et al., 2012) return to the nucleus as well to help export the vRNPs into the cytoplasm (Neumann et al., 2000).

1.4.4 Post-translational modifications

Besides the arrangement, depending on their function, post-translational modifications have to be accomplished (Dawson and Mehle, 2018; Dawson et al., 2020). These modifications occur in the ER and Golgi apparatus. Different post-translational modifications for IAV proteins include SUMOylation, phosphorylation (e.g. M1, NP, NS1), ubiquitination (e.g. PB2, PB1, PA), glycosylation (e.g. HA, NA) and palmitoylation (HA, M2) (Han et al., 2014; Kirui et al., 2016). SUMOylation, which is the conjugation of the Small Ubiquitin-like Modifier (SUMO) to a target protein affects PB1, NP, NS1 and M1. It is important for intracellular trafficking, nuclear export and virus replication (Gao et al., 2015; Santos et al., 2013). Phosphorylation is the attachment of phosphoryl groups on conserved sites of threonine (Thr, T), serine (Ser, S) or less frequently tyrosine (Nishi et al., 2014). Phosphorylation affects the stability, activity, subcellular localization as well as protein-protein-interaction of all IAV structural proteins and NS1 (Hutchinson et al., 2012). PB1, NP and M2 are ubiquitinated, which is the addition of ubiquitin to viral proteins. It plays important roles in degradation via the proteasome, trafficking, transcription/translation, nuclear transport, polymerase activity, protein-protein interaction, virus packaging, production of apoptosis and immune response (Fu et al., 2015; Kirui et al., 2016; Liao et al., 2010; Su et al., 2018). *N*-Glycosylation, i.e. the attachment of oligosaccharides to *N*-glycosidic linkages (NGS) of asparagine (Asn, N) side chain, is the most prominent modification for the HA and NA (Tate et al., 2014). Glycosylation takes place in the ER and trimmed in the Golgi apparatus. The number and pattern of glycosylation of the HA and NA vary in HxNx IAV subtypes (Altman et al., 2019; Tong et al., 2012). Palmitoylation is the addition of palmitic acid by the attachment of fatty acids to highly conserved cysteine (Cys, C) residues in the cytoplasmic tail of HA as well as M2 (Veit, 2012; Veit and Schmidt, 1993), a mechanism which might be affected by NS1 protein (Gadalla et al., 2021).

1.4.5 Assembly and virus release

The last steps are virus assembly and virus release which take place at the apical plasma membrane called “budozone”. All eight newly synthesized vRNPs as well as the structural proteins have to assemble at this site, before a new infectious virus can be released from the plasma membrane (Hutchinson et al., 2010). Some vRNPs, like HA, NA and M2 are membrane integrated proteins and contain sorting signals which navigate them from the cytoplasm over the ER and the trans-Golgi-network (TGN) to the budozone (Schmitt and Lamb, 2005). RNA segments contain specific packaging signals at both terminal ends of each gene segment which are important for the correct packaging into the new virion, otherwise false packaging occurs (Gerber et al., 2014; Muramoto et al., 2006). To release the virus, NA is necessary to cleave the linkage between HA of the newly formed virions and the SA on the cell membrane (Colman, 1994).

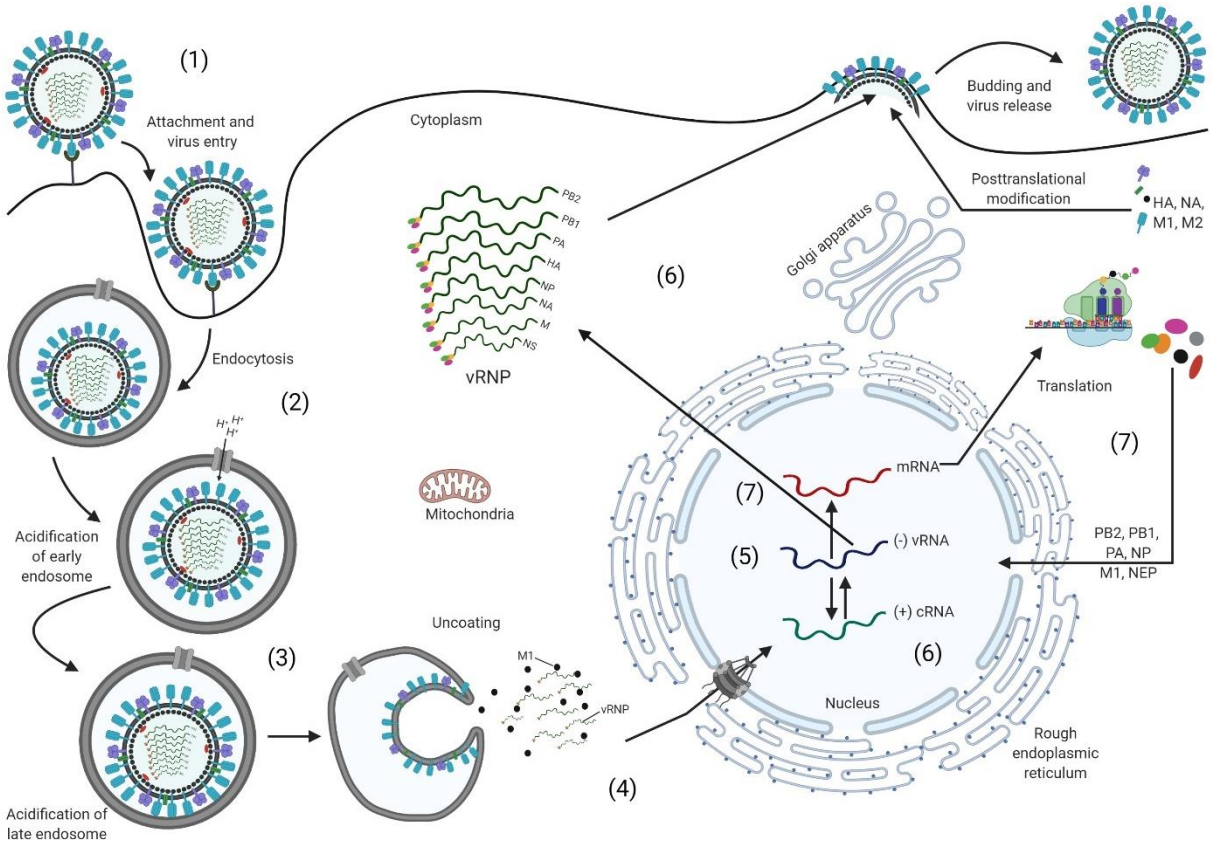

Figure 2: Replication cycle of influenza A virus. After the attachment of HA to sialic acid, the virus enters the cell by endocytosis. Acidification of the endosome leads to conformational changes in the HA which results in membrane fusion and the uncoating of the vRNPs. Replication and transcription of viral genes take place in the nucleus, whereas translation of viral proteins occurs in the cytoplasm. vRNAs and the viral core proteins meet at the “budozone” and the virus is released. Created with Biorender.

1.5 Evolution of influenza viruses

The nature of the influenza segmented genome and error-prone activity of the heterotrimeric vRdRp are two driving factors for continuous evolution and adaptation of influenza viruses in different hosts (Drake, 1993; Holland et al., 1982). Moreover, the spontaneous mutation rate of RNA viruses compared to DNA viruses is around 300-fold higher (Peck and Lauring, 2018). IAV can alter its genome by accumulation of point mutations (known as antigenic drift) or reassortment caused by exchanging gene segments between two IAV upon co-infection of one host cell (antigenic shift). Therefore, a high genetic diversity of IAV is present and infection of a wide range of hosts is possible. There are three mechanisms known by which influenza virus can undergo evolutionary changes, resulting in a constant evolution particularly of the surface glycoproteins HA and NA (Connor et al., 1994; Shao et al., 2017).

1.5.1 Antigenic drift

Antigenic drift is defined as the occurrence of single mutations in the virus genome, which lead to changes in the amino acid sequence. These changes alter the protein structure and subsequently its biological functions (e.g. HA and NA) (Figure 3). These mutations occur due to the lack of the proofreading function of the influenza vRdRp which results in a rate of integration of false nucleotides between 10^{-3} to 10^{-4} (Drake, 1993; Shao et al., 2017). This can result in immune escape by changing or masking immunogenic epitopes of circulating virus which will not be efficiently recognized by vaccine-induced antibodies. The biggest impact in immune escape is mostly due to changes in the epitopes A and B of HA, since neutralizing antibodies are directed against the HA protein and cannot recognize the pattern of the antigen-antibody-interaction anymore (Gamblin et al., 2004). Antigenic drift is the main reason for vaccination failure in humans and poultry which requires regular update of influenza virus vaccines (e.g. annual or biennial) (Grund et al., 2011; Wen et al., 2021). The NA contains three immunogenic epitopes (A-C) as well, but immune escape is far less frequent compared to the HA (Munoz and Deem, 2005). Moreover, amino acid exchanges in the HA of H1-, H2-, H3-, H4-, H5- and H9-subtypes have been also associated with changes in the receptor preferences or affinities which play a role in animal-to-human transmission of IAV (Reperant et al., 2012).

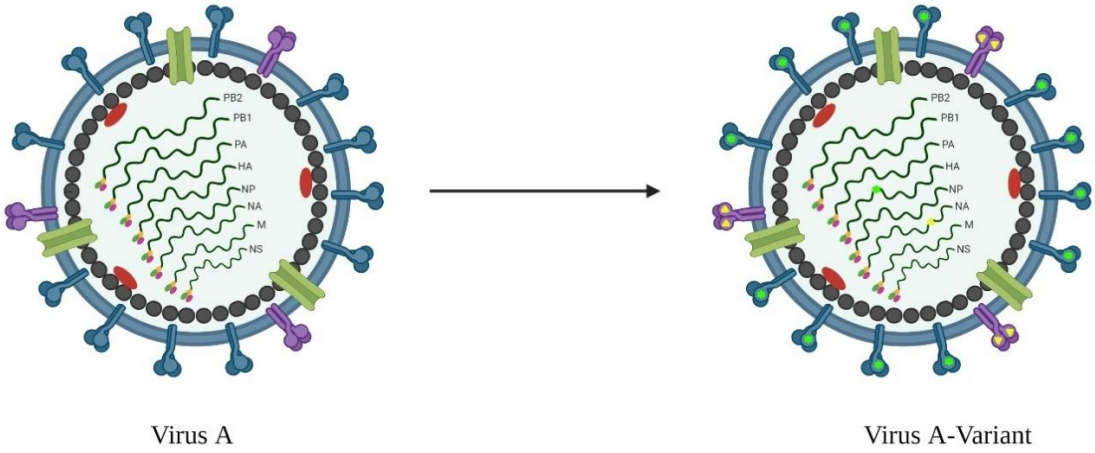

Figure 3: Antigenic drift of influenza A virus. Occurrence of mutations in the virus genome (green star and yellow triangle) which lead to changes in the structure of mainly HA and NA (green star and yellow triangle) is defined as antigenic drift. Created with Biorender.

1.5.2 Reassortment

The second important mechanism for the evolution of IAV is called "reassortment". Here, two or more different IAV can simultaneously infect one cell and swap their gene segments (Mostafa et al., 2018; Reid and Taubenberger, 2003) (Figure 4). Reassortment between avian, swine and human influenza viruses can result in "antigenic shift". All pandemic IAV (e.g. H1N1 in 1918/1919 and 2009) acquired gene segments from avian and/or swine influenza viruses. Similarly, H9N2 donated gene segments to a number of AIVs (e.g., H5N1, H6N1, H7N4, H7N7, H7N9, H9N2, H10N8), which crossed the species barrier to infect humans inducing asymptomatic to fatal infections (Chen et al., 2014; Lam et al., 2013; Monne et al., 2013).

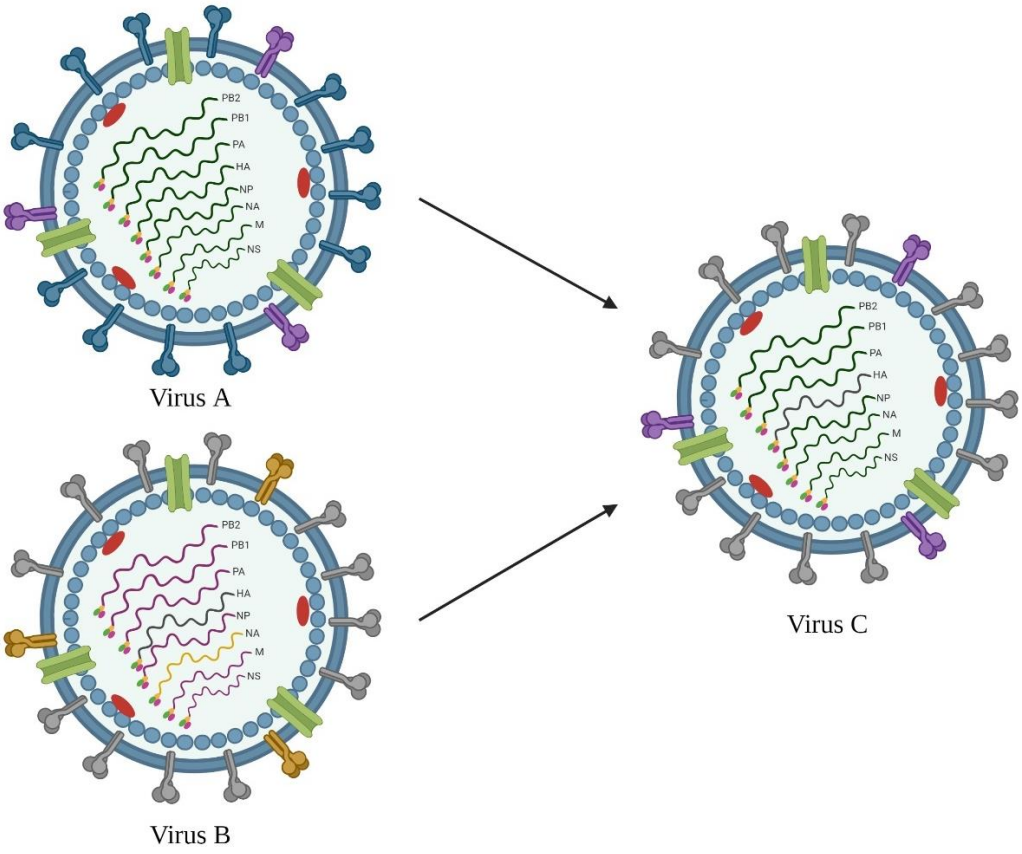

Figure 4: Reassortment of influenza A virus. A host cell can be infected by two different viruses (Virus A and B) simultaneously, which results in swapping gene segments (reassortment) and emergence of new viruses. Created with Biorender.

1.5.3 Recombination

The third mechanism is known as recombination. Here, parts of IAV gene segments (homologous recombination) or host cellular RNA (non-homologous recombination) are integrated in other gene segments. Recombination can abruptly affect virus properties. Recombination in the Hemagglutinin cleavage site (HACS) resulted in the evolution of HPAIV from LPAIV in several occasions (Gultyaev et al., 2021). Intersegmental recombination of HACS with 30 nucleotides from the NP segment or 21 nucleotides from the M segment resulted in the conversion of LPAIV to HPAIV H7N3 in Chile in 2002 and in Canada in 2004, respectively (Pasick et al., 2005; Suarez et al., 2004). Similarly, the evolution of HPAIV H7N9 in China in 2017 and H7N3 in Mexico in 2012 was due to insertion nucleotides from 28S ribosomal ribonucleic acid (rRNA) into the HACS (Gultyaev et al., 2021; Maurer-Stroh et al., 2013). Conversely, shuffling of PA sequences in the NA resulted in the attenuation of an HPAIV H5N1 in chickens due to insertion of stop codon and subsequently deletion of the NA head domain (Kalthoff et al., 2013).

1.6 AIV infection in birds and mammals

1.6.1 AIV infection in wild birds

AIV has been isolated from more than 100 wild bird species (26 families). However, some species act as the main reservoirs for AIV (e.g. wild aquatic birds) (Olsen et al., 2006; Webster et al., 1992). The species are mainly from the order *Anseriformes*, like ducks (particularly Mallards), geese, and swans as well as from the order *Charadriiformes* including gulls and shorebirds. It is worth mentioning that susceptibility of wild birds to AIV differ according to virus strain, bird species and age (Spackman, 2009). Generally, the infection of waterfowl (e.g. ducks and geese) is mostly asymptomatic due to the adaptation of the virus to these birds (Alexander, 2000; Pantin-Jackwood and Swayne, 2009; Spackman, 2009). Waterfowls like Mallard ducks exhibit no symptoms upon AIV-infection, partially due to the upregulation of the retinoic acid-inducible gene-I (RIG-I), an important inducer of type I interferons (Barber et al., 2010; Evseev and Magor, 2019; Weber-Gerlach and Weber, 2016a). Nevertheless, few reports have described high mortality in wild birds after infection with different H5Nx (e.g. H5N3 in South Africa in 1960s, H5N1 in 2002/2003, H5N8 in 2020 and H5N3 in 2021) (Becker, 1966; Capua and Mutinelli, 2001; FLI, 2021b; Verhagen et al., 2021). Due to the replication of the virus in the epithelial cells of the gastrointestinal tract (GIT), viruses are excreted at high levels and for a long time in the feces (Olsen et al., 2006; Webster et al., 1978). Influenza viruses are stable and can remain infectious in lake water at different temperatures for several weeks. Since many *Anseriformes* or *Charadriiformes* are migratory birds and fly long distances, AIV can be translocated between countries or continents (Bodewes and Kuiken, 2018; Global Consortium for and Related Influenza, 2016; Lycett et al., 2020; van der Kolk, 2019).

1.6.2 AIV infection in domestic birds (i.e. poultry)

Chickens and turkeys (Gallinaceous birds) are known to be highly susceptible to AIV infections, although turkeys are more vulnerable than chickens to AIV-induced morbidity and mortality (Alexander, 2000; Alexander et al., 1986). It is believed that poultry gets infected by AIV via direct or indirect contact with wild birds. The shedding of infectious virus from wild birds into the environment (e.g. water or feed) is the most common source for infection of poultry. Live poultry markets are also an important source for transmission of AIV from wild birds to poultry (Alexander, 2000). In chickens (and turkeys), AIV exhibit two pathotypes: LP and HP. According to the OIE, HPAIV can be identified by the polybasic HACS or degree of virulence after intravenous injection. HPAIV produce an intravenous pathogenicity index (IVPI) greater than 1.2, while viruses with IVPI less than 1.2 are considered as LPAIV (Alexander, 2000). LPAIV replicate in the epithelial cells of the respiratory and digestive tracts and lead only to mild or subclinical infections in poultry (Pantin-Jackwood and Swayne, 2009). Few LPAIV (e.g. H9N2) can cause moderate to severe clinical signs and even induce mortality in chicken flocks (Bano et al., 2003) and the co-infection with bacteria, fungi or other viruses causes severe symptoms and increased mortality rates (Belkasmi et al., 2020; Umar et al., 2018). Moreover, clinical signs in chickens and turkeys are often non-specific but birds may show e.g. ruffled feathers,

oedema, coughing and sneezing, depression, ocular and nasal discharge, weight loss, decreased activity and decreased egg production as well as decreased uptake of food and water (Morales et al., 2009; Spickler et al., 2008; Tumpey et al., 2004). Moreover, swelling of the sinuses, conjunctivitis and diarrhoea have been reported (Mondal et al., 2013). Independent of the species, post-mortem lesions are commonly found in the respiratory and gastrointestinal tracts (Alexander, 2000). Conversely, the systemic replication of HPAIV causes severe clinical signs and up to 100% mortality in a short time. Symptoms vary according to bird species. Congestion, cyanosis and haemorrhages (e.g. on the shanks, legs, comb and wattle) in chickens are common, while turkeys exhibit mostly nervous signs including paralysis, convulsions, tremors, paresis and paralysis (Alexander, 2000; Alexander et al., 1978; Narayan et al., 1969; Scheibner et al., 2019b; Swayne and Slemons, 2008).

In contrast to chickens and turkeys, ducks infected with HPAIV exhibit no or mild symptoms since they are more resistant to HPAIV infections (Fleming-Canepa et al., 2019; Scheibner et al., 2019a). Ducks can spread AIV asymptomatically to poultry (e.g. chickens, turkeys), therefore, they have been described as a "Trojan horse" (Kim et al., 2009). Nevertheless, morbidity and mortality may vary according to the duck species (Pekin *vs.* Mallard *vs.* Muscovy duck), age and inoculation route (intranasal, intraocular, intramuscular) and virus strain (Cagle et al., 2012; Pantin-Jackwood et al., 2013; Pantin-Jackwood et al., 2012; Scheibner et al., 2019a; Scheibner et al., 2019b). Generally, Pekin and Mallard ducks are more resistant to HPAIV infections compared to Muscovy ducks (Scheibner et al., 2019b).

1.6.3 AIV infections in mammals including humans

Human influenza viruses belong to H1, H2, H3, N1 and N2 subtypes (Glezen, 1996; Kilbourne, 2006; Taubenberger and Morens, 2006). Infection of humans with AIV or human influenza viruses carrying gene segments from avian sources have been frequently reported. The latter was the reason for the emergence of the "Spanish flu" H1N1 in 1918/1919 which killed more than 50 million people (Monto and Fukuda, 2020), the "Asian flu" H2N2 in 1957 which killed 1.1 million people, H3N2 emerged in Hong Kong in 1968 which killed 1 million people and last but not least the "swine flu" pandemic in 2009 (Garten et al., 2009; Schulman and Kilbourne, 1969). Direct bird to human transmission of AIV (e.g. H5N1, H5N6, H6N2, H7N3, H7N7, H7N9, H9N2, H10N8) has also been reported. Symptoms ranged from self-limiting flu-like illness to death (Abdelwhab et al., 2014; Kalthoff et al., 2010; Mostafa et al., 2018). In 2021, the first cases of AIV H5N8 infections in humans were reported in Russia (WHO, 2021b). AIV can also infect mammals including swine, horses or seals and the infection ranges from subclinical signs to high mortality (e.g. in seals) (Dittrich et al., 2018; Reperant et al., 2012).

1.7 Genetic determinants for virulence of avian influenza viruses in poultry

Using reverse genetics, several studies have been conducted to elucidate the genetic determinants for adaptation and virulence of AIV in poultry and mammals. However, these efforts are still insufficient to

fully understand the molecular mechanism which underlies the shift in virulence or higher adaptation in different animal species. In the next points, I will focus on the role of HA, NA and NS1 as main virulence determinants in poultry. However, that does not exclude the role of other gene segments, alone or in combinations, in virulence of some AIV in different poultry species (Tada et al., 2011), particularly in ducks (Hu et al., 2013; Kajihara et al., 2013).

1.7.1 Hemagglutinin

1.7.1.1 Structure and function

The HA is essential for virus entry, spread throughout the organism, antigenicity and virulence. The HA consists of three identical subunits building up a homotrimer spike-like structure with head and stalk domains which is anchored with the carboxy-terminus in the viral membrane (Mair et al., 2014). The HA is synthesized as a fusion-inactive molecule, known as HA0, and undergoes posttranslational modifications like proteolytic cleavage or glycosylation. For IAV to be infectious, the HA0 has to be cleaved at the HACS by host proteases into two polypeptides: HA1 and HA2 (Skehel and Wiley, 2000). The head domain of the IAV is formed exclusively by the HA1 polypeptide, while the HA stalk domain is formed by both HA1 and HA2. The receptor binding domain (RBD), proteolytic CS and most of the immunogenic sites are located in the globular head domain. The latter harbours five antigenic sites (known as epitopes A, B, C, D and E) (Gamblin and Skehel, 2010; Iba et al., 2014; Kaverin et al., 2007). Epitopes A and B are the major epitopes and therefore changes in these epitopes are crucial for vaccine efficiency and immune-escape. The HA2 has three important structures: the transmembrane domain (TMD), the hydrophobic fusion peptide and conformational immunogenic epitopes. The fusion peptide in the N-terminus of the HA2 mediates the fusion of the viral membrane with the endosomal membrane during the replication cycle (Chen et al., 1998; Steinhauer, 1999).

1.7.1.2 Host proteases and hemagglutinin cleavage site

Proteolytic activation of HA0 is essential for virus infectivity. Therefore, the distribution of HA-activating proteases in the host cells and the sequence of HACS are main determinants for replication and virulence of AIV. Different host proteases can cleave HA0 into HA1 and HA2 depending on the structure of the HACS. LPAIV contain a monobasic HACS motif RXR/K*G (R, arginine- x, any amino acid- K, lysine * G, glycine). Cleavage occurs between R/K and G. These motifs are recognized by trypsin and trypsin-like enzymes (e.g. human airway trypsin-like protease “HAT”, transmembrane protease serine member 2 “TMPRSS2”), which are restricted to the respiratory and intestinal tracts. Therefore, LPAIV infections may cause local respiratory and digestive tract disorders (Baron et al., 2013; Bottcher et al., 2006; Laporte and Naesens, 2017). Human influenza viruses possess a monobasic HACS as well (Schrauwen et al., 2011). Conversely, HPAIV of H5 and H7 subtypes may contain polybasic HACS motifs (R-X-K/R-R/G), which are recognized and activated by ubiquitously expressed furin-like proteases (Luczo et al., 2015; Stieneke-Grober et al., 1992). Since these proteases are located at the plasma membrane as well as in the TGN in many cells and organs, systemic infections result in

up to 100% mortality. It is known that HPAIV evolve from LPAIV progenitors. Changing the monobasic HACS to a polybasic motif is the main virulence determinant of HPAIV in birds (Abdelwhab et al., 2016b; Kobayashi et al., 1996; Scheibner et al., 2019b). However, glycosylation in the vicinity of the HACS may sterically hinder the access of furin proteases and prevent the exhibition of high virulence (Kawaoka, 1991; Kawaoka and Webster, 1989). Moreover, the high virulence in chickens of some H5 viruses require mutations in the NA (Stech et al., 2015) or NS1 (Li et al., 2006). Importantly, the impact of the polybasic HACS on virulence of H5 and H7 viruses differs among poultry species and breeds. For instance, insertion of a polybasic HACS into a LPAIV H7N7 increased the virulence in chickens and to a lesser extent in turkeys, whereas in ducks (i.e. Mallards, Pekin and Muscovy) the virus remained avirulent (Scheibner et al., 2019b). Muscovy ducks were more vulnerable than Pekin ducks to mortality and morbidity to H5N1 and H5N8 (Cagle et al., 2011; Cagle et al., 2012). Furthermore, insertions of several basic amino acids into the HACS of non-H5/non-H7 LPAIV subtypes resulted in increased virulence of H6 and H9 in chickens (Munster et al., 2010; Soda et al., 2011), while other studies showed that mutations in other gene segments are required to increase virulence of H2, H4, H8, H9 and H14 with polybasic HACS (Gischke et al., 2020; Gohrbandt et al., 2011; Veits et al., 2012). Together, virulence of AIV in poultry is a multigenic trait. Although the HACS is the main virulence determinant in poultry, mutations in other gene segments or host-factors play a role.

1.7.2 Neuraminidase

1.7.2.1 Structure and function

The NA protein comprises 454 amino acids (aa) and is a homotetramer of four identical subunits that form a mushroom-like spike on the viral membrane. The NA monomer is formed of N-terminus, TMD, stalk domain and head domain (Colman, 1994; Gamblin and Skehel, 2010; McAuley et al., 2019). The stalk domain varies between different AIV due to natural deletions (Li et al., 2011). The head domain harbours the sialidase enzyme pocket, which is formed of highly conserved functional and framework residues. The NA is the second major surface glycoprotein of the virion and its main role is the removal of SA from the surface of the infected host cells or mucoid decoys in the upper respiratory tract. The balance between HA receptor-binding and NA receptor-destroying activities is important for an optimal infection, transmission, viral replication, pathogenesis and host adaptation for the virus (Arai et al., 2020; Chen et al., 2020; Mok et al., 2017; Stech et al., 2015; Wagner et al., 2002). Furthermore, the NA has three immunogenic epitopes (A, B and C) and can provide partial protection against homologous virus challenge in poultry (Sylte et al., 2007).

1.7.2.2 NA stalk deletions and glycosylation pattern

The NA stalk domain of some AIV has a deletion of 1 to 39 aa (Li et al., 2011). While these deletions have been detected upon transmission of e.g. H5N1, H7N1, H9N2, H2N2 from wild aquatic birds to domestic poultry (Banks et al., 2001; Hoffmann et al., 2012; Matsuoka et al., 2009; Sorrell et al., 2010; Sun et al., 2013), they were very rare in N4, N8 and N9 NA-subtypes (Li et al., 2011). The mechanism

underlying the evolution of a short NA stalk in some AIV but not in others, is not well-understood. Furthermore, the impact of the NA stalk domain deletions on replication, virulence and transmission in poultry species varies in different strains and different poultry species. For example, a deletion in the NA stalk domain of an H7N1 virus resulted in increased replication and excretion in chickens but it was detrimental for virus replication in ducks (Hoffmann et al., 2012). For H5Nx viruses, several studies showed that shortening the NA of H5N1 (mostly of aquatic or wild bird origins) increased virus adaptation in chickens and ducks (Li et al., 2014b; Stech et al., 2015). The reasons behind the efficient replication of some AIV with short NA stalk domain in chickens compared to viruses with full-length is not fully clear. However, it has been speculated that reducing the NA activity is important to avoid early cleavage of the SA during virus entry and thus promotes virus replication and subsequently virulence in chickens (Li et al., 2011). Moreover, the NA stalk domain has three to four glycosylation sites which are important for maturation, structure and stability of the NA (Wu et al., 2017). The deletion in the NA stalk removes one to four glycosylation sites (Tong et al., 2012). H5N1 lacking these NA glycosylation sites were more virulent in Mallard ducks (Chen et al., 2020).

1.7.3 Non-structural protein 1

The NS segment is the smallest gene segment of IAV (890 nucleotides) and encodes the NS1 protein as well as the NS2/NEP protein, which results from an alternative splicing of NS mRNA. For some IAV, NS3 (174 aa) has been detected as well (Bouvier and Palese, 2008; Selman et al., 2012; Vasin et al., 2014). NS1 is translated from the unspliced transcript of the eighth vRNA segment (NS) and is a small, multifunctional protein with a typical size of 26 kilo Dalton (kDa). Phylogenetic analysis indicated that NS1 has two distinct genetic alleles: allele A (mammalian and avian viruses) and allele B (mainly avian viruses), where allele A is more common than allele B (Kawaoka et al., 1998; Marc, 2014; Suarez and Perdue, 1998).

1.7.3.1 Structure of NS1

NS1 typically encompasses 230 aa, but the size can vary among different strains (Krug, 2015; Wacquiez et al., 2020). NS1 which forms homodimers has two structural domains, which are connected through a flexible linker (Figure 5). The N-terminal domain, the RNA binding domain (RBD; aa residue 1 to 73), is made of three alpha-helices (Chien et al., 1997). The RBD is connected through a linker region (LR) (aa 74 to 87) to the effector domain (ED). The ED (aa 88 to 230) is composed of three alpha helices and seven beta-strands (Hale et al., 2008a). The RBD has the capacity to bind different types of cellular and viral RNA including double-stranded RNA (e.g. the panhandle-like structure in each influenza gene segment). This is important to prevent the stimulation of antiviral innate immunity triggered by sensing viral RNA through e.g. RIG-I (Hale et al., 2008a; Marc, 2014). The RBD also interacts with the NP and can affect the activity of the viral polymerase (Robb et al., 2011). The ED interacts with many cellular proteins (Figure 5) particularly those involved in host-immune response (e.g. Myxoma resistance protein 1; Mx1), host mRNA maturation (e.g. cleavage and polyadenylation specificity factor 30;

CPSF30) and mRNA export (e.g. nuclear export factor 1; NXF1) (Marc, 2014). Moreover, NS1 interacts with PDZ-domain-containing proteins. These proteins function in cell signalling and cellular polarity. The NS1 PDZ domain is located in the C-terminus (residues 226-230) and the consensus PDZ-binding motif of AIV in the NS1 is mostly "^{226}ESEV^{230}" and for human influenza viruses is "^{226}RKSV^{230}" (Obenauer et al., 2006).

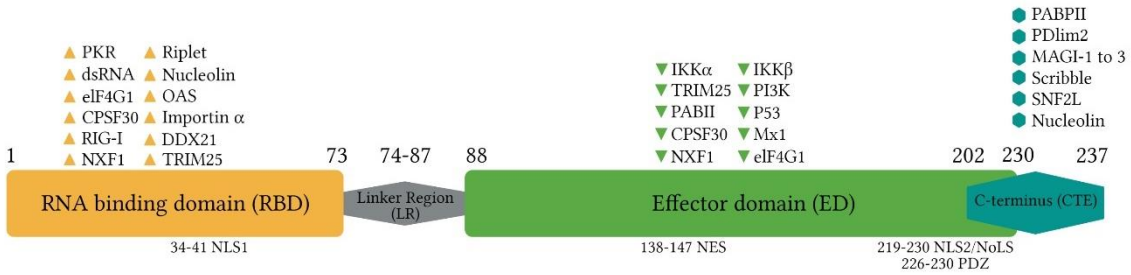

Figure 5: Structure of NS1 and binding to cellular proteins and factors. The RNA binding domain (RBD) and effector domain (ED) are connected through with a linker region (LR). The RBD can bind different types of cellular and viral RNA, while the ED interacts with many cellular proteins (the figure is modified with Biorender from (Rosario-Ferreira et al., 2020)).

1.7.3.2 Nuclear/nucleolar localization and nuclear export signals of NS1

NS1 has two NLSs: NLS1 and NLS2. NLS1 is part of the RBD. It is highly conserved in all IAV and is composed of aa 34 to 41. NLS2 is localized between aa 219 and 230 (Greenspan et al., 1988; Hale et al., 2008b). Besides NLS1 and NLS2, a nucleolar localization signal (NoLS) was found to overlap the sequence of NLS2 (Figure 5). In addition, NS1 has nuclear export signals (NES) in the ED (residues 138–147). These signals control the subcellular localization of NS1 in the nucleo-cytoplasm in host cells (Melen et al., 2007; Volmer et al., 2010). Nevertheless, the localization depends on different factors e.g. virus strain, cell type and time post-infection. Since NS1 contains two NLSs, it can accumulate in the nuclei of infected cells independent of other viral proteins. During infection, NS1 accumulates at early time points in the nucleus of infected cells and is present later on in the cytoplasm (Hale et al., 2008a; Krug and Etkind, 1973). The presence of NS1 in the nucleus at early stages of infection is important to shut-off host mRNA synthesis including those encoding for immune system elements (e.g. Interferon) (Mok et al., 2017). Furthermore, mutations in the NES compensate the lack of NLS2 in some AIV due to natural truncation in the C-terminus of some AIV (Keiner et al., 2010).

1.7.3.3 NS1 is a virulence determinant in poultry

NS1 plays an important role in the inhibition of type I IFN-mediated antiviral response and is involved in evasion from the innate immune system (Garcia-Sastre et al., 1998). Therefore, NS1 contributes to the efficient virus replication in infected cells and is a virulence factor for some IAV (Noah and Krug, 2005). Due to the interaction with different proteins or other partners, NS1 can either inhibit (e.g. IFN and antiviral response) or enhance (e.g. translation of viral mRNAs in the cytoplasm; activity of the viral polymerase in the nucleus) different viral or cellular mechanisms (Burgui et al., 2003) (Figure 6).

Mutations in different regions of NS1 have been described to play diverse roles in virus pathogenicity in birds. For example, a deletion of 5-aa in the flexible linker region (aa 80 to 84) along with the D92E mutation in the ED in an HPAIV H5N1 increased virulence in chickens (Long et al., 2008). Similarly, V149A in the ED contributed to virulence of HPAIV in chickens (Li et al., 2006). The C-terminus (CTE) of NS1 (aa 202 to 237) is disordered and prone to deletion or extension due to variable stop codons. About 13 different forms of deletions or extensions in CTE are present so far in AIV (Abdelwhab et al., 2016a; Marc, 2014; Suarez and Perdue, 1998). The impact of the variable NS1 CTE on virus virulence and transmission in different poultry species is not fully understood and mostly controversial due to variable study designs, the use of different strains and different cells or animal species.

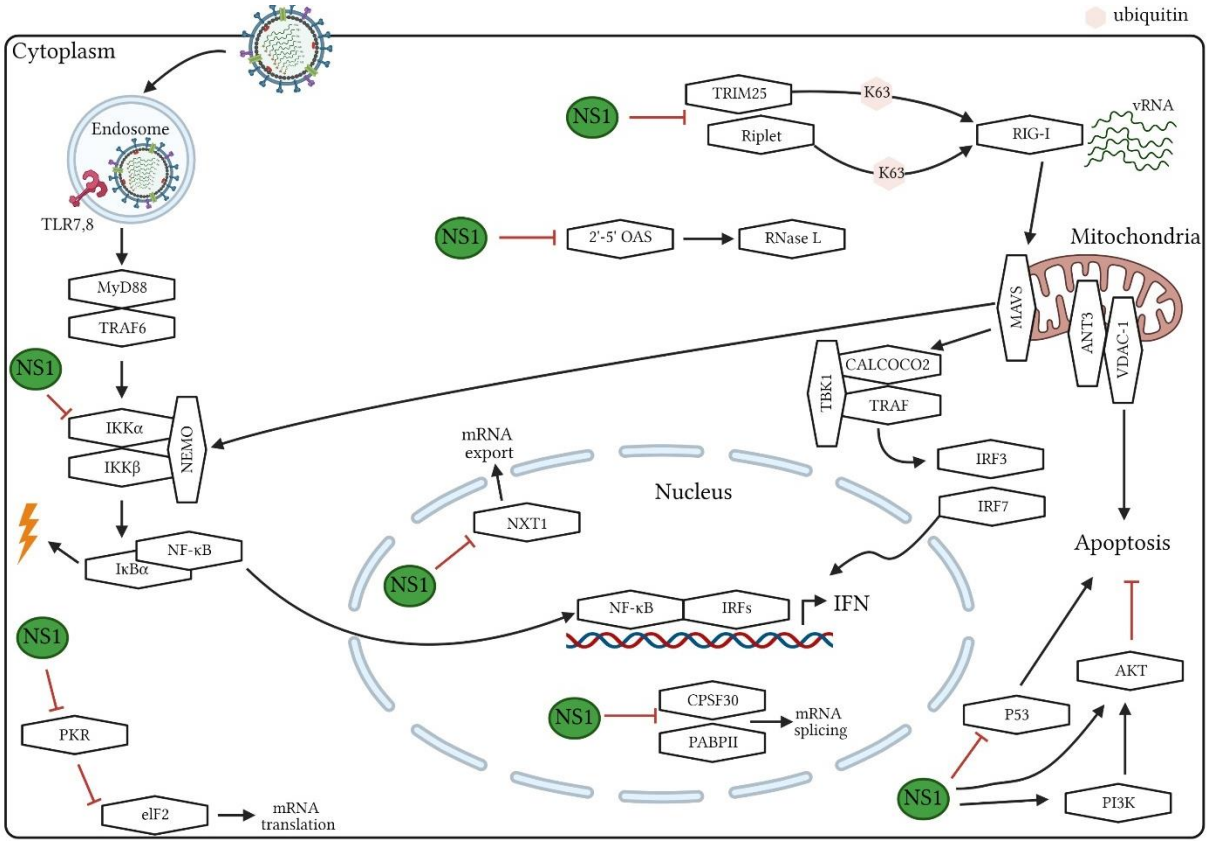

Figure 6: Interaction of NS1 with cellular factors. NS1 inhibits the interferon regulatory factor 3 (IRF3) activation by blocking RIG-I resulting in the suppression of host innate immunity (type I IFN expression) as well as it is also involved in host gene expression shutoff, apoptosis and viral replication (the figure is modified with Biorender after (Hao et al., 2020)).

1.7.4 Genetic determinants for virulence of avian influenza viruses in mammals

Apart from the acquisition of seasonal or pandemic human influenza viruses to gene segments from AIV via reassortment, some AIV, *per se*, are able to cross the species barrier and infect mammals including humans (reviewed in detail in (Abdelwhab et al., 2014; Kalthoff et al., 2010; Mostafa et al., 2018)). Genetic determinants for interspecies transmission and virulence in mammals have been extensively studied in the last two decades. Mutations in almost all gene segments linked to the high adaptation of

these AIV in mammalian cells *in vitro*, animal models *in vivo* and or infected patients have been described (Fouchier, 2015; Fouchier et al., 2004; Imai et al., 2012; Watanabe et al., 2011). Most of the studies revealed key mutations in the HA, polymerase complex and NS1 across different AIV subtypes (Lycett et al., 2009; Mostafa et al., 2018; Zielecki et al., 2010).

1.7.4.1 Hemagglutinin

1.7.4.1.1 Receptor binding

The HA of IAV is the main determinant of host range since it recognizes and binds SA on the surface of the host cell (Mostafa et al., 2018). Influenza viruses have different receptor specificities and recognise the *N*-acetylneuraminic SA linked to the sugar galactose with alpha(α)(2,3) or α(2,6) linkage. Sialic acids are either nitrogen (N)- or oxygen (O)-substituted derivatives of neuraminic acid (Byrd-Leotis et al., 2017; Webster et al., 1992). Avian influenza viruses and equine influenza viruses preferentially bind to glycans harbouring sialic acids with α(2,3) linkage to galactose (α2,3-SA), whereas human influenza viruses preferably bind to α2,6-SA. The distribution of SA varies from one host to another, since aquatic birds contain α2,3-SA in the respiratory and intestinal tract and humans contain mostly α2,6-SA in the upper respiratory tract and to a lesser extent α2,3-SA in the lungs (Franca et al., 2013; Kumlin et al., 2008; Pillai and Lee, 2010). It is important to mention that some AIV have dual receptor specificity and can recognize the avian and mammalian receptors. Switching from avian α2,3-SA to mammalian α2,6-SA is required for efficient transmission of AIV to mammals including humans (Ito et al., 1998; Ito et al., 1997; Watanabe et al., 2011). Point mutations in the receptor binding site (e.g. Q226L as well as G228H (H3 numbering)) of the HA enabled AIV (e.g. H5, H7, H9) as well as human adapted influenza virus strains (e.g. H1N1, H3N2) to increase binding affinity of these viruses to α2,6-SA receptors (Vines et al., 1998). Besides binding affinity, host range, replication efficiency and pathogenicity can be affected as well. It is important to mention that swine and quails harbour α2,3-SA and α2,6-SA and therefore they are considered as a "mixing vessels" for generation of reassortant viruses with higher replication efficiency in humans (Russell et al., 2006b; Shelton et al., 2011).

1.7.4.2 The polymerase subunits

Mutations in the polymerase segments play a major role in AIV adaptation to mammalian hosts (Subbarao et al., 1993). Several specific aa exchanges in the PB2 subunit (e.g. 271A, 627E, 253N, 591K, 526R, 590S, 591R, 627K) lead to an increased viral polymerase activity as well as in increased virus replication and pathogenicity in mammals (e.g. mice, swine) (Liu et al., 2012; Mok et al., 2011; Song et al., 2014). Most PB2 segments of AIV contain glutamic acid (E) at position 627 (PB2-627E), whereas human IAV contain lysine at this position (PB2-627K). PB2-627K plays a key role in mammalian-adapted viruses and therefore position 627 is an important determinant of host range (Yamada et al., 2010). Besides position 627, position 701 in the PB2 segment plays a role in AIV adaptation in mammals (Steel et al., 2009), since aa exchange D701N contributes to high pathogenicity in mice (e.g. H5N1) (Czudai-Matwich et al., 2014). Nevertheless, not all isolated mammalian influenza viruses contain these

amino acid exchanges and therefore other additional residues in different segments might play roles in virus adaptation to mammals.

It has been described that internal-protein coding genes of H9N2 are able to reassort with multiple viruses (e.g. H7N9, H7N7, H5N6) and that certain reassortants (e.g. those carrying H9N2-PB1) show increased pathogenicity in mice (Lam et al., 2013; Shen et al., 2016; Su et al., 2015). Reassortment of PB1 of H9N2 with H7N9 increased virulence in mice, but did not confer efficient transmission to guinea pigs by airborne route (Su et al., 2015). Position 375 in PB1 varies between avian IAV and human IAV. In AIV asparagine and to lesser extent serine or threonine are present at position 375, while human IAV contain a serine and it is suggested that it plays a critical role for adaptation and virulence (Taubenberger et al., 2005). PB1-F2 is a small protein which is encoded by a +1 alternative ORF of PB1 and influences the innate immune response and viral pathogenicity (Zamarin et al., 2006). However, the role of PB1-F2 in adaptation to mammals is mostly strain- and host-dependent. For example, S at position 66 (66S) contributed to high pathogenicity of the pandemic H1N1/1918 and H5N1 in mammals (Conenello et al., 2011; Varga et al., 2011). Conversely, complete deletion or truncations of PB1-F2 did not alter pathogenicity of different H5N1 and H1N1 viruses in mice (Chen et al., 2010; McAuley et al., 2010).

PA containing 97I increased virulence of an AIV in mice compared to chickens. Further specific PA residues, e.g. 70V and/or 224S enhanced viral polymerase activity and increased replication in mammals (Sun et al., 2014). Besides, R195K, K206R and P210L in PA-X of H1N1 increase the virulence and transmission of IAV in mice and ferrets when present in a H9N2 virus background (Sun et al., 2020).

1.7.4.3 NS1

The role of NS1 for adaptation of AIV in mammalian cells or animal models has been described. Changing the amino acid serine to proline (P) at position 42 (P42S), as well as F103M and M106I in the NS1 protein increased the virulence of H5N1 in mammals (e.g. mice) dramatically (Jiao et al., 2008). Likewise, a deletion of amino acid 80-84 in the linker region along with the D92E mutation in the ED in an HPAIV H5N1 virus increased virulence in mice (Long et al., 2008). Conversely, some studies showed no impact for the NS1 on virulence or interferon induction in mice and/or in ferrets (Hale et al., 2010a; Hale et al., 2010b).

1.8 Innate immune system

Rapid response of the innate immune system depends on the recognition of certain molecular structures of invading organisms that are detected as a foreign antigen (Campbell and Magor, 2020). These molecular structures are pathogen associated molecular patterns (PAMPs) and are usually essential for the survival of pathogens and include for example lipopolysaccharides (LPS), single-strand RNA (ssRNA) or double-strand RNA (dsRNA). The immune system of the host possesses various pattern recognition receptors (PRRs) that recognize these PAMPs. Retinoic acid-inducible gene-I-like receptors

(RLRs), toll-like receptors (TLR) and nucleotide-binding oligomerization domain (NOD)-like receptors (NLRs) are the three main PRR, which respond to influenza infections in mammals and birds. They are mainly found in cytosolic compartments (e.g. RLR, NLR) or on the cell surface (e.g. TLR) (Campbell and Magor, 2020; Chen et al., 2013). The resulting antiviral response include cytokines, chemokines and the upregulation of antiviral effectors. Particularly the Interferon (IFN) system is able to prevent the spread of intracellular pathogens through its rapid activation until adaptive immunity takes over (Evseev and Magor, 2019).

1.8.1 RIG-I-like receptors

RLRs which recognize IAV include RIG-I, Melanoma differentiation-associated gene 5 (MDA5) as well as laboratory of genetics and physiology 2 (LGP2) which are expressed in immune cells and somatic cell types (Campbell and Magor, 2020; Chen et al., 2013). RIG-I and MDA5 are the main cytosolic PRR for IAV in mammals and birds and detect nucleic acids of invading viruses to activate the interferon system. Type I interferons (IFN-α and IFN-β) or pro-inflammatory cytokines (e.g. Interleukin (IL)-6, Tumor necrosis factor (TNF)) are produced as soon as cytosolic sensors recognize viral RNA (Evseev and Magor, 2019). Besides detection of viral replication in the cytoplasm, RIG-I is also able to detect viral replication in the nuclear compartment. RIG-I recognizes short dsRNA, which is produced during IAV replication, and short 5'-ppp-dsRNA in infected cells (Brisse and Ly, 2019; Weber et al., 2015). RIG-I is ubiquitously expressed in human tissues, and the expression in birds is highly variable. Chickens and turkeys lack RIG-I, which might explain their vulnerability to morbidity and mortality after AIV infections. Ducks possess RIG-I but the expression levels vary among different duck species (Barber et al., 2010; Campbell and Magor, 2020; Chen et al., 2013; Evseev and Magor, 2019). During an influenza infection, IFN-β expression is dependent on RIG-I and cannot be compensated by IFN-α (Koerner et al., 2007). To compensate the absence of RIG-I, chickens express MDA5 (Xu et al., 2016). MDA5 recognizes long dsRNA in chickens, while mammalian MDA5 recognizes long polyinosinic-polycytidylic acid (poly(I:C)). In Muscovy ducks the MDA5 expression is similar to RIG-I expression (Brisse and Ly, 2019; Campbell and Magor, 2020; Lee et al., 2012). MDA5 expression has been detected during LPAIV and HPAIV infections in chickens as well as in Muscovy and Pekin ducks (Cornelissen et al., 2012; Cornelissen et al., 2013; Fleming-Canepa et al., 2019; Wei et al., 2014).

1.8.2 Toll-like receptors

Triggering of TLRs by PAMPs induces innate immune responses and leads to the induction of signaling pathways like NF-κB, type I IFN or mitogen-activated protein kinase. These activations lead to the production of pro-inflammatory cytokines/chemokines and type I IFNs (IFN-α expression) (Kaiser, 2010). Extra- and intracellularly expression of TLR is possible, e.g. on plasmacytoid dendritic cells (pDCs) (TLR7, 8, 9). The classification of TLR in birds differs from the classification in humans (Temperley et al., 2008). For mice, 13 TLR have been described, so far (Chuang et al., 2020). Chickens contain ten TLR, whereas only four TLR have been described in ducks. Interestingly, chickens contain

two TLRs (TLR15 and TLR21) which are not found in mammals, but were found in lower vertebrates. In mammals, TLR3, 7 and 8 recognize viral RNA and therefor are important in the defense against IAV. Chickens do not contain TLR8, 9 and 10, but TLR3 and 7 can detect IAV during infection in birds (for extensive review see (Chen et al., 2013; Diebold et al., 2004)). The tissue expression of TLR3, which upregulates the expression of type I IFN, varies between chickens, different duck breeds and mammals (Campbell and Magor, 2020; Pantin-Jackwood et al., 2013).

1.8.3 Type I, II and III Interferons

Interferons are inducible cytokines, which have antiviral activity and can be divided into three families (types I, II and III). Type I IFNs include IFN-alpha (α), -beta (β) as well as the less characterized IFN-epsilon (ε), -tau (τ), -kappa (κ), -delta (δ), -omega (ω) and -zeta (ζ) (also known as limitin) (Lazear et al., 2019; Oritani et al., 2000). So far, only IFN-α and IFN-β are well-characterized in birds and during viral infection, airway epithelium, macrophages and pDC are the primary site where type I IFN are produced (Campbell and Magor, 2020; Santhakumar et al., 2017). Type I IFNs act as immunomodulators of the adaptive immune system by activating e.g. natural killer cells (NK), dendritic cells and macrophages. Pekin ducks show a short but efficient type I IFN response during HPAIV H5N1 infection at 1 and 2 days post inoculation (dpi) (Saito et al., 2018). Type I IFN expression is dependent on the PRR localization. While TLR are responsible for IFN-α expression, RIG-I is in charge of IFN-β expression (Opitz et al., 2007). Type II IFN consist of IFN-gamma (γ), which is secreted by NK cells, $CD8^+$ lymphocytes and $CD4^+$ T helper cells and are present in birds as well (Schroder et al., 2004). Like type I IFN, type III IFN is predominantly expressed by immune and tissue specific cells, but its function and signaling is mainly restricted to mucosal epithelial cells. Chickens and ducks express only one type III IFN (IFN-lambda (λ)), whereas other vertebrates (e.g. humans) can produce up to four type III IFNs (IFN-λ1-4) (Santhakumar et al., 2017; Stanifer et al., 2019).

1.8.4 Interferon-stimulated genes

IFN-α and IFN-β are able to attach to type I IFN-receptor (IFNAR1/IFNAR2) which is present on most cells and induce a cascade (Janus kinases/signal transducer and activator of transcription proteins (JAK/STAT) signaling pathway) resulting in the induction of many interferon-stimulated genes (ISGs) which can interact with the viral components to suppress replication (Evseev and Magor, 2019; Nan et al., 2017; Weber-Gerlach and Weber, 2016b). IFN-λ is able to bind to IFNLR1/IL-10R2 receptor starting a cascade as well. Ducks can upregulate many different ISGs during HPAIV infections (for extensive review see (Campbell and Magor, 2020; Evseev and Magor, 2019; Stanifer et al., 2019)), while in mammals, more than one hundred ISGs can be upregulated (e.g. Mx, OAS, PKR, Viperin). HPAIV infections in humans, mice and birds can result in an overwhelming inflammatory immune response called “cytokine storm” (Evseev and Magor, 2019).

1.9 Infection of birds with H9N2 and H5N8 in Germany

1.9.1 Low pathogenic H9N2 avian influenza virus

H9N2 is an LPAIV and was first isolated from turkeys in Wisconsin, United States of America (USA) in 1966 (A/turkey/Wisconsin/1966) (Homme and Easterday, 1970; Peacock et al., 2019). After 1966, H9N2 was isolated from wild birds and domestic poultry in North America and has since been detected in different avian species in Europe, Africa, Asia and the Middle East. It is nowadays the most prevalent LPAIV worldwide and is endemic in poultry in many countries. To date, more than 60 human infections have been reported (Peacock et al., 2020; Pusch and Suarez, 2018). H9N2 viruses can donate internal protein coding-gene segments to other AIVs, e.g. H7N9 which infected over 1000 humans in China since 2013 (Pu et al., 2018). In addition, several studies have shown that several H9N2 isolates are able to bind both human-and avian-type SA receptors without prior adaptation in mammals (Li et al., 2014a; Peacock et al., 2020).

Little is known about H9N2 in poultry in Europe, although the virus has been frequently isolated from wild and domestic birds in the last 20 years (Peacock et al., 2019). H9N2 outbreaks, particularly in turkeys, have been reported in the United Kingdom (UK), the Netherlands, Romania, Russia, Poland, Hungary, Italy, France, Belgium and Ireland (Peacock et al., 2019; Reid et al., 2016; Swieton et al., 2018; Verhagen et al., 2017). Besides outbreaks in poultry, H9N2 has been detected in wild birds in Finland (Lindh et al., 2014) and Coman et al. (2013) reported serological evidence for H9N2 infections among agriculture workers in Romania. In Germany, H9N2 was isolated from chickens, turkeys and ducks in 1994-1996, 1998, 2004, 2012 - 2013 and 2015-2017 (Alexander, 2000; Parvin et al., 2020; Peacock et al., 2019). The isolates belonged to two genetic lineages designated Y439 and G1-W. To date, so far there is no recorded human case due to H9N2 infection in Germany.

1.9.2 Highly pathogenic H5N8 avian influenza virus

In 1996, in Guangdong (GD) province, China, a new H5N1 virus was isolated from domestic geese which established in a new lineage called goose/Guangdong (Gs/GD lineage). This virus acquired internal gene segments from H9N2 and H6N1 viruses after reassortment. It killed 6 out of 18 infected humans in Hong Kong in 1997. The virus evolved rapidly and therefore a classification system was adopted by the WHO/OIE/FAO H5N1 Evolution Working Group (Smith et al., 2015; World Health Organization/World Organisation for Animal and Agriculture Organization, 2014). Based on the sequence and phylogenetic analyses, the HA of H5N1 Gs/GD lineage is classified into clade 0 to clade 9, which are further divided into one, two, three and four order clades (e.g. clade 2.3.4.4) and sub-clades (e.g. 2.3.4.4A and 2.3.4.4B). H5N1 Gs/GD has undergone several reassortment events which resulted in H5N2, H5N3, H5N2, H5N5, H5N6, and H5N8 subtypes. These viruses caused unprecedented scale of outbreaks worldwide. Therefore, they are considered panzootic viruses (Lee et al., 2017). The HPAIV H5N1 (Gs/GD) was initially introduced into Europe in autumn and winter 2005/2006. H5N8 clade 2.3.4.4A reached Europe in autumn 2014 and the second wave of H5N8 clade 2.3.4.4B in 2016 (Globig et al., 2017; Harder et al., 2015; King et al., 2020a; Pohlmann et al., 2017; Zhong et al., 2014).

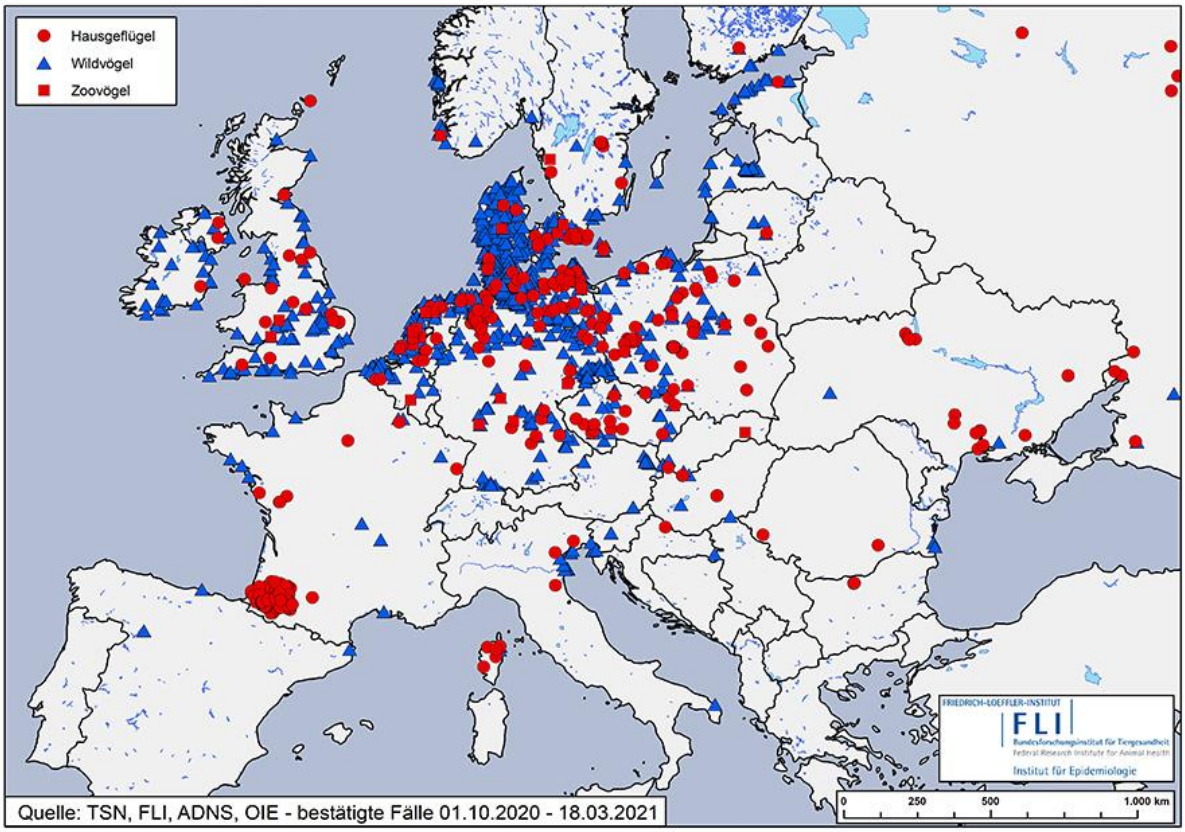

Figure 7: HPAIV H5 cases in European domestic (red dot), wild (blue triangle) and zoo birds (red square). (https://www.fli.de/de/aktuelles/tierseuchengeschehen/aviaere-influenza-ai-gefluegelpest/karten-zur-klassischen-gefluegelpest/; 23.03.2021, 10:20 Uhr).

In Germany, the outbreak of H5N8 clade 2.3.4.4A in 2014 was limited. It affected a 31,000 meat-turkey flock in Heinrichswalde, Mecklenburg Western Pomerania (Harder et al., 2015). The farm was closely located to Lake Galenbeck (1,3 km distance), which is a frequent home for wild birds. The first report of HPAIV H5N8 clade 2.3.4.4B in Germany was on November 7th in 2016 in Tufted ducks (*Aythya fuligula*) at Lake Constance in Baden-Wuerttemberg (southwest Germany), shortly after reports of an increased mortality of tufted ducks in Hungary and Poland. On November 8th, many Tufted ducks were found dead at lake Ploen in Schleswig-Holstein (northern Germany) (Pohlmann et al., 2017). Thereafter, HPAIV H5N8 clade 2.3.4.4B caused lethal infections in hundreds of wild and domestic birds in Germany and Europe. More than 1150 cases of HPAIV H5Nx clade 2.3.4.4B were reported in Germany from November 8th 2016 until September 30st 2017. A total of 107 outbreaks were reported in 15 zoos or animal parks in Germany, where birds were kept in captivity. So far, this HPAIV epidemic was the most severe epidemic recorded in Germany (Globig et al., 2017). In January and February 2020, a novel HPAIV clade 2.3.4.4B H5N8 virus occurred in wild and domestic birds in Germany and other European countries (King et al., 2020a; King et al., 2020b).

Since October 2020, about 1200 HPAIV H5 cases were reported in wild birds, poultry and captive birds in all federal states of Germany except of Saarland (Figure 7) (FLI, 2021a, b). H5N8 was identified in

all reported cases, while HPAIV H5N5 was detected in one case only. Epidemiological data indicated that HPAIV H5 spread from northern Germany in Schleswig-Holstein and Mecklenburg Western Pomerania to the southern states (FLI, 2020). Turkeys and chickens are the most affected poultry species in Germany, in addition to captive birds like ducks and geese. A wide range of wild bird species were affected including Barnacle goose (*Branta leucopsis*), Eurasian wigeon (*Mareca Penelope*), gulls, owls, peregrine falcon (*Falco peregrinus*), white-tailed eagle (*Haliaeetus albicilla*) and the Eurasian eagle-owl (*Bubo bubo*). Furthermore, more than 16000 dead or moribund waders and aquatic birds were found in the area of the Wadden Sea coast in Schleswig-Holstein and more than 1.6 million birds are affected since the beginning of the 2020/2021 epidemic. Besides Germany, more than 650 outbreaks were reported in 25 European countries, especially along the coasts of the Netherlands, United Kingdom (UK), Ireland, Denmark, Belgium, Sweden, Norway, Finland, Lithuania, Latvia and Estonia resulting in losses of millions of animals. Since February 2021, the infection was mostly reported in swans and geese and the virus spread to Czech Republic, Austria, Switzerland, Hungary, Bulgaria and Romania. This epidemic is still ongoing and is more severe and widespread than the 2016/2017 epidemic (OIE, 2021). Importantly, UK reported HPAIV H5N8 in a fox (*Vulpes Vulpes*), four harbour seals (*Phoca vitulina*) and one grey seal (*Halichoerus grypus*). Recently, seven asymptomatically-infected poultry farm workers in Russia were identified during stamping-out of H5N8-infected chickens (EFSA, 2021; OIE, 2021).

2 Aim

Avian influenza viruses evolve rapidly through mutations, reassortment and/or recombination of the virus genome. They infect a wide range of host species and the infection ranges from asymptomatic to sudden death. Viral factors that contribute to the adaptation and virulence of AIV vary among bird species as well as in mammals. Due to the tremendous economic losses in poultry and the continuous threat to public health, it is highly important to study the genetic determinants for adaptation and virulence of AIV in poultry and assess their zoonotic potential. In this dissertation we focused on two widely spread zoonotic AIV, H9N2 and H5N8.

H9N2 infected humans and donated gene segments to other AIV (e.g. H5N1, H7N9), which caused fatal infections in humans. It is the most widespread LPAIV in chickens and turkeys worldwide and has been frequently reported in birds in Europe including Germany since 2012. Little is known about the genetic signatures in the European H9N2 compared to non-European viruses, particularly mutations in the hemagglutinin cleavage site, a major virulence determinant of HPAIV in chickens. No data is available on the impact of these signatures on virus fitness *in vitro* and *in vivo* in gallinaceous birds or replication efficiency in mammalian cells.

Furthermore, the panzootic H5N8 clade 2.3.4.4 viruses caused severe losses in poultry in several countries worldwide, including Germany. The clade B infection 2020/2021 was the largest known AIV epidemic in birds in Germany and therefore there is a risk for reassortment with co-circulating with the semi-endemic H9N2. It is not known whether reassortment between German H9N2 and H5N8 can change the virus fitness in birds and mammals, which is important for zoonotic risk assessment. Moreover, while H5N8 clade A virus was avirulent in Pekin ducks, clade B virus was highly virulent. Viral markers, particularly in NS1, which contribute to high virulence of clade B virus in ducks are largely unknown. Therefore, work in this dissertation tried to answer the following questions:

(I) Do non-basic amino acids in the HACS of German H9N2 viruses have an effect on virulence in chickens and turkeys or replication in mammalian cells *in vitro*?

(II) Is reassortment between German H9N2 and H5N8 clade 2.3.4.4 viruses possible and what are the biological propensities of H5N8-H9N2 reassortants in poultry and mammals?

(III) Does the unique variation in the C-terminal domain of NS1 of H5N8 clade 2.3.4.4 viruses affect virulence in chickens, ducks or mice?

3 Publications

(I) Non-basic amino acids in the hemagglutinin proteolytic cleavage site of a European H9N2 avian influenza virus modulate virulence in turkeys

Claudia Blaurock, David Scheibner, Maria Landmann, Melina Vallbracht, Reiner Ulrich, Eva Böttcher-Friebertshäuser, Thomas C. Mettenleiter & Elsayed M. Abdelwhab

Scientific reports

Sci Rep 10, 21226 (2020)

doi: 10.1038/s41598-020-78210-8

scientific reports

Check for updates

OPEN

Non-basic amino acids in the hemagglutinin proteolytic cleavage site of a European H9N2 avian influenza virus modulate virulence in turkeys

Claudia Blaurock[1], David Scheibner[1], Maria Landmann[2], Melina Vallbracht[1], Reiner Ulrich[2], Eva Böttcher-Friebertshäuser[3], Thomas C. Mettenleiter[1] & Elsayed M. Abdelwhab[1]✉

H9N2 avian influenza virus (AIV) is the most widespread low pathogenic (LP) AIV in poultry and poses a serious zoonotic risk. Vaccination is used extensively to mitigate the economic impact of the virus. However, mutations were acquired after long-term circulation of H9N2 virus in poultry, particularly in the hemagglutinin (HA) proteolytic cleavage site (CS), a main virulence determinant of AIV. Compared to chickens, little is known about the genetic determinants for adaptation of H9N2 AIV to turkeys. Here, we describe 36 different CS motifs in Eurasian H9N2 viruses identified from 1966 to 2019. The European H9N2 viruses specify unique HACS with particular polymorphism by insertion of non-basic amino acids at position 319. Recombinant viruses carrying single HACS mutations resembling field viruses were constructed (designated G319, A319, N319, S319, D319 and K319). Several viruses replicated to significantly higher titers in turkey cells than in chicken cells. Serine proteases were more efficient than trypsin to support multicycle replication in mammalian cells. Mutations affected cell-to-cell spread and pH-dependent HA fusion activity. In contrast to chickens, mutations in the HACS modulated clinical signs in inoculated and co-housed turkeys. G319 exhibited the lowest virulence, however, it replicated to significantly higher titers in contact-turkeys and in vitro. Interestingly, H9N2 viruses, particularly G319, replicated in brain cells of turkeys and to a lesser extent in mammalian brain cells independent of trypsin. Therefore, the silent circulation of potentially zoonotic H9N2 viruses in poultry should be monitored carefully. These results are important for understanding the adaptation of H9N2 in poultry and replication in mammalian cells.

Avian influenza viruses (AIV) belong to genus Influenza A Virus (IAV) in the family *Orthomyxoviridae*. AIV are enveloped viruses with a segmented single-strand RNA genome of negative polarity. The genome is composed of eight gene segments (PB2, PB1, PA, HA, NP, NA, M, and NS) which encode more than 11 viral proteins[1]. According to the different antigenic properties of the two surface glycoproteins hemagglutinin (HA) and neuraminidase (NA), AIV are classified into 16 HA (H1—H16) and 9 NA (N1 – N9) subtypes. Each virus contains one HA and one NA subtype with possible 144 HxNy combinations[2]. Wild birds are the natural reservoir for all AIV subtypes and domestic birds acquire AIV infection after direct or indirect contact with wild birds. In poultry, H1-H16 subtypes are low pathogenic (LP), while H5 and H7 subtypes can become highly pathogenic (HP) to cause up to 100% mortality. Therefore, preventive culling of H5 and H7 infected poultry is recommended by the World Organization for Animal Health (OIE)[3]. The HA plays an important role in virus virulence and interspecies transmission[4–6]. Activation of HA by proteolytic cleavage into HA1 and HA2 subunits is important for exposing the HA2-fusion peptide, which mediates pH-dependent merge of viral and host cell membranes and subsequently the release of viral RNA into the host cell[7,8]. The HA cleavage site motifs (CS) of HPAIV specify a stretch of basic amino acids (aa) which comply with the minimum polybasic motif required for the

[1]Friedrich-Loeffler-Institut, Federal Research Institute for Animal Health, Südufer 10, 17493 Greifswald-Insel Riems, Germany. [2]Institute of Veterinary Pathology, Faculty of Veterinary Medicine, Leipzig University, An den Tierkliniken 33, 04103 Leipzig, Germany. [3]Institute of Virology, Philipps University Marburg, Hans-Meerwein-Straße 2, 35043 Marburg, Germany. ✉email: Sayed.abdel-whab@fli.de

cleavage by ubiquitous furin-like enzymes (R-X-K/R-R)[9]. LPAIV possess monobasic HACS, which is activated by trypsin-like enzymes (e.g. trypsin, airway-trypsin like enzymes, transmembrane serine proteases "TMPRSS") which are restricted to the respiratory and digestive tracts[10,11]. Therefore, replication of LPAIV is usually limited, and morbidity and mortality are reduced compared to the HPAIV which cause systemic infections resulting in multiple organ failure and up to 100% mortality[3].

H9N2 viruses are the most widespread AIV in poultry worldwide. They infect a wide range of birds and mammals including humans[12,13]. In birds, the virus is endemic in many countries and a number of genetic lineages are established (e.g. G1, Y280, Korean lineages)[14]. H9N2 are classified as LPAIV and some H9N2 viruses are poorly adapted to poultry, however, they may cause severe morbidity and considerable mortality in chickens even without concomitant bacterial or viral co-infections[15–17]. Although chickens and turkeys belong to Galliformes, turkeys are generally more vulnerable to AIV-induced morbidity and mortality than chickens[3]. Compared to mammals[18,19], genetic determinants for adaptation of H9N2 in both species are not well understood. In chickens, mutations in the HA head domain of Asian-H9N2 contributed to efficient virus transmission[20] and insertion of basic aa in the HACS increased pathogenicity of some strains[21,22]. In turkeys, molecular markers for the adaptation of H9N2 are not known.

In Europe, H9N2 outbreaks, particularly in turkeys, have been reported from Poland, UK and the Netherlands[23–25]. In Germany, recurrent outbreaks caused by Korean-like H9N2 lineage have been increasingly observed since 2012 mainly in turkeys, and autogenous vaccines have been used in some regions[26,27]. In this study, polymorphism in the HACS was determined after analysis of the HA sequences of European and non-European H9N2 viruses. Recombinant viruses were constructed and the impact of these mutations on virus fitness in vivo and in vitro in turkeys and chickens was studied.

Materials and methods

Sequence analysis. All HA protein sequences of European and non-European H9N2 viruses were retrieved from GenBank and GISAID until 21–01-2020. Sequences of laboratory adapted viruses and those with ambiguous amino acid sequences were deleted. The remaining sequences were aligned using Multiple Alignment using Fast Fourier Transform (MAFFT)[28] and further analyzed using Geneious Prime. The polymorphism in position 4 (P4) to position 1 (P1) in the cleavage site (positions 317 – 320 H9 HA numbering after removal of the signal peptide sequence) was determined.

Cells, viruses and plasmids. Human-embryonic kidney 293 T cells (HEK-293 T), Madin-Darby canine kidney cells (MDCK), MDCK type II (MDCKII) cells, bat brain cells (FLG-R, CVCL_0I97) cat brain cells (CEB1-R), warthog brain cells (PHA-B-1-R) and mouse brain cells (MDIG-1-R) were obtained from the cell-culture collection at the Veterinary Medicine of Friedrich-Loeffler-Institut (FLI), Germany. MDCK-HAT and MDCK-TMPRSS2 cells have been previously described[29]. Primary chicken embryo kidney (CEK) cells were prepared from 18–19 day-old chicken embryos and primary turkey embryo kidney (TEK) cells from 23 day-old turkey embryos[30]. Turkey embryo brain (TEB) cells were prepared from 23 day-old turkey embryos according to the standard protocols[30]. A/turkey/Germany/AR1685/2016 (H9N2) (GISAID ID: 486,439) (designated hereafter as K319) was obtained from the repository of FLI kindly provided by Timm C. Harder. All plasmids of K319 were cloned in a previous project (Mostafa et al. submitted) as previously published[31]. pCAGGS-expression plasmid was kindly provided by Stefan Finke. Cloning of the HA gene into pCAGGS was done after amplification of the HA genes from pHW-HA plasmids using specific primers containing XhoI and ClaI restriction sites (available upon request). Green fluorescence protein (GFP) pcDNA-expression plasmid was kindly provided by Barbara Klupp.

Generation of recombinant viruses. The HA of K319 virus was modified using QuikChange II XL Site-Directed Mutagenesis Kit (Agilent Technologies, USA). Primers used for mutagenesis are available upon request. Mutagenesis reactions were treated with 10 U/µl DpnI for one hour at 37 °C. Transformation of XL Gold ultracompetent cells was performed according to the manufacturer's instructions (Agilent Technologies, USA) and 400 µl were plated on Luria–Bertani (LB)-agar (Invitrogen, USA) supplemented with ampicillin (Roth, Germany) overnight at 37 °C. Colonies were inoculated in LB broth supplemented with ampicillin and incubated overnight in a shaker at 37 °C/300 rpm. Plasmids were extracted by QIAprep Plasmid Kits (Qiagen, Germany) and the concentration was adjusted to 1 µg/µl. Viruses were rescued in HEK293T and MDCKII co-culture using Lipofectamine 2000 and OptiMEM (Gibco, USA) as previously described[32]. Supernatants of transfected cells were inoculated into 9–11 day-old specific pathogen free (SPF) embryonated chicken eggs (ECEs) (VALO BioMedia GmbH, Germany). Eggs were examined daily for embryo activity for 5 days post-inoculation (dpi) and chilled at 4—8 °C for 1—2 days. Then, the allantoic fluid was collected under sterile conditions from each inoculated egg and the hemagglutination titer was determined using hemagglutination (HA) test according to the standard protocol[33]. Sterile allantoic fluids (after plating on sheep blood agar) with HA titer > 16 were pooled together and aliquots were stored at—70 °C until use. Virus titration of working stocks was determined by plaque test as described below. Furthermore, unwanted mutations were excluded by sequencing of plasmids and virus stocks. Sequences of all viruses in this study were generated after amplification of all gene segments using One-Step RT-PCR kit (Qiagen, Germany) and universal primers[31] or internal primers (available upon request). Amplicons were extracted in 1% (w/v) agarose (Biozym Scientific GmbH, Germany) gels using QIAquick Gel Extraction Kit (Qiagen, Germany). Purified gene products were subjected for Sanger sequencing by an ABI BigDye Terminator v.1.1 Cycle Sequencing Kit (Applied Biosystems, Germany). Nucleotide and deduced aa sequences were analyzed using Geneious Prime.

Replication kinetics in different cell lines. The replication of recombinant viruses in primary CEK and TEK cells as well as indicated cell lines was compared using a multiplicity of infection (MOI) of 0.001. Viruses were incubated with the indicated cells in 12-well plates at 37 °C and 5% CO_2 for 1 h (h). The virus inoculum was removed and cells were treated with citrate buffered (pH 3.0) saline (CBS) for 2 min (min) to inactivate extracellular virions. Afterwards, cells were washed twice with phosphate buffer saline (PBS). Finally, cells (except MDCK-HAT and MDCK-TMPRSS2) were covered with minimal essential medium (MEM) containing 2.8% bovine serum albumin (BSA) (MP Biomedicals, USA) and with or without 2 µg/mL TPCK-treated trypsin (Sigma-Aldrich, USA) and incubated at 37 °C and 5% CO_2. MDCK-HAT and MDCK-TMPRSS2 were covered with MEM containing BSA and 0.2 µg/ml Doxycycline (Sigma-Aldrich, USA) as described[29]. Cells were harvested at the indicated time points and stored at − 70 °C until use. The replication kinetics were conducted in duplicates and repeated two times for each type of cells. Virus progeny was titrated by plaque test as described below. The results are expressed as mean and standard deviation of all replicates as log_{10} plaque forming unit per ml (Log_{10} pfu/ml).

Plaque test. Virus titration was done in MDCKII cells in 12-well plates using standard plaque assay. Briefly, viruses were ten-fold serial diluted in MEM. Confluent cells were infected for 1 h with virus dilutions at 37 °C and 5% CO_2. The extracellular viruses were adsorbed and cells were washed twice with PBS. Cells were covered by semi-solid agar (Bacto Agar; BD, France) containing MEM, 2 µg/ml TPCK-trypsin and 4% BSA (MP Biomedicals, USA). Plates were incubated at 37 °C and 5% CO_2 for 3 days, cells were fixed with 10% formaldehyde containing 0.1% crystal violet and were incubated at room temperature (rt) for at least 24 h. Virus titration was performed in duplicates. Virus titers were calculated after counting the number of plaques multiplied by the reciprocal of virus dilution. The final titers were calculated and expressed as Log_{10} pfu/ml. Cell-to-cell spread was determined by measuring the diameter of 100 plaques of each virus using Nikon NIS-Elements imaging software (Nikon, Düsseldorf, Germany). Plaque diameter is shown as mean and standard deviation.

Western Blot. The impact of trypsin, HAT or TMPRSS2 on HA cleavability was investigated using standard Western Blot procedures. CEK cells were transfected with 5 µg of the different HA-pCAGGS plasmids using Lipofectamine 2000 and OptiMEM for 24 h. Moreover, CEK cells were cotransfected with 2 µg pCAGGS-HA-plasmid and 500 ng TMPRSS2 plasmid, incubated for 24 h and harvested as described below. Furthermore, MDCK-HAT cells were infected with the six different viruses using a MOI of 0.1 for 24 h at 37 °C. At 24 h post transfection or post-infection, cells and supernatant were harvested and subjected for two cycles of centrifugation at 13,000 rpm for 10 min and washing of the pellets with 1 × PBS. Finally, pellets were solved in PBS and Laemmli buffer (Serva, Germany). The samples were heated for 5 min at 95 °C, then stored at -20 °C or directly used for detection of viral proteins in 12% Sodium Dodecyl Sulfate Polyacrylamide Gel Electrophoresis (SDS-PAGE). Briefly, 20 µl of each sample was transferred to a polyacrylamide gel to separate proteins with a molecular mass between 10 and 100 kDa. An electrophoresis chamber (BioRad, Germany) was filled with 1 × SDS-PAGE-buffer (10xPAGE Buffer: 0.25 M Tris, 2 M Glycin, 1% SDS), protein solutions containing SDS-sample buffer were loaded onto the gel and separated at 200 V for 45—60 min. Size of the indicated proteins was assessed against PageRuler protein ladder (Thermo Fisher, USA). Binding of viral proteins to a polyvinylidene fluoride membrane (PVDF) (GE Healthcare Life science, Germany) was done after electrotransfer at 20 V for 90 min per blot. After blocking the membrane with 5% skim milk in 1 × Tris-buffer-saline 2.5% containing 0.25% Tween20 (TBS-T) (Applichem GmbH, Germany) for 1 h at rt on a rocking platform. Serum of an infected turkey (1:100) in the current study was incubated with each membrane overnight at 4 °C. Membranes were washed by 1 × TBS-T and incubated with TBS-T containing peroxidase-labelled secondary anti-turkey antibodies (1:20,000) for 60 min at rt. Visualization of viral proteins was done by chemiluminescence using Clarity Western ECL Substrate (BioRad, Germany) Kit. Images were captured by Bio-Rad Versadoc 4000 Molecular Imager (BioRad, Germany) and Quantity One software (BioRad, Germany).

Syncytium formation assay. Monolayers of CEK cells in a 24-well-plate were transiently transfected with 100 ng of GFP-pcDNA plasmid and 600 ng of the different pCAGGS-HA-plasmids using Lipofectamine 2000 and OptiMEM as previously done[34]. After 210 min of incubation at 37 °C, OptiMEM was exchanged to 1 ml MEM with 5% fetal calf serum (FCS) (Biowest, Germany). The transfected cells were incubated for 16 h at 37 °C. Cells were treated with 0.05% trypsin for 10 min at rt and incubated for 15 min at 37 °C with 1 ml MEM containing Earle's balanced salts and 10% FCS. To induce membrane fusion, cells were incubated with 1 ml of PBS which was adjusted to pH 4.0, 4.2, 4.4, 4.6, 4.8, 5.0, 5.2, 5.2, 5.4, 5.6, 5.8 or 6.0 with HCl, for 4 min at rt. Cells were washed twice with 1xPBS and were then incubated with MEM containing 10% FCS for 4 h and finally fixed with 4% PFA. The number and the area of green-fluorescing syncytia with three or more nuclei within 10 fields of view (5.5 mm^2 each) using an Eclipse Ti-S Fluorescence microscope and the NIS-Elements software (Nikon) as described[34]. The area of syncytia was divided by the number of syncytia to determine the average syncytia area. The larger the average area of syncytia, the higher the fusion activity.

Animal experiment

Ethical statement. The animal experiments were carried out in the experimental animal facilities of the FLI, Germany following the German Regulations for Animal Welfare. All experiments were approved by the authorized ethics committee of the State Office of Agriculture, Food Safety, and Fishery in Mecklenburg – Western Pomerania (LALLF M-V; permission number 7221.3–1.1–051-12) and the commissioner for animal welfare at the FLI representing the Institutional Animal Care and Use Committee (IACUCs).

Experimental design. SPF ECE were incubated in the hatchery facilities at the FLI for 21 days and one-day old turkeys were purchased from commercial source. The turkey poults were tested to exclude bacterial (i.e. Salmonella, E.coli, ORT), viral (i.e. AIV, NDV, TRT) and protozoal (i.e. Coccidia) infections. All birds received water and feed ad-libitum. Six week-old chickens or turkeys were allocated to different groups of 15 birds each in separate animal rooms. Ten birds were inoculated with each recombinant virus oculonasally (ON) with $10^{5.7}$pfu/bird. At 1 day post inoculation (dpi), 5 sentinel chickens or turkeys were added to assess chicken-to-chicken or turkey-to-turkey transmission. Furthermore, 10 chickens were intravenously (IV) inoculated with selected viruses to determine the intravenous pathogenicity index (IVPI). A negative control group was left un-inoculated. All birds were observed daily for 10 days. Oropharyngeal (OR) and cloacal (CL) swabs were collected at 4 dpi using serum-free MEM containing antibiotics (in 1 L: 5.6 ml BSA, 1% enrofloxacin (Bayer, Germany), 0.5% lincomycin (WDT, Germany), 0.1% gentamycin (aniMedica GmbH, Germany). Swabs were frozen at −70 °C until use. At 4 dpi, 3 birds per group were slaughtered and organ samples from nare, trachea, lung, airsac, pancreas, duodenum, kidney, thymus, bursa and brain were used for virus titration and/or histopathological examination. At the end of the experiment, all birds were humanely killed under deep anesthesia using Isoflurane (CP-Pharma, Germany).

Detection of viral RNA. RNA was extracted from swabs and organ samples using NucleoMagVet 8/96 PCR Clean-up Core Kit (Macherey & Nagel GmbH, Germany) in KingFisher Flex Purification System (Thermo Fisher Scientific, USA). The amount of viral RNA was determined in different samples using SuperScript III Platinum One-Step qRT-PCR Kit (Invitrogen, Germany). A generic quantitative real-time polymerase chain reaction (RT-qPCR) targeting partial AIV-M gene sequence[35] was performed in AriaMx Real-time PCR System (Agilent, Germany). Standard curves were run in each RT-qPCR plate using ten-fold serial dilutions of K319 virus (10^{1} to 10^{5} pfu/ml). The relative amount of viral RNA was quantified by plotting the Ct-values in the standard curves and results are expressed as mean and standard deviation (equivalent Log_{10} pfu/ml). Moreover, selected samples were inoculated in SPF ECE for virus isolation as recommended[36]. Furthermore, virus excreted in oropharyngeal (OR) and cloacal (CL) swabs from inoculated and contact birds was subjected for Sanger sequencing.

Seroconversion. Blood samples were collected at the end of the animal experiment from all chickens and turkeys, and serum was separated after 24 h incubation in the fridge. Sera were tested for anti-AIV nucleoprotein (NP) using enzyme-linked immunosorbent assay (ELISA) by ID screen Influenza A Antibody Competition Multispecies kit (IDvet, France) and plates were read using Tecan ELISA reader. According to the manufacture guideline samples below 45% were considered negative.

Histopathology and immunohistochemistry. Histopathological lesions and distribution of AIV matrixprotein (MP) antigen in different organs were studied by histopathological and immunohistochemical (IHC) techniques. Samples were embedded in paraffin wax and sectioned at 2 – 4 µm. For histopathological examination, slides were stained with hematoxylin and eosin and the severity of lesions was determined using an ordinal scale: 0 = no; 1 = mild; 2 = moderate, and 3 = severe necrosis and/or necrotizing inflammation. Furthermore, for immunohistochemical examination slides were stained using the avidin–biotin–peroxidase complex method (Vectastain PK 6100, Vector Laboratories Burlingame, USA) with citric buffer pretreatment, a primary monoclonal mouse anti-MP antibody (M1Hb-64, 1:100), and a secondary biotinylated anti-mouse IgG (BA 9200, Vector Laboratories Burlingame, USA) antibody (1:200) in IHC as described[37]. The distribution of parenchymal and endothelial MP antigen in different organs was semi-quantitatively scored, each on an ordinal scale: 0 = negative; 1 = focal or oligofocal, 2 = multifocal, and 3 = coalescing to diffuse antigen.

Statistics. Data were analyzed using GraphPad Prism version 8.1.0 and differences were considered significant at a p value of $p < 0.05$. Plaque diameter was analyzed with Kruskal–Wallis with Dunn's test. Replication kinetics in different cell lines were analyzed using one-way ANOVA with post hoc Tukey tests and Kruskal–Wallis with Dunn's test. Viral shedding in oral swabs at 4 dpi were compared using Mann–Whitney Wilcoxon test. Results were considered significant when p value in both tests were < 0.05.

Results

European H9N2 viruses specify unique HACS motifs, mostly due to substitutions of non-basic amino acids. Polymorphism in the cleavage sites (Fig. 1A,B) from position P4 to position P1 (residue 317 to 320 in H9 numbering) in European (n = 82) and non-European (n = 2926) H9N2 viruses from 1966 to 2019 were analyzed (Fig. 1C,D; Table 1, Supplementary Table S1). Sequences of the European viruses represent 21 turkey, 15 chicken and 46 wild bird isolates. In total, 36 different HACS motifs were identified (P4-P1 only). The European viruses had 12 different motifs and the non-European viruses exhibited 32 different HACS motifs (Table 1). Four HACS motifs were observed only in the European and 24 only in the non-European viruses (Table 1). While the majority of non-European H9N2 possessed RSSR/G (81.5%), KSSR/G (5.9%) or KSKR/G (3.3%) in the HACS, the European viruses specified different motifs due to accumulation of non-basic aa including ASDR/G (47.6%), ASNR/G (13.4%), ASAR/G (7.3%) or RSSR/G (11.0%). Only 4 out of 36 HACS motifs (motifs #6, 7, 27 and 35) contain dibasic or multibasic HACS. Motif #6 (AS**KR**/G) was seen in 4 European H9N2 sequences and motif #7 (**RSKR**/G) in 1 and 6 European and non-European H9N2 sequences, respectively. Moreover, the non-European viruses have variations in all four positions. Conversely, serine (S) in P3 and arginine (R) in P1 in the European viruses were highly conserved (100%), while P4 and P2 specified 5 (A, I, R, T, V)

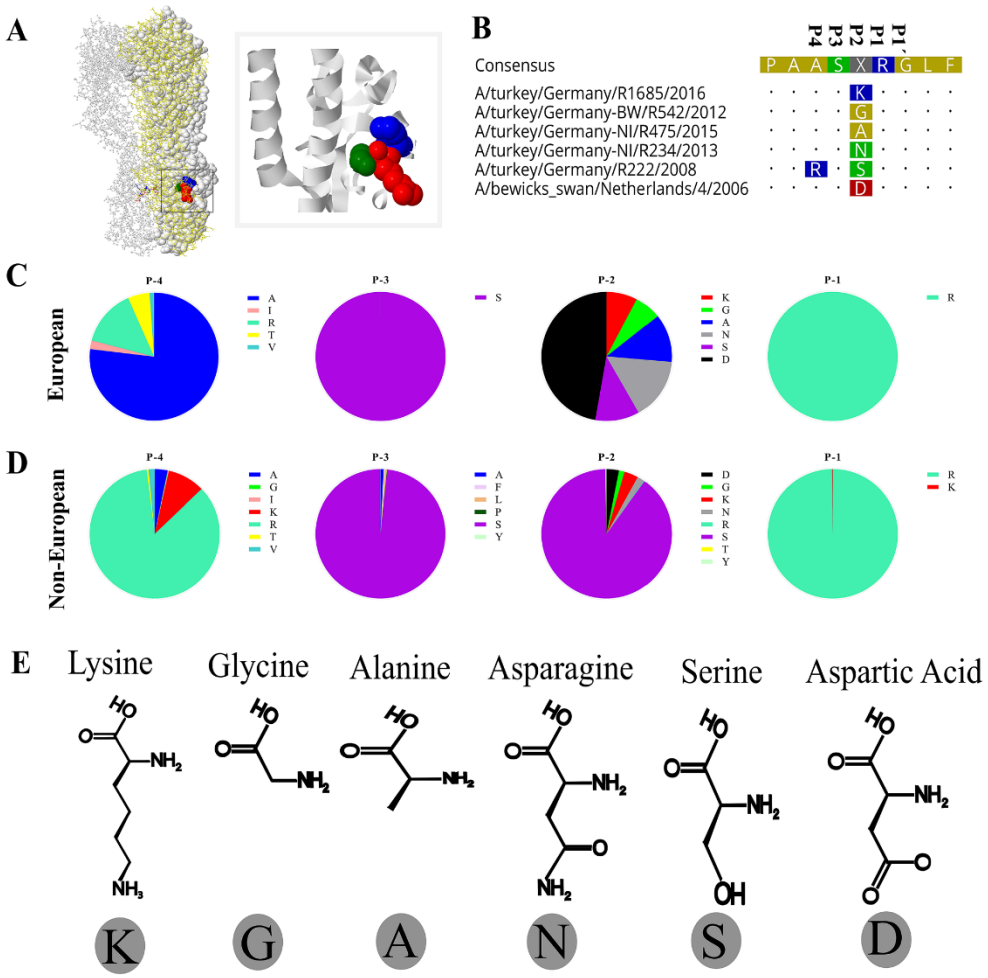

Figure 1. Polymorphism in the hemagglutinin cleavage site (HACS) of European and non-European H9N2 sequences. The 3D structure of H9N2-K319 HA trimer showing P2 (residue 319) in blue, arginine in P1 (red) and glycine in P1′(green) was generated by SWISS-Model and further edited by Geneious (**A**). Alignment of the cleavage site of representative European viruses showing polymorphism (K, G, A, N, S, D) in position P2 (**B**). Prevalence of polymorphism in the HACS of European H9N2 (n = 82) (**C**) and Non-European H9N2 (n = 2926) (**D**) in H9N2-HA sequences retrieved from GISAID and GenBank on 20–01-2020. All sequences specifying S contains R in position P4. Positions P1 and P3 are highly conserved, while position P2 was more variable than P4, particularly in the European-H9N2 sequences (C-D). Structure and size of amino acids in position P2 are shown (**E**).

and 6 (G, A, N, S, D, K) different aa, respectively (Fig. 1B). At P2, the European viruses had G (6.1%), A (7.3%), N (15.9%), S (11.0%), D (50.0%) or K (9.8%), while the prevalence rate of these aa in non-European viruses was 1.4, 0.0, 1.7, 89.7, 3.1 and 3.5%, respectively. These results indicate that the HACS sequences of European H9N2 viruses differ from the non-European viruses. While serine at P2 dominated the non-European H9N2, the European H9N2 viruses had relatively comparable prevalence of G, A, N, S and K (6.1 to 15.9%), while D had a prevalence of 50.0%. G is the smallest and K is the largest aa (Fig. 1E). Since mutation (i.e. to tyrosine (Y)) at P2 affected cleavability of non-European H9N2 viruses in cell culture[38] and replication of WSN/H1N1 in the brain of mice[39], we decided to study the impact of non-basic aa in P2 (hereafter referred to 319) in the European H9N2 viruses in vitro and in vivo.

		European H9N2 (total 91)		Non-European H9N2 (total 2926)	
	Motif (P1/P1´)	No	%	No	%
1	ASGR/G	2	2.4	13	0.4
2	ASAR/G	6	7.3	0	0.0
3	ASNR/G	11	13.4	3	0.1
4	RSSR/G	9	11.0	2384	81.5
5	ASDR/G	39	47.6	70	2.4
6	ASKR/G	4	4.9	0	0.0
7	RSKR/G	3	3.7	6	0.2
8	VSDR/G	1	1.2	20	0.7
9	TSNR/G	2	2.4	0	0.0
10	TSGR/G	3	3.7	16	0.5
11	ISGR/G	1	1.2	2	0.1
12	ISDR/G	1	1.2	0	0.0
13	RSGR/G			3	0.1
14	RSNR/G			35	1.2
15	ASDK/G			1	0.0
16	VSNR/G			7	0.2
17	VSGR/G			7	0.2
18	VSSR/G			9	0.3
19	ASYR/G			7	0.2
20	ISNR/G			3	0.1
21	KSSR/G			172	5.9
22	ISSR/G			1	0.0
23	KASR/G			2	0.1
24	RYSR/G			2	0.1
25	RASR/G			21	0.7
26	RLSR/G			13	0.4
27	RSRR/G			7	0.2
28	GSSR/G			3	0.1
29	RPSR/G			2	0.1
30	RFSR/G			9	0.3
31	RSTR/G			2	0.1
32	RSSK/G			4	0.1
33	RCSR/G			1	0.0
34	RSIR/G			1	0.0
35	KSKR/G			96	3.3
36	RSNK/G			1	0.0
	Total	82	100.0	2926*	100.0

Table 1. Cleavage site motifs of European and Non-European H9N2 viruses from 1966 to 2019. A total of 2926 non-European viruses were retrieved from GISAID and GenBank on 21–01-2020. Three sequences from chickens (2 from Iran in 2007 and 1 from Egypt in 2013) had RSNR/**R**, RSNK/**R** and KSSR/**A** motifs assuming wrong or unusual sequences in the HA2 (i.e. underlined R or A). Only motifs No. 6, 7, 27 and 35 (highlighted in grey) encode dibasic or multibasic HACS. Using reverse genetics, we generated six recombinant viruses with polymorphism at position P2 resembling the first 6 motifs (no. 1 to 6).

Generation of six recombinant viruses with variable HACS motifs. To get an insight into the impact of non-basic aa variation at P2, six recombinant viruses were generated. In addition to the wild type K319 virus, five mutants carrying G, A, N, S or D at position 319 (designated G319, A319, N319, S319 and D319, respectively), resembling the field viruses (Fig. 1C), were rescued. Viruses were propagated in SPF ECE and the virus titers ranged from $10^{5.7}$ (G319) to $10^{6.2}$ (S319) pfu/ml (data not shown).

Variable replication of recombinant viruses in primary turkey and chicken cells in the presence or absence of trypsin. Replication of the recombinant viruses was studied in TEK and CEK in the presence and absence of trypsin for 1, 8, 24, 48 and 72 hpi, and virus titers were determined by plaque test in MDCKII cells (Fig. 2A–D). In TEK cells, in the presence of trypsin, the peak of virus replication was reached 24 hpi, except for K319 at 48 hpi. G319 replicated at significantly lower levels than S319 at 8 hpi ($p < 0.002$), while G319 and

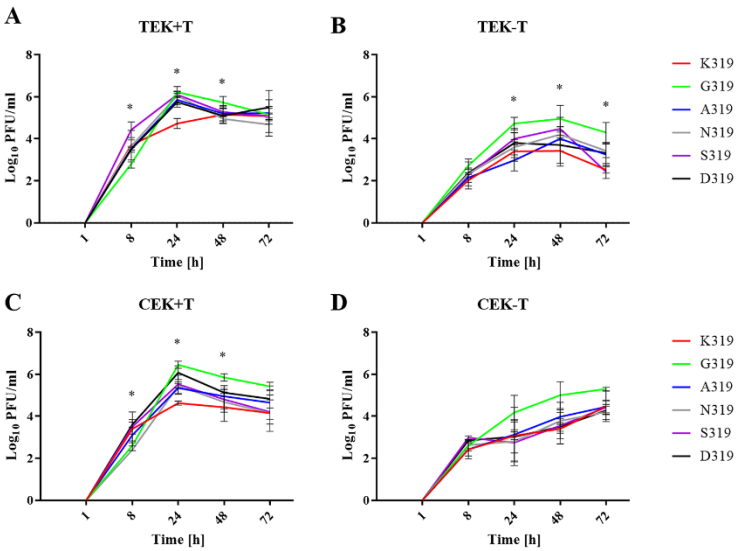

Figure 2. Virus replication in cell culture in the presence or absence of trypsin. Shown are the replication kinetics of the recombinant viruses 1, 8, 24, 48 and 72 h post inoculation (hpi) at an MOI of 0.001 in turkey embryo kidney (TEK) cells (**A**,**B**) and chicken embryo kidney (CEK) cells (**C**,**D**) with (+T) and without trypsin (-T). Titers are expressed as PFU/ml and are shown as the mean and the standard deviation. The kinetics were done twice in duplicates for each cell types and data were analyzed using one-way ANOVA with post hoc Tukey tests and Kruskal–Wallis with Dunn's test. The results were considered significant when p value in both tests were < 0.05 as indicated by asterisk and explained in the main text.

S319 replicated at higher levels than K319 at 24 hpi ($p < 0.04$). At 48 hpi, G319 replicated at higher levels than N319 ($p < 0.04$) and all viruses replicated at similar levels at 72 hpi (Fig. 2A). Without trypsin, all viruses replicated at comparable levels at 8 and 48 hpi and reached the peak of replication at 48 hpi. G319 replicated at significantly higher levels than A319 at 24 hpi and higher than K319 and S319 at 72 hpi ($p < 0.006$) (Fig. 2B). Although trypsin increased virus titers in TEK cells compared to cells without trypsin, only significant differences were obtained for S319 at 8 and 24 hpi ($p < 0.04$). In CEK cells, in the presence of trypsin, peak of virus replication was reached 24 hpi. G319 replicated at significantly higher titers than K319 at 24 and 48 hpi ($p < 0.03$) (Fig. 2C). D319 replicated at significantly higher titers than N319 at 8 hpi and higher than K319 at 24 hpi ($p < 0.02$) (Fig. 2C). Without trypsin, virus titers were comparably lower than in the presence of trypsin, although it was not statistically significant ($p > 0.052$) and peak of virus replication was delayed to 72 hpi (Fig. 2D). Comparing TEK and CEK, in the presence of trypsin, N319 replicates significantly higher in TEK than in CEK cells at 8 hpi ($p < 0.003$) (Fig. 2A,C). Without trypsin, only K319, A319 and S319 replicated at 72 hpi to significantly higher levels in TEK cells than in CEK cells (Fig. 2B,D). Taken together, all recombinant viruses replicated to higher levels and reach their maximum titer in primary turkey and chicken cells faster in the presence of trypsin. Non-basic amino acids, particularly G319, supported rapid and higher replication of H9N2 in turkey cells. Regardless of their different physiochemical properties, mutations in the HACS enhanced virus replication in TEK than in CEK. These results indicate that mutations in P2 affect virus replication in avian cells.

TMPRSS2 and to a lesser extent HAT can support multiple-cycle replication of viruses with non-basic amino acids in the HACS. Using Western blot, the HA of all viruses was shown to be cleaved by trypsin, TMPRSS2 and HAT whereas no cleavability was observed in the absence of these proteases (Fig. 3A–C). The proteolytic activation of HAT and TMPRSS2 to support multiple-cycle replication was studied in different MDCK cells for 24 hpi. In MDCK cells which do not produce endogenous HAT or TMPRSS2, virus titers were generally lower than in MDCK-TMPRSS2 and MDCK-HAT cells (Fig. 3D). Without trypsin, G319 and S319 replicated to higher levels than K319, A319 and N319. S319 replicated at significantly higher titers than D319 ($p < 0.02$) (Fig. 3D). In the presence of trypsin, the titer of G319 was higher than A319 and K319. In MDCK-TMPRSS2 cells, all viruses replicated at comparable levels ($p > 0.2$), except G319 which replicated at significantly higher titer than other viruses ($p < 0.015$) (Fig. 3D). In MDCK-HAT cells, all viruses replicated at comparable levels ($p > 0.1$) (Fig. 3D). Viruses replicated at higher titers in MDCK-TMPRSS2 than in MDCK-HAT cells, but it was not statistically significant ($p > 0.9$). All viruses except S319 replicated at significantly higher titers in MDCK-TMPRSS2 than in MDCK cells ($p < 0.001$), while only K319 and D319 replicated at significantly

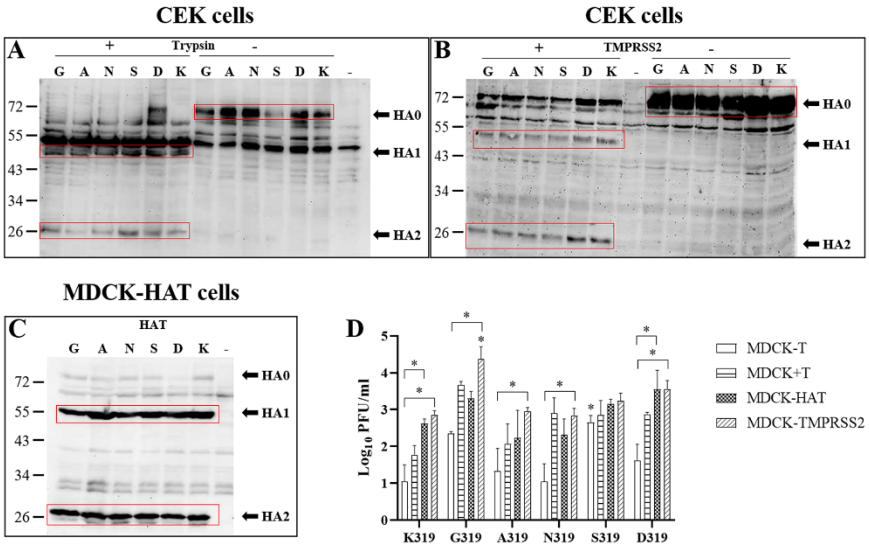

Figure 3. HA proteolytic activation and replication of recombinant viruses in different MDCK cell lines. Cleavage-activation of the HA of recombinant viruses carrying single mutations in the HACS in CEK cells with (+) or without (+) trypsin (**A**), in CEK after transfection with TMPRSS2 (+) or left untransfected (-) (**B**) or MDCK cells expressing HAT (**C**). Western Blot figures were acquired by Quantity One Software Version 4.4 (Biorad, Germany) (https://www.bio-rad.com/webroot/web/pdf/lsr/literature/4000126-14A.pdf). Multiple cycle replication after infection of MDCK with or without trypsin, MDCK-TMPRSS2 or MDCK-HAT with different recombinant viruses at MOI of 1 for 24 h. Titers were determined by plaque assay in MDCKII cells in the presence of trypsin. Titers are expressed as PFU/ml and are shown as the mean and the standard deviation. The kinetics were done twice in duplicates for each cell types (**D**). Data were analyzed using one-way ANOVA with post hoc Tukey tests and Kruskal–Wallis with Dunn's test. Asterisk indicates significant differences compared to K319 ($p < 0.05$).

higher titers in MDCK-HAT than in MDCK cells ($p < 0.05$). Together, although mutations in P2 did not affect HA-cleavability by trypsin, HAT and TMPRSS2, they modulated H9N2 virus replication in a protease-dependent manner with a remarkable impact of TMPRSS2 and to a lesser extent HAT on virus replication.

Non-basic amino acids in the HACS increased cell-to-cell spread and influenced the optimal pH-range for HA fusion activity. Cell-to-cell spread of the different virus variants was investigated by plaque assays on MDCKII cells. While K319 produced significantly smaller plaques compared to other viruses ($p < 0.0001$), largest plaque diameter was observed for G319 ($p < 0.01$) (Fig. 4A). Binding of protons in the low pH environment of the endosome serves as fusion trigger for HA. The pH-dependence and optimal pH of fusion of the different HA variants was investigated in a transient-transfection based cell–cell fusion assay. For this, CEK cells were transfected with the different pCAGGS-HA plasmids and GFP-pcDNA which was used as a marker and fusion was triggered with PBS buffer at pH 4.0 to 6.0 in 0.2 intervals. 4 h after the pH shift, syncytia were measured to determine the pH for membrane fusion. All HA variants produced syncytia at pH 4.0 to 5.2. Exposure to pH 5.4 could trigger all HA variants except D319. Only S319-HA and G319-HA produced syncytia at pH 5.6. No syncytia formation was observed by any HA at pH ≥ 5.8. The highest fusion activity was observed after exposure to pH 4.2 for K319-HA, pH 5.0 for D319-HA, pH 5.2 for G319-HA and S319-HA and pH 5.4 for A319-HA and N319-HA (Fig. 4B). These results indicate that mutations in P2 have an impact on cell-to-cell spread and pH fusion activation of H9N2.

Mutations in the HACS did not increase H9N2 virulence or transmission in chickens. All ON or IV challenged chickens remained healthy and PI values for all viruses were 0.0, however, all birds seroconverted (Supplementary Table S2). Viral RNA of all viruses was only detected in OR swabs of inoculated chickens 4 dpi and at low titers (Fig. 5A), where RNA of K319, G319, A319, N319, S319 and D319 was detected in 8/10, 7/10, 8/10, 5/10, 9/10 and 4/10 OR swabs, respectively (Supplementary Table S2). G319 and S319 had significantly lower titers than K319 and A319 ($p < 0.04$) (Fig. 5A). Viral RNA was reported in the nare of inoculated chickens with N319 and to a lesser extent in A319- or K319-inoculated chickens (Fig. 5B). No infectious virus was obtained after direct titration of any sample in plaque test. All contact chickens remained healthy and neither

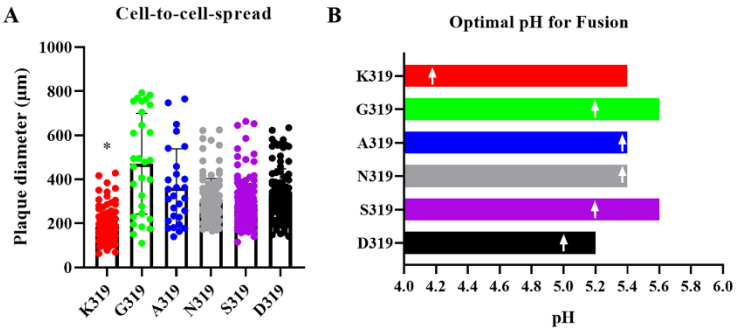

Figure 4. Cell-to-cell spread and pH fusion activity of recombinant viruses. Cell-to-cell spread was assessed in MDCKII cells in the presence of trypsin. Asterisk indicates that K319 induced the lowest plaque diameter compared to all other viruses ($p < 0.05$). Plaque diameter was measured by Nikon NIS Software (Nikon, Germany) (https://www.microscope.healthcare.nikon.com/de_EU/products/software/nis-elements) and analyzed with Kruskal–Wallis with Dunn's test (**A**). pH activation of membrane fusion was determined by treating HA-transfected chicken embryo kidney cells with pH 4.0 to 6.0 at 0.2 pH-intervals. The mean size of measured syncytia (> 50) was calculated. Shown is the range of pH values at which HA fusion activity was detectable. White arrows indicate the pH at which fusion activity was highest for each HA variant (**B**).

antibodies nor viral RNA were detectable (Supplementary Table S2). Collectively, H9N2 used in this study is poorly transmissible in chickens and mutations in P2 have no impact on virus transmission in chickens.

In turkeys, H9N2 exhibited higher adaptation than in chickens and some non-basic amino acids in the HACS affected virulence, replication and transmission. Direct inoculated and co-housed turkeys exhibited clinical signs including swelling of infraorbital sinus, facial edema, ruffled feather, rales and/or diarrhea. These clinical signs were observed in inoculated turkeys with N319 (10/10; PI = 0.6), K319 and D319 (9/10; PI = 0.4), S319 (3/10; PI = 0.1), A319 (2/10; PI = 0.1) and G319 (1/10; PI = 0.1) (Table 2) and in 2/5, 3/5, 4/5, 1/5, 1/5 and 1/5 co-housed turkeys, respectively (Table 2). At 4 dpi, caseous material was observed in the swollen sinuses during autopsy. Viral RNA was detected in almost all OR swabs obtained 4 dpi in inoculated turkeys and no significant differences were observed between the groups ($p > 0.1$) (Fig. 5C). In contact turkeys, G319 was shed in significantly higher amounts compared to K319, A319 and D319 ($p < 0.03$) (Fig. 5D). Cloacal shedding was only detected in two K319- and one A319-inoculated turkeys, although at very low titers (data not shown). In all inoculated groups, viral RNA was detectable only in the nare obtained 4 dpi and to a lesser extent in the brain (except for A319) (Fig. 5E,F). Direct titration of samples was not successful. Sequence of the HA in swab samples revealed no changes in the HACS and no additional mutations in the HA except G319 which an additional G61D mutation (H9 numbering) in inoculated turkeys. All ON-inoculated and contact turkeys seroconverted, except for one contact turkey inoculated with S319 (Table 2). Using IHC, MP antigen was detected in the nare of all inoculated turkeys, mainly in the epithelial cells of nasal chambers, infraorbital sinus and nasal glands. K319 and N319 were detected at slightly higher levels than others. MP antigen was neither detected in other examined organs nor in the endothelial cells. Histopathological changes in the nare were mostly multifocal, acute to sub-acute, lymphocytic and purulent, partially necrotizing sinusitis, rhinitis and inflammation of the nasal glands with associated edema of surrounding tissue. The inflammation caused by K319 and N319 was slightly more severe than other viruses. In the brain, mild multifocal lymphocytic perivascular infiltration was observed in turkeys inoculated with D319, A319 and S319. In the kidneys, focal interstitial lymphocytic infiltration was observed in one turkey inoculated with A319. Together, turkeys succumbed to H9N2 infection more severely than chickens. Mutations in P2 in the HACS affected virulence in turkeys.

HACS mutations have an effect on virus replication in different brain cells in the presence or absence of trypsin. Because low amounts of H9N2 RNA and mild lesions were observed in the brain of turkeys, multiple-cycle replication efficiency in brain cells obtained from different species was studied. All recombinant viruses replicated in TEB, PHA-B-1-R and CEB1-R cells independent of trypsin at an MOI of 0.001 for 24 h (Fig. 6A–C). In TEB, the addition of trypsin significantly increased virus replication and G319 revealed the highest titers ($p < 0.01$) (Fig. 6A). In PHA-B-1-R and CEB1-R cells, viruses replicated at significantly lower titers than in TEB without significant impact of trypsin in virus replication (Fig. 6B,C). Moreover, G319 was able to replicate in bat and mouse brain cells independent of trypsin, although at lower titers when compared to PHA-B-1-R and CEB1-R cells (data not shown). These data indicated that the H9N2 virus used in this study can infect brain cells of turkeys and mammals independent of trypsin, and mutations in the HACS can affect multiple-cycle replication of the virus in turkey brain cells.

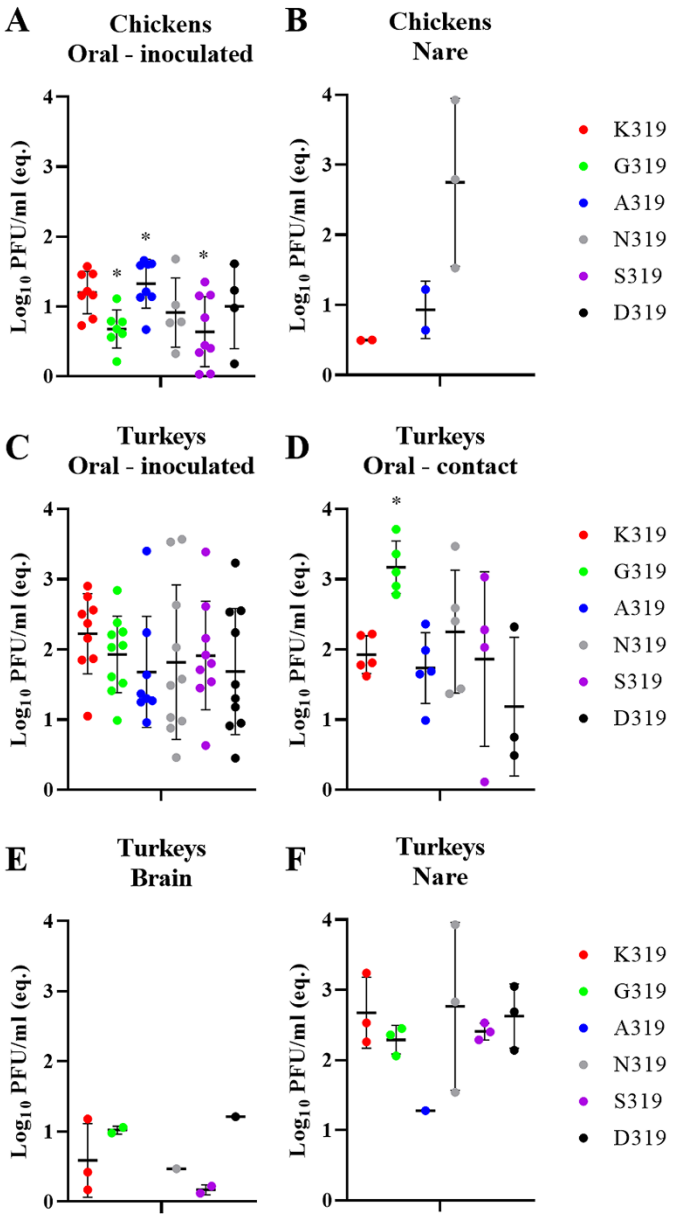

Figure 5. Virus detection in oropharyngeal swabs and organ samples in chickens and turkeys. Detection of viral RNA in inoculated chickens in oropharyngeal swabs (**A**) or organs (nasal cavity) (**B**) at 4 dpi was determined by RT-qPCR targeting the M gene and are expressed as equivalent Log_{10} PFU/ml. Virus excretion in oropharyngeal swabs (**C**,**D**) as well as in brain (**E**) and nasal cavity (**F**) at 4 dpi was determined by RT-qPCR targeting the M gene and are expressed as equivalent Log_{10} PFU/ml. Asterisk indicates significant difference compared to K319.

	PI	Inoculated Turkeys			Contact Turkeys		
		Morbidity	Shedding	Seroconversion	Morbidity	Shedding	Seroconversion
K319	0.4	9/10*	9/10	7/7	3/5	5/5	5/5
K319G	0.1	1/10	10/10	7/7	1/5	5/5	5/5
K319A	0.1	2/10	8/10	7/7	1/5	5/5	5/5
K319N	0.6	10/10	10/10	7/7	2/5	5/5	5/5
K319S	0.1	3/10	9/10	7/7	1/5	4/5	4/5
K319D	0.4	9/10	10/10	7/7	4/5	3/5	5/5

Table 2. Clinical examination of turkeys after oculonasal inoculation. * Number of positive birds/total examined. Turkeys were challenged with $10^{5.7}$ pfu/bird and 1 dpi 5 birds were added to assess transmission. At 4 dpi, 3 directly-inoculated turkeys were euthanized to assess virus distribution and lesions in different organs. Seroconversion (number of positive birds / total examined) was tested at 10 dpi using ELISA. Clinical scoring was conducted as recommended by the OIE on a scale 0 to 3: 0 = apparently healthy, 1 = birds showed 1 clinical sign (ruffled feather, respiratory disorders, diarrhea), 2 = birds showed more than 1 clinical signs and 3 = dead birds. The pathogenicity index (PI) is the mean of all clinical scores for all inoculated birds in 10 day-observation period. Clinical examination was done blindly by two veterinarians. Shedding was determined by RT-qPCR.

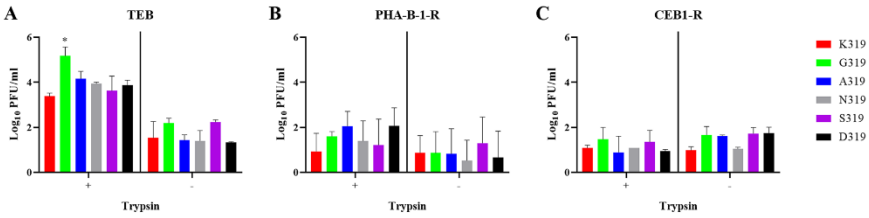

Figure 6. Replication of recombinant viruses in brain cells of turkeys, pigs and cats. Replication of indicated viruses was tested in primary turkey embryo brain (TEB) cells (**A**), Warthog brain PHA-B-1-R cell line (**B**) and Cat brain CEB1-R cell line (**C**) after infection with recombinant viruses at an MOI of 0.001 for 24 h in the presence (+) or absence (-) of trypsin. Virus titers are expressed as log10 PFU/ml and are shown as the mean and standard deviation of three independent rounds. Asterisk indicate significant differences ($p < 0.05$) compared to wt-H9N2 K319.

Discussion

The wide distribution of H9N2 affects the poultry industry worldwide. The virus is endemic in chickens and turkeys in several African and Asian countries, and recurrent outbreaks have been reported in Europe. European H9N2 viruses analyzed in this study had HACS motifs, which are different from the non-European H9N2 viruses. Compared to the Asian H9N2 G1-like lineage, little is known about the virulence of European H9N2 in chickens and turkeys[40,41]. Several studies have shown that non-European H9N2 viruses can increase in virulence after the insertion of basic aa in the HACS with or without reassortment with HPAIV H5N1[21,22]. Our analysis showed that the European H9N2 virus acquired several non-basic amino acids particularly in position P2 (residue 319 H9 numbering). Some of these alterations have been previously reported in Polish H9N2 viruses[42]. While amino acids at P3 and P1 are highly conserved, the variation in position 2 is remarkable. Six different amino acids were observed in European H9N2 viruses (G, A, N, S, D, K) while three were seen in the non-European viruses (Y, T, I). These results indicate a preferential selection for accumulation of non-basic amino acids in non-European viruses at this position. The inserted non-basic amino acids at P2 have different physiochemical properties, including size and polarity. These different characteristics may have an impact on the HACS conformation which could result in increased accessibility for certain proteases and thus enhanced HA cleavability, and/or the degree of exposure of the fusion peptide, resulting in the observed enhanced cell-to-cell spread (Fig. 4A) and altered optimal pH-range to trigger HA fusion (Fig. B).

Viruses used in this study replicated in different cultured cells without trypsin, although cells were infected with low multiplicity and extracellular virions were removed by treatment of cells with citrate buffered saline and washing with PBS. The efficient replication of some H9N2 viruses in primary chicken cells without exogenous trypsin has been previously reported[43]. Our results showed that TMPRSS2 and to a lesser extent HAT can support multiple-cycle replication of different viruses, particularly G319, better than trypsin. Several studies have also shown that S, R or K in P2 can affect cleavage activation of the R-S-X-R motifs in non-European H9N2 viruses by different proteases (i.e. matriptase, HAT, TMPRSS2 and furin)[11,44]. Similarly, a tyrosine at P2 affected cleavability of non-European H9N2 viruses in cell culture[38].

Cleavage of the fusion-inactive HA0 by host proteases into HA1/HA2 subunits results in irreversible conformational changes, enabling HA2 to mediate low-pH dependent fusion of the viral and cellular membranes in

the endosomal compartment and subsequently release of the viral RNA into the cytoplasm[6]. The pH value in the early endosome is about 6 to 6.3, 5 to 6 in the late endosome, and 4 to 5[45] in the lysosome[46]. Thus, rapid fusion may enhance early virus replication before triggering the host-immune response or lysis of the virus particles. Nevertheless, pH stability is also important for persistence of AIV in the environment or in the acidic milieu of the upper airways. Therefore, AIV optimal ranges for pH-fusion-activation vary from 4.4 to 6.4[46,47]. Mutations in P2 affected pH-fusion activation in the range of pH 4.0 to 5.6. Although the mechanism is not fully understood, it is possible that the insertion of non-basic amino acids enhanced cleavability of the HA in the extracellular environment by HAT or intracellularly by TMPRSS2. It has been also reported that mutations in the head domain of the HA1 apart from the fusion peptide can trigger HA2 fusion activity of H9N2 at different pH values[48,49].

Although chickens and turkeys are both galliform birds, they vary in their susceptibility to AIV. Generally, turkeys are more vulnerable to AIV-induced morbidity and mortality than chickens[3]. The virus used here is a turkey-origin virus similar to the vast majority of European viruses analyzed in this study, thus it is conceivable that adaptation to turkey-cells or turkeys was superior to chickens. Similarly, Turkey/Wisconsin/66(H9N2) caused no clinical signs in chickens, although all chickens seroconverted, while inoculated-turkeys exhibited mild depression, sinusitis and respiratory signs and almost all turkeys seroconverted[50]. Likewise, all chickens inoculated with a recent polish H9N2 virus of turkey origin from the 2013/2014 outbreak and 1 of 2 contact-chickens seroconverted[42]. Poor replication of two Dutch wild-bird-origin H9N2 viruses in chickens as indicated by lack of clinical signs, low virus titers in swabs and respiratory organs and low seroconversion has been reported[41]. Conversely, efficient replication and transmission of a chicken-adapted virus Ck/Hebei/LC/2008 H9N2 in chickens and turkeys have been reported, although cloacal excretion was not seen in turkeys[51].

There is a gap in understanding the genetic determinants responsible for adaptation in chickens *vs.* turkeys. Interestingly, N337K (corresponding to N319K in our study) in the HACS was detected in the 6th passage of a turkey-origin H9N2 isolated in Poland in 2013/2014 outbreak in chickens as low frequency variant and became predominant in the 7th passage indicating a role of this particular amino acid for virus adaptation in chickens[52]. However, in our study, neither N319 nor K319 exhibited any increased virulence or transmissibility in chickens or turkeys, and both viruses replicated in a trypsin-dependent manner at significantly higher levels in turkey cells than in chicken cells. It seems that variation in P2 alone is not sufficient for adaptation in chickens and additional mutations e.g. in HA, PA, NP and PB1[52] or in the NA[53] are probably required. Furthermore, sequence of swab samples from inoculated and contact turkeys at 4 dpi indicated that mutations in the HACS were stable except for G319 which acquired one additional mutation in the HA. Whether this mutation resulted in increased virus titers in the nasal cavity in sentinel turkeys remained to be investigated. Studies showed that H9N2 HACS was stable after passaging in cell culture or in embryonated eggs[54,55]. Conversely, passaging of H9N2 in tracheal organ cultures or different birds (i.e. turkeys, quails and ducks) resulted in accumulation of mutations in the HACS, among other segments[40,56]. These different results may be explained by using different H9N2 viruses or variable host-specific selection pressure. Moreover, we detected RNA but not infectious virus in brain samples. Evidence for the extra-pulmonary spread of H9N2 in different organs in poultry has been described[48,57,58].

Human infections caused by H9N2 have been reported[59]. Importantly, several AIV with high fatality rate in humans acquired non-HA/NA gene segments from H9N2 (e.g. H5N1, H7N9, H10N8). In addition to human hosts, H9N2 AIV has also infected mammals including pigs, dogs, cats, horses and bats[13]. Without prior adaptation, AIV H9N2 in this study succeeded in multiple-cycle replication in brain cells of pigs, cats and mice independent of trypsin, albeit to low levels. Mutation to tyrosine at P2 increased replication of WSN/H1N1 in the brain of mice[39]. Virulence of these viruses remains to be studied in mammalian models, but zoonotic risk of H9N2 AIV (e.g. G319) should be monitored carefully. G319-like H9N2 viruses may infect and replicate at higher levels in the upper respiratory tract of turkeys without causing severe disease. The threat of H9N2 AIV as a zoonotic agent is neglected[60] and there is an urgent need to reassess containment of the H9N2 AIV in poultry[61].

In conclusion, our analysis indicated preferential substitutions of non-basic amino acids in the HACS of European-H9N2 viruses, which were different from non-European viruses. These mutations increased virus replication in *vitro* and in vivo and contributed to virus fitness in turkeys, but not in chickens. H9N2 viruses in this study, particularly G319 replicated in mammalian cells without trypsin. The findings of this study are important to better understand adaptation of H9N2 in turkeys and mammalian cells.

Received: 16 September 2020; Accepted: 20 November 2020
Published online: 04 December 2020

References

1. Bouvier, N. M. & Palese, P. The biology of influenza viruses. *Vaccine* **26**(Suppl 4), D49-53 (2008).
2. Fouchier, R. A. M. *et al.* Characterization of a novel influenza A virus hemagglutinin subtype (H16) obtained from black-headed gulls. *J. Virol.* **79**, 2814 (2005).
3. Alexander, D. J. A review of avian influenza in different bird species. *Vet. Microbiol.* **74**, 3–13 (2000).
4. Herfst, S. *et al.* Airborne transmission of influenza A/H5N1 virus between ferrets. *Science* **336**, 1534–1541 (2012).
5. Sorrell, E. M., Wan, H., Araya, Y., Song, H. & Perez, D. R. Minimal molecular constraints for respiratory droplet transmission of an avian–human H9N2 influenza A virus. *Proc. Natl. Acad. Sci. U. S. A.* **106**, 7565–7570 (2009).
6. Steinhauer, D. A. Role of hemagglutinin cleavage for the pathogenicity of influenza virus. *Virology* **258**, 1–20 (1999).
7. Skehel, J. J. & Wiley, D. C. Receptor binding and membrane fusion in virus entry: the influenza hemagglutinin. *Annu. Rev. Biochem.* **69**, 531–569 (2000).
8. Böttcher-Friebertshäuser, E., Garten, W., Matrosovich, M. & Klenk, H. D. in *Influenza Pathogenesis and Control - Volume I* (eds Richard W. Compans & Michael B. A. Oldstone) 3–34 (Springer International Publishing, Berlin, 2014).
9. Rott, R. The pathogenic determinant of influenza virus. *Vet. Microbiol.* **33**, 303–310 (1992).

10. Bottcher, E. *et al.* Proteolytic activation of influenza viruses by serine proteases TMPRSS2 and HAT from human airway epithelium. *J. Virol.* **80**, 9896–9898 (2006).
11. Baron, J. *et al.* Matriptase, HAT, and TMPRSS2 activate the hemagglutinin of H9N2 influenza A viruses. *J. Virol.* **87**, 1811–1820 (2013).
12. Nagy, A., Mettenleiter, T. C. & Abdelwhab, E. M. A brief summary of the epidemiology and genetic relatedness of avian influenza H9N2 virus in birds and mammals in the Middle East and North Africa. *Epidemiol. Infect.* **145**, 3320–3333 (2017).
13. Peacock, T. H. P., James, J., Sealy, J. E. & Iqbal, M. A global perspective on H9N2 avian influenza virus. *Viruses* **11** (2019).
14. Hu, M. *et al.* Genetic characteristic and global transmission of influenza A H9N2 virus. *Front. Microbiol.* **8**, 2611 (2017).
15. Nili, H. & Asasi, K. Natural cases and an experimental study of H9N2 avian influenza in commercial broiler chickens of Iran. *Avian Pathol* **31**, 247–252 (2002).
16. Nili, H. & Asasi, K. Avian influenza (H9N2) outbreak in Iran. *Avian Dis.* **47**, 828–831 (2003).
17. Guo, Y. J. *et al.* Characterization of the pathogenicity of members of the newly established H9N2 influenza virus lineages in Asia. *Virology* **267**, 279–288 (2000).
18. Sun, X., Belser, J. A. & Maines, T. R. Adaptation of H9N2 influenza viruses to mammalian hosts: a review of molecular markers. *Viruses* **12**(5), 541 (2020).
19. Wan, H. & Perez, D. R. Amino acid 226 in the hemagglutinin of H9N2 influenza viruses determines cell tropism and replication in human airway epithelial cells. *J. Virol.* **81**, 5181–5191 (2007).
20. Zhong, L. *et al.* Molecular mechanism of the airborne transmissibility of H9N2 avian influenza A viruses in chickens. *J. Virol.* **88**, 9568–9578 (2014).
21. Soda, K., Asakura, S., Okamatsu, M., Sakoda, Y. & Kida, H. H9N2 influenza virus acquires intravenous pathogenicity on the introduction of a pair of di-basic amino acid residues at the cleavage site of the hemagglutinin and consecutive passages in chickens. *Virol. J.* **8**, 64 (2011).
22. Gohrbandt, S. *et al.* H9 avian influenza reassortant with engineered polybasic cleavage site displays a highly pathogenic phenotype in chicken. *J. Gen. Virol.* **92**, 1843–1853 (2011).
23. Swieton, E., Jozwiak, M., Minta, Z. & Smietanka, K. Genetic characterization of H9N2 avian influenza viruses isolated from poultry in Poland during 2013/2014. *Virus Genes* **54**, 67–76 (2018).
24. Reid, S. M. *et al.* The detection of a low pathogenicity avian influenza virus subtype H9 infection in a turkey breeder flock in the United Kingdom. *Avian Dis.* **60**, 126–131 (2016).
25. Verhagen, J. H. *et al.* Discordant detection of avian influenza virus subtypes in time and space between poultry and wild birds; Towards improvement of surveillance programs. *PLoS ONE* **12**, e0173470 (2017).
26. Parvin, R. *et al.* Comparison of pathogenicity of subtype H9 avian influenza wild-type viruses from a wide geographic origin expressing mono-, di-, or tri-basic hemagglutinin cleavage sites. *Vet. Res.* **51**, 48 (2020).
27. Harder, T. C. Endemic non-notifiable avian influenza virus infections in poultry. Available online at: NRL Avian Influenza. (Accessed 25 August 2020); https://ec.europa.eu/food/sites/food/files/animals/docs/ad_cm_20180710_24-annual-meetings_ai-pres-08.pdf. (2018).
28. Katoh, K. & Standley, D. M. MAFFT: iterative refinement and additional methods. *Methods Mol. Biol.* **1079**, 131–146 (2014).
29. Bottcher, E., Freuer, C., Steinmetzer, T., Klenk, H. D. & Garten, W. MDCK cells that express proteases TMPRSS2 and HAT provide a cell system to propagate influenza viruses in the absence of trypsin and to study cleavage of HA and its inhibition. *Vaccine* **27**, 6324–6329 (2009).
30. Choi, J. W. *et al.* Optimal conditions for cryopreservation of primary chicken embryo kidney cells with dimethyl sulfoxide. *Mol. Biotechnol.* **35**, 237–241 (2007).
31. Hoffmann, E., Stech, J., Guan, Y., Webster, R. G. & Perez, D. R. Universal primer set for the full-length amplification of all influenza A viruses. *Arch. Virol.* **146**, 2275–2289 (2001).
32. Stech, J. *et al.* Rapid and reliable universal cloning of influenza A virus genes by target-primed plasmid amplification. *Nucleic Acids Res.* **36**, e139 (2008).
33. OIE. Chapter 2.3.4. Avian influenza. Available at: http://www.oie.int/fileadmin/Home/fr/Health_standards/tahm/2.03.04_AI.pdf. (2015).
34. Vallbracht, M., Schröter, C., Klupp, B. & Mettenleiter, T. Transient transfection-based fusion assay for viral proteins. *Bio-Protocol* **7**, e2162 (2017).
35. Hoffmann, B., Hoffmann, D., Henritzi, D., Beer, M. & Harder, T. C. Riems influenza a typing array (RITA): An RT-qPCR-based low density array for subtyping avian and mammalian influenza a viruses. *Sci. Rep.* **6**, 27211 (2016).
36. Alexander, D. J. *Avian Influenza*, https://www.oie.int/fileadmin/Home/eng/Health_standards/tahm/2.03.04_AI.pdf (2015).
37. Graaf, A. *et al.* A viral race for primacy: co-infection of a natural pair of low and highly pathogenic H7N7 avian influenza viruses in chickens and embryonated chicken eggs. *Emerg. Microbes Infect.* **7**, 204 (2018).
38. Tse, L. V. & Whittaker, G. R. Modification of the hemagglutinin cleavage site allows indirect activation of avian influenza virus H9N2 by bacterial staphylokinase. *Virology* **482**, 1–8 (2015).
39. Sun, X., Tse, L. V., Ferguson, A. D. & Whittaker, G. R. Modifications to the hemagglutinin cleavage site control the virulence of a neurotropic H1N1 influenza virus. *J. Virol.* **84**, 8683–8690 (2010).
40. Swieton, E., Tarasiuk, K., Olszewska-Tomczyk, M., Iwan, E. & Smietanka, K. A turkey-origin H9N2 avian influenza virus shows low pathogenicity but different within-host diversity in experimentally infected turkeys, quail and ducks. *Viruses* **12**(3), 319 (2020).
41. Bergervoet, S. A. *et al.* Susceptibility of chickens to low pathogenic avian influenza (LPAI) viruses of wild bird- and poultry-associated subtypes. *Viruses* **11**(11), 1010 (2019).
42. Smietanka, K. *et al.* Avian influenza H9N2 subtype in Poland–characterization of the isolates and evidence of concomitant infections. *Avian Pathol.* **43**, 427–436 (2014).
43. Tombari, W., ElBehi, I., Amouna, F. & Ghram, A. Variability of tropism and replicative capacity of two naturally occurring influenza A H9N2 viruses in cell cultures from different tissues. *Avian Pathol.* **45**, 212–220 (2016).
44. Tse, L. V., Hamilton, A. M., Friling, T. & Whittaker, G. R. A novel activation mechanism of avian influenza virus H9N2 by furin. *J. Virol.* **88**, 1673–1683 (2014).
45. DiCiccio, J. E. & Steinberg, B. E. Lysosomal pH and analysis of the counter ion pathways that support acidification. *J. Gen. Physiol.* **137**, 385–390 (2011).
46. Russell, C. J., Hu, M. & Okda, F. A. Influenza hemagglutinin protein stability, activation, and pandemic risk. *Trends Microbiol.* **26**, 841–853 (2018).
47. Scholtissek, C. Stability of infectious influenza-a viruses to treatment at low pH and heating. *Arch. Virol.* **85**, 1–11 (1985).
48. Song, Y. *et al.* Genetic characteristics and pathogenicity analysis in chickens and mice of three H9N2 avian influenza viruses. *Viruses* **11**, 1127 (2019).
49. Peacock, T. P. *et al.* Variability in H9N2 haemagglutinin receptor-binding preference and the pH of fusion. *Emerg. Microbes Infect.* **6**, e11–e11 (2017).
50. Dundon, W. G., Maniero, S., Toffan, A., Capua, I. & Cattoli, G. Appearance of serum antibodies against the avian influenza non-structural 1 protein in experimentally infected chickens and turkeys. *Avian Dis.* **51**, 209–212 (2007).
51. Sun, H. *et al.* The infection of turkeys and chickens by reassortants derived from pandemic H1N1 2009 and avian H9N2 influenza viruses. *Sci. Rep.* **5**, 10130 (2015).

52. Świętoń, E., Olszewska-Tomczyk, M., Giza, A. & Śmietanka, K. Evolution of H9N2 low pathogenic avian influenza virus during passages in chickens. *Infect. Genet. Evol.* **75**, 103979 (2019).
53. Sun, Y. *et al.* Amino acid 316 of hemagglutinin and the neuraminidase stalk length influence virulence of H9N2 influenza virus in chickens and mice. *J. Virol.* **87**, 2963–2968 (2013).
54. Shaib, H. A. *et al.* Impact of embryonic passaging of H9N2 virus on pathogenicity and stability of HA1- amino acid sequence cleavage site. *Med. Sci. Monit.* **16**, BR333–337 (2010).
55. Lee, C. W. *et al.* Sequence analysis of the hemagglutinin gene of H9N2 Korean avian influenza viruses and assessment of the pathogenic potential of isolate MS96. *Avian Dis.* **44**, 527–535 (2000).
56. Petersen, H., Matrosovich, M., Pleschka, S. & Rautenschlein, S. Replication and adaptive mutations of low pathogenic avian influenza viruses in tracheal organ cultures of different avian species. *PLoS ONE* **7**, e42260 (2012).
57. Post, J., de Geus, E. D., Vervelde, L., Cornelissen, J. B. & Rebel, J. M. Systemic distribution of different low pathogenic avian influenza (LPAI) viruses in chicken. *Virol. J.* **10**, 23 (2013).
58. Lenny, B. J. *et al.* Replication capacity of avian influenza A(H9N2) virus in pet birds and mammals Bangladesh. *Emerg. Infect. Dis.* **21**, 2174–2177 (2015).
59. Freidl, G. S. *et al.* Influenza at the animal–human interface: a review of the literature for virological evidence of human infection with swine or avian influenza viruses other than A(H5N1). *Euro Surveill.* **19**, 20793 (2014).
60. Carnaccini, S. & Perez, D. R. H9 influenza viruses: an emerging challenge. *Cold Spring Harb. Perspect. Med.* **10**(6), a038588 (2020).
61. Sims, L. D., Tripodi, A. & Swayne, D. E. Spotlight on avian pathology: can we reduce the pandemic threat of H9N2 avian influenza to human and avian health?. *Avian Pathol.* https://doi.org/10.1080/03079457.2020.1796139 (2020).

Acknowledgments
Dajana Helke and Nadine Bock are thanked for laboratory technical assistance, Günter Strebelow for his assistance in sequencing, Dr. Christine Fast, Bärbel Hammerschmidt, Frank Klipp, Mathias Jan, Harald Manthei, Doreen Fiedler, Bärbel Berger, Thomas Möritz and Ralf Henkel for their support in the animal experiments and to Silvia Schuparis and Hilke Gräfe for histotechnological preparations. Barbara Klupp and Stefan Finke are thanked for providing the plasmids.

Author contributions
C.B. performed the in vitro characterization and statistical analysis, E.M.A., T.C.M. and E.F. conceived and designed the experiments, C.B., D.S. and E.M.A. conducted the animal experiments, R.U. and M.L. conducted the histopathological examination, M.V. and C.B. conducted the fusion assay, C.B. and E.M.A. wrote the draft of the manuscript, all authors discussed the results, commented on the manuscript, and approved the final version.

Funding
Open Access funding enabled and organized by Projekt DEAL. This work was supported by grants from the Deutsche Forschungsgemeinschaft DFG AB 567 and Delta Flu Project DELTA-FLU, Project ID: 727922 funded by the European Union under: H2020-EU. M. Landmann is supported for this work through a doctoral scholarship from the European Social Fund (ESF). The funders had no role in study design, data collection and analysis, decision to publish or preparation of the manuscript.

Competing interests
The authors declare no competing interests.

Additional information
Supplementary information is available for this paper at https://doi.org/10.1038/s41598-020-78210-8.

Correspondence and requests for materials should be addressed to E.M.A.

Reprints and permissions information is available at www.nature.com/reprints.

Publisher's note Springer Nature remains neutral with regard to jurisdictional claims in published maps and institutional affiliations.

Supplementary Material

Non-basic amino acids in the hemagglutinin proteolytic cleavage site of a European H9N2 avian influenza virus modulate virulence in turkeys

Claudia Blaurock[1], David Scheibner[1], Maria Landmann[2], Melina Vallbracht[1], Reiner Ulrich[2], Eva Böttcher-Friebertshäuser[3], Thomas C. Mettenleiter[1] and Elsayed M. Abdelwhab[1*]

[1]Friedrich-Loeffler-Institut, Federal Research Institute for Animal Health, Suedufer 10, 17493 5 Insel Riems-Greifswald, Germany 6

[2]Institute of Veterinary Pathology, Faculty of Veterinary Medicine, Leipzig University, Germany

[3]Institute of Virology, Philipps University Marburg, Marburg, Germany

Supplementary Figure S1: Cleavability of H9N2 viruses carrying single mutations in the HACS by trypsin in chicken embryo kidney (CEK) cells.

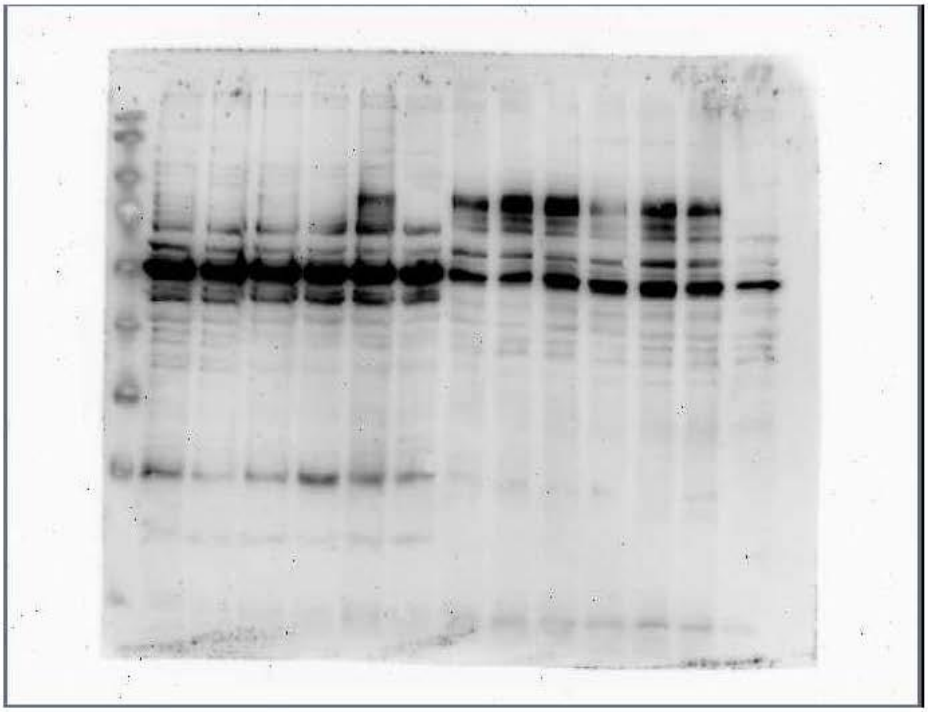

The cleavability of HA0 into HA1 and HA2 subunits was studied using Western Blot after the transfection of CEK cells with 5µg pCAGGS-HA-plasmid in the presence (+) or absence (-) of trypsin for 24 hours. Detection of the HA of all viruses was detected with serum of an infected turkey (1:100) in the current study after separation in a 12 % polyacrylamide gel. Shown, from left to right: the protein marker, G319 (+), A319 (+), N319 (+), S319 (+), D319 (+), K319 (+), G319 (-), A319 (-), N319 (-), S319 (-), D319 (-), K319 (-) and the mock control (non-infected CEK cells). For full annotation, please refer to Figure 3 panel A.

Supplementary Figure S2: Cleavability of H9N2 viruses carrying single mutations in the HACS by TMPRSS2 in chicken embryo kidney (CEK) cells.

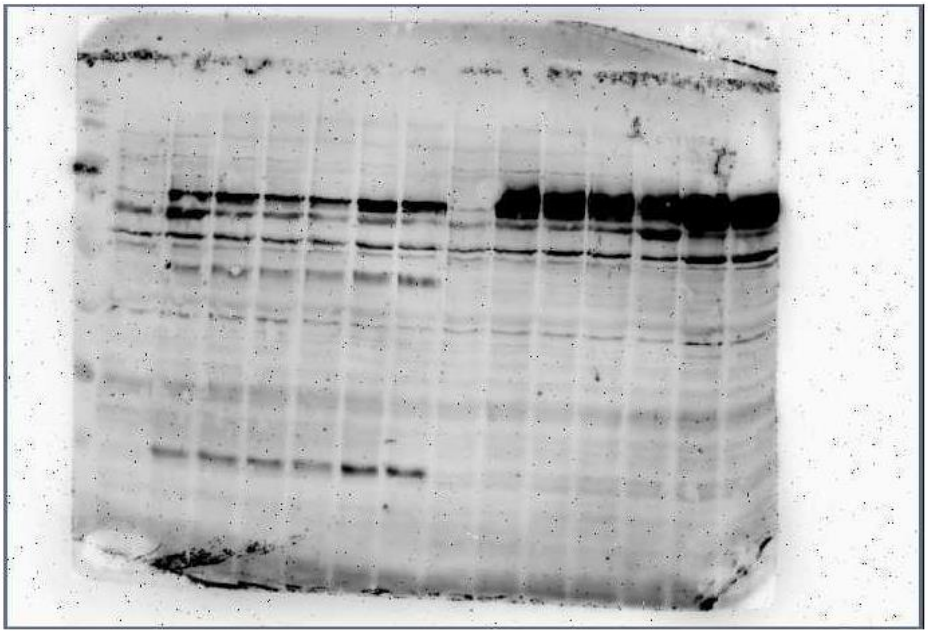

The cleavability of HA0 into HA1 and HA2 subunits was studied using Western Blot after the transfection of CEK cells with 2µg pCAGGS-HA-plasmid and with or without 500ng TMPRSS2 plasmid for 24 hours. Detection of the HA of all viruses was detected with serum of an infected turkey (1:100) in the current study after separation in a 12 % polyacrylamide gel. Shown, from left to right: protein marker, mock control (non-infected CEK cells), G319 (+TMPRSS2), A319 (+TMPRSS2), N319 (+TMPRSS2), S319 (+TMPRSS2), D319 (+TMPRSS2), K319 (+TMPRSS2), mock control (non-infected CEK cells), G319 (-TMPRSS2), A319 (-TMPRSS2), N319 (-TMPRSS2), S319 (-TMPRSS2), D319 (-TMPRSS2) and K319 (-TMPRSS2). For full annotation, please refer to Figure 3 panel B.

Supplementary Figure S3: Cleavability of H9N2 viruses carrying single mutations in the HACS by MDCK cells expressing HAT.

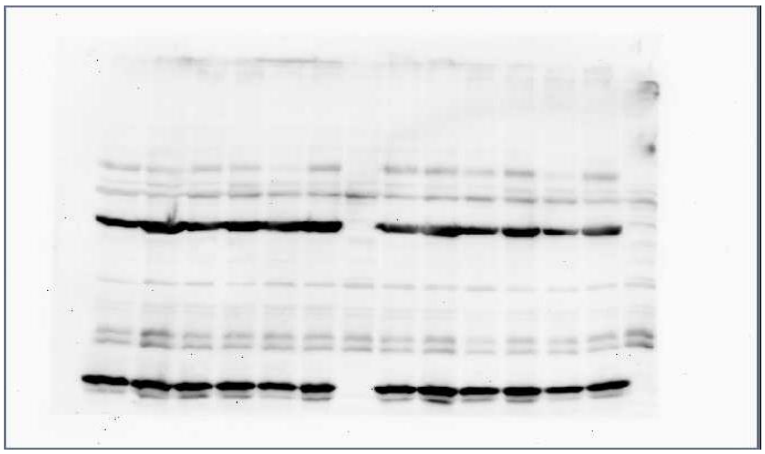

The cleavability of HA0 into HA1 and HA2 subunits was studied using Western Blot after the infection of MDCK-HAT cells with an MOI of 0.1 for 24 hours (+ 0.2 µg/ml Doxycycline). Detection of the HA of all viruses was done with serum of an infected turkey (1:100) generated in the current study after separation in a 12 % polyacrylamide gel. Shown, from left to right: protein marker, G319 (MOI = 0.1), A319 (MOI = 0.1), N319 (MOI = 0.1), S319 (MOI = 0.1), D319 (MOI = 0.1), K319 (MOI = 0.1), mock control (non-infected MDCK-HAT cells). T G319 (1 ml virus), A319 (1 ml virus), N319 (1 ml virus), S319 (1 ml virus), D319 (1 ml virus) and K319 (1 ml virus) and the mock control (non-infected MDCK-HAT cells). For full annotation, please refer to Figure 3 panel C.

Non-basic amino acids in the hemagglutinin proteolytic cleavage site of a European H9N2 avian influenza virus modulate virulence in turkeys

Claudia Blaurock[1], David Scheibner[1], Maria Landmann[2], Melina Vallbracht[1], Reiner Ulrich[2], Eva Böttcher-Friebertshäuser[3], Thomas C. Mettenleiter[1] and Elsayed M. Abdelwhab[1*]

[1]Friedrich-Loeffler-Institut, Federal Research Institute for Animal Health, Suedufer 10, 17493 Insel Riems-Greifswald, Germany

[2]Institute of Veterinary Pathology, Faculty of Veterinary Medicine, Leipzig University, Germany

[3]Institute of Virology, Philipps University Marburg, Marburg, Germany

Supplementary Table S1: Prevalence of cleavage site motifs of H9N2 in different species

	Motif (P1/P1´)	European H9N2				Non-European H9N2			
		Total No.	Chicken	Turkey	Other*	Total No.	Chicken	Turkey	Other
1	AS**G**R/G	2	0	0	2	13	6	0	7
2	AS**A**R/G	6	0	5	1	0	0	0	0
3	AS**N**R/G	11	0	8	3	3	0	0	3
4	RS**S**R/G	9	9	0	0	2384	1842	11	531
5	AS**D**R/G	39	0	0	39	70	1	1	68
6	AS**K**R/G	4	0	4	0	0	0	0	0
7	RSKR/G	3	3	0	0	6	0	5	1
8	VSDR/G	1	0	0	1	20	0	6	14
9	TSNR/G	2	1	1	0	0	0	0	0
10	TSGR/G	3	1	2	0	16	14	0	2
11	ISGR/G	1	0	1	0	2	0	0	2
12	ISDR/G	1	1	0	0	0	0	0	0
13	RSGR/G					3	2	1	0
14	RSNR/G					35	21	0	14
15	ASDK/G					1	0	0	1

16	VSNR/G					7	0	0	7
17	VSGR/G					7	0	1	6
18	VSSR/G					9	2	6	1
19	ASYR/G					7	6	0	1
20	ISNR/G					3	0	0	3
21	KSSR/G					172	135	0	37
22	ISSR/G					1	1	0	0
23	KASR/G					2	1	0	1
24	RYSR/G					2	2	0	0
25	RASR/G					21	4	0	17
26	RLSR/G					13	11	0	2
27	RSRR/G					7	4	0	3
28	GSSR/G					3	3	0	0
29	RPSR/G					2	1	0	1
30	RFSR/G					9	8	0	1
31	RSTR/G					2	2	0	0
32	RSSK/G					4	3	0	1
33	RCSR/G					1	0	0	1

34	RSIR/G					1	0	0	1
35	KSKR/G					96	41	0	55
36	RSNK/G					1	1	0	0
	Total	82	15	21	46	2926§	2111	31	781

* "Other" refers to e.g. ducks, mallards, teals, wigeons, pheasants, ostriches, swans, pigeons or environment.

§ Three sequences from chickens (2 from Iran in 2007 and 1 from Egypt in 2013) had RSNR/**R**, RSNK/**R** and KSSR/**A** motifs assuming wrong or unusual sequences in the HA2 (i.e. underlined R or A).

Non-basic amino acids in the hemagglutinin proteolytic cleavage site of a European H9N2 avian influenza virus modulate virulence in turkeys

Claudia Blaurock[1], David Scheibner[1], Maria Landmann[2], Melina Vallbracht[1], Reiner Ulrich[2], Eva Böttcher-Friebertshäuser[3], Thomas C. Mettenleiter[1] and Elsayed M. Abdelwhab[1*]

[1]Friedrich-Loeffler-Institut, Federal Research Institute for Animal Health, Suedufer 10, 17493 Insel Riems-Greifswald, Germany

[2]Institute of Veterinary Pathology, Faculty of Veterinary Medicine, Leipzig University, Germany

[3]Institute of Virology, Philipps University Marburg, Marburg, Germany

Supplementary Table S2: Clinical examination of chickens after oculonasal challenge

	Inoculated chickens				Contact chickens		
	PI	Morbidity	Shedding	Seroconversion	Morbidity	Shedding	Seroconversion
K319		0/10*	8/10	7/7	0/5	0/5	0/5
K319G		0/10	7/10	7/7	0/5	0/5	0/5
K319A		0/10	8/10	7/7	0/5	0/5	0/5
K319N		0/10	5/10	7/7	0/5	0/5	0/5
K319S		0/10	9/10	7/7	0/5	0/5	0/5
K319D		0/10	4/10	7/7	0/5	0/5	0/5

* Number of positive birds/total examined

Chickens were challenged with $10^{5.7}$ pfu/bird and 1 dpi 5 birds were added to assess transmission. At 4 dpi, 3 directly-inoculated chickens were euthanized to assess virus distribution and lesions in different organs. Seroconversion (number of positive birds / total examined) was tested at 10 dpi using ELISA. Clinical scoring was conducted as recommended by the OIE on a scale 0 to 3: 0= apparently healthy, 1= birds showed 1 clinical sign (ruffled feather, respiratory disorders, diarrhea), 2 = birds showed more than 1 clinical signs and 3 = dead birds. The pathogenicity index (PI) is the mean of all clinical scores for all inoculated birds in 10 day-observation period. All birds remained healthy. Clinical examination was done blindly by two veterinarians. Shedding was determined by RT-qPCR.

(II) Genetic incompatibilities and reduced transmission in chickens may limit the evolution of reassortants between H9N2 and panzootic H5N8 clade 2.3.4.4 avian influenza virus showing high virulence for mammals

Ahmed Mostafa, Claudia Blaurock, David Scheibner, Christin Müller, Ulrike Blohm, Alexander Schäfer, Marcel Gischke, Ahmed H. Salaheldin, Hanaa Z. Nooh, Mohamed A. Ali, Angele Breithaupt, Thomas C. Mettenleiter, Stephan Pleschka, and Elsayed M. Abdelwhab

Virus Evolution

Virus Evol 6 (2), veaa077 (2020)

doi: 10.1093/ve/veaa077

VIRUS EVOLUTION

Virus Evolution, 2020, 6(2): veaa077

doi: 10.1093/ve/veaa077
Research Article

Genetic incompatibilities and reduced transmission in chickens may limit the evolution of reassortants between H9N2 and panzootic H5N8 clade 2.3.4.4 avian influenza virus showing high virulence for mammals

Ahmed Mostafa,[1,2,*,†] Claudia Blaurock,[3,†] David Scheibner,[3] Christin Müller,[1] Ulrike Blohm,[4] Alexander Schäfer,[4] Marcel Gischke,[3] Ahmed H. Salaheldin,[3] Hanaa Z. Nooh,[5] Mohamed A. Ali,[2] Angele Breithaupt,[6] Thomas C. Mettenleiter,[3] Stephan Pleschka,[1] and Elsayed M. Abdelwhab[3,*,‡]

[1]Institute of Medical Virology, Justus Liebig University Giessen, Schubertstrasse 81, 35392 Giessen, Germany, [2]Center of Scientific Excellence for Influenza Viruses, National Research Centre (NRC), Dokki, 12622, Giza, Egypt, [3]Institute of Molecular Virology and Cell Biology and , [4]Institute of Immunology, Friedrich-Loeffler-Institut, Federal Research Institute for Animal Health, Südufer 10, 17493 Greifswald-Insel Riems, Germany, [5]Department of Anatomy and Histology, College of Medicine, Jouf University, Sakaka 72442, Aljouf Province, Saudi Arabia and [6]Department of Experimental Animal Facilities and Biorisk Management, Friedrich-Loeffler-Institut, Federal Research Institute for Animal Health, Südufer 10, 17493 Greifswald-Insel Riems, Germany

*Corresponding author: E-mail: sayed.abdel-whab@fli.de or ahmed_elsayed@daad-alumni.de

†Ahmed Mostafa and Claudia Blaurock contributed equally to this work. Author order was determined both alphabetically and in order of seniority.

‡https://orcid.org/0000-0003-2103-0922

Abstract

The unprecedented spread of H5N8- and H9N2-subtype avian influenza virus (AIV) in birds across Asia, Europe, Africa, and North America poses a serious public health threat with a permanent risk of reassortment and the possible emergence of novel virus variants with high virulence in mammals. To gain information on this risk, we studied the potential for reassortment between two contemporary H9N2 and H5N8 viruses. While the replacement of the PB2, PA, and NS genes of highly pathogenic H5N8 by homologous segments from H9N2 produced infectious H5N8 progeny, PB1 and NP of H9N2 were not able to replace the respective segments from H5N8 due to residues outside the packaging region. Furthermore, exchange of the PB2, PA, and NS segments of H5N8 by those of H9N2 increased replication, polymerase activity and interferon antagonism of the H5N8 reassortants in human cells. Notably, H5N8 reassortants carrying the H9N2-subtype PB2 segment and to lesser extent the PA or NS segments showed remarkably increased virulence in mice as indicated by rapid onset of mortality, reduced mean time to death and increased body weight loss. Simultaneously, we observed that in chickens the H5N8 reassortants, particularly with the H9N2 NS segment, demonstrated significantly reduced transmission to co-housed chickens. Together, while the limited capacity for reassortment between co-circulating H9N2 and H5N8 viruses and the reduced bird-to-bird transmission of possible H5N8 reassortants in chickens may limit the evolution of such reassortant viruses, they show a higher replication potential in human cells and increased virulence in mammals.

Importance

The segmented nature of avian influenza viruses (AIV) genome enables the evolution of new virus variants by exchanging segments (reassortment) between two viruses upon co-infection of the same host-cell. Reassortment resulted in the evolution of pandemic and highly virulent influenza viruses in humans. Here, we studied the potential reassortment of two German AIV H5N8 and H9N2 and the impact on virus fitness in human cells, mice, and chickens. We found that H9N2 PB1 and NP were not compatible to replace the respective segments from H5N8, interestingly, due to genetic differences outside the packaging region. Importantly, H5N8 viruses carrying H9N2 PB2, PA, and NS segments exhibited high adaptation in human cells and remarkably increased virulence in mice. However, the reassortment between H5N8 and H9N2 negatively affected transmission in chickens. This study is important for zoonotic risk assessment after reassortment of H5N8 and H9N2 AIV similar to those used in this study.

Key words: avian influenza; H5N8, H9N2, clade 2.3.4.4, interspecies transmission; zoonoses; pandemic; reassortment; chicken; mice; interferon antagonism; polymerase activity.

1. Introduction

Avian influenza viruses (AIV) are members of the genus influenza A virus (IAV) in the family *Orthomyxoviridae*. The single-stranded negative-sense RNA genome consists of eight segments, which encode at least 10 viral proteins (Bouvier and Palese 2008) divided into two categories: structural (i.e. part of the virion) and non-structural components. The virion consists of the internal ribonucleoprotein (RNP) complex (encompassing polymerase basic subunit 1 (PB1) and subunit 2 (PB2), polymerase acidic protein (PA), nucleoprotein (NP), and viral RNA), the matrix protein 1 (M1), and the nuclear export protein (NEP). The virion envelope contains the hemagglutinin (HA), neuraminidase (NA), and matrix protein 2 (M2). Several non-structural proteins (e.g. NS1, PB1-F2, and PA-x) are not packaged into the virus particles, but are expressed in the host cell, and play important roles, for example, in interferon-antagonism, inflammatory response, or apoptosis. Some non-structural proteins are not necessarily present upon infection with every influenza virus (e.g. PB1-F2) (Bouvier and Palese 2008). The HA and NA of IAV are classified into 18 and 11 distinct subtypes, respectively (Bouvier and Palese 2008). H17, H18, N10, and N11 have not been found in avian species. The majority were identified in AIV from wild birds but also frequently isolated in poultry. While most of AIV exhibit low pathogenicity (LP) in the wild bird reservoir, AIV specifying H5 and H7 can become highly pathogenic (HP) after circulation of LP precursors in poultry (Alexander 2000). Due to the segmented nature of the viral genome, these segments can be exchanged (i.e. reassortment) between different viruses upon co-infection of the same host leading to the evolution of new virus variants with altered characteristics. Reassortment has resulted in strains that have caused pandemic outbreaks with devastating impacts on the human population (Mostafa et al. 2018).

H9N2 is the most widespread AIV subtype in poultry worldwide. Several clades of AIV H9N2 (e.g. G1, Y280, Korean or European lineages) are endemic in many countries in Asia, Europe and the Middle East (Fusaro et al. 2011). In poultry, some Asian H9N2 viruses exhibited mild-to-moderate virulence with or without co-infections with other viruses or bacteria (Guo et al. 2000; Kishida et al. 2004; Lee et al. 2011). Moreover, H9N2 viruses were isolated from humans in several countries (Freidl et al. 2014; Nagy, Mettenleiter, and Abdelwhab 2017). Importantly, H9N2 viruses donated internal segments to other AIV generating zoonotic reassortant viruses, like AIV A/Goose/Guangdong/1/1996 H5N1 (GsGD96) (Guan et al. 1999), the 2013 H10N8 (Chen et al. 2014), and the continuously circulating 2013 H7N9 (Pu et al. 2015).

GsGD96-like viruses continue to pose a serious public health threat. From 1996 to date, the virus evolved into 10 phylogenetic clades (clade 0 to 9) and multiple subclades. While most of these subclades disappeared, clade 2.3.4.4 viruses are still circulating in wild and domestic birds. Since 2009, the reassortment of the H5 HA segment of clade 2.3.4.4 with other AIV subtypes resulted in the evolution of H5N1-, H5N2-, H5N3-, H5N5-, H5N6- and H5N8-subtypes in wild and domestic birds (Lee et al. 2017). These viruses have spread from South Korea and China to many Asian, European, and North American countries. This panzootic spread of AIV H5 clade 2.3.4.4 was alarming for both poultry and human health. Although the pathogenicity of clade 2.3.4.4 H5Nx viruses in mammals varied considerably, some viruses (e.g. H5N6, H5N2) were able to infect mammals including humans causing mild to fatal infections (Kim et al. 2014; Pulit-Penaloza et al. 2015; Kaplan et al. 2016; Pan et al. 2016; Wang et al. 2016, 2017; Kwon et al. 2018; Lee et al. 2018). Interestingly, unlike human-pathogenic H7N9 or H10N8 AIVs (Guan et al. 1999; Chen et al. 2014; Pu et al. 2015), sequence analysis of the H5N8 clade 2.3.4.4 indicated no relationship to H9N2-derived segments (Kwon et al. 2018). Since 2016, an unprecedented number of H5N8 clade 2.3.4.4 outbreaks was reported in birds in Europe (Napp et al. 2018; Pohlmann et al. 2018), where H9N2 is semi-endemic posing a continuous risk for reassortment (Reid et al. 2016; Świętoń et al. 2018). The reassortment of avian and human transmission influenza viruses may result in the occurrence of influenza pandemics, since the human population is naïve for such viruses and high mortality rates are expected (Mostafa et al. 2018). The relevance of a scenario is highlighted by the fact that pandemic influenza viruses in 1957, 1968, and 2009 possessed segments, particularly PB2, PB1, and/or PA, from avian origin viruses (Mostafa et al. 2018).

Here, we studied the impact of potential reassortment between two recent German H5N8 clade 2.3.4.4 and H9N2 viruses on replication in human cells and virulence in mice and chickens.

2. Materials and methods

2.1 Viruses and cells

German H5N8, H9N2, and Tk14 were provided by Timm Harder at FLI, Riems and H9N2-G1-like was obtained from the Center of Scientific Excellence for Influenza Viruses, National Research Centre, Egypt. MDCK-II and HEK293T were obtained from the cell culture collection at FLI Insel Riems. Calu-3 and A549 were obtained from the Institute of Medical Virology, Justus Liebig

University Giessen, Germany. NHBE (Lonza) were prepared according to manufacturer's instructions. CEK cells were prepared from 18-day-old SPF embryonated chicken eggs (VALO BioMedia) (Hennion and Hill 2015).

2.2 Generation of Recombinant Viruses

All genomic segments of H5N8 and H9N2 were amplified and cloned in pHW vector and viruses were rescued in MDCK-II and HEK293T cells (Stech et al. 2008; Mostafa et al. 2015). H9N2 was rescued and propagated in cell culture in the presence of N-tosyl-L-phenyalanine chloromethyl ketone (TPCK)-trypsin. All viruses were propagated in 9- to 11-day-old SPF eggs and viruses were maintained at −80 °C until use.

2.3 Sequence Analysis

RNA of recombinant viruses was extracted using the QIAamp Viral RNA Mini Kit and transcribed into cDNA using the Omniscript Reverse Transcription Kit (Qiagen). All segments were purified from gel slices after Phusion RT-PCR (Stech et al. 2008) using the Qiagen Gel Extraction Kit (Qiagen) and subjected for Sanger sequencing using the ABI BigDye Terminator v.1.1 Cycle Sequencing Kit (Applied Biosystems). Sequences of German viruses in this study were submitted to GISAID and assigned isolate identity numbers 486439, 486440, and 486441. The Egyptian H9N2 virus had NCBI accession numbers MK190705 to MK190710 for the internal gene segments. Comparison between H9N2 and H5N8 genomes was done by Geneious v.11.1.5 (Biomatters). Tertiary structures of PB1 and NP were generated using SWISS-Model (https://swissmodel.expasy.org) and PyMol software (https://pymol.org).

2.4 Replication kinetics in primary human and chicken cells

NHBE cells were differentiated under air-liquid conditions as described (Matrosovich et al. 2004). NHBE and CEK were infected with recombinant viruses at an MOI of 0.01 for the indicated time periods. TPCK-trypsin was added for the replication of H9N2 in CEK, but not in NHBE cells. Cells were harvested and the virus titer was determined using foci assay (FA) (Ma et al. 2010). TPCK-trypsin was used for the titration of H9N2 only. The test was performed in triplicates and in three independent biological replicates. Each sample was titrated in duplicates.

2.5 Replication kinetics in human cells

Replication of recombinant H5N8/H9N2 viruses in human cells was determined in A549 and Calu-3 cells infected at an MOI of 0.01 for 1 h. The inoculum was removed and cells were treated with citrate buffer saline pH 3 and washed using phosphate buffer saline (PBS, MP Biomedicals). Minimal essential medium (MEM) containing 0.2 per cent bovine serum albumin (BSA) was added and cells were incubated for the indicated time periods at 33 °C, 37 °C, and/or 39 °C. TPCK-trypsin was added for the replication of H9N2 in A549 cells. Cell culture supernatants were harvested and stored at −80 °C until titration.

2.6 Virus titration

Virus titration in this study was determined by plaque assay in MDCK-II cells (Abdelwhab et al. 2016) except for replication in human cell culture which was performed by FA as described (Ma et al. 2010). TPCK-trypsin was added for the titration of H9N2 only.

2.7 Minigenome luciferase assay

The luciferase assay was performed using Dual-Luciferase Reporter Assay System (Promega) (Petersen et al. 2018). Briefly, confluent HEK293T cells were transfected with 1 µg of PB2, PB1, PA, and NP from H5N8 and/or H9N2 or empty pHW2000 plasmids mixed with 40 ng Renilla luciferase expression plasmid pRL-SV40 (Promega) and 200 ng p125-Luc Firefly luciferase expression plasmid containing the luciferase reporter gene (Yoneyama et al. 1998). Transfection was performed using Trans-IT2020 (Mirus) for 8 h at 33 °C and 39 °C (Mostafa et al. 2013). Relative luminometer units (RLU) of each reaction were normalized to Renilla luciferase and the results are expressed as x-fold change compared to the negative control.

2.8 Detection of interferon-beta (IFN-β) response in cell culture

Amplification of the IFN-β mRNA in A549 infected with the indicated viruses at an MOI of 1 for 24 h was done as previously published (Petersen et al. 2018). The relative expression in infected and non-infected cells was calculated using the 2^-(ΔΔct) method (Livak and Schmittgen 2001).

2.9 Flow cytometry

A549 cells were infected at an MOI of 1 with H5N8, H5N8_NS, and H5N8_PB2-PA-NS at 33 °C or 39 °C. At 24 hpi, cells and supernatant were harvested and centrifuged at 1,100 rpm for 5 min and washed with PBS. Separated cells were stained with live/dead dye Zombie Aqua™ Fixable (Biolegend) for 20 min, then washed with MEM media containing 10 per cent FCS and fixed and permeabilized with True-Nuclear™–reagent (Biolegend) for 30 min. Cells were stained with primary mouse-anti-NP antibody (ATCC-HB65) for 30 min followed by rat-anti-mouse IgG2a-PE (Dianova) as secondary antibody for 30 min. Cells were washed with FACS-Buffer and analyzed via FACS. Cells were analyzed by excluding doublets (FSC-A vs. FSC-H) and dead cells (Zombie Aqua+).

2.10 Ethic statement

Experiments were carried out in the biosafety level-3 animal facilities of the FLI according to the German Regulations for Animal Welfare and after approval of the authorities (permission number: 7221.3-1-060/17) and the commissioner for animal welfare at the FLI representing the Institutional Animal Care and Use Committee (IACUC).

2.11 Infection of mice

Four-week-old female BALB/C mice (Charles River) were allocated in closed ISOcage system (Tecniplast) and were left to adapt for 5 days before challenge. At the day of challenge (d0), all mice were weighed and individually marked. For each virus, mice received either 10^5 ($n=11$) or 10^3 ($n=8$) pfu in 50 µl MEM. One control group ($n=8$) received 50 µl sterile medium (sham group). Inoculation was performed under mild anesthesia using Isoflurane (CP-Pharma). Mice were observed daily for clinical signs and the daily BW per gram was expressed relative to the BW of each mouse at d0. All mice that had lost more than 25 per cent of the d0-BW were humanely killed and scored dead. After

3 dpi, three mice per group were euthanized using isoflurane. The whole brain, one lung, and half of the spleen were collected and homogenized using TissueLyzer® (Qiagen) at ratio 1 g/1 ml PBS and stored at −80 °C until further use. The second half of the spleen was used for flow cytometry analysis. The experiment ran for 11 dpi, all surviving mice were humanely killed using isoflurane and cervical dislocation. MTD was calculated.

2.12 Virus replication in mice

Brain, lungs, and spleen of mice were weighed (w/v) and homogenized and the virus titer was determined by plaque assay. Viral RNA was extracted automatically by RNA Extraction Kit (Macherey Nagel). The amount of viral RNA in homogenized samples was also detected by RT-qPCR (Hoffmann et al. 2016).

2.13 Detection of IFN-β response in the lung of mice

Lungs were collected at 3 dpi, weighed (w/v), and homogenized. The total RNA was extracted from homogenized lung tissues using Trizol and RNeasy Kit (Qiagen). The cDNA was synthesized from 400 ng RNA using the Prime Script 1st Strand cDNA Synthesis Kit (TaKaRA) and Oligo dT Primer (TaKaRa). Quantification of IFN-β transcripts was done using SYBR® GreenER™ qPCR SuperMIX Universal Kit (Invitrogen) and generic primers (Kim et al. 2003; Li, Moltedo, and Moran 2012). The x-fold change of normalized samples to β-actin transcripts (Petersen et al. 2018) compared to the control mice was calculated using the 2^-(ΔΔct) method.

2.14 Detection of cell-mediated immunity in the spleen of mice

At 3 dpi, the spleen was removed and single cell suspensions were prepared for flow cytometry analysis. T-cell subsets and activation status were identified with fluorescent dye-labeled antibodies against the following murine surface antigens: CD3 (clone 17A2), APC-Cy7; CD4 (clone GK1.5), FITC; CD8 (clone 53-6.7), APC; CD69 (clone H1.2F3), PE-Cy7 (Biolegend). All incubation steps were carried out for 15 min at 4 °C in the dark. The iNKT cell subtype was detected by PE-labeled, empty or PBS57-loaded, CD1d Tetramer (NIH tetramer Core Facility). For iNKT staining, tetramers were incubated for 30 min, in the dark. Cells were washed in fluorescence-activated cell sorting (FACS) buffer and analyzed by Flow cytometer BD Fortessa and FACS DIVA software (BD Biosciences).

2.15 Infection of chickens

Six-week-old SPF chickens were randomly allocated into six groups. Ten chickens were inoculated with $10^{3.7}$ pfu/bird and five naïve birds were added at 1 dpi to each group. Birds were observed daily for morbidity and mortality. Clinical scoring was given and the PI and MTD were calculated as previously done (Abdelwhab el et al. 2016). Chickens were kept on the floor in separate rooms (one group per room) at the BSL3 facilities of the FLI. In each room, water was supplied with cup and bell drinkers and feed was provided in wide grid metal troughs and flat containers. Temperature and light were regulated automatically and all stables were cleaned daily by water. Each room contained a video camera.

2.16 Virus excretion and seroconversion

Swabs were collected from surviving or freshly dead birds and virus titer was determined by plaque assay. Furthermore, detection of viral RNA was determined as previously described (Hoffmann et al. 2016) after automatic extraction. Sera collected at the end of experiments were examined using 'ID screen Influenza A Antibody Competition Multispecies Kit' enzyme-linked immunosorbent assay (ELISA) (IDvet) in Infinite® 200 PRO reader (TECAN).

2.17 Histopathology and immunohistochemistry

Tissues from chickens ($n=3$ per group) inoculated with H5N8, H5N8_NS, or H5N8_PB2-PA-NS were collected in 10 per cent neutral phosphate buffer formalin. Sample processing, hematoxylin and eosin (HE) staining, and immunohistochemistry was performed as published (Breithaupt et al. 2011), but with using a monoclonal antibody against the M protein of IAV (ATCC clone HB-64, 1:200, at 4 °C overnight). Necrosis was scored on a scale 0 to 3+: 0 = no lesion, 1+ = mild, 2+ = moderate, 3+ = severe. Viral antigen was scored on a labeling scale 0 to 3+: 0 = negative, 1+ = focal to oligofocal, 2+ = multifocal, 3+ = coalescing foci or diffuse labelling (blinded study).

2.18 Statistics

Statistical analysis for swab and organ samples, replication kinetics, immune response, polymerase activity, and bodyweight gain were done using non-parametric Kruskal–Wallis and Mann–Whitney Wilcoxon tests with post-hoc Tukey tests. Survival durations were analyzed using log-rank Mantel–Cox test. Results were considered statistically significant at p value < 0.05. All analysis was done by GraphPad Prism software.

3. Results

3.1 Compatibility of European H9N2 and clade 2.3.4.4 H5N8 segments in reassortment

To assess the ability of A/turkey/Germany/R1685/2016 (H9N2) (designated H9N2) to reassort with HPAIV A/tufted duck/Germany/8444/2016 (H5N8) clade 2.3.4.4 subclade B (designated H5N8) in human-embryonic kidney 293T (HEK293T) cells, genome segments of H5N8 were replaced by single segments of H9N2 using reverse genetic systems in a 7+1 approach. All H9N2 segments, except PB1 and NP, yielded H5N8 infectious viruses indicating an incompatibility for exchanging these two segments (Fig. 1A). These results were confirmed in two different laboratories and using different rescue strategies. Conversely, H9N2 virus carrying H5N8 PB1 and/or NP segments were successfully rescued (data not shown). Reassortment of H5N8 with H9N2 M segment, however, produced only low progeny virus titers after propagation in eggs and, therefore, was not used for further characterization.

To further determine whether H9N2 segments generally show a restricted compatibility to reassort with HPAIV H5N8, segments of H5N8 were replaced by segments of G1-like A/chicken/Egypt/S12568C/2016 (H9N2) (designated H9N2-G1-like). Only the PB2 and PA of H9N2-G1-like yielded infectious H5N8 viruses and the rescue of a reassortant H5N8 virus with NS from H9N2-G1-like was not successful. Interestingly, NS1 proteins of H5N8 and H9N2-G1-like belong to allele A, while German H9N2 NS1 belongs to allele B (w). Moreover, swapping single segments of the current H5N8 virus with another HPAIV A/turkey/

A

No.	Virus	PB2	PB1	PA	HA	NP	NA	M	NS	HA titer	pfu/mL (log10)
1	**H5N8**									256	6.3
2	**H9N2**	■	■	■	■	■	■	■	■	128	6.6
3	**H5N8_PB2**	■								256	6.3
4	H5N8_PB1		■							neg	neg
5	**H5N8_PA**			■						256	6.3
6	H5N8_HA				■					1024	7.4
7	H5N8_NP					■				neg	neg
8	H5N8_NA						■			16	7.9
9	H5N8_M							■		16	5.1
10	**H5N8_NS**								■	256	6.3
11	**H5N8_PB2-PA-NS**	■		■					■	256	6.6
12	H5N8_PB1-NP-M		■			■		■		neg	neg
13	H5N8_PB1-HA		■		■					neg	neg
14	H5N8_PB1-NA		■				■			neg	neg
15	H5N8_NP-HA				■	■				neg	neg
16	H5N8_NP-NA					■	■			neg	neg
17	H5N8_PB1-Chimera1		▒							4	4.1
18	H5N8_PB1-Chimera2		▒							neg	neg
19	H5N8_NP-Chimera3					▒				16	5.3
20	H5N8_NP-Chimera4					▒				neg	neg

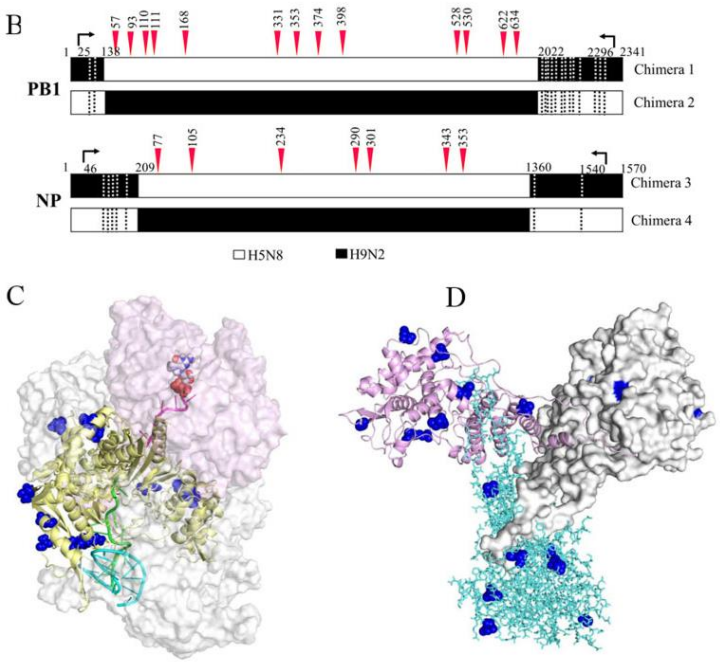

Figure 1. Genetic compatibility of H5N8 and H9N2 viruses in this study. Results of H5N8 virus rescue after exchanging segments with European H9N2 virus showing hemagglutination (HA) titer and virus titers in plaque forming units (pfu/ml). neg – virus rescue was not successful (A). Chimera of PB1 and NP segments were generated by exchanging the non-coding regions at the 5and 3ends of H5N8 (white) and H9N2 (black). Silent mutations in these non-coding regions are shown as dotted lines while amino acid exchanges are shown in red triangles and the positions are written in black. The length of PB1 and NP was 2341 and 1570 nucleotides, respectively. Amino acid sequences were deduced from ORFs of PB1 (positions 25 to 2296) and NP (positions 46 to 1540). Numbering of the amino acids starts from the start codon (B). Tertiary structures of the H5N8-PB1 (yellow ribbons) interacting with PA and PB2 (C) and homotrimers of NP (D) were predicted using SWISS-Model. RNAs interacting with PB1 residues are shown in red, green, and cyan. Amino acid differences in the H5N8 PB1 and NP are shown as blue spheres.

Table 1. Genetic identity of different gene segments of H5N8 and H9N2 used in this study.

Segment	Number of nt differences (%)	Number of aa differences (%)	Positions (H9N2-x-H5N8)
PB2	188 (91.8%)	5 (99.3%)	I260V, R376K, D678F, V717A, N759K
PB1	119 (94.8%)	13 (98.3%)	M57T, S93A, T110A, V111M, K168R, D331E, R353K, A374T, E398D, A528T, V530I, C622G, Q634H
PA	117 (94.6%)	16 (97.8%)	L4F, A85T, V86M, D101E, K113R, E216D, A277S, L290F, I311M, P325L, I354V, G386D, V407I, K615R, D629E, I649L
NP	42 (97.2%)	7 (98.6%)	R77K, G105V, V234A, N290D, V301I, I343V, I353F
M1	40 (94.7%)	7 (97.2%)	A33V, R134K, F144L, M165I, V166A, K230R, R242K
M2	10 (96.6%)	5 (94.9%)	D13N, V28I, R45H, I51V, E66G
NS1	211 (69.6%)	76 (65.0%)	Too many to count
NS2	75 (79.5%)	24 (80.2%)	I6M, T7L, Q14M, V19M, E22G, V26E, E36G, R37S, R39K, I40L, S48T, A63G, T64K, N67E, E68Q, S70G, A81E, C83V, N85H, I86R, T88K, K89I, L100M, S111Q

nt, nucleotides; aa, amino acids.

Germany-MV/AR2487/2014 (H5N8) clade 2.3.4.4 subclade A (designated tk14) yielded infectious viruses (data not shown). This indicates that there are genetic incompatibilities for reassortment between H5N8 and H9N2 viruses used in this study.

To determine possible constraints for reassortment of H9N2 PB1 and NP with H5N8, we compared sequences between H5N8 and H9N2 segments (Table 1). Fifteen and seven silent nucleotide (nt) differences in the PB1 and NP, respectively, were observed in the non-coding regions (NCR), but no differences in the amino acid (aa) sequence (Fig. 1B and Table 1). Conversely, thirteen and seven non-synonymous differences were found in the respective open reading frame (ORF) (Fig. 1B). We therefore generated four chimeric PB1 and NP segments carrying exchanged NCRs from either H5N8 or H9N2 (Chimera 1: $PB1_{H5N8}$/$NCRs_{H9N2}$; Chimera 2: $PB1_{H9N2}$/$NCRs_{H5N8}$; Chimera 3: NP_{H5N8}/$NCRs_{H9N2}$; Chimera 4: NP_{H9N2}/$NCRs_{H5N8}$). Infectious H5N8 viruses were obtained only with PB1 or NP chimeras containing the ORFs from H5N8 (Chimeras 1 and 3) indicating that the NCRs of the different genomes do not affect functionality of the respective H5N8 genes (Fig. 1A and B). These results suggest that differences in the gene coding sequences and not in the packaging signal regions are responsible for the genetic incompatibility between H5N8 and H9N2 segments.

To achieve a better understanding of the possible effects caused by the aa differences between the H9N2 and H5N8 PB1 and NP proteins (Table 1), we superimposed the aa differences in the two H9N2 proteins onto the tertiary structure of the respective H5N8 proteins (Fig. 1C and D). The aa differences in the H5N8 PB1 are positioned in 'finger' or 'thumb' domains (Lo, Tang, and Shaw 2018). The aa differences in the H5N8 NP are highly variable among IAVs (Kukol and Hughes 2014) and are essential for NP-NP homo-oligomerization, PB2 binding and/or interaction with the tail loop (Ng, Wang, and Shaw 2009).

To study the impact of H9N2 segments on H5N8 fitness, we rescued six recombinant viruses: H5N8, H9N2, and H5N8 variants carrying H9N2 PB2 (H5N8_PB2), H9N2 PA (H5N8_PA), H9N2 NS (H5N8_NS), or H9N2 PB2, PA, and NS (H5N8_PB2-PA-NS). The replication of these viruses in two primary cell cultures (chicken embryo kidneys (CEK) and normal human bronchial epithelial cells (NHBE)) and two human cell lines (A549 and Calu-3 cells) was studied. Polymerase activity and interferon (IFN)-β response in A549 cells were determined. Furthermore, the impact of reassortment on H5N8 virulence, replication, IFN-β response, and T-cell activation in mice and virulence, excretion, tissue distribution, and transmission in chickens was studied.

3.2 Influence of H9N2 segments on H5N8 replication in CEK cells

CEK cells were infected at multiplicity of infection (MOI) of 0.01 for 1, 8, 12, 24, and 36 h at 37 °C. AIV H5N8 replicated to significantly higher levels than AIV H9N2 at each time point ($P < 0.003$) (Fig. 2A–D). Exchange of the PA and NS segments significantly increased replication of H5N8 at 8 hour post-infection (hpi) ($P < 0.0006$), while substitution of PB2 or all three segments had no effect ($P > 0.3$). At 12 and 36 hpi, all H5N8 reassortants replicated to similar levels as H5N8 virus ($P > 0.1$). At 24 hpi, H5N8_PB2-PA-NS replicated to slightly higher titers than H5N8 virus ($P = 0.045$) (Fig. 2A–D). Together, small differences in virus titers in CEK were only observed at 8 hpi for H5N8_PA and H5N8_NS and at 24 h for H5N8_PB2-PA-NS.

3.3 H9N2 NS segment alone or in combination with the PB2 and PA segments increased replication of H5N8 in NHBE cells

NHBE cells represent a good *ex vivo* model for studying IAV-infection of well-differentiated human primary airway cells with characteristics such as goblet and ciliated cells (Davis et al. 2015). NHBE cells were infected at an MOI of 0.01 for 1, 6, 12, 24, and 36 hpi at 37 °C. While H9N2 did not replicate on NHBE cells, the H5N8 replicated at moderate levels. Although H5N8_PB2 and H5N8_PA replicated at comparable levels as H5N8, H5N8_NS, and H5N8_PB2-PA-NS replicated to significantly higher titers ($P < 0.001$). Remarkably, replication of H5N8_PB2-PA-NS was observed earlier than other viruses (Fig. 2E–H). Taken together, H9N2 NS segment alone or in combination with the PB2 and PA segments increased replication of H5N8 in primary human bronchial epithelial cells.

3.4 H5N8 reassortants carrying either H9N2 NS or PB2, PA and NS gain significantly increased replication ability in human lung cells at lower respiratory tract temperature

Virus replication in human cells at 33 °C (e.g. upper respiratory tract temperature), 37 °C (e.g. lower respiratory tract

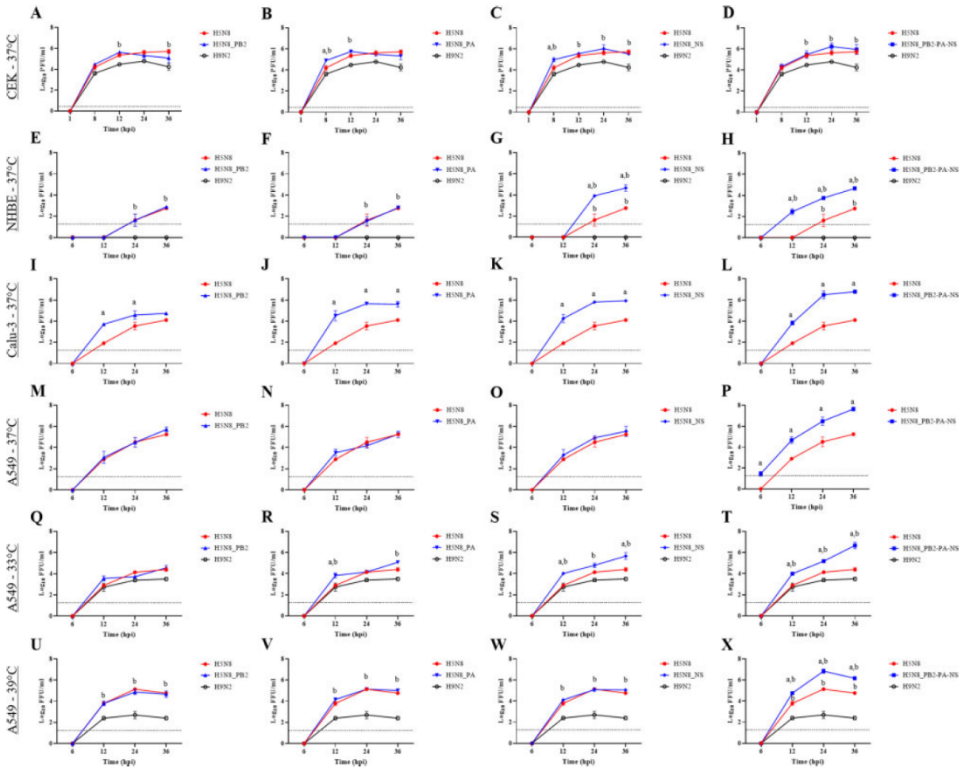

Figure 2. Replication of selected recombinant viruses in cells of avian or human origin. Replication of indicated viruses was analyzed in chicken embryo kidney cells (A–D), differentiated normal human bronchial epithelial cells (E–H), Calu-3 (I–L), and A549 (M–X) infected with an MOI of 0.01 for indicated time points. Significant differences compared to H5N8 and H9N2 viruses at P-value <0.05 are shown by letters 'a' and 'b', respectively. All cells were incubated after infection at 37 °C and additionally A549 cells were incubated at 33 °C (Q–T) or 39 °C (U–X). TPCK-trypsin was added for the replication of H9N2 in all cells, except NHBE cells. 0 values shown in the y-axis indicate no plaques or foci were detected in 400 µl or 50 µl per well, respectively. Dashed lines indicate the predicted low detection limit (LOD) of plaque and foci assays in this study (i.e. < 1 pfu/ffu in 400 µl or 50 µl, respectively).

temperature), and/or 39 °C (e.g. fever) was studied. Replication kinetics of recombinant viruses were compared in Calu-3 cells at 37 °C (Fig. 2I–L) and in A549 cells at 33 °C, 37 °C and 39 °C (Fig. 2M–X). At 37 °C, recombinant H5N8 replicated to only low titer compared to other reassortant H5N8 viruses in Calu-3 cells and virus progeny was first detected at 12 hpi and reached a maximum titer at 36 hpi (Fig. 2I–L). The replication of H5N8 increased significantly after reassortment with H9N2 PB2, PA, and/or NS (Fig. 2I–L). In A549 cells at 37 °C, the reassortment with PB2, PA, or NS segments independently did not affect the replication of the reassortant H5N8 (Fig. 2M–P). However, H5N8_PB2-PA-NS replicated earlier and exhibited significantly higher titers than other viruses (Fig. 2P).

In A549 cells, H5N8 virus replication was significantly higher at 39 °C than at 33 °C ($P < 0.05$) (Fig. 2Q–X), while H9N2 replicated at lower titers than H5N8 viruses particularly at 39 °C (Fig. 2Q–X). At 33 °C, the H5N8_NS demonstrated significantly higher titers at 12 and 36 hpi (Fig. 2S) and replication of H5N8_PB2-PA-NS was significantly higher than H5N8 at all periods (Fig. 2T). At 39 °C, H5N8_PB2-PA-NS replicated to higher levels compared to the H5N8 virus (Fig. 2X). In summary, the combination of H9N2 PB2, PA, and NS segments significantly increased the replication of H5N8 in different human lung cells at different temperatures.

3.5 H9N2 PA reduced the polymerase activity of H5N8 at 33 °C and 39 °C, while PB2 only increased the polymerase activity at 39 °C

The impact of PB2 and PA on polymerase activity was assessed by a minigenome luciferase assay in HEK293T cells. The relative luciferase activity of the different minigenome compositions was compared to the wild-type H5N8 segments (Fig. 3A). At 33 °C, the activity of H9N2 polymerase was similar to that of H5N8, but greatly (75%) reduced at 39 °C. However, the H9N2 PB2 or PA combined with NP and the remaining polymerase subunits of H5N8 reduced the polymerase activity at 33 °C by 20 per cent ($P < 0.001$) (Fig. 3A). At 39 °C, the H9N2 PA resulted in a stronger reduction of the polymerase activity leading to a 55 per cent activity reduction compared to the wild-type H5N8 ($P < 0.001$). Conversely, H9N2 PB2 significantly increased (40%)

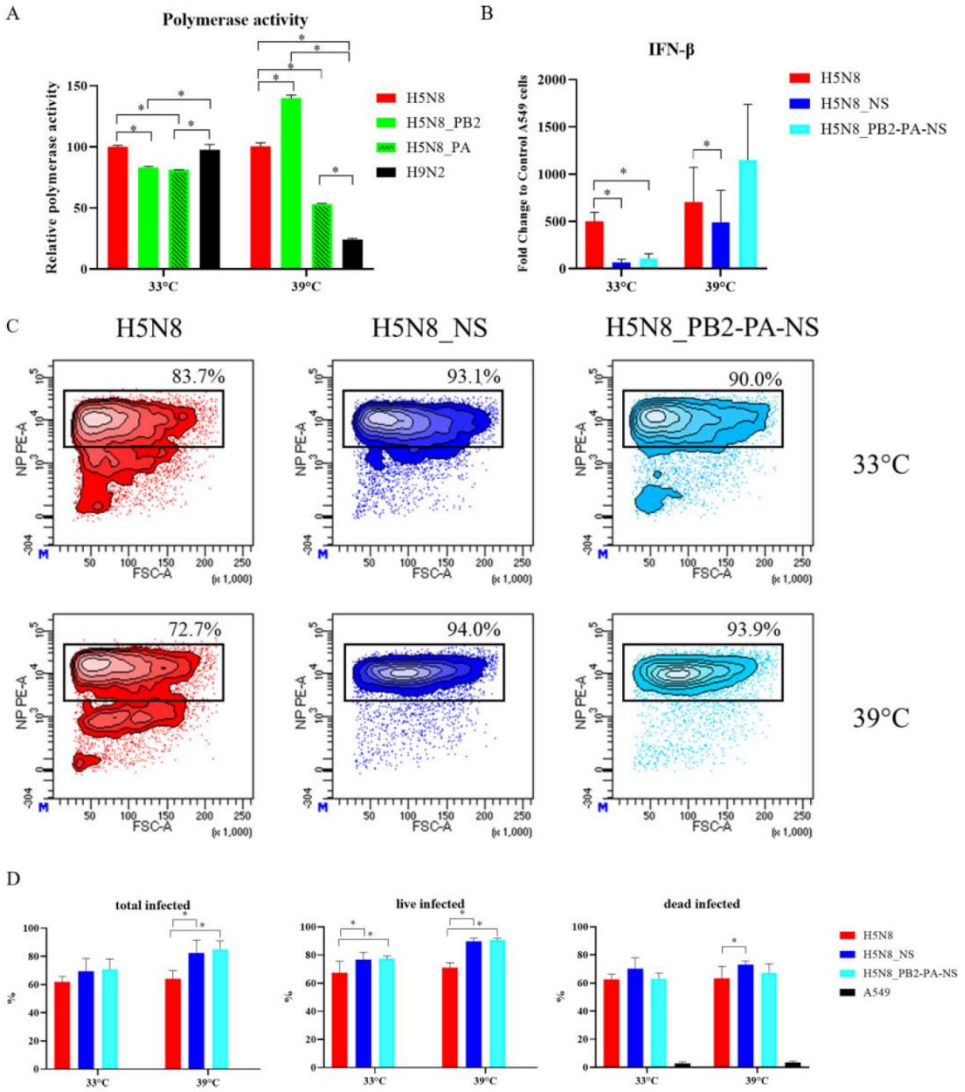

Figure 3. The impact of H9N2 segments on polymerase activity, interferon response, and number of infected A549 cells. Polymerase activity in human kidney embryonic cells (HEK293T) of indicated viruses normalized to the activity of H5N8 and expressed as x-fold change at 33 and 39 °C (A). Fold change induction of interferon-β in A549 cells of indicated viruses normalized to cells without infection inoculated with PBS at 33 °C or 39 °C (B). Representative results of flow cytometry after infection of A549 at MOI of 1 with H5N8 (red), H5N8_NS (dark blue), or H5N8_PB2-PA-NS (light blue) for 24 h at 33 °C (upper panel) or 39 °C (lower panel) (C). Infected, NP highly positive cells are given as percentages from total living cells based on uninfected control cells. The test was done in duplicates and repeated three times and results are shown as average and standard deviations of all replicates (D). Significant differences compared to H5N8 and H9N2 viruses at P-value <0.05 are shown.

the polymerase activity in combination with the other H5N8 NP and subunits at 39 °C ($P < 0.001$) (Fig. 3A). Generally, H9N2 PA and PB2 affected the polymerase activity of H5N8 in a temperature-dependent manner. While H9N2 PB2 supported higher polymerase activity of H5N8 at human lower respiratory tract temperature, PA significantly reduced the polymerase activity, which may explain the low activity of H9N2 at human lower respiratory tract temperature.

3.6 Compared to H5N8, the reassortant H5N8 carrying the H9N2 NS increased the IFN-β response in human A549 lung cells in a temperature-dependent manner

The amount of IFN-β gene expression was quantified via real-time reverse-transcription PCR (RT-qPCR) by amplification of mRNA of A549 cells 24 hpi with H5N8_NS or H5N8_PB2-PA-NS at either 33 °C or 39 °C. The results were normalized to the β-actin mRNA and expressed as x-fold change. The IFN-β response in H5N8 virus infected cells at 33 °C was 207-fold lower than the response at 39 °C (Fig. 3B). At 33 °C, the level of IFN-β gene expression in cells infected with H5N8_NS or H5N8_PB2-PA-NS was reduced compared to the H5N8 by 392- and 432-fold, respectively (Fig. 3B). Conversely, at 39 °C, H5N8_NS increased the IFN-β response by 441-fold compared to wild-type H5N8 infected cells and by 1,040-fold compared to cells infected with the reassortant H5N8_NS at 33 °C (Fig. 3B). Collectively, H9N2 NS inhibited IFN-β response of H5N8 at human upper respiratory tract temperature and increased IFN-β response at lower respiratory tract temperature.

3.7 Compared to H5N8, the reassortant H5N8 carrying the H9N2 NS significantly infected higher number of human A549 lung cells

To test whether the number of infected cells correlate with the pattern for IFN-β response, A549 cells were infected at MOI of 1 for 24 h with H5N8, H5N8_NS, or H5N8_PB2-PA-NS at either 33 °C or 39 °C (Fig. 3C and D). The total number of cells as well as the number of viable or dead cells infected with different viruses were calculated using flow cytometry and standard anti-NP-antibodies (Fig. 3C and D). The results showed that the total number of cells and the number of viable cells infected with H5N8 was slightly higher, although not statistically significant, at 39 °C than at 33 °C ($P > 0.4$). Conversely, the total number and number of viable cells infected with H5N8_NS or H5N8_PB2-PA-NS was higher at 39 °C than at 33 °C ($P < 0.03$). The total number of cells infected with H5N8_NS or H5N8_PB2-PA-NS was higher than H5N8 at 33 °C and 39 °C although statistical differences were only observed at 39 °C ($P < 0.0003$). The number of viable cells infected with H5N8_NS or H5N8_PB2-PA-NS was significantly higher than H5N8 at 33 °C and 39 °C ($P < 0.01$). There were no statistical differences between the number of cells infected with H5N8_NS or H5N8_PB2-PA-NS at both temperatures ($P \geq 0.1$). The number of dead cells was significantly higher after the infection with H5N8_NS than H5N8 at 39 °C ($P < 0.02$). Altogether, H9N2 NS significantly increased the number of live infected cells, which is partially correlated with the inhibition of IFN-β response particularly at the human upper respiratory tract temperature.

3.8 H5N8 reassortants carrying the H9N2 PB2, PA or NS alone or in combination demonstrated increased virulence in mice as indicated by rapid onset of mortality

Mice inoculated intra-nasally with 10^5 plaque forming units (pfu) (high dose) (Fig. 4A) or 10^3 pfu (low dose) of each virus (Fig. 4B) were observed for 11 days and the mean time to death (MTD) was calculated. Four days after high dose inoculation only two mice infected with H9N2 had to be sacrificed because of drastic (>25%) body weight (BW) reduction (Fig. 4A). Mice infected with H5N8 virus died between 3 and 6 dpi with MTD of 4.1 days (Fig. 4A) similar to mice infected with reassortant H5N8 carrying segments from H9N2 that died within 4 dpi. Mice infected at high dose with H5N8_PB2 started to die at 1 dpi with MTD of 2.8 days. In the groups infected with H5N8_PA, H5N8_NS, and H5N8_PB2-PA-NS mice started to die at day 3 and the MTD values were estimated to be 3.2, 3.5, and 3.5 days, respectively (Fig. 4A). The survival durations of H5N8_PB2 and H5N8_PA inoculated mice were significantly shorter than those inoculated with H5N8 ($P < 0.008$). None of the mice in the sterile medium-inoculated group (sham group) died. After low dose inoculation, all mice inoculated with H9N2 survived. Mice infected with H5N8 virus died within 9 dpi with MTD of 7.2 days (Fig. 4B). Mortality started at day 5 in groups of mice inoculated with H5N8_PB2 and H5N8_PB2-PA-NS and 6 dpi in groups of mice inoculated with H5N8_NS or H5N8_PA with MTD values of 6.2, 7, 7.2, and 5.6 days, respectively (Fig. 4B). Mice inoculated with H5N8_PB2-PA-NS exhibited significantly shorter survival duration than H5N8-inoculated mice ($P < 0.013$). Taken together, H9N2 segments increased virulence of H5N8 in mice as indicated by rapid onset of mortality and short survival durations.

3.9 The impact of reassortment of H5N8 with H9N2 on body weight of inoculated mice

After high dose inoculation, animals showed reduction in BW at 1 dpi compared to the relative BW immediately before infection and compared to the control group (Fig. 4C). H9N2 inoculated mice exhibited a transient reduction in BW at 2 and 3 dpi and the BW started to increase at 4 dpi to the end of the experiment, although at significantly lower levels than the control group ($P < 0.01$) (Fig. 4C). Mice inoculated with H5N8 viruses showed drastic reduction in BW until the day of death or killing and the reduction in BW gain was statistically significant compared to the sham and H9N2-inoculated groups ($P < 0.001$). Compared to H5N8, significant reduction in BW was observed in H5N8_NS inoculated mice at 1–3 dpi ($P < 0.0002$), in H5N8_PA and H5N8_PB2 inoculated mice at 1 and 3 dpi ($P < 0.0001$) and in H5N8_PB2-PA-NS at 2 dpi ($P < 0.001$) (Fig. 4C). After low dose inoculation, H9N2 had no effect on the BW, while H5N8 viruses caused significant reduction in BW of inoculated mice. The reassortment with H9N2 PA or NS did not significantly alter the impact of H5N8 on BW. However, H5N8_PB2 and H5N8_PB2-PA-NS viruses at 3–5 dpi and 2–5 dpi, respectively caused significant increased reduction in the BW compared to the wild-type H5N8 virus ($P < 0.001$) (Fig. 4D). These results indicate a specific impact of the H9N2 PB2, PA, and NS segments particularly when combined in BW loss after infection with H5N8.

3.10 Reassortment of H5N8 with H9N2 did not lead to significant increase of viral titers in the lungs of infected mice

The titer of viruses in the lungs, brain, and spleen homogenates from humanely killed or deceased high-dose inoculated mice at 3 dpi was determined by plaque test in MDCKII (Fig. 4E). Viruses were recovered from the lungs of all inoculated mice at comparable titers (~10^4 PFU/g) and there was no significant difference in viral titers between different groups (Fig. 4E). Infectious virus was detected in the brain of H5N8-inoculated mice (~$10^{3.3}$ PFU/g), H5N8_PB2 (~$10^{2.0}$ PFU/g), and H5N8_PA (~$10^{2.0}$ PFU/g) only (data not shown). No infectious virus was detected in the spleen of any mouse. Generally, H9N2 PB2, PA, or NS segments did not significantly increase H5N8 load in the lungs of infected mice.

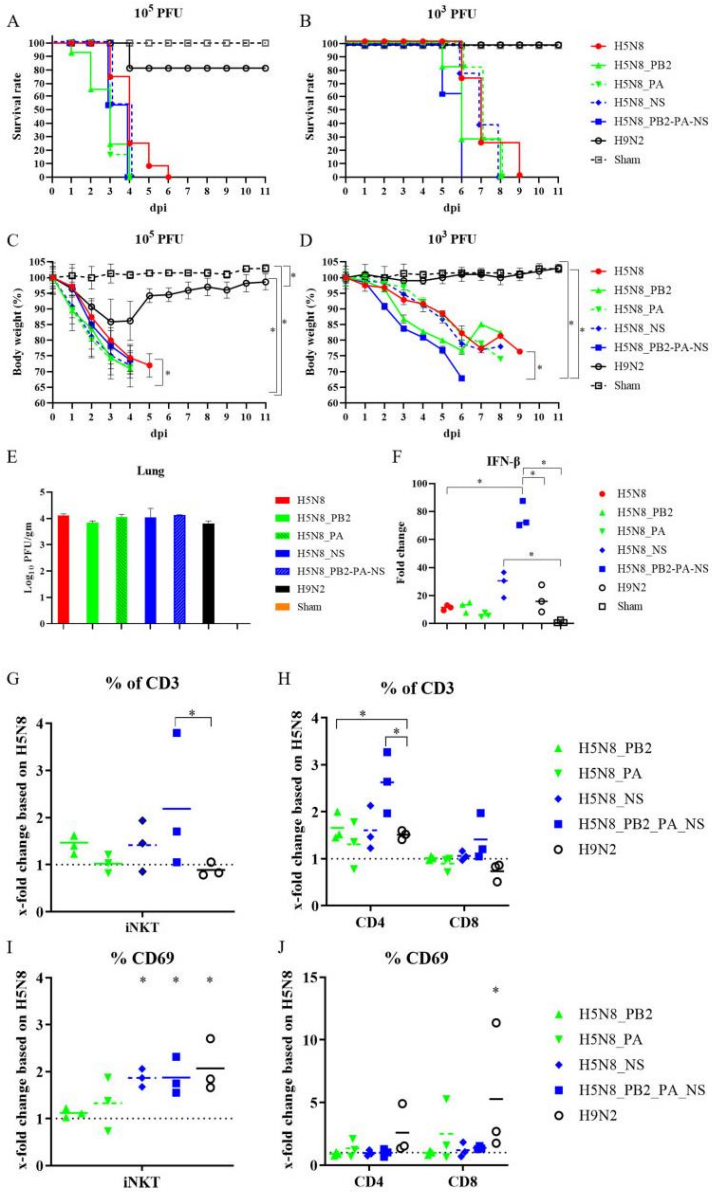

Figure 4. The impact of H9N2 PB2, PA, and NS segments on viral fitness of reassortant H5N8 in mice. Mortality and BW loss after intra-nasally high dose inoculation (10^5 pfu/mouse) (A, C) or with low dose 10^3 pfu/mouse (B, D). Mice that lost more than 25 per cent of BW at day 3 were humanely killed after deep anesthesia by Isoflurane and cervical dislocation. Significant differences compared to mice inoculated with H5N8, H9N2, or sham group at *P*-value <0.05 are shown (C, D). Viral titers in lung samples obtained from high-dose inoculated mice were determined by plaque assay in MDCKII and expressed as plaque forming unit per gram (PFU/gm). (E). Results of IFN-β expression in the lungs of high-dose inoculated mice at 3 dpi ($n-3$). Fold change of IFN-β mRNA was normalized to sham mice shown as individual and average values (F). T-cell frequencies and activation in the spleen of high-dose inoculated mice ($n-3$) at 3 dpi. Frequency of iNKT cells and CD4+ and CD8+ T-cells among CD3+ cells (G, H) and frequency of CD69+ iNKT cells (I). Asterisks in panels I and J refer to significant differences compared to H5N8. Results were normalized to H5N8-inoculated mice with 10^5 pfu.

3.11 H9N2 NS alone or in combination with PB2 and PA significantly increased IFN-β response in the lungs of infected mice

IFN-β mRNA in the lungs of high-dose inoculated mice at 3 dpi was quantified and normalized to the β-actin mRNA for each sample (Fig. 4F) (Livak and Schmittgen 2001). H5N8_PB2-PA-NS and H5N8_NS increased the expression of IFN-β by 59- and 22-fold, respectively. H9N2 infection increased the IFN-β response by 13-fold, while the recombinant wild-type H5N8 and H5N8_PB2 mounted an IFN-β activation at similar levels, ~9-fold. H5N8_PA was slightly less efficient to induce IFN-β response compared to other viruses, although H5N8_PA inoculated mice expressed IFN-β at 5-fold higher than the control group (Fig. 4F). These results indicate that H9N2 segments particularly NS affected IFN-β response in the lungs of H5N8-infected mice.

3.12 Reassortment with H9N2 activated iNKT cells in the spleen of inoculated mice in a dose-dependent manner

To get an insight into the impact of H5N8 reassortment with H9N2 on T-cell response using flow cytometry analysis, spleen samples were collected from mice at 3 dpi. Results were normalized to the H5N8 response after subtraction of values from the control group (Fig. 4G–J). High dose inoculation with H5N8_PB2-PA-NS resulted in increased frequencies of iNKT, CD4+, and CD8+ cells among CD3+ lymphocytes in the spleen compared to the wild-type H5N8 infected mice. Interestingly, H5N8_NS and H5N8_PB2-PA-NS significantly activated iNKT cells, measured by CD69 expression, in the same amount as the H9N2 control and in contrast to wild-type H5N8. Activation of classical CD4+ and CD8+ T cells failed after infection with these viruses (Fig. 4G–J). Inoculation of mice with 10^3 pfu H9N2 did not significantly affect the stimulation of iNKT cells compared to the control group (data not shown). Altogether, H9N2 NS increased activation of early responding iNKT cells in the spleen after infection with high dose of H5N8 virus.

3.13 In chickens, reassortment with H9N2 NS had a negative impact on chicken-to-chicken transmission

Ten chickens were inoculated oculonasally and five contact chickens were added 1 dpi to each group. Birds were observed for 10 dpi. The pathogenicity index (PI) based on the daily clinical scoring for each bird ranging from 0 (avirulent) to 3 (highly virulent) and MTD were calculated. All H9N2-inoculated birds survived without showing clinical signs. All H5N8 inoculated birds died within 2 days (H5N8_NS, H5N8_PB2-PA-NS, and H5N8 inoculated chickens) or 3 days (H5N8_PB2 and H5N8_PA inoculated chickens) with comparable PI values of 2.7 and MTD of 2.8 (H5N8_PB2), 2.2 (H5N8_PA), or 2.0 (H5N8_NS, H5N8_PB2-PA-NS, and H5N8) (Fig. 5A). Contact birds to chickens inoculated with H9N2, H5N8_NS or H5N8_PB2-PA-NS did not show any clinical signs and remained healthy. All contact birds to chickens inoculated with H5N8 and H5N8_PB2 died with MTD of 4 and 7.6 dpi (3 and 6.6 days post contact). Only 3/5 contact chickens to chickens inoculated with H5N8_PA died with MTD of 4.7 dpi (3.7 days post contact) (Fig. 5B) and the two remaining birds did not exhibit any clinical signs. The survival durations of contact chickens to H5N8_PB2 and H5N8_PA-inoculated chickens were significantly longer than that of chickens cohoused with H5N8-inoculated chickens ($P < 0.002$). These results indicate that the reassortment with H9N2, particularly H9N2 NS segment, reduced bird-to-bird transmission of H5N8 virus without significant impact on virulence in inoculated chickens.

Virus excretion was determined in oropharyngeal (OP) and cloacal (CL) swabs and different organs 2 dpi by plaque assay in MDCKII cells. The results are expressed as plaque forming units per ml (PFU/ml) (Fig. 5C). The titers of all H5N8 viruses in inoculated chickens were comparable ($P > 0.1$). H9N2 was not recovered from any chicken although all inoculated chickens seroconverted, while H5N8 viruses were excreted at higher levels from the cloaca than the oropharynx. All H5N8-inoculated chickens died within 3 dpi and, therefore, no swabs were taken at 4 dpi. No infectious virus was obtained from contact chickens after titration of samples using plaque test at any time point and all surviving contact chickens were negative for anti-NP antibodies. However, viral RNA was detected in 4/5 and 3/5 chickens co-housed with chickens inoculated with H5N8_PB2 or H5N8_PA at 4 dpi, respectively (data not shown). These results indicate that the reassortment with H9N2 NS segment reduced the excretion of H5N8 viruses to undetectable limits in contact chickens.

Replication and viral tissue tropism were compared at 2 dpi in chickens inoculated with H5N8, H5N8_NS, or H5N8_PB2-PA-NS by plaque test (Fig. 6), histopathology, and immunohistochemistry (Table 2 and Supplementary Fig. S1). Compared to H5N8, the titer of infectious viruses in organs of inoculated chickens was generally reduced after inoculation with H5N8_NS and to lesser extent with H5N8_PB2-PA-NS (Fig. 6). H5N8 yielded the highest tissue necrosis score and most abundant viral antigen distribution, followed by H5N8_NS and least H5N8_PB2-PA-NS (Table 2 and Supplementary Fig. S1). Differences in necrosis scores were most obvious in duodenum, liver, and thymus, and for antigen distribution in liver, kidney, and thymus (Table 2). In the lung and heart, antigen distribution and necrosis did not differ significantly between groups. In particular, H5N8 was associated with a ubiquitous endotheliotropism that was markedly restricted after H5N8_NS and even more after H5N8_PB2-PA-NS infection, particularly in the liver, kidney, pancreas, and gastrointestinal tract (Table 2 and Supplementary Fig. S1). Together, the results from the chicken experiments indicate that the reassortment of H5N8 virus particularly with H9N2 NS segment has a negative impact on transmission and virus excretion in contact chickens.

4. Discussion

Although AIV H9N2 was the donor of non-HA/NA segments for AIV, which were highly virulent in humans (Guan et al. 1999; Fusaro et al. 2011; Pu et al. 2015), there are no published data for natural reassortment of the internal genes of H9N2 with H5N8, since 2016 so far. Here, we analyzed the compatibility of two recent German H9N2 and H5N8 clade 2.3.4.4 viruses to reassort and studied the impact of reassortment on H5N8 fitness *in vitro* and *in vivo*. Only the H9N2 PB2, PA, and NS segments resulted in infectious reassortant H5N8 viruses with high titers, while H9N2 PB1 and NP were not compatible with productive replication of the other H5N8 segments used in this study. It is worth mentioning that the adaptation of AIV in specific hosts (wild vs. domestic birds) may affect the range of reassortment between H5N8 and H9N2 in this study (Lu, Lycett, and Leigh Brown 2014). While H9N2 viruses can circulate undetected in poultry, HPAIV-infected poultry are usually culled (Alexander 2000). Therefore, some H9N2-AIV may adapt to domestic birds, while the unprecedented incursions of H5N8 into poultry worldwide was mostly via separate direct or indirect contact at the wildlife-domestic

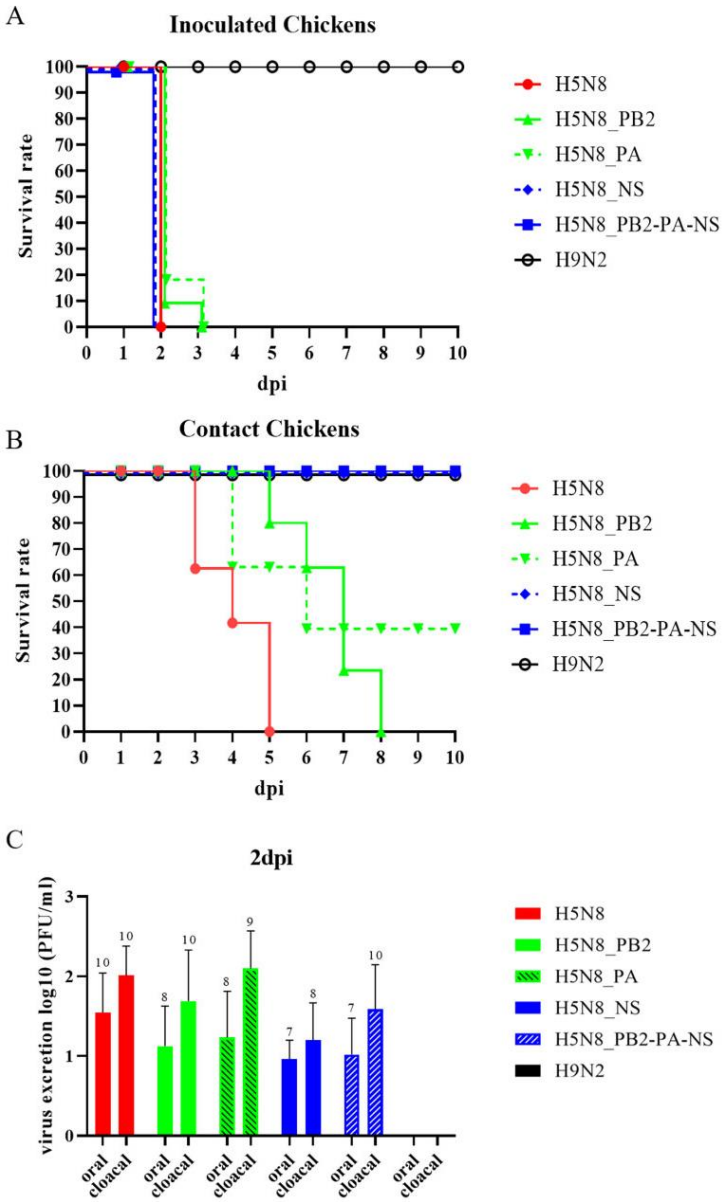

Figure 5. The impact of H9N2 PB2, PA, and NS on H5N8 virus fitness in chickens. Survival rate of chickens inoculated with different viruses via oculonasal route (A) and survival rate of contact chickens (B). Virus excretion at 2 dpi from inoculated chickens was determined using plaque test in MDCKII. Numbers refer to number of chickens tested positive out of 10 inoculated chickens (C).

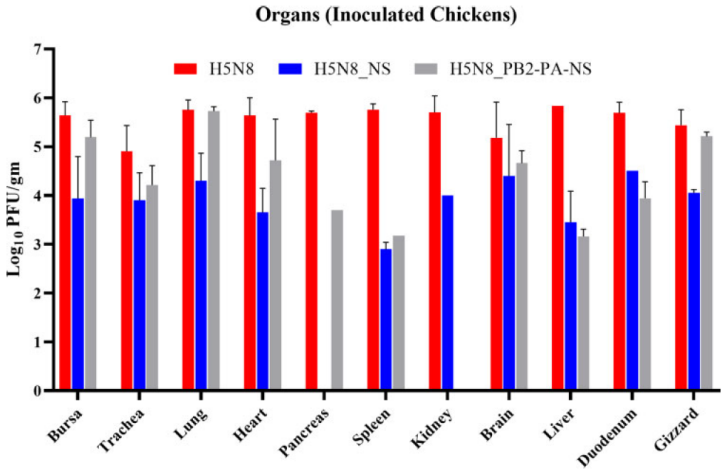

Figure 6. The impact of H9N2 PB2, PA, and NS on H5N8 virus replication in chicken organs. Viral titers in different organs of inoculated-chickens at 2 dpi were determined using plaque test in MDCKII cells. Results are shown as average and standard deviation of positive samples.

animal interface with limited lateral spread in poultry holdings (Mulatti et al. 2018; Poen et al. 2018; Pohlmann et al. 2018). Furthermore, the reassortment of H5 clade 2.3.4.4 yielding diverse H5Nx viruses occurred mainly via exchange of the NA segment and it occurred mostly in wild birds (Lee et al. 2017). Recently, the isolation of reassortant H5N2 viruses from poultry in Egypt, where both H5N8- and H9N2-AIV are endemic, has been described in farmed broilers and ducks after obtaining the H9N2 NA or H5N8 HA segments (Hagag et al. 2019; Hassan et al. 2020). No evidence is available for reassortment of internal segments. Interestingly, H5N8 detected in wild birds in Germany in 2016/2017 were found to possess varying PB1 segments and the evolution of H5N5 was associated with acquisition of novel PB1 and NP segments (Pohlmann et al. 2018). Findings of this study may explain this variation of PB1 and NP during the introduction of H5N8 in Europe in 2016/2017.

Reassortment may be limited due to RNA–RNA, RNA–protein or protein–protein interaction constrains (Lowen 2017). Along this line, it has recently been reported that RNA packaging signal regions restrict reassortment of human H3N2 and avian H5N8 and H7N9 viruses (White et al. 2019). Another study showed that the interaction of RNA with specific NP amino acids governed the successful reassortment of bat H17N10 and seal H7N7 viruses in mammalian cells (Moreira et al. 2016; Bolte et al. 2019). In the current study, H9N2 PB1 and NP were not compatible with the other H5N8 proteins although they were more similar on the nucleotide level than the compatible PB2, PA, and NS segments. Intriguingly, this incompatibility was due to differences in the ORF and not in the packaging region and was not associated with HA and/or NA genes as previously observed (White et al. 2019). Therefore, it is tempting to assume that incompatibility of H5N8 and H9N2 segments occurs possibly on the protein–protein interaction level, which remains to be investigated. No data are available so far on the biological function of these peculiar H5N8 PB1 and NP differences, which merit further investigation.

The efficient influenza virus replication, including H9N2, in mammalian cells via increased replication speed or decreased sensitivity to antiviral effectors can be strain specific (Kurokawa et al. 1999; Grimm et al. 2007; Dittmann et al. 2008). Compared to some Asian H9N2 viruses (SJCEIRS-H9-Working-Group 2013), H9N2 virus in this study did not replicate efficiently in human cells probably due to high adaptation to birds conferred by the HA (e.g. receptor binding). Despite limitations for H5N8/H9N2 reassortment, findings in the current study provide strong evidence that H9N2 internal segments can increase the replication of H5N8 virus in mammalian cells as recently described for some Egyptian H5N1/H9N2 reassortants (Arai et al. 2019). Although H9N2 segments had minor effect on virus replication in primary chicken cells, the synergism between H9N2 PB2, PA, and NS resulted in significant high replication of H5N8 in all human cells used in this study independent of temperature. Nevertheless, different replication levels of H5N8/H9N2 reassortants were observed in NHBE, A549, and Calu-3, which is in line with variable replication of some influenza viruses in these cells in other studies (Gerlach et al. 2013; Kanrai et al. 2016). Although it remains to be identified, this variation in replication of H5N8/H9N2 reassortants in different cells may be attributed to some cellular and viral factors. NHBE cells are a pseudostratified primary differentiated bronchial epithelial cell culture containing ciliated and non-ciliated cells and are more closely related to the *in-vivo* situation. Calu-3 cells are a bronchial epithelial adenocarcinoma cell line isolated from a 25-year-old Caucasian male, while A549 cells are thought to be a type II alveolar epithelial cell line isolated from a human pulmonary adenocarcinoma (Papazian, Würtzen, and Hansen 2016). Calu-3 and NHBE cells are airway epithelial cells; however, in Calu-3 each H9N2 segment increased H5N8 replication, while in NHBE cells only H9N2 NS segment had a significant impact on multiple-cycle replication of H5N8.

An obvious shortcoming here is that we did not measure IFN-β expression in different cell cultures after the infection

Table 2. Histopathology and tissue tropism in chickens.

		H5N8_NS		H5N8_PB2-PA-NS		H5N8	
	Cell tropism and necrosis score	Max score[a]	Group score[b]	Max score[a]	Group score[b]	Max score[a]	Group score[b]
Lung	Endothelium	+++	6	+++	8	+++	9
	Respiratory epithelium	++	6	+++	7	+++	8
	Necrosis score	+++	7	+++	9	+++	9
Heart	Endothelium	++	4	+	3	+++	8
	Myocardium	++	6	++	6	++	6
	Necrosis score	++	4	++	5	++	4
Proventriculus	Endothelium	++	4	+++	7	+++	9
	Mucosal / glandular epithelium	++	5	++	6	+++	7
	Necrosis score	+	2	+	3	++	5
Gizzard	Endothelium	+++	3	+++	n.c.[c]	+++	n.c.[c]
	Mucosal epithelium	+	2	+	n.c.[c]	++	n.c.[c]
	Necrosis score	+	2	+	n.c.[c]	+	n.c.[c]
Duodenum	Endothelium	+++	4	++	4	+++	9
	Mucosal epithelium	0	0	+	1	++	5
	Necrosis score	0	0	0	0	+	2
Cecum	Endothelium	++	3	++	4	+++	9
	Mucosal epithelium	++	3	++	2	++	4
	Necrosis score	+	1	++	2	++	3
Cecal tonsil	Endothelium	+	2	+	3	+++	9
	Immune cells	+	1	+	2	++	5
	Necrosis score	++	6	++	6	+++	9
Pancreas	Endothelium	++	2	0	0	+++	8
	Parenchymal epithelium	+	2	+	1	+	3
	Necrosis score	0	0	+	1	+	2
Liver	Endothelium	+	1	+	1	+++	9
	Parenchymal epithelium	+	1	++	4	++	6
	Necrosis score	+	2	+	2	++	6
Kidney	Endothelium	+	2	+	1	+++	9
	Parenchymal epithelium	+	2	+	1	++	4
	Necrosis score	+	1	+	1	++	5
Spleen	Endothelium	++	n.c.[c]	++	4	+++	n.c.[c]
	Immune cells	++	n.c.[c]	++	6	++	n.c.[c]
	Necrosis score	++	n.c.[c]	+++	9	+++	n.c.[c]
Bursa	Endothelium	++	4	++	6	+++	9
	Mucosal epithelium	0	0	0	0	0	0
	Immune cells	+	3	+	3	++	5
	Necrosis score	++	4	+	3	++	6
Thymus	Endothelium	++	5	++	6	+++	9
	Immune cells	++	5	+++	8	+++	9
	Necrosis score	++	5	+++	7	+++	8
Brain	Endothelium	++	3	+++	6	+++	9
	Neurons, glia, epithelium	++	5	++	3	++	6
	Necrosis score	++	4	++	3	++	6

Necrosis scoring and detection of viral antigen in chickens infected with H5N8_NS, H5N8_PB2-PA-NS, or H5N8, three animals per group. Necrosis scoring on a scale 0 to 3+: 0 = no lesion, 1+ = mild, 2+ = moderate, 3+ = severe. Antigen detection on a labeling scale 0 to 3: 0 = negative, 1+ = focal to oligofocal, 2+ = multifocal, 3+ = coalescing foci or diffuse labeling.

[a]Max score: maximum of tissue score reached in this group.

[b]Group score, sum of '+' in this group.

[c]n.c.: not calculated, not all tissues present for evaluation.

with different H5N8/H9N2 reassortants to elucidate the role of PB2 and PA in the inhibition of IFN-response (Hayashi, MacDonald, and Takimoto 2015a; Gao et al. 2019) or to quantify IFN-β levels in different cells (Hsu et al. 2012). Nevertheless, our results revealed that H5N8 viruses carrying H9N2 NS was more efficient to inhibit IFN-β response, which was correlated with the increased number of live infected cells. Therefore, it is likely that after the infection of NHBE cells with H5N8_PB2 or H5N8_PA H5N8 NS was not as efficient as H9N2 NS to block the IFN-β response or the number of infected cells was too low to support high virus replication and thus increased IFN-β-inhibition. Conversely, in Calu-3 H9N2 PA and to lesser extent PB2 increased the replication of H5N8. The differentiated NHBE cells differ physiologically from the monoculture cells (e.g. Calu-3 or A549) in mucin secretion, receptor distribution, proteases, and IFN-β response and the replication of different influenza viruses may vary in different cells of the human respiratory tract (Matrosovich et al. 2004; Chan et al. 2010; Kreft et al. 2015; Gerlach et al. 2017). Moreover, PB2 and PA play a role in the inhibition of innate immune response (e.g. IFN-β) (Graef et al. 2010; Zhao et al. 2014; Hayashi, MacDonald, and Takimoto 2015a; Gao et al. 2019), and synergism with NS1 is required for efficient virus replication *in vivo* and *in vitro* (Varga et al. 2011; Nogales et al. 2017). It is worth mentioning that NS1 inhibit the innate immune response mostly by shutoff-active host IFN-related mRNAs and cytokine release, while PA-x preferentially degrades genes associated with cellular protein metabolism and protein repair (Chaimayo et al. 2018). Therefore, it is plausible that H9N2 PB2 or PA, through different cell-dependent pathways than by NS1, may inhibit the innate immune responses in Calu-3 cells. Furthermore, it is reasonable to suggest that higher replication of H5N8_PB2 in Calu-3 is also attributed to the higher polymerase activity conferred by PB2 at high temperature as previously described (Bradel-Tretheway et al. 2008). Although H9N2 NS significantly reduced IFN-β response and increased the number of H5N8-infected alveolar epithelial cells (i.e. A549) at different temperature, it was astonishing that single H9N2 did not increase H5N8 replication at high temperature. Surprisingly, data on the underlying mechanism for variable susceptibility of Calu-3 and A549 to influenza viruses are scarce, although both cell lines are commonly used in influenza virus research. Calu-3 and A549 are different cell lines and they vary physiologically with different cell internalization and trafficking pathways (Capel et al. 2016; Papazian, Würtzen, and Hansen 2016; Lujan et al. 2019). Efficient replication of some influenza viruses in Calu-3 than in A549 was attributed to such physiological variations (e.g. to proteolytic enzymes (Böttcher et al. 2006; Bottcher-Friebertshauser et al. 2011)). The impact of H9N2 PB2, PA, and NS on different steps of virus replication in Calu-3 and A549 and interaction with cellular factors should be further investigated.

Another notion was that H5N8_PB2-PA-NS had higher IFN-β response at 39 °C, although not statistically significant, compared to H5N8. It should not be totally excluded that some influenza viruses can replicate at high levels despite the high interferon response (Penski et al. 2011; Petersen et al. 2018). Moreover, this relative inefficiency to block the IFN-β response can be probably compensated by the higher and early replication (Kurokawa et al. 1999) and/or higher polymerase activity conferred by PB2 at high temperature. Although at 33 °C the activity of H9N2 was similar to that of H5N8, H9N2 PB2, and PA reduced the polymerase activity of H5N8. Conversely, at 39 °C compared to H5N8, H9N2 exhibited significantly lower polymerase activity, which is mostly driven by the H9N2 PA. Recently, lower polymerase activity conferred by PA has been shown to drive the acquisition of mammal-adaptation markers in H7N9 PB2 (i.e. E627K) (Liang et al. 2019), known to increase polymerase activity in mammals. It has been recently shown that H5N8 viruses from 2016 to 2017 outbreak had a lower polymerase complex activity in human cells with minor impact on virus replication in cell culture (Vigeveno et al. 2020). This low polymerase activity was markedly increased with either the PB2 or PA of an H5N8 from 2014 to outbreak (Vigeveno et al. 2020). Similarly, PA of the pandemic-H1N1/2009 enhanced polymerase activity of chicken-origin H3N2 in mammalian cells at 37 °C, but not at the lower temperature of 34 °C (Bussey et al. 2011), which was restored by reassortment with PB2 (Hayashi et al. 2015b). Therefore, H9N2 PB2 and PA may balance the replication of the virus in human cells at different temperatures (i.e. in upper vs. lower respiratory tracts). It is worth mentioning that polymerase activity does not always correlate with the level of replication of influenza viruses in cell culture (Chin et al. 2014).

Previous studies showed the high compatibility of H5N1 and H9N2 for reassortment and increased virulence of reassortant H5N1 viruses in mammals after acquisition of H9N2 PB2, PA, NP, and/or NS (Hao et al. 2016; Arai et al. 2019). In the current study, H9N2 exhibited low virulence in mice. Conversely, H5N8 killed all mice inoculated with low or high dose and reassortment of H5N8 with H9N2 segments, particularly PB2, increased virus virulence as indicated by rapid onset of mortality, shorter MTD, and higher BW loss. PB2 was also associated with high virulence observed for some H5Nx in mice (Park et al. 2015; Wang et al. 2017). The interplay of NS1 with the immune system and the impact on mortality is well known. Here, H9N2 NS alone or in combination with PB2 and PA was not as efficient as the respective H5N8 segments to inhibit IFN-β or T-cell immune responses in lungs of infected mice. H5N8 NS in this study belongs to allele A, while H9N2 NS belongs to allele B, which blocked the IFN-β response less efficiently than allele A NS at 37 °C (Zohari et al. 2010). However, the ability of H9N2 NS to inhibit innate immune response in the upper respiratory tract as seen in A549 at 33 °C may support virus replication at early stage of infection. Conversely, H9N2 NS was not efficient to inhibit the IFN-β response at 39 °C (Szretter et al. 2009). Furthermore, an elevated IFN-β expression was mostly accompanied by an increased activation of early responding iNKT cells, which are able to improve the outcome of influenza virus infections (Kok et al. 2012) by mediating efficient NK and CD8+ T cell activation (Ishikawa et al. 2010). However, the infection exacerbated too fast to mount specific antiviral responses.

The reassortment between H5N8 and H9N2 segments did not affect virulence or early excretion of H5N8 in inoculated chickens. Strikingly, the reassortment with H9N2, particularly with the H9N2 NS segment, had a strong impact on chicken-to-chicken transmission as indicated by extended MTD or lack of morbidity, mortality, and virus excretion in contact birds. The impact of the NS segment was also previously demonstrated by our groups and others showing that the NS segment was important for virus replication and endotheliotropism of H7N1 in chickens (Abdelwhab el et al. 2016), virulence of H5N1 and transmission in chickens and/or mice (Li et al. 2006; Jiao et al. 2008), and increased replication of AIV and swine influenza viruses in mammalian cells (Kanrai et al. 2016; Petersen et al. 2018). Moreover, a recent study has shown that a Chinese H9N2 PB2 segment enhanced the fitness of H5N1 and H5N8 from earlier 2.3 clades in chickens (Hao et al. 2019), even though they are genetically different compared to the recent H5N8 clade 2.3.4.4b viruses.

In conclusion, findings of this study showed that the two recent European H9N2 and H5N8-clade 2.3.4.4b viruses used in this study had restricted compatibility for reassortment due to mutations outside the packing region. Although reassortment with H9N2 increased replication of H5N8 in human cells, it had a detrimental effect on transmission in chickens. This study is important for zoonotic risk assessment after reassortment of contemporary H5N8 and H9N2 AIV similar to those used in this study. Nevertheless, findings in this study might indicate the potential of reassortment in the evolution of H5N8 viruses with higher replication ability in human cells and virulence in mammals if reassortment occurred in other avian hosts (e.g. turkeys or ducks).

Data Availability

Viral genomic data is available in GISAID under accession numbers 486439, 486440 and 486441. All the other data are available upon request.

Supplementary data

Supplementary data are available at *Virus Evolution* online.

Acknowledgements

The authors are grateful to Timm C. Harder for providing the wild-type viruses, Takashi Fujita for providing the firefly-luciferase plasmid p125-Luc, Jana Schulz for help in statistical analysis, Dajana Helke, Nadine Bock, Stephanie Knoefel, Silke Rehbein and Silvia Schuparis for laboratory technical assistance, to Günter Strebelow for his assistance in sequencing, to Allison Groseth for providing positive controls for cytokine RT-qPCR, to Donata Hoffmann for providing the TissueLyzer, and to Steffen Weigend, Silvia Wittig and the animal caretakers at the FLI for their support in the animal experiments.

Conflict of interest: None declared.

Funding

This work was partially supported by grants from the Deutsche Forschungsgemeinschaft, Germany (DFG; AB 567/1-2 and DFG VE780/1-1 to E.M.A.), DELTA-FLU, Project ID: 727922 funded by the European Union under: H2020-EU as well as the German Centre for Infection Research (DZIF), partner site Giessen, Germany (TTU 01.806 Broad-spectrum Antivirals to Co-PI SP), DFG funded SFB 1021 (RNA viruses: RNA metabolism, host response, and pathogenesis, TP C01 to Co-PI SP), Science and Technology Development Fund (STDF), Egypt (contract number 5175 to M.A.A.), and National Research Centre (TT110801 and 12010126 to A.M.). The funders had no role in study design, data collection and analysis, decision to publish, or preparation of the manuscript.

References

Abdelwhab el, S. M. et al. (2016) 'Prevalence of the C-Terminal Truncations of NS1 in Avian Influenza a Viruses and Effect on Virulence and Replication of a Highly Pathogenic H7N1 Virus in Chickens', *Virulence*, 7: 546–57.

Alexander, D. J. (2000) 'A Review of Avian Influenza in Different Bird Species', *Veterinary Microbiology*, 74: 3–13.

Arai, Y. et al. (2019) 'Genetic Compatibility of Reassortants between Avian H5N1 and H9N2 Influenza Viruses with Higher Pathogenicity in Mammals', *Journal of Virology*, 93: e01969–18.

Bolte, H. et al. (2019) 'Packaging of the Influenza Virus Genome is Governed by a Plastic Network of RNA- and Nucleoprotein-Mediated Interactions', *Journal of Virology*, 93: e01861–18.

Böttcher, E. et al. (2006) 'Proteolytic Activation of Influenza Viruses by Serine Proteases TMPRSS2 and HAT from Human Airway Epithelium', *Journal of Virology*, 80: 9896–8.

Bottcher-Friebertshauser, E. et al. (2011) 'Inhibition of Influenza Virus Infection in Human Airway Cell Cultures by an Antisense Peptide-Conjugated Morpholino Oligomer Targeting the Hemagglutinin-Activating Protease TMPRSS2', *Journal of Virology*, 85: 1554–62.

Bouvier, N. M., and Palese, P. (2008) 'The Biology of Influenza Viruses', *Vaccine*, 26: D49–53.

Bradel-Tretheway, B. G. et al. (2008) 'The Human H5N1 Influenza a Virus Polymerase Complex is Active In Vitro over a Broad Range of Temperatures, in Contrast to the WSN Complex, and This Property Can Be Attributed to the PB2 Subunit', *Journal of General Virology*, 89: 2923–32.

Breithaupt, A. et al. (2011) 'Neurotropism in Blackcaps (*Sylvia atricapilla*) and Red-Billed Queleas (*Quelea quelea*) after Highly Pathogenic Avian Influenza Virus H5N1 Infection', *Veterinary Pathology*, 48: 924–32.

Bussey, K. A. et al. (2011) 'PA Residues in the 2009 H1N1 Pandemic Influenza Virus Enhance Avian Influenza Virus Polymerase Activity in Mammalian Cells', *Journal of Virology*, 85: 7020–8.

Capel, V. et al. (2016) 'Insight into the Relationship between the Cell Culture Model, Cell Trafficking and siRNA Silencing Efficiency', *Biochemical and Biophysical Research Communications*, 477: 260–5.

Chaimayo, C. et al. (2018) 'Specificity and Functional Interplay between Influenza Virus PA-X and NS1 Shutoff Activity', *PLoS Pathogens*, 14: e1007465.

Chan, R. W. et al. (2010) 'Influenza H5N1 and H1N1 Virus Replication and Innate Immune Responses in Bronchial Epithelial Cells Are Influenced by the State of Differentiation', *PLoS One*, 5: e8713.

Chen, H. et al. (2014) 'Clinical and Epidemiological Characteristics of a Fatal Case of Avian Influenza a H10N8 Virus Infection: A Descriptive Study', *The Lancet*, 383: 714–21.

Chin, A. W. H. et al. (2014) 'Influenza a Viruses with Different Amino Acid Residues at PB2-627 Display Distinct Replication Properties In Vitro and In Vivo: Revealing the Sequence Plasticity of PB2-627 Position', *Virology*, 468–470: 545–55.

Davis, A. S. et al. (2015) 'Validation of Normal Human Bronchial Epithelial Cells as a Model for Influenza a Infections in Human Distal Trachea', *Journal of Histochemistry & Cytochemistry*, 63: 312–28.

Dittmann, J. et al. (2008) 'Influenza a Virus Strains Differ in Sensitivity to the Antiviral Action of Mx-GTPase', *Journal of Virology*, 82: 3624–31.

Freidl, G. S. et al. (2014) 'Influenza at the Animal–Human Interface: A Review of the Literature for Virological Evidence of Human Infection with Swine or Avian Influenza Viruses Other than A(H5N1)', *Euro Surveillance*, 19: 20793.

Fusaro, A. et al. (2011) 'Phylogeography and Evolutionary History of Reassortant H9N2 Viruses with Potential Human Health Implications', *Journal of Virology*, 85: 8413–21.

Gao, W. et al. (2019) 'Prevailing I292V PB2 Mutation in Avian Influenza H9N2 Virus Increases Viral Polymerase Function and Attenuates IFN-Beta Induction in Human Cells', *Journal of General Virology*, 100: 1273–81.

Gerlach, R. L. et al. (2013) 'Early Host Responses of Seasonal and Pandemic Influenza a Viruses in Primary Well-Differentiated Human Lung Epithelial Cells', *PLoS One*, 8: e78912.

Gerlach, T. et al. (2017) 'pH Optimum of Hemagglutinin-Mediated Membrane Fusion Determines Sensitivity of Influenza a Viruses to the Interferon-Induced Antiviral State and IFITMS', *Journal of Virology*, 91: e00246.

Graef, K. M. et al. (2010) 'The PB2 Subunit of the Influenza Virus RNA Polymerase Affects Virulence by Interacting with the Mitochondrial Antiviral Signaling Protein and Inhibiting Expression of Beta Interferon', *Journal of Virology*, 84: 8433–45.

Grimm, D. et al. (2007) 'Replication Fitness Determines High Virulence of Influenza a Virus in Mice Carrying Functional Mx1 Resistance Gene', *Proceedings of the National Academy of Sciences of the United States of America*, 104: 6806–11.

Guan, Y. et al. (1999) 'Molecular Characterization of H9N2 Influenza Viruses: Were They the Donors of the "Internal" Genes of H5N1 Viruses in Hong Kong?', *Proceedings of the National Academy of Sciences of the United States of America*, 96: 9363–7.

Guo, Y. J. et al. (2000) 'Characterization of the Pathogenicity of Members of the Newly Established H9N2 Influenza Virus Lineages in Asia', *Virology*, 267: 279–88.

Hagag, N. M. et al. (2019) 'Isolation of a Novel Reassortant Highly Pathogenic Avian Influenza (H5N2) Virus in Egypt', *Viruses*, 11: 565.

Hao, X. et al. (2016) 'Reassortant H5N1 Avian Influenza Viruses Containing PA or NP Gene from an H9N2 Virus Significantly Increase the Pathogenicity in Mice', *Veterinary Microbiology*, 192: 95–101.

—— et al. (2019) 'The PB2 and M Genes of Genotype S H9N2 Virus Contribute to the Enhanced Fitness of H5Nx and H7N9 Avian Influenza Viruses in Chickens', *Virology*, 535: 218–26.

Hassan, K. E. et al. (2020) 'Novel Reassortant Highly Pathogenic Avian Influenza A(H5N2) Virus in Broiler Chickens', *Emerging Infectious Diseases*, 26: 129–33.

Hayashi, T., MacDonald, L. A., and Takimoto, T. (2015a) 'Influenza a Virus Protein PA-X Contributes to Viral Growth and Suppression of the Host Antiviral and Immune Responses', *Journal of Virology*, 89: 6442–52.

—— et al. (2015b) 'Identification of Influenza a Virus PB2 Residues Involved in Enhanced Polymerase Activity and Virus Growth in Mammalian Cells at Low Temperatures', *Journal of Virology*, 89: 8042–9.

Hennion, R. M., and Hill, G. (2015) 'The Preparation of Chicken Kidney Cell Cultures for Virus Propagation', *Methods in Molecular Biology*, 1282: 57–62.

Hoffmann, B. et al. (2016) 'Riems Influenza a Typing Array (RITA): An RT-qPCR-Based Low Density Array for Subtyping Avian and Mammalian Influenza a Viruses', *Scientific Reports*, 6: 27211.

Hsu, A. C. et al. (2012) 'Critical Role of Constitutive Type I Interferon Response in Bronchial Epithelial Cell to Influenza Infection', *PLoS One*, 7: e32947.

Ishikawa, H. et al. (2010) 'IFN-Gamma Production Downstream of NKT Cell Activation in Mice Infected with Influenza Virus Enhances the Cytolytic Activities of Both NK Cells and Viral Antigen-Specific CD8+ T Cells', *Virology*, 407: 325–32.

Jiao, P. et al. (2008) 'A Single-Amino-Acid Substitution in the NS1 Protein Changes the Pathogenicity of H5N1 Avian Influenza Viruses in Mice', *Journal of Virology*, 82: 1146–54.

Kanrai, P. et al. (2016) 'Identification of Specific Residues in Avian Influenza a Virus NS1 That Enhance Viral Replication and Pathogenicity in Mammalian Systems', *Journal of General Virology*, 97: 2135–48.

Kaplan, B. S. et al. (2016) 'Novel Highly Pathogenic Avian A(H5N2) and A(H5N8) Influenza Viruses of Clade 2.3.4.4 from North America Have Limited Capacity for Replication and Transmission in Mammals', *Msphere*, 1:e00003-16.

Kim, T. S. et al. (2003) 'Induction of Interleukin-12 Production in Mouse Macrophages by Berberine, a Benzodioxoloquinolizine Alkaloid, Deviates CD4+ T Cells from a Th2 to a Th1 Response', *Immunology*, 109: 407–14.

Kim, Y. I. et al. (2014) 'Pathobiological Features of a Novel, Highly Pathogenic Avian Influenza A(H5N8) Virus', *Emerging Microbes & Infections*, 3: e75.

Kishida, N. et al. (2004) 'Co-Infection of *Staphylococcus aureus* or *Haemophilus paragallinarum* Exacerbates H9N2 Influenza a Virus Infection in Chickens', *Archives of Virology*, 149: 2095–104.

Kok, W. L. et al. (2012) 'Pivotal Advance: Invariant NKT Cells Reduce Accumulation of Inflammatory Monocytes in the Lungs and Decrease Immune-Pathology during Severe Influenza a Virus Infection', *Journal of Leukocyte Biology*, 91: 357–68.

Kreft, M. E. et al. (2015) 'The Characterization of the Human Cell Line Calu-3 under Different Culture Conditions and Its Use as an Optimized in Vitro Model to Investigate Bronchial Epithelial Function', *European Journal of Pharmaceutical Sciences*, 69: 1–9.

Kukol, A., and Hughes, D. J. (2014) 'Large-Scale Analysis of Influenza a Virus Nucleoprotein Sequence Conservation Reveals Potential Drug-Target Sites', *Virology*, 454-455: 40–7.

Kurokawa, M. et al. (1999) 'Influenza Virus Overcomes Apoptosis by Rapid Multiplication', *International Journal of Molecular Medicine*, 3: 527–30.

Kwon, H. I. et al. (2018) 'Comparison of the Pathogenic Potential of Highly Pathogenic Avian Influenza (HPAI) H5N6, and H5N8 Viruses Isolated in South Korea during the 2016-2017 Winter Season', *Emerging Microbes & Infections*, 7: 1–10.

Lee, D. H. et al. (2017) 'Evolution, Global Spread, and Pathogenicity of Highly Pathogenic Avian Influenza H5Nx Clade 2.3.4.4', *Journal of Veterinary Science*, 18: 269–80.

Lee, Y. N. et al. (2011) 'Isolation and Characterization of a Novel H9N2 Influenza Virus in Korean Native Chicken Farm', *Avian Diseases*, 55: 724–7.

—— et al. (2018) 'Evaluation of the Zoonotic Potential of Multiple Subgroups of Clade 2.3.4.4 Influenza A (H5N8) Virus', *Virology*, 516: 38–45.

Li, W., Moltedo, B., and Moran, T. M. (2012) 'Type I Interferon Induction during Influenza Virus Infection Increases Susceptibility to Secondary *Streptococcus pneumoniae* Infection by Negative Regulation of Gammadelta T Cells', *Journal of Virology*, 86: 12304–12.

Li, Z. et al. (2006) 'The NS1 Gene Contributes to the Virulence of H5N1 Avian Influenza Viruses', *Journal of Virology*, 80: 11115–23.

Liang, L. et al. (2019) 'Low Polymerase Activity Attributed to PA Drives the Acquisition of the PB2 E627K Mutation of H7N9 Avian Influenza Virus in Mammals', *mBio*, 10: e01162.

Livak, K. J., and Schmittgen, T. D. (2001) 'Analysis of Relative Gene Expression Data Using Real-Time Quantitative PCR and the 2(-Delta Delta C(T)) Method', *Methods*, 25: 402–8.

Lo, C. Y., Tang, Y. S., and Shaw, P. C. (2018) 'Structure and Function of Influenza Virus Ribonucleoprotein', *Sub-Cellular Biochemistry*, 88: 95–128.

Lowen, A. C. (2017) 'Constraints, Drivers, and Implications of Influenza a Virus Reassortment', *Annual Review of Virology*, 4: 105–21.

Lu, L., Lycett, S. J., and Leigh Brown, A. J. (2014) 'Reassortment Patterns of Avian Influenza Virus Internal Segments among Different Subtypes', *BMC Evolutionary Biology*, 14: 16.

Lujan, H. et al. (2019) 'Refining In Vitro Toxicity Models: Comparing Baseline Characteristics of Lung Cell Types', *Toxicological Sciences*, 168: 302–14.

Ma, W. et al. (2010) 'The NS Segment of an H5N1 Highly Pathogenic Avian Influenza Virus (HPAIV) Is Sufficient to Alter Replication Efficiency, Cell Tropism, and Host Range of an H7N1 HPAIV', *Journal of Virology*, 84: 2122–33.

Matrosovich, M. N. et al. (2004) 'Human and Avian Influenza Viruses Target Different Cell Types in Cultures of Human Airway Epithelium', *Proceedings of the National Academy of Sciences of the United States of America*, 101: 4620–4.

Moreira, E. A. et al. (2016) 'A Conserved Influenza a Virus Nucleoprotein Code Controls Specific Viral Genome Packaging', *Nature Communications*, 7: 12861.

Mostafa, A. et al. (2013) 'Improved Dual Promotor-Driven Reverse Genetics System for Influenza Viruses', *Journal of Virological Methods*, 193: 603–10.

—— et al. (2015) 'Efficient Generation of Recombinant Influenza a Viruses Employing a New Approach to Overcome the Genetic Instability of HA Segments', *PLoS One*, 10: e0116917.

—— et al. (2018) 'Zoonotic Potential of Influenza a Viruses: A Comprehensive Overview', *Viruses*, 10: 497.

Mulatti, P. et al. (2018) 'Integration of Genetic and Epidemiological Data to Infer H5N8 HPAI Virus Transmission Dynamics during the 2016–2017 Epidemic in Italy', *Scientific Reports*, 8: 18037.

Nagy, A., Mettenleiter, T. C., and Abdelwhab, E. M. (2017) 'A Brief Summary of the Epidemiology and Genetic Relatedness of Avian Influenza H9N2 Virus in Birds and Mammals in the Middle East and North Africa', *Epidemiology and Infection*, 145: 3320–33.

Napp, S. et al. (2018) 'Emergence and Spread of Highly Pathogenic Avian Influenza A(H5N8) in Europe in 2016–2017', *Transboundary and Emerging Diseases*, 65: 1217–26.

Ng, A. K., Wang, J. H., and Shaw, P. C. (2009) 'Structure and Sequence Analysis of Influenza a Virus Nucleoprotein', *Science in China Series C: Life Sciences*, 52: 439–49.

Nogales, A. et al. (2017) 'Interplay of PA-X and NS1 Proteins in Replication and Pathogenesis of a Temperature-Sensitive 2009 Pandemic H1N1 Influenza a Virus', *Journal of Virology*, 91: e00720.

Pan, M. et al. (2016) 'Human Infection with a Novel, Highly Pathogenic Avian Influenza A (H5N6) Virus: Virological and Clinical Findings', *Journal of Infection*, 72: 52–9.

Papazian, D., Würtzen, P. A., and Hansen, S. W. K. (2016) 'Polarized Airway Epithelial Models for Immunological Co-Culture Studies', *International Archives of Allergy and Immunology*, 170: 1–21.

Park, S. J. et al. (2015) 'Dynamic Changes in Host Gene Expression Associated with H5N8 Avian Influenza Virus Infection in Mice', *Scientific Reports*, 5: 16512.

Penski, N. et al. (2011) 'Highly Pathogenic Avian Influenza Viruses Do Not Inhibit Interferon Synthesis in Infected Chickens but Can Override the Interferon-Induced Antiviral State', *Journal of Virology*, 85: 7730–41.

Petersen, H. et al. (2018) 'NS Segment of a 1918 Influenza a Virus-Descendent Enhances Replication of H1N1pdm09 and Virus-Induced Cellular Immune Response in Mammalian and Avian Systems', *Frontiers in Microbiology*, 9: 526.

Poen, M. J. et al. (2018) 'Local Amplification of Highly Pathogenic Avian Influenza H5N8 Viruses in Wild Birds in The Netherlands, 2016–2017', *Euro Surveillance*, 23: 17–00449.

Pohlmann, A. et al. (2018) 'Swarm Incursions of Reassortants of Highly Pathogenic Avian Influenza Virus Strains H5N8 and H5N5, Clade 2.3.4.4b, Germany, Winter 2016/17', *Scientific Reports*, 8: 15.

Pu, J. et al. (2015) 'Evolution of the H9N2 Influenza Genotype That Facilitated the Genesis of the Novel H7N9 Virus', *Proceedings of the National Academy of Sciences of the United States of America*, 112: 548–53.

Pulit-Penaloza, J. A. et al. (2015) 'Pathogenesis and Transmission of Novel Highly Pathogenic Avian Influenza H5N2 and H5N8 Viruses in Ferrets and Mice', *Journal of Virology*, 89: 10286–93.

Reid, S. M. et al. (2016) 'The Detection of a Low Pathogenicity Avian Influenza Virus Subtype H9 Infection in a turkey Breeder Flock in the United Kingdom', *Avian Diseases*, 60: 126–31.

SJCEIRS-H9-Working-Group. (2013) 'Assessing the Fitness of Distinct Clades of Influenza A (H9N2) Viruses', *Emerg Microbes Infect*, 2: e75.

Stech, J. et al. (2008) 'Rapid and Reliable Universal Cloning of Influenza a Virus Genes by Target-Primed Plasmid Amplification', *Nucleic Acids Research*, 36: e139–e139.

Świętoń, E. et al. (2018) 'Genetic Characterization of H9N2 Avian Influenza Viruses Isolated from Poultry in Poland during 2013/2014', *Virus Genes*, 54: 67–76.

Szretter, K. J. et al. (2009) 'Early Control of H5N1 Influenza Virus Replication by the Type I Interferon Response in Mice', *Journal of Virology*, 83: 5825–34.

Varga, Z. T. et al. (2011) 'The Influenza Virus Protein PB1-F2 Inhibits the Induction of Type I Interferon at the Level of the MAVS Adaptor Protein', *PLoS Pathogens*, 7: e1002067.

Vigeveno, R. M. et al. (2020) 'Outbreak Severity of Highly Pathogenic Avian Influenza A(H5N8) Viruses Is Inversely Correlated to Polymerase Complex Activity and Interferon Induction', *Journal of Virology*, 94: e00375.

Wang, X. et al. (2016) 'Characteristics of Two Highly Pathogenic Avian Influenza H5N8 Viruses with Different Pathogenicity in Mice', *Archives of Virology*, 161: 3365–74.

—— et al. (2017) 'Synergistic Effect of PB2 283M and 526R Contributes to Enhanced Virulence of H5N8 Influenza Viruses in Mice', *Veterinary Research*, 48: 67.

White, M. C. et al. (2019) 'H5N8 and H7N9 Packaging Signals Constrain HA Reassortment with a Seasonal H3N2 Influenza a Virus', *Proceedings of the National Academy of Sciences of United States of America*, 116: 4611–8.

Yoneyama, M. et al. (1998) 'Direct Triggering of the Type I Interferon System by Virus Infection: Activation of a Transcription Factor Complex Containing IRF-3 and CBP/p300', *The EMBO Journal*, 17: 1087–95.

Zhao, Z. et al. (2014) 'PB2-588I Enhances 2009 H1N1 Pandemic Influenza Virus Virulence by Increasing Viral Replication and Exacerbating PB2 Inhibition of Beta Interferon Expression', *Journal of Virology*, 88: 2260–7.

Zohari, S. et al. (2010) 'Differences in the Ability to Suppress Interferon Beta Production between Allele a and Allele B NS1 Proteins from H10 Influenza a Viruses', *Virology Journal*, 7: 376.

Supplementary Material

Supplementary Figure S1:

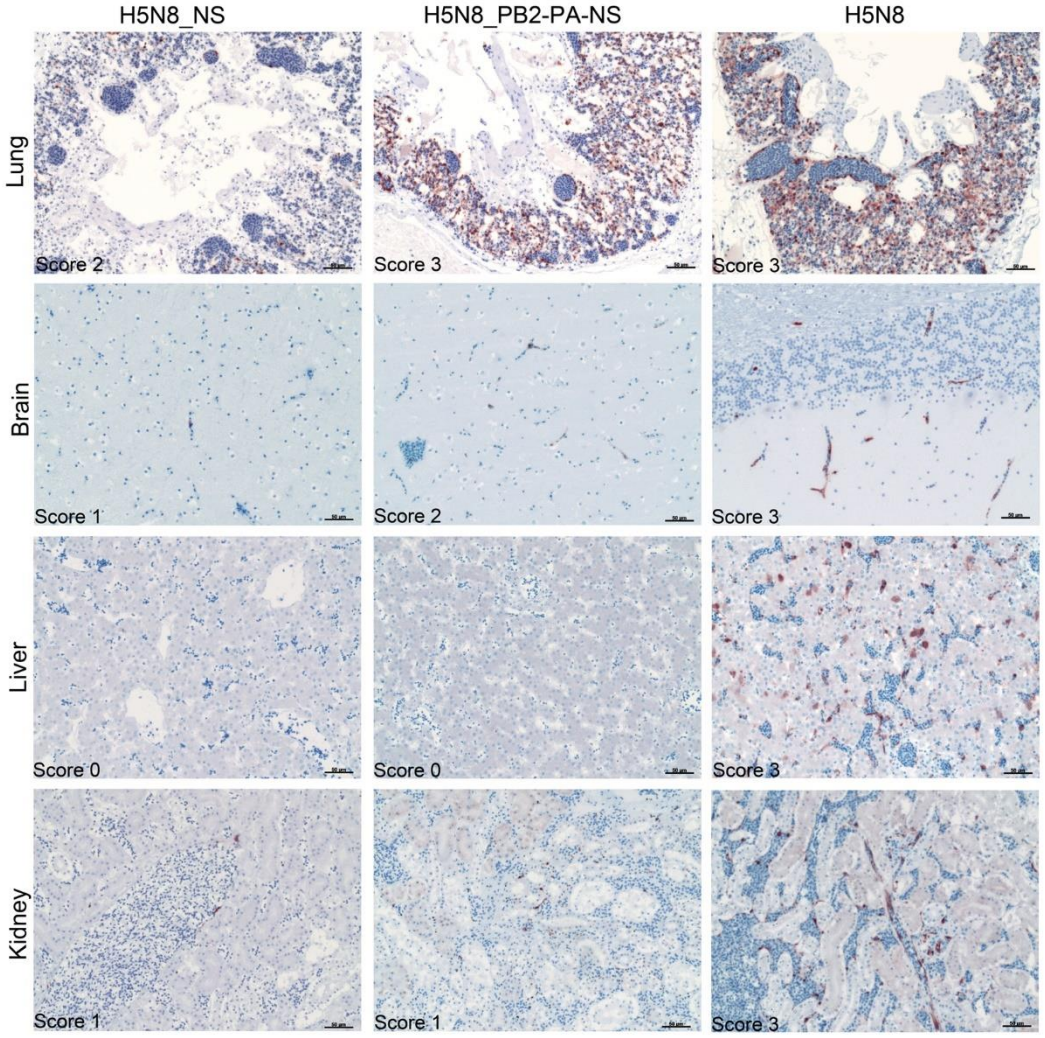

(III) Preferential selection and contribution of non-structural protein 1 (NS1) to the efficient transmission of the panzootic avian influenza H5N8 2.3.4.4 clades A and B viruses in chickens and ducks

Claudia Blaurock, Angele Breithaupt, David Scheibner, Ola Bagato, Axel Karger, Thomas C. Mettenleiter and Elsayed M. Abdelwhab

Submitted to Journal of Virology

Preferential selection and contribution of non-structural protein 1 (NS1) to the efficient transmission of the panzootic avian influenza H5N8 2.3.4.4 clades A and B viruses in chickens and ducks

Running Title: Contribution of NS1 to Transmission of H5N8 in Ducks

Claudia Blaurock[1], Angele Breithaupt[2], David Scheibner[1], Ola Bagato[1,4], Axel Karger[1], Thomas C. Mettenleiter[3] and Elsayed M. Abdelwhab[1*]

[1]Institute of Molecular Virology and Cell Biology, [2]Department of Experimental Animal Facilities and Biorisk Management, [3]Friedrich-Loeffler-Institut, Federal Research Institute for Animal Health, Südufer 10, 17493 Greifswald-Insel Riems, Germany, [4]Center of Scientific Excellence for Influenza Viruses, National Research Centre (NRC), Dokki, 12622 Giza, Egypt

* Corresponding author: Elsayed M. Abdelwhab
Tel: +49 38351 7 1139;
Fax: +49 38351 7 1188
sayed.abdel-whab@fli.de

Subject category: Animal, RNA Viruses

Counts:

Abstract	**244 words**
Text	6807 words
Table	1
Figure	6

Abstract

Highly pathogenic avian influenza viruses H5N8 clade 2.3.4.4 caused outbreaks in poultry at an unprecedented global scale. The virus was spread by wild birds in Asia in two waves: clade-2.3.4.4A in 2014/2015 and clade-2.3.4.4B since 2016 up to today. Both clades were highly virulent in chickens, but only clade-B viruses exhibited high virulence in ducks. Viral factors which contribute to virulence and transmission of these panzootic H5N8 2.3.4.4 viruses are largely unknown. The NS1 protein, typically composed of 230 amino acids (aa), is a multifunctional protein which is also a pathogenicity factor. Here, we studied the evolutionary trajectory of H5N8 NS1 proteins from 2013 to 2019 and their role in the fitness of H5N8 viruses in chickens and ducks. Sequence analysis and *in-vitro* experiments indicated that clade-2.3.4.4A and clade-2.3.4.4B viruses have a preference for NS1 of 237-aa and 217-aa, respectively over NS1 of 230-aa. NS217 was exclusively seen in domestic and wild birds in Europe. The extension of the NS1 C-terminus of clade-B virus reduced virus transmission and replication in chickens and ducks and partially impaired the systemic tropism to the endothelium in ducks. Conversely, lower impact on fitness of clade-A virus was observed. Remarkably, the NS1 of clade-A and clade-B, regardless of length, was efficient to block interferon induction in infected chickens and changes in the NS1 C-terminus reduced the efficiency for interferon antagonism. Together, the NS1 C-terminus contributes to the efficient transmission and high fitness of H5N8 viruses in chickens and ducks.

Importance

The panzootic H5N8 highly pathogenic avian influenza viruses of clade 2.3.4.4A and 2.3.4.4B devastated poultry industry globally. Clade 2.3.4.4A was predominant in 2014/2015 while clade 2.3.4.4B was widely spread in 2016/2017. Both clades exhibited different pathotypes in ducks. Virus factors contributing to virulence and transmission are largely unknown. The NS1 protein is typically composed of 230 amino-acids (aa) and is an essential interferon (IFN) antagonist. Here, we found that the NS1 protein of clade 2.3.4.4A preferentially evolved toward long NS1 with 237-aa, while clade 2.3.4.4B evolved toward shorter NS1 with 217-aa (exclusively found in Europe) due stop-codons in the C-terminus (CTE). We showed that the NS1 CTE of H5N8 is required for efficient virus replication, transmission and endotheliotropism in ducks. In chickens, H5N8 NS1 evolved toward higher

55 efficiency to block IFN-response. These findings may explain the preferential pattern for
56 short NS1 and high fitness of the panzootic H5N8 in birds.

57 **Key words:** Highly Pathogenic Avian Influenza Virus, H5N8, Clade 2.3.4.4, Evolution, NS1,
58 Virulence, Transmission, Ducks, Interferon-antagonism

Introduction

Avian influenza viruses (AIV) infect a wide range of birds and mammals exhibiting high pathogenic (HP) or low pathogenic (LP) phenotypes. AIV belongs to genus Influenza A Virus (IAV) in the family *Orthomyxoviridae* with an RNA genome of eight gene segments (segments 1 to 8) which encode more than ten structural and non-structural proteins (1). The non-structural protein-1 (NS1), encoded by segment 8 encompassing 890 nucleotides, occurs in two distinct alleles (phylogroups) in birds, where allele A is more common than allele B (2-4). NS1 typically encompasses 230 amino acids (aa) arranged in two domains: the RNA binding domain (RBD) from aa 1 to 73 and an effector domain (ED) from aa 88-230 which are connected by a linker (residues 74-87) (5). It is present as a homodimer. Upon infection of cells, the interactions of NS1 RBD with many viral and host RNA species prevents the activation of host cellular sensors and suppresses cellular gene expression. Likewise, the ED interacts with a plethora of host proteins to, among other functions, antagonize host immune response (5, 6).

Although, NS1 has a typical length of 230 aa, several influenza viruses (e.g. H5Nx) have a shorter NS1 due to a 5-aa deletion in the linker region (80-84 aa) (5) or a deletion in the C-terminus (ΔCTE) of the ED. We and others showed that there are up to 13 different forms of the ΔCTE in AIV (4, 7, 8). The most common ΔCTE form (88%) was NS with 217-aa lacking aa 218-230, while the extension in CTE to 237 aa was rarely observed (n= 112/13026, 0.9%) (8). Generally, in poultry the impact of NS1 CTE variations on virulence of AIV is controversial and the contribution to virus transmission or tropism was rarely studied. Species-specific variations in the PDZ domain (aa 227-230) of NS1 affected LPAIV H7N1 and HPAIV H5N1 replication in duck cell cultures but not in chicken embryo fibroblasts (9, 10). *In-vivo*, no significant difference in virulence of HPAIV H5N1 in chickens was observed due to variation of the PDZ domain (10) and it was dispensable for virus replication in chickens and ducks (11). Conversely, a deletion of the PDZ domain in the HPAIV H7N1 NS1 was advantageous for virus replication in chicken embryo fibroblasts (8, 12) and in infected chickens (8) but did not significantly affect the high virulence of the virus in infected chickens (8). In another study, extension of 217-aa NS1 to 230 or 237 aa did not have a significant impact on LPAIV H9N2 replication in avian cells, but increased virus replication and transmission in chickens without significant impact on virulence (13). No information is available on the impact of CTE elongation on HPAIV fitness, particularly transmissibility, in ducks.

The HPAIV Goose/Guangdong (GsGd96) H5N1 first reported in Hong Kong in 1996/1997, with full NS1 CTE, devastated poultry in more than 60 countries (14) and 455 out of 861 (53%) infected humans died (15). Since then, the virus evolved into tens of clades and subclades and underwent several reassortment events. In recent years, H5N8 clade 2.3.4.4 spread globally in an unprecedented panzootic (14). In 2013-2015, H5N8 clade 2.3.4.4A (designated H5N8-A) was transported by wild birds from Asia to birds and poultry in Europe and North America (16, 17). In 2016, the second wave of H5N8 caused by clade 2.3.4.4B (designated H5N8-B) resulted in devastating outbreaks in poultry in several countries in Asia, Europe, Africa and the Middle East (18-20). H5N8-A viruses were avirulent in Pekin ducks, while H5N8-B viruses were highly virulent (21). We have recently shown that NS1 is a major virulence determinant of an H5N8-B virus in ducks (Scheibner et al. in preparation) and swapping NS gene segment of H5N8-B and LPAIV H9N2 reduced virus transmission in chickens (22). Little is known about the global evolution of NS1 gene of clade 2.3.4.4 viruses overtime and the role of CTE on virus fitness in gallinaceous birds and waterfowls. In this study, we analysed all sequence of NS1 of clade 2.3.4.4 H5Nx viruses and studied the impact of NS1 CTE deletion and extension on replication, virulence and transmission of recent HPAIV H5N8-A and H5N8-B in chickens and ducks.

Materials and Methods

Sequence analysis. A total of 8185 complete NS1 protein sequences were retrieved from GISAID (n= 2872) and Influenza Virus Resources (n= 5313) available publicly from 1996 to 2019. Sequences were edited manually (e.g. to remove the laboratory-viruses and viruses with ambiguous sequences or nomenclature, etc.), aligned using MAFFT and further edited using Geneious version 2019.2.3. Furthermore, statistical programming language R (23) was used to analyse the prevalence of sequences of H5N8 viruses from 2013 to 2019 and the R package ggplot2 (24) to construct graphs. MrBayes was used to analyse the phylogenetic relatedness after selection of bestfit Model in Topali v2 software (25) and further edited using Dendroscope and Inkscape free software.

Viruses and cell lines. A/turkey/Germany-MV/AR2487/2014 (H5N8) carrying NS with 237-aa (designated hereafter A_NS237) and A/tufted duck/Germany/8444/2016 (H5N8) carrying NS with 217-aa (designated hereafter B_NS217) were kindly provided by Timm C. Harder, the head of reference laboratory for avian influenza virus, Friedrich-Loeffler-Institut (FLI),

Greifswald Insel-Riems, Germany. The HA of both viruses belonged to clade 2.3.4.4A and 2.3.4.4B, respectively. Madin-Darby canine kidney type II cells (MDCKII) and human embryonic kidney cells (HEK293T) were provided by the Cell Culture Collection in Veterinary Medicine of the FLI. Primary chicken embryo kidney (CEK) and duck embryo kidney (DEK) cells were prepared according to the standard protocol and as described below (26).

Construction of recombinant wild and mutant viruses. All viruses were handled in biosafety level 3 (BSL3) facilities at the FLI. Recombinant B_NS217 virus was generated in a previous study (22). To generate a recombinant A_NS237 virus, viral RNA was extracted from allantoic fluid using Trizol reagent (Thermo Fischer, Germany) and Qiagen RNeasy Kit (Qiagen, Germany) following the manufacturers' guidelines. cDNA was transcribed using reverse primer targeting the conserved termini of influenza gene segments and the Omniscript Reverse Transcription Kit (Qiagen, Germany). Each gene segment was amplified using segment-specific primers and extracted from 1% gel slices using Qiagen Gel Extraction Kit (Qiagen, Germany). Purified gene segments were cloned into the plasmid pHW*Ccd*B as previously done (27). Plasmids containing different gene segments were extracted from transformed *E. coli* XL1-Blue™ or SURE2™ Supercompetent Cells (Agilent, Germany) using QIAGEN Plasmid Mini and Midi Kit (Qiagen, Germany) and subjected for Sanger sequencing (Eurofins, Germany). The NS gene segments of A_NS237 and B_NS217 were modified using QuikChange II Site Directed Mutagenesis Kit according to the instruction manual (Agilent, Germany). The sequence of mutagenesis primers is available upon request.

HEK293T/MDCKII co-culture were transfected with 1 µg plasmids of each gene segment (27) in a mixture of Opti-MEM containing GlutaMAX and Lipofectamine 2000 (Fischer Scientific, Germany). After 2 days, 9-11 day-old specific pathogen free (SPF) embryonated chicken eggs (ECE) (VALO BioMedia GmbH, Germany) were inoculated via the allantoic sac with the supernatant of transfected cells (28). Eggs were checked daily for embryo mortality and the hemagglutination activity in the allantoic fluid was tested against 1% chicken erythrocytes following the standard protocol. Allantoic fluids with titre higher than 16 hemagglutination units were tested for bacterial contamination using Columbia sheep blood agar (Thermo Fisher, Germany). Virus stocks were dispensed in 2 mL-cryotubes and stored at -80°C until further use.

Virus titration. Virus titration in this study was done using standard plaque assay. Briefly, viruses were serially diluted in ten-fold dilutions in PBS and were added to MDCKII cells in 12-well plates for 1 h at 37°C/5% CO_2. Cells were washed with phosphate buffer saline (PBS, pH= 7.4). Semisolid agar (Bacto^{TM} Agar, BD, France) and minimal essential medium (MEM) containing 4% bovine serum albumin (BSA) (MP Biomedicals, USA) were mixed to equal parts and was added to each well. After three days at 37°C, cells were fixed by 4% formaldehyde containing 0.1% crystal violet for 24 h and plaques were counted. Viral titres were expressed as plaque forming units per ml (PFU/ml).

Preferential selection of NS segment in vitro. To determine the preferential selection of the authentic NS segment (NS237 in clade-A or NS217 in clade-B) over NS230, HEK293T cells were co-transfected with 9 plasmids in 4 different settings. Cells were co-transfected with plasmids containing all gene segments of clade-A A_NS217 virus in addition to clade-A NS segments with NS230 or NS237, each in two independent experiments. Similarly, cells were co-transfected with plasmids containing all gene segments of clade-B B_NS237 virus in addition to clade-B NS segments with NS230 or NS217. Transfection was done as described above using OptiMEM and Lipofectamine. Two days after transfection, 2 eggs per transfection were inoculated with the transfected-cell supernatant and daily checked for embryo mortality. The allantoic fluid was harvested and plaque assay was conducted. A total of 70 plaques were randomly selected and RNA was extracted using NucleoSpin 96 Virus Core Kit (Macherey & Nagel GmbH, Germany). cDNA Synthesis was performed with OneStep RT-PCR Kit (Qiagen, Germany) and NS specific primers. Purified gel products were subjected for Sanger sequencing (Eurofins, Germany). Prevalence of different NS variants was analysed using Geneious version 2019.2.3.

Replication kinetics in primary chicken embryo kidney (CEK) and duck embryo kidney (DEK) cells. CEK cells were prepared from 18-day-old SPF ECE and DEK cells were prepared from 23-day-old duck eggs. Briefly, embryos were decapitated using sterile scissors and the kidney was removed in sterile petri dish. Cell suspensions were prepared by trypsinization and mechanically by sterile scissors in presence of MEM containing 10% foetal calf serum (FCS) (Biowest, Germany). Trypsinized cells were collected in a flask containing MEM and subjected for stirring using magnetic bar at 200 rpm at room temperature (rt) for 25 minutes. The suspension was purified by decanting the whole amount in gauze pads in a beaker followed by centrifugation for 5 min at 1200 rpm. The pellet was suspended in MEM containing 10% FCS, penicillin- streptomycin (1:100) (Thermo Fisher Scientific, USA) and

amphotericin B (1:1000) (Biowest, Germany). Finally, ~500,000 cells per well were distributed in 12-well plates. After 24 h, semi-confluent cells were infected at a multiplicity of infection (MOI) of 1 PFU per 1000 cells in MEM and left for 1 h at 37°C/5% CO_2. Thereafter, the inoculum was removed and extracellular virions were inactivated by citric acid buffer (pH= 3) for two minutes and the cells were washed twice with PBS. MEM with 0.2% BSA was added to each well. All plates were incubated at 37°C/5% CO_2. At indicated hours post infection (hpi), cells were collected and kept at -80°C until use. The assay was run in duplicates for each virus and repeated twice. Virus titres were determined by plaque assay in MDCKII as described above. The results were expressed as mean and standard deviation of all replicates.

Protein expression in avian cells using Western Blot. To study the impact of CTE on expression of NS1, CEK cells were infected at an MOI of 0.1 in duplicates for 1 h at 37°C and 40 °C. Cells were treated with citrate buffer saline for 2 minutes then washed twice with PBS before adding MEM containing 0.2 % BSA and further incubation for 2, 4, 8 and 24 hours. At the indicated time points, cells were collected and subjected for two rounds of centrifugation for 10 min at 13,000 rpm and washing by PBS. Cell pellets were dissolved in Laemmli buffer (SERVA, Germany) and PBS at ratio 1:1 and heated for 5 min at 95° C. Proteins were separated in standard procedures using 12% polyacrylamide gel (SDS-PAGE) and transferred to polyvinylidene fluoride (PVDF) membranes (GE Healthcare Life science, Germany) using TransBlot semi dry transfer cell (Bio-Rad, Germany). After saturation of non-specific protein binding using 5% low-fat milk diluted in TBS-T at rt for one hour, the membranes were incubated overnight under constant shaking at 4°C with the primary polyclonal rabbit anti-NS1 antibody. Furthermore, β-actin as well as NP were detected using monoclonal anti-β-actin (Sigma-Aldrich, USA) as well as polyclonal-anti-NP rabbit antibodies, respectively. After washing the membrane three times with 1xTBS-T (each step 5 min), secondary peroxidase-conjugated rabbit and mouse IgG at a dilution of 1:20000 in TBS-T were added to the membrane for 1 h at rt. Thereafter, the membranes were washed 3 times with 1 x TBS-T and antibody binding was detected in a BioRad Versa Doc System with the Quantity One software (BioRad, Germany) by chemiluminescence using the Clarity Western ECL Substrate (BioRad, Germany).

Animal experiments

Ethic statement. All experiments in this study were carried out according to the German Regulations for Animal Welfare after obtaining the necessary approval from the authorized ethics committee of the State Office of Agriculture, Food Safety, and Fishery in Mecklenburg – Western Pomerania (LALLF M-V) under permission number: 7221.3-1-060/17 and approval of the commissioner for animal welfare at the FLI representing the Institutional Animal Care and Use Committee (IACUC). All animal experiments were conducted in the BSL3 animal facilities at the FLI.

Experimental design. The impact of CTE on virulence and transmission was assessed in White Leghorn chickens and Pekin ducks. One-day-old SPF chicks hatched at the FLI, Celle, Germany and one-day old Pekin ducklings (Duck-Tec Brueterei, Germany) were used for this study. Ducks were tested to exclude bacterial (e.g. Salmonella spp.) and viral (i.e. influenza) infections. Two days before challenge, 15 chickens (6-week old) and ducks (2-week old) were allocated into six groups in separate experimental rooms. Ten birds were challenged with indicated viruses by oculonasal (ON) inoculation and 1 day-post-inoculation (dpi), 5 naïve birds were added to each inoculated group to assess bird-to-bird transmission. All birds were observed daily for morbidity and mortality for 10 days. Clinical scoring was adopted as previously done (8): 0 for clinically healthy birds, 1 for moribund birds showing one clinical sign including respiratory disorders, cyanosis, nervous signs or diarrhoea and 2 for moribund birds showing two or more clinical signs and 3 for dead birds. Severely moribund birds which were not able to eat or drink were humanely killed using isoflurane (CP Pharma, Germany) and were given score 3 at the next day. Furthermore, the pathogenicity index (PI) for each virus was calculated as the mean value for daily-scores of all birds in 10 days divided by 10. The mean time to death (MTD) was calculated by multiplying the number of birds that died per day as day of death divided by the total number of dead birds in each group.

Virus excretion. To determine the impact of CTE on virus excretion in inoculated and sentinel chickens and ducks, oropharyngeal (OP) and cloacal (CL) swabs were obtained from surviving or freshly dead birds at 2 and 4 dpi in MEM containing 0.2% BSA and antibiotics. Extraction of viral RNA from swab media was done using Viral RNA/DNA Isolation Kit (NucleoMagVET) (Macherey & Nagel GmbH, Germany) in a KingFisher Flex Purification System (Thermo Fisher Scientific, USA). Partial amplification of AIV-M gene was done using SuperScript III One-Step RT-PCR System with Platinum Taq DNA Polymerase (Invitrogen, Germany) and generic real-time reverse-transcription PCR (RT-qPCR) as previously published (29) in AriaMx real-time cycler (Agilent, Germany). Standard curves

generated by serial dilutions of B_NS217 (10 to 100000 pfu) were used in each plate. To semi-quantify the viral RNA, plotting of the Ct-value and the corresponding dilution in the standard curve was automatically done. Results are shown as mean and standard deviation of positive birds.

Seroconversion. At the end of the experiment, blood samples were collected from the jugular vein in all surviving birds after deep anaesthesia. Serum samples were collected after 24 h at 4 °C and centrifugation. Anti-AIV NP was detected using ID screen Influenza A Antibody Competition Multispecies ELISA Kit (IDvet, France). Plates were read in Infinite 200 PRO reader (Tecan Trading AG, Switzerland).

Histopathology and immunohistochemistry. To determine the impact of CTE on microscopic lesions and distribution of AIV in different tissues, samples were collected from freshly dead or slaughtered inoculated birds (n=3 per group) at 2 dpi. Samples from beak, trachea, lungs, brain, heart, pancreas, liver, kidney, spleen, proventriculus, gizzard, duodenum, cecum, cecal tonsils, bursa of Fabricius and thymus were collected in 4% phosphate-buffered neutral formaldehyde. The tissues were embedded in paraffin, cut at 3 µm thickness and stained with haematoxylin and eosin (HE) for light microscopical examination (blinded study). Scoring of microscopic lesions was performed on a necrosis scale 0 to 3+: 0 = no lesion, 1+ = mild, 2+ = moderate, 3+ = severe. Furthermore, viral antigen detection was performed using the avidin-biotin-complex (ABC) in immunohistochemistry (IHC) method (30). The M1 protein of influenza A virus was detected by ATCC HB-64 monoclonal antibody diluted 1:200 in Tris-buffered saline, pH 7.6 at 4°C overnight and goat anti-mouse IgG (#BA 9200, Vector Laboratories, Burlingame, CA) diluted 1:200. Bright red signals were generated with an ABC Kit (Vectastain Elite #PK6100, Vector Laboratories) and the AEC substrate 3-amino-9-ethylcarbazole (Dako, Carpinteria, CA). Moreover, sections were counterstained with Mayer's haematoxylin. Positive control tissue samples and a nonrelated control antibody were included in each run. Scoring was done on a scale 0 to 3+: 0 = negative, 1+ = focal to oligofocal, 2+ = multifocal, 3+ = coalescing foci or diffuse labeling.

Detection of cytokines in chickens and ducks. To get an insight into the impact of CTE on immune response, interferons were measured by generic RT-qPCR (31, 32). Chickens and ducks (n=3) were inoculated with different viruses in a separate experiment. Lungs and spleen of chickens were collected at 2 dpi, weighed (w/v) and homogenized using TissueLyzer® (Qiagen, Germany). The total RNA was extracted from homogenized tissues using Trizol and

RNeasy Kit following the manufacturer's instructions (Qiagen, Germany). The cDNA was transcribed from 400 ng RNA by the Prime Script 1st Strand cDNA Synthesis Kit (TaKaRa, Germany) and Oligo dT Primer (TaKaRa) in a total 20 µl reaction as recommended by the producers. Quantification of IFN-α, IFN-β and IFN-γ transcripts was done using TaqMan probes for chickens or SYBR GreenER qPCR SuperMIX Universal Kit (Invitrogen) for ducks (31, 32). Normalization was done using 28S rRNA transcripts (33). Results were calculated using the 2^-(ΔΔct) method and expressed as fold change of normalized samples compared to samples obtained from non-infected birds (n=3).

Statistics. Data were analysed for statistics using GraphPad Prism software. Non-parametric Kruskal-Wallis (Dunn's multiple comparsions) test was used for statistical anaysis of replication kinetics. One-way ANOVA with post hoc Tukey's test was used for statistical analysis of swab and organ samples as well as for the analysis of the fold-change induction of interferon. Survival time was analysed by Log-rank (Mantel-Cox) test. Data were consideres statistically significant at p-value<0.05.

Results

Temporal and spatial variations in the NS1 C-terminus of clade 2.3.4.4 H5N8 viruses. To understand the global evolution of NS1 CTE in H5 viruses, we analysed 8185 NS1 protein sequences from H5Nx viruses available in GenBank and GISAID. Our analysis revealed that NS1 exhibits 15 size variants. The parental virus GsGD96 had a typical NS1 of 230-aa with full CTE. From 1997, other NS1 with variable aa lengths including 202, 212, 215, 217, 220, 223, 224, 225, 227, 228, 230, 232, 236, 237 and 238 aa were found (data not shown). The most predominant forms were NS217, NS225, NS230 and NS237. NS225 and NS230 have a complete CTE, but vary due to a deletion of aa 80 to 84. Other variants have deletions or insertions in the CTE. For instance, NS217 and NS237 have a 13-aa deletion or 7-aa insertion in the CTE due to variable stop codons in the NS1 CTE, respectively.

To determine the origin and evolution of the NS segment in H5N8-A and H5N8-B, 1068 H5N8 sequences from 2013 (n=12), 2014/2015 (n= 465) and 2016/2019 (n=591) from Asia and Europe were analysed. The NS1 of both viruses clustered in two phylogroups within the Eurasian lineage along with other contemporary H5N8 viruses from Europe and Asia (Figure 1A). H5N8 sequences had either NS230, NS237 or NS217. In 2013, Asian H5N8 viruses as

315 well as the putative predecessors (H4N2, H11N9, H4N6 and H5N2 (34)) had NS1 with a
316 length of 230-aa (Figure 1B). In 2014/2015, 428/465 (~92%) sequences were of 237-aa
317 length, while NS230 was reported only in 37/465 (~8%) (35 from wild birds mainly
318 waterfowl and 2 from domestic chickens and ducks). In 2016/2019, 201/591 (~34%) and
319 390/591 (~66%) sequences had NS230 or NS237, respectively (Figure 1B). NS230 was
320 reported mainly in Asia in wild birds or environment (n= 155/201; ~77.1%) and domestic
321 birds (n= 44/201; ~21.9%). Only 2/201 (1%) viruses with NS230 were reported in turkeys in
322 Italy and Poland. NS217 was not reported in Asia (except one sequence from wild birds in
323 Iran), while in Europe NS217 was reported in 214/390 (~54.9%) from wild birds or
324 environmental samples and 176/390 (~45.1%) from domestic birds. No single sequence with
325 NS217 was reported in 2013/2015 and no NS237 was found in 2016/2019 in sequences
326 analysed in this study. These results indicate temporal and spatial patterns for NS1 CTE in
327 H5N8 viruses from 2013 to 2019. In Asia, H5N8 with NS230 and NS237 in 2014/2015 were
328 common in wild birds. Conversely, NS217 was reported in wild and domestic birds
329 exclusively in Europe in 2016/2019. These findings suggest a preferential selection for NS237
330 and NS217 over NS230 in H5N8-A in 2014/2015 and H5N8-B in 2016/2019, respectively.

331 **Generation of recombinant H5N8-A and H5N8-B viruses with NS217, NS230 and NS237**
332 **NS1 proteins.** Two H5N8 clade A and clade B viruses were selected for this study. Both
333 viruses were closely related to the contemporary H5N8 viruses (Figure 1A). The NS1 of
334 A_NS237 and B_NS217 viruses share 92.6% nucleotides and 90.8% aa identity with 48
335 nucleotides and 20 aa differences, respectively. Seven aa differences were found in the RBD
336 (V6M, S7L, H17Y, S48N, D53G, L65V, G70E), 4 in the linker region (N80T, I81V, V84S,
337 T86S) and 9 in the ED (T127N, I129T, D139N, T143A, L166F, I176N, T202A, S205N,
338 S216P). No deletion in aa positions 80-84 was found. Extension of NS1 CTE (clade-A) and
339 truncation (clade-B) was observed (Figure 1C). To study the impact of NS1 CTE on the
340 fitness of H5N8-A and H5N8-B viruses *in vitro* and *in vivo*, recombinant viruses were
341 generated using A_NS237 and B_NS217. We constructed four more recombinant viruses:
342 A_NS230 and A_NS217 were generated from A_NS237 and B_NS230 and B_NS237 were
343 generated from B_NS217. These viruses carry NS1 with different length due to insertion or
344 removal of stop codons in the NS1 CTE (Figure 1C). Sequence of recombinant virus stocks
345 were confirmed by Sanger sequencing and compared to the sequences of the parent viruses.
346 All viruses were propagated in ECE and reached titres ranged from 3.6×10^5 to 2.3×10^7
347 PFU/ml.

Preferential selection of H5N8-A and H5N8-B viruses to NS1 with variable C-terminus length. To test whether there is a preference of clade-A and clade-B viruses to certain NS1 variants, we co-transfected HEK293T cells with 8 segments from A_NS237 and plasmids containing A_NS230 or A_NS217. The same experiment was done with 8 segments from B_NS217 and plasmids containing B_NS230 or B_NS237. The experiment was conducted in two independent replicates. After two days, supernatant from transfected cells was inoculated in ECE for two days. Allantoic fluid was serially diluted and titrated in plaque test in MDCKII cells (Figure 2A). Seventy plaques were randomly selected, 37 from clade-A sets and 33 from clade-B sets. RNA was extracted and sequencing of NS segment was generated. Results showed that A_NS237 dominated other clade-A viruses with NS230 and NS217, where 8/16 and 13/21 plaques had NS237 and 8/16 and 8/21 plaques were mixed with A_NS230-NS237 and NS217-NS237, respectively. No single plaque contained A_NS217. Likewise, the B_NS217 dominated other longer NS variants, where 2/11 and 13/22 plaques had NS217, 9/11 and 9/22 plaques were mixed with NS217-NS230 and NS217-NS237 plaques, respectively. No single plaque contained A_NS230 alone (Figure 2A). These results indicate that H5N8 clade-A and clade-B have strain-specific preference for NS1 proteins with long and short C-terminus, respectively.

Changes in the CTE did not have a significant impact on NS1 expression in avian cells at different temperatures. The expression of NS1 in CEK cells at 2, 4, 8 and 24 hpi at 37°C and 40 °C was studied in duplicates in two independent rounds using Western Blot. At 2 hpi, NS1 was neither detected at 37°C nor at 40 °C (data not shown). At 4, 8 and 24 hpi, the NS1 of all viruses according to the expected molecular weight were detected without significant differences in the amount of NS1 at 37 and 40 °C (Figure 2B). Together, changes in the CTE didn't affect the NS1 expression in chicken cells at different temperatures.

Extension of NS1 CTE of H5N8-B reduced virus replication in duck cells, but not in chicken cells. The impact of NS1 CTE on virus replication in primary CEK and DEK cells at 1, 8, 24, 48 and 72 h was studied (Figure 2C-F). No significant differences for the replication of H5N8-A viruses in CEK and DEK and replication of H5N8-B in CEK cells were observed (Figure 2C-E). In DEK cells, B_NS217 replicated to significantly higher titres than B_NS230 and/or B_NS237 at 8, 48 and 72 hpi ($p < 0.05$) (Figure 2F) and higher than A_NS237 viruses at 24 hpi ($p < 0.01$). Together, these results indicate that changes in the NS1 CTE did not affect H5N8-A and H5N8-B replication in chicken cells. Conversely, the elongation of the NS1 reduced H5N8-B virus replication in duck cells.

Elongation of NS1 of H5N8-B virus partially or fully compromised virus transmission to naïve chickens. Virulence of the 6 different viruses was assessed in ten ON-inoculated chickens per group. All birds died within 3 dpi and with the same PI value of 2.7 (Table 1). The MTD was also comparable ranging from 2 to 2.6 days in H5N8-A inoculated groups and 2 to 2.2 days in H5N8-B inoculated groups. All contact chickens in groups inoculated with H5N8-A viruses died within 6 days (5 day-post-contact "dpc"), with MTD of 5.2, 4.8 and 5.4 days in groups co-housed with A_NS237, A_NS230 and A_NS217 inoculated chickens, respectively (Table 1). All chickens co-housed with B_NS217 died within 4 dpi (3 dpc), while 4/5 chickens co-housed with B_NS230 inoculated chickens died within 6 days. None of the contact chickens co-housed with B_NS237 died. Surviving contact chickens in the latter two groups did not seroconvert at 10 dpi (9 dpc) (Table 1). Together, NS1 did not affect virus virulence in chickens. The impact of CTE on chicken-to-chicken transmission is virus dependent. While the elongation of the CTE of H5N8-B compromised virus transmission in chickens, no significant impact on H5N8-A virus was observed.

Changes in the CTE reduced H5N8-B virus oral and cloacal excretion in chickens. Virus excretion at 2 dpi was determined in OP and CL swabs. Viral RNA was detected in all inoculated chickens (Figure 3A, B). RNA levels were comparable in OP and CL swabs in chickens inoculated with H5N8-A viruses. However, B_NS230 was excreted at significantly lower levels than B_NS237 and B_NS217 in the OP and CL swabs ($p < 0.04$) (Figure 3B). Cloacal excretion of B_NS217 and B_NS237 was higher than in the OP swabs ($p < 0.002$) (Figure 3B). RNA was not detected in contact chickens in any group. These results indicate that short NS1 CTE is important for the excretion of H5N8-B virus in chickens, but not for H5N8-A.

Changes in the CTE altered H5N8-A and H5N8-B distribution and severity of lesions in different tissues of chickens. The histopathological changes and distribution of influenza antigen in different organs of chickens which died at 2 dpi were evaluated. All H5N8-A and H5N8-B viruses induced comparable levels of necrotic inflammation in different organs. Using IHC, virus antigen was detected in the endothelial cells and parenchyma of all organs at comparable levels (Figure 3C, D). These results revealed the systemic distribution of H5N8-A and H5N8-B viruses in chickens without obvious impact of NS1 CTE on lesions or distribution in vital organs.

412 **Elongation of NS1 of H5N8-B virus reduced virulence in Pekin ducks.** Previous studies
413 showed that H5N8-A virus was avirulent in Pekin ducks after ON inoculation, while H5N8-B
414 was highly virulent (21). Furthermore, we showed that NS from H5N8-B virus increased
415 virulence of H5N8-A in ducks (Scheibner et al. in preparation). Here, we assessed the impact
416 of CTE on virus fitness in ducks. A_NS237 and the short NS1-derivatives exhibited low
417 virulence in ducks and no mortality was observed (Figure 4A, B). All ducks seroconverted 10
418 dpi (data not shown). Conversely, all ducks inoculated with B_NS217 died within 4 days with
419 MTD of 2.5 days (Figure 4C) and PI value of 2.7. Elongation of the NS1 CTE reduced H5N8-
420 B virulence as indicated by reduced mortality and increased survival periods. After
421 inoculation of ducks with B_NS230 and B_NS237, 9/10 and 7/10 ducks died with PI values
422 of 1.8 and 1.7, respectively. The survival period was significantly longer; 6.5 and 4.4 days in
423 ducks inoculated with B_NS230 ($p < 0.0001$) and B_NS237 ($p < 0.001$), respectively (Figure
424 4C). All co-housed ducks in groups inoculated with B_NS217 died within 6 dpi (5 dpc) with
425 MTD of 4.6 dpi (3.6 dpc) (Figure 4D). Only 2/5 contact ducks died in either group inoculated
426 with B_NS230 or B_NS237. The contact ducks died at 10 or 8 dpi (9 and 7 dpc), respectively
427 which was significantly longer than contact ducks co-housed with B_NS217 ($p = 0.003$)
428 (Figure 4D). All surviving ducks seroconverted 10 dpi (data not shown). These data confirm
429 that H5N8-B is more virulent than H5N8-A in Pekin ducks. NS1 alone does not play a main
430 role in virulence or transmission of H5N8-A, but elongation of NS1 CTE reduced virulence of
431 H5N8-B in inoculated and contact ducks.

432 **Changes in the NS1 CTE reduced H5N8-B virus excretion in cloacal swabs in ducks.**
433 Virus excretion was determined in OP and CL swabs obtained at 2 dpi in inoculated and 1 dpc
434 in contact ducks. Inoculated ducks excreted more virus orally than via the cloacae. B_NS217
435 was excreted at significantly higher levels than A_NS237 in inoculated ducks (Figure 4E, F).
436 No significant differences were observed in H5N8-A inoculated groups (Figure 4E), but the
437 level of virus shedding in the OP swabs was significantly higher than in the CL swabs ($p \leq$
438 0.0001). Conversely, B_NS217 was excreted at significantly higher levels than B_NS230 and
439 B_NS217 ($p < 0.005$) with about 15 and 1000 average folds, respectively (Figure 4F). In
440 contact ducks, all H5N8-A viruses were excreted at similarly low levels in the OP swabs and
441 viral RNA was detected in 1/5 duck only in the cloacal swabs. B_NS217 and B_NS237 were
442 detected at similar levels in the OP swabs, and at ~10 times higher levels than B_NS230 (data
443 not shown). Only 1/5 ducks cohoused with B_NS217 inoculated ducks excreted virus in the
444 CL swabs (10^4 pfu/ml), other contact ducks were negative (data not shown).

445 **Changes in the CTE altered H5N8-B distribution and lesions in different tissues of**
446 **ducks.** H5N8-A viruses induced focal to multifocal necrosis and inflammation in the lungs,
447 brain, heart and nasal conchae, without impact of CTE on the distribution of the lesions.
448 H5N8-B viruses caused more consistent and more widespread (multifocal to diffuse) necrosis
449 and inflammation in these tissues and additionally in the spleen, thymus, bursa, pancreas and
450 kidney. Remarkably, hepatic necrosis was decreased or abolished by gradually shortening the
451 H5N8-A NS1 or extension of H5N8-B NS1. Viral antigen detection in the endothelium was
452 only seen in B_NS217 with a broad spectrum of affected tissues (systemic
453 endotheliotropism). In accordance with the lesion profile, H5N8-A viruses were mainly found
454 in the lungs, heart, nasal conchae and liver but clearly less consistent and less abundant
455 compared to H5N8-B viruses (Figure 4G,H). Interestingly, only A_NS237 showed viral
456 antigen in the parabronchial epithelium of air sac ostia. The tropism of H5N8-B viruses was
457 extended to the brain, thymus, spleen, intestine, pancreas and kidney but elongation of NS1
458 resulted in reduced M1 antigen detection in all organs. Neither B_NS230 nor B_NS237 was
459 detected in the gastrointestinal tract (Figure 5, detailed data not shown). Together, compared
460 to H5N8-A virus, the high virulence of H5N8-B virus in ducks was associated with more
461 widespread necrosis and inflammation as well as lymphocyte depletion in the lymphatic
462 organs and in case of B_NS217 with systemic endotheliotropism. The NS1 CTE abolished the
463 diffuse endotheliotropism of H5N8-B virus, but alone did not affect the lack of
464 endotheliotropism of H5N8-A virus and gradually reduced the hepatic necrosis caused by
465 both H5N8-A and H5N8-B and the antigen distribution of H5N8-B in all tissues.

466 **Detection of cytokine response in the lungs and spleen of inoculated chickens and ducks.**
467 The detection of IFN-α, IFN-β and IFN-γ mRNA in the lungs and spleen of inoculated
468 chickens and ducks at 2 dpi was done using generic RT-PCR and expression levels were
469 normalized to 28S rRNA. The results are expressed as fold change compared to negative
470 controls (Figure 6). In the lungs of chickens, H5N8-A and H5N8-B viruses induced
471 comparable expression levels for IFN-α and IFN-γ, while IFN-β expression induced by
472 A_NS237 (Figure 6B) was significantly lower than that induced by clade B_NS217 ($p < 0.05$)
473 (Figure 6E). A_NS237 was more efficient to block IFN-α induction than A_NS230 and
474 A_NS217 (Figure 6A) and was able to significantly block IFN-γ induction compared to
475 A_NS230 Figure 6C). B_NS230 was significantly less efficient to inhibit IFN-α induction
476 than B_NS217 and B_NS237 (Figure 6D). In the spleen, A_NS217 was less efficient than
477 A_NS230 and A_NS237 in inhibiting the IFN-α response. No significant differences were
478 observed in the spleen of chickens inoculated with H5N8-B viruses (data not shown). In

479 ducks, the expression of IFN was limited compared to chickens. There were no significant
480 differences in the levels of expression of IFN in the lungs and spleen between different groups
481 (Figure 6G-L, data not shown). These results indicate that in chickens the original NS1 of
482 H5N8-A and H5N8-B viruses, regardless of the length of the CTE, evolved toward higher
483 efficiency to block IFN-α response in the lungs. Extension or shortening of the NS1 reduced
484 the efficiency of the virus to block IFN response. IFN response in ducks was limited
485 compared to chickens and NS1 CTE did not affect IFN expression in the lungs and spleen.

486

487 **Discussion**

488 The continuous circulation of the panzootic H5N8 clade 2.3.4.4 is threatening the poultry
489 industry worldwide. It is important to understand the viral factors which contribute to the high
490 fitness of HPAIV H5N8 in chickens and ducks. It has been previously suggested that H5N8
491 clade-A viruses acquired the NS segment from A/duck/Eastern China/1111/2011 (H5N2),
492 while clade-B viruses acquired the NS segment by reassortment with
493 A/environment/Jiangxi/28/2009 (H11N9) or A/duck/Hunan/8-19/2009 (H4N2) (34). We
494 found that all putative ancestors for clades A or B possess NS1 with 230-aa. In contrast,
495 Eurasian H5N8 in 2013/2014 (clade-A) or European 2015/2016 (clade-B) have NS1 with
496 237-aa or 217-aa, respectively. We did not find NS217 in 2013/2014 or NS237 in 2016/2018.
497 These results indicate that NS1 rapidly acquired longer (clade-A) or shorter (clade-B) NS1
498 and dominated their ancestors indicating selective advantages for virus replication in a clade-
499 specific pattern. Indeed, our competition experiments in cell culture confirmed this
500 assumption with preferential selection of the authentic NS over NS with a typical length of
501 230-aa. The latter was disadvantageous for virus fitness *in vitro* and/or *in vivo*. The negative
502 impact of NS230 on the fitness of clade-A virus was limited compared to clade-B virus. In
503 clade-A virus, the only significant difference due to shortening of the NS237 to 230-aa or
504 217-aa was the less ability to block IFN-α response in the lungs of chickens compared to the
505 wild type A_NS237 virus. Conversely, the extension of NS1 CTE of clade-B virus to 230-aa
506 or 237-aa reduced virus replication in duck cells and virulence, transmission, excretion and/or
507 replication in different organs of inoculated chickens and ducks. These results may explain
508 the preferential selection of H5N8 clade 2.3.4.4 for a certain length of the NS1 protein.

509 While chickens died after inoculation with H5N8-A and H5N8-B viruses, H5N8-B was more
510 virulent in Pekin ducks than H5N8-A virus which is in accordance with previous results (21).

511 The virulence determinants of HPAIV vary in chickens and ducks. In chickens, the HA,
512 particularly the polybasic cleavage site (HACS), is the main determinant of virulence.
513 However, mutations in other gene segments (i.e. PB1, NP and NA) contributed to the high
514 virulence of an American HPAIV H5N2 clade 2.3.4.4A in chickens (35). Moreover, previous
515 studies have shown that NS1 V149A contributed to the virulence of an H5N1 virus in
516 chickens (36) and replacing the NS segment of the current H5N8-B with that of an H9N2
517 reduced transmission and replication of H5N8-B in chickens (22). In ducks, several studies
518 found that the HA alone is not sufficient for high virulence (37-42) and we recently found that
519 H5N8-B NS segment, in addition to the HA and NP, increased virulence and transmission of
520 H5N8-A in Pekin ducks (Scheibner et al. in preparation) indicating a significant role for NS in
521 H5N8-B virulence and bird-to-bird transmission efficiency. Here, we showed that the NS1
522 CTE is important for virus transmission in chickens and ducks in a virus-specific manner.
523 Although it remains to be studied, H5N8-A virus may have compensatory mutations in the
524 NS1 or other proteins and, thus, shortening the CTE have less impact on virus fitness
525 compared to H5N8-B. In fact, the synergism between NS1 CTE and mutations in the NS1
526 RBD (i.e. I38Y) (43) or mutations in the PB1-F2 (44) affected virulence of HPAIV H5N1 in
527 mice. Similarly, mutations in the nuclear export signal (e.g. D139N as seen in this study) can
528 compensate the absence of nuclear/nucleolus localisation signals due to a 6-aa-deletion in the
529 NS1 CTE of an H7N7 virus (12).

530 Virulence in inoculated chickens and ducks was associated with systemic dissemination of
531 viral antigen, histopathological lesions and in particular with systemic endotheliotropism in
532 chickens and H5N8-B virus in ducks. Interestingly, in contrast to the systemic replication of
533 H5N8-A virus in chickens, replication of H5N8-A virus in ducks was limited to the
534 respiratory tract, heart and liver resembling some LPAIV and HPAIV (45). Viral or host
535 factors which contribute to the different endotheliotropism in chickens and ducks of some
536 AIV are not well understood (46). It has been shown that the polybasic HACS is important for
537 the endotheliotropism in chickens and/or ducks (47, 48). However, although both H5N8
538 viruses used in this study possess a polybasic HACS, they showed a striking difference in
539 endotheliotropism in ducks indicating that factors beyond the HACS are essential for the
540 tropism to endothelial cells. Scheibner et al. (49) described diffuse endotheliotropism in
541 chickens but not in ducks after inoculation with an HPAIV H7N7. In this study, the NS1 CTE
542 did not significantly affect the endotheliotropism in chickens, however, it reduced H5N8-B
543 virus distribution in the endothelial cells as well as in vital organs including the brain, heart,
544 lung and spleen in ducks. The extension of CTE in HPAIV H7N1 NS1 decreased virus

545 excretion and tropism to the endothelial cells and epithelium in the central nervous system
546 and respiratory tract without significant difference in virulence in chickens (8). The specific
547 impact of NS1 CTE on the endotheliotropism of H5N8-B virus in ducks merits further
548 investigation.

549 Chickens mount robust IFN-responses, but fail to limit viral replication and succumb to a
550 "cytokine storm" (50). Compared to chickens, we found that the IFN response in the lungs
551 and spleen in Pekin ducks was limited as described before (51-55). Interestingly, NS1 is a
552 main antiviral antagonist for influenza viruses which is mediated by different NS1 domains
553 (6). Our results showed that CTE has no impact on IFN-β and IFN-γ responses, while H5N8-
554 A and H5N8-B viruses with NS of 230-aa were less efficient to block IFN-α induction in
555 chickens which might also explain the disfavor to NS with 230-aa. A previous study has
556 shown that extension of NS1 of H9N2 to 230-aa or 237-aa did not affect the levels of IFN-α
557 and IFN-β but increased the IFN-γ in the lungs of chickens (13). Conversely, a deletion of 6-
558 aa in the NS1 CTE of an LPAIV H7N1 did not affect type I or type II IFN-response in
559 chickens or ducks (11). This discrepancy is probably due to the use of different virus strains or
560 subtypes.

561 In conclusion, there is a preferential selection for a certain NS1 CTE in 2.3.4.4 H5N8 clade-A
562 (with 237-aa) and clade-B (with 217-aa) viruses over NS1 with 230-aa, the common length of
563 NS1 in AIV. The latter had a negative impact on virus fitness *in vitro* and *in vivo*. CTE can
564 affect the virulence in a species and clade-specific manners. In chickens, NS1 CTE of H5N8-
565 A and H5N8-B evolved toward higher efficiency to block IFN-α response. In ducks, NS1
566 CTE is essential for efficient transmission, replication and high virulence of H5N8-B which
567 correlated with (i) systemic endotheliotropism and (ii) widespread tissue damage. These
568 results are important to understand the evolution of the panzootic H5N8 clade 2.3.4.4 and the
569 role of NS1 in virus fitness in chickens and ducks.

570

571 **Acknowledgment**

572 Dajana Helke, Nadine Bock, Sarah Knapp and Silvia Schuparis are thanked for laboratory
573 technical assistance, Günter Strebelow for his assistance in sequencing, Dr. Christine Fast,
574 Prof. Steffen Weigend, Bärbel Hammerschmidt, Frank Klipp, Harald Manthei, Doreen
575 Fielder, Bärbel Berger, Thomas Moeritz and Ralf Henkel for their support in the animal

576 experiments, Silvia Schuparis for histological preparations and Dr. Daniel Marc for providing
577 the anti-NS1 antibodies. Emmelie Eckhardt and Luca Zaeck are thanked for technical support.
578 This work was supported by grants from Horizon 2020 "Delta Flu" (project ID: 727922) and
579 the Deutsche Forschungsgemeinschaft (DFG; AB 567/1-1 and DFG VE780/1-1). The funders
580 had no role in study design, data collection and analysis, decision to publish, or preparation of
581 the manuscript.

582

583 **Declaration of interest statement**

584 The authors declare no conflict of interest

Table 1: Impact of NS1 CTE in chickens after challenge with recombinant H5N8 viruses

Clade	Viruses	Inoculated Chickens			Contact Chickens		
		Mortality*	Scoring	MTD	Mortality*	MTD	Seroconversion
A	A_NS217	10/10	2.7	2.6	5/5	5.4	n.a.
	A_NS230	10/10	2.7	2.1	5/5	4.8	n.a.
	A_NS237	10/10	2.7	2.0	5/5	5.2	n.a.
B	B_NS217	10/10	2.7	2.0	5/5	4.0	n.a.
	B_NS230	10/10	2.7	2.2	4/5	5.5	0/1
	B_NS237	10/10	2.7	2.0	0/5	n.a.	0/5

Mortality = number of dead chickens to number of inoculated

MTD= mean time to death

n.a.= not applicable because all birds died

Figure 1: Evolution of NS1 of clade 2.3.4.4A and 2.3.4.4B H5N8 viruses

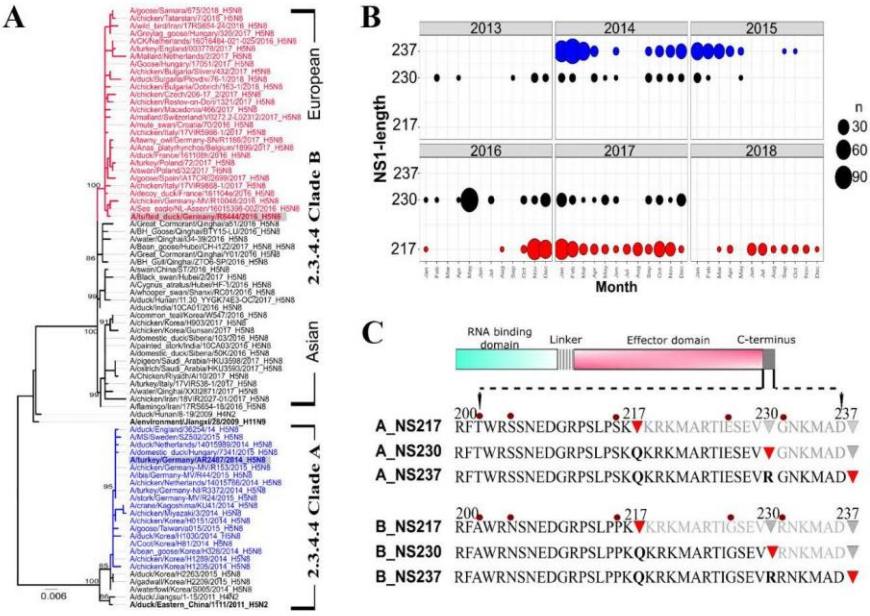

NS gene sequences were retrieved from GISAID and were aligned using MAFFT. A mid-point rooted phylogenetic tree was generated by MrBayes in Toplai v2. Two independent runs of 1,000,000 replicates and 10% burn-in were used. Shown is the phylogenetic relatedness of NS segments allele A of representative viruses. Clade-A and clade-B viruses used in this study are highlighted in grey. Viruses written in black have NS230, in red have NS217 and in blue have NS237. The putative ancestors are written in bold. Similar topology was obtained using NJ and ML trees (data not shown) (A). R was used to determine the temporal distribution of NS1 length in sequences collected between 2013 to 2018 (B). Recombinant H5N8 clade-A and clade-B 2.3.4.4 viruses were generated carrying different NS1 CTE. Clades A and B wild-type viruses have 237 and 217-aa, respectively. Deep-red circles indicate point mutations in clade-A compared to clade-B. Red triangles indicate stop codons (C).

Figure 2: Preferential selection and impact of NS1 CTE on expression and replication of H5N8 viruses in cell culture

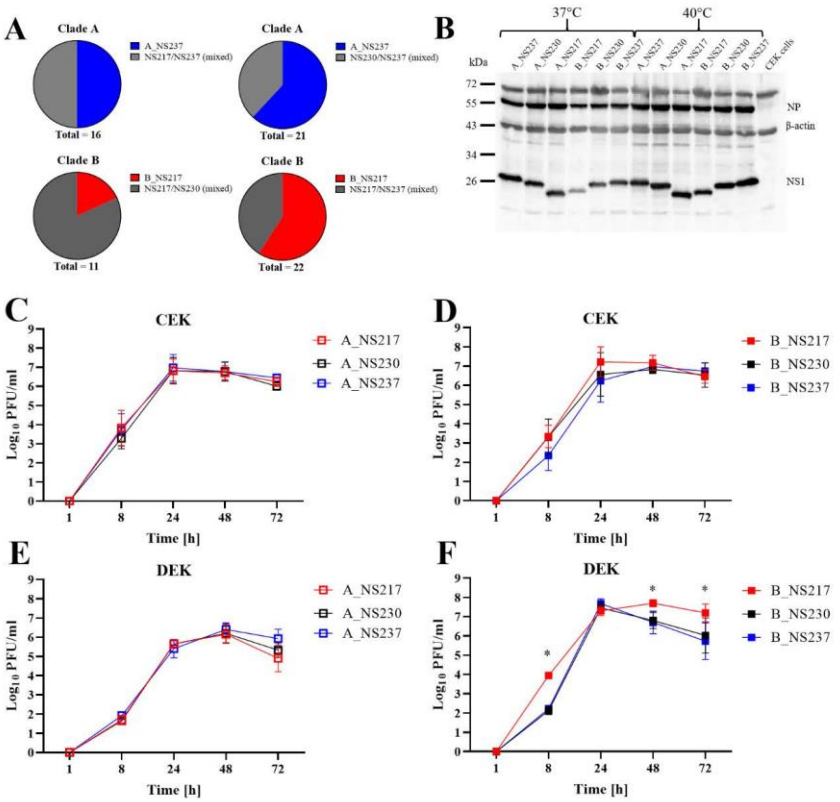

Preferential selection of NS1 was studied by co-transfection of cells for 2 days and propagation in ECE. Plaques were randomly selected and NS1 was subjected for Sanger sequencing after RNA extraction and amplification of the NS1. The transfection was run in two separate rounds (A). Expression of NS1 4 hours post infection of CEK cells with an MOI of 0.1. NS1 was detected by rabbit polyclonal NS1 antibodies, NP was detected by polyclonal NP rabbit-antibody and beta-actin with a commercial monoclonal antibody. Similar results were obtained at 8 and 24 hpi (data not shown) (B). Replication of different viruses at MOI of 0.001 at indicated time points in primary embryo kidney cells obtained from chickens (CEK) (C, D) or ducks (DEK) (E, F). Virus titres were determined by plaque assay in MDCKII cells. Statistical significance * $p < 0.05$.

Figure 3: The impact of NS1 on virus excretion and endotheliotropism in chickens

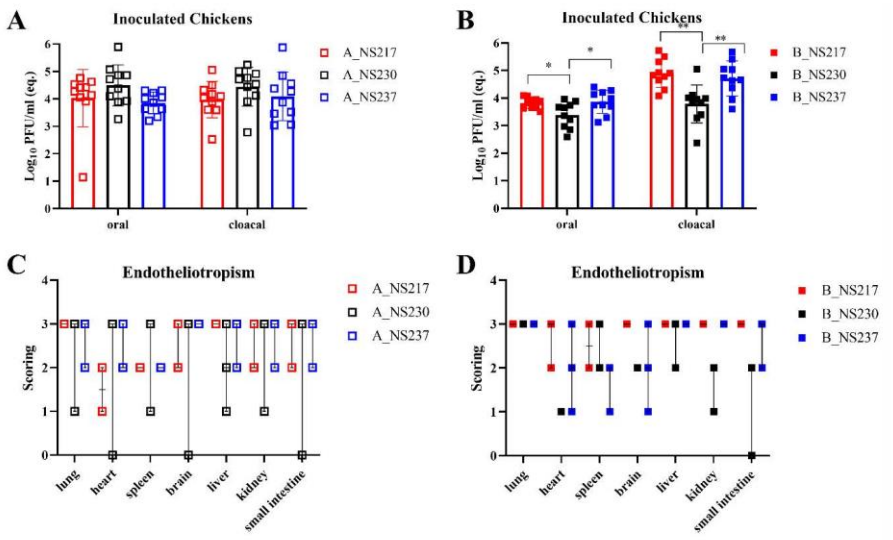

Virus excretion determined in oropharyngeal and cloacal swabs in inoculated chickens 2 dpi using quantitative RT-qPCR was expressed as log10 pfu/ml (eq.) (A, B). Endotheliotropism was determined by IHC. Scores indicate 0 = negative, 1 = focal to oligofocal, 2 = multifocal, 3 = coalescing foci or diffuse labelling, dots represent individual animals, bar = median with interquartile range (C, D). Statistical significance * $p < 0.05$, ** $p < 0.01$.

Figure 4: The impact of NS1 on virulence, transmission, virus excretion and endotheliotropism in ducks

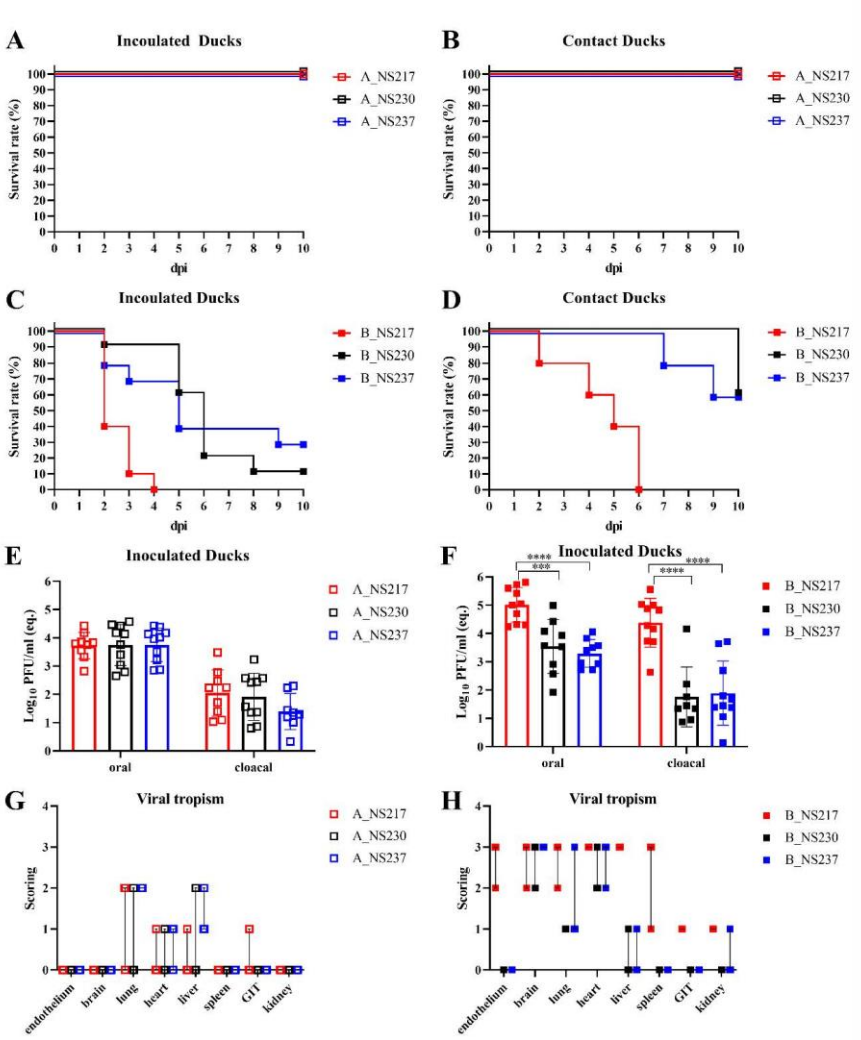

Survival curves were generated using Kaplan Meyers for clade-A inoculated (A) and contact ducks (B) and clade-B inoculated (C) and contact ducks (D). Virus excretion determined in oropharyngeal and cloacal swabs in inoculated ducks with clade-A (E) or clade-B viruses (F) using quantitative RT-qPCR was expressed as log10 pfu/ml (eq.) in inoculated ducks. Viral tropism in ducks was determined by IHC at 2 dpi of ducks with clade-A (G) or clade-B (H)

631 viruses. Scores indicate 0 = negative, 1 = focal to oligofocal, 2 = multifocal, 3 = coalescing
632 foci or diffuse labelling, dots represent individual animals, bar = median with interquartile
633 range. Endothelium scores indicate the maximum score found in all tissue affected. Statistical
634 significance * $p < 0.05$, ** $p < 0.01$, ***, $p < 0.001$, ****, $p < 0.0001$.

635 **Figure 5: Immunohistopathological detection of Matrix antigen in selected organs in**
636 **ducks**

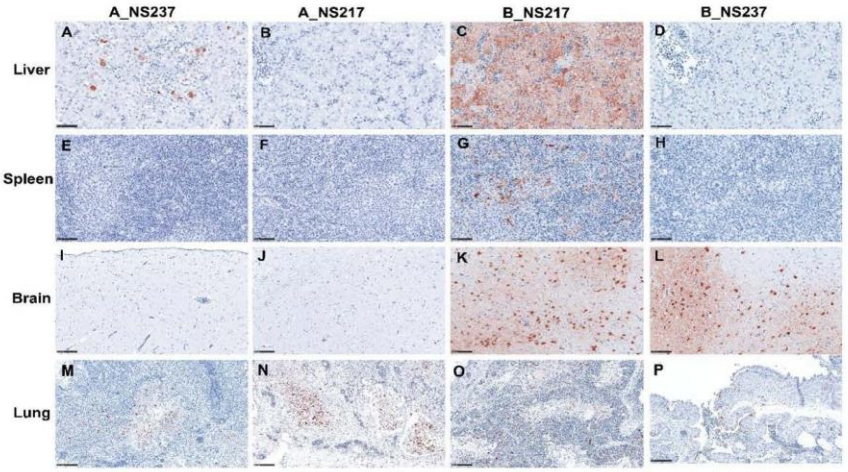

637

638 Organs were obtained from inoculated-ducks, euthanized 2 dpi. Immunohistochemistry, ABC
639 Method using anti-Matrix-1 protein antibody, AEC chromogen (red-brown), Hematoxylin
640 (blue) counterstain. (A-H) bar 50 µm, (I-P) bar 100 µm.

641 **Figure 6: Interferon induction in lungs of chickens and ducks inoculated with clade A**
642 **and B H5N8 viruses**

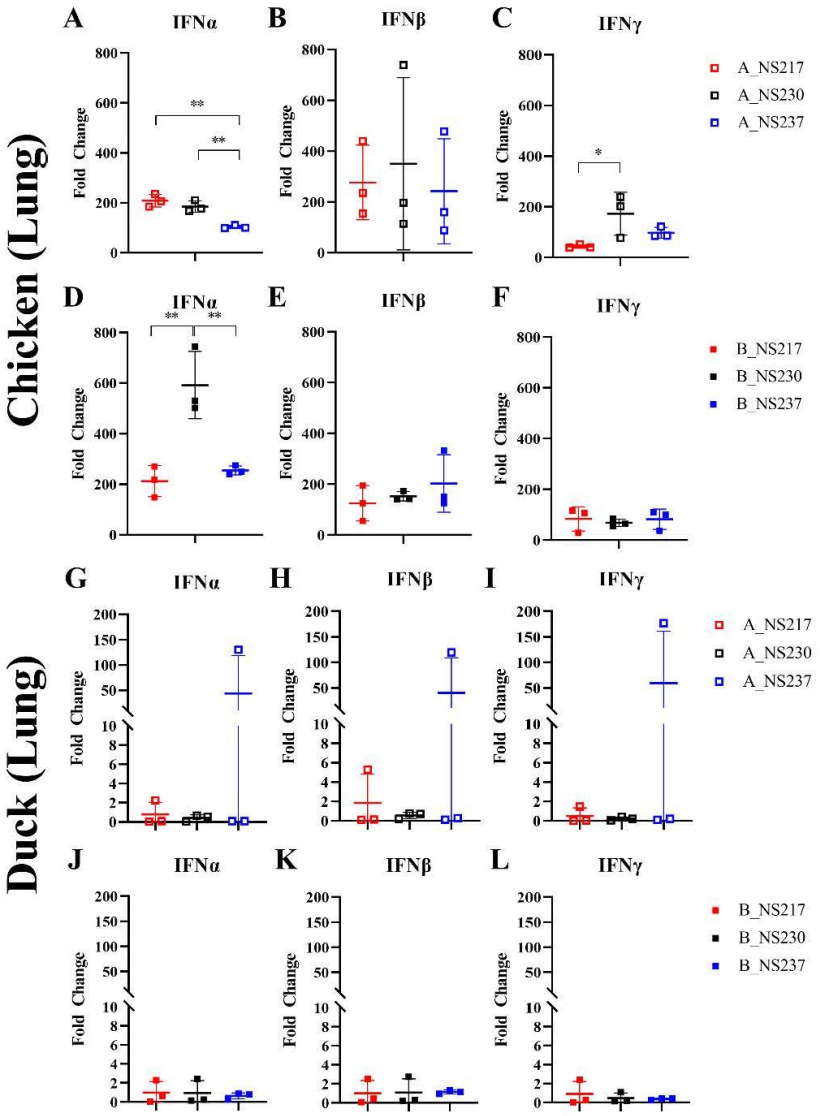

643

644 Shown are the fold changes in IFN-levels in the lungs of chickens and ducks inoculated with
645 clade A and B H5N8 viruses 2 dpi. Tissues were collected, weighed (w/v) and homogenized.

646 The mRNA of IFN-α, IFN-β or IFN-γ were measured by generic RT-qPCR from 3 birds in
647 each group. Normalization was done using 28S rRNA transcripts. Results were calculated
648 using the 2^-(ΔΔct) method and expressed as fold change of normalized samples compared to
649 samples obtained from non-infected birds (n=3). Statistical significance * $p < 0.05$, ** $p <$
650 0.01.

651 **References**

652 1. Webster RG, Bean WJ, Gorman OT, Chambers TM, Kawaoka Y. 1992. Evolution and
653 ecology of influenza A viruses. Microbiol Rev 56:152-79.
654 2. Lin YP, Shu LL, Wright S, Bean WJ, Sharp GB, Shortridge KF, Webster RG. 1994.
655 Analysis of the influenza virus gene pool of avian species from southern China.
656 Virology 198:557-66.
657 3. Kawaoka Y, Gorman OT, Ito T, Wells K, Donis RO, Castrucci MR, Donatelli I,
658 Webster RG. 1998. Influence of host species on the evolution of the nonstructural
659 (NS) gene of influenza A viruses. Virus Res 55:143-56.
660 4. Suarez DL, Perdue ML. 1998. Multiple alignment comparison of the non-structural
661 genes of influenza A viruses. Virus Res 54:59-69.
662 5. Marc D. 2014. Influenza virus non-structural protein NS1: interferon antagonism and
663 beyond. J Gen Virol 95:2594-2611.
664 6. Hale BG, Randall RE, Ortin J, Jackson D. 2008. The multifunctional NS1 protein of
665 influenza A viruses. J Gen Virol 89:2359-2376.
666 7. Dundon WG, Milani A, Cattoli G, Capua I. 2006. Progressive truncation of the Non-
667 Structural 1 gene of H7N1 avian influenza viruses following extensive circulation in
668 poultry. Virus Res 119:171-6.
669 8. Abdelwhab el SM, Veits J, Breithaupt A, Gohrbandt S, Ziller M, Teifke JP, Stech J,
670 Mettenleiter TC. 2016. Prevalence of the C-terminal truncations of NS1 in avian
671 influenza A viruses and effect on virulence and replication of a highly pathogenic
672 H7N1 virus in chickens. Virulence 7:546-57.
673 9. Soubies SM, Volmer C, Croville G, Loupias J, Peralta B, Costes P, Lacroux C, Guerin
674 JL, Volmer R. 2010. Species-specific contribution of the four C-terminal amino acids
675 of influenza A virus NS1 protein to virulence. J Virol 84:6733-47.
676 10. Zielecki F, Semmler I, Kalthoff D, Voss D, Mauel S, Gruber AD, Beer M, Wolff T.
677 2010. Virulence determinants of avian H5N1 influenza A virus in mammalian and
678 avian hosts: role of the C-terminal ESEV motif in the viral NS1 protein. J Virol
679 84:10708-18.
680 11. Soubies SM, Hoffmann TW, Croville G, Larcher T, Ledevin M, Soubieux D, Quere P,
681 Guerin JL, Marc D, Volmer R. 2013. Deletion of the C-terminal ESEV domain of NS1
682 does not affect the replication of a low-pathogenic avian influenza virus H7N1 in
683 ducks and chickens. J Gen Virol 94:50-58.
684 12. Keiner B, Maenz B, Wagner R, Cattoli G, Capua I, Klenk HD. 2010. Intracellular
685 distribution of NS1 correlates with the infectivity and interferon antagonism of an
686 avian influenza virus (H7N1). J Virol 84:11858-65.
687 13. Kong W, Liu L, Wang Y, He Q, Wu S, Qin Z, Wang J, Sun H, Sun Y, Zhang R, Pu J,
688 Liu J. 2015. C-terminal elongation of NS1 of H9N2 influenza virus induces a high
689 level of inflammatory cytokines and increases transmission. J Gen Virol 96:259-268.
690 14. Guan Y, Smith GJ. 2013. The emergence and diversification of panzootic H5N1
691 influenza viruses. Virus Res 178:35-43.
692 15. WHO. 2019. Cumulative number of confirmed human cases of avian influenza
693 A(H5N1) reported to WHO available online at:
694 https://www.who.int/influenza/human_animal_interface/H5N1_cumulative_table_arch
695 ives/en/ (last accessed 12-03-2021).
696 16. Ip HS, Torchetti MK, Crespo R, Kohrs P, DeBruyn P, Mansfield KG, Baszler T,
697 Badcoe L, Bodenstein B, Shearn-Bochsler V, Killian ML, Pedersen JC, Hines N,
698 Gidlewski T, DeLiberto T, Sleeman JM. 2015. Novel Eurasian highly pathogenic
699 avian influenza A H5 viruses in wild birds, Washington, USA, 2014. Emerg Infect Dis
700 21:886-90.

17. Pasick J, Berhane Y, Joseph T, Bowes V, Hisanaga T, Handel K, Alexandersen S. 2015. Reassortant highly pathogenic influenza A H5N2 virus containing gene segments related to Eurasian H5N8 in British Columbia, Canada, 2014. Sci Rep 5:9484.
18. Lee DH, Bertran K, Kwon JH, Swayne DE. 2017. Evolution, global spread, and pathogenicity of highly pathogenic avian influenza H5Nx clade 2.3.4.4. J Vet Sci 18:269-280.
19. Pohlmann A, Starick E, Grund C, Hoper D, Strebelow G, Globig A, Staubach C, Conraths FJ, Mettenleiter TC, Harder T, Beer M. 2018. Swarm incursions of reassortants of highly pathogenic avian influenza virus strains H5N8 and H5N5, clade 2.3.4.4b, Germany, winter 2016/17. Sci Rep 8:15.
20. Hassan KE, El-Kady MF, El-Sawah AAA, Luttermann C, Parvin R, Shany S, Beer M, Harder T. 2019. Respiratory disease due to mixed viral infections in poultry flocks in Egypt between 2017 and 2018: Upsurge of highly pathogenic avian influenza virus subtype H5N8 since 2018. Transbound Emerg Dis doi:10.1111/tbed.13281.
21. Grund C, Hoffmann D, Ulrich R, Naguib M, Schinkothe J, Hoffmann B, Harder T, Saenger S, Zscheppang K, Tonnies M, Hippenstiel S, Hocke A, Wolff T, Beer M. 2018. A novel European H5N8 influenza A virus has increased virulence in ducks but low zoonotic potential. Emerg Microbes Infect 7:132.
22. Mostafa A, Blaurock C, Scheibner D, Muller C, Blohm U, Schafer A, Gischke M, Salaheldin AH, Nooh HZ, Ali MA, Breithaupt A, Mettenleiter TC, Pleschka S, Abdelwhab EM. 2020. Genetic incompatibilities and reduced transmission in chickens may limit the evolution of reassortants between H9N2 and panzootic H5N8 clade 2.3.4.4 avian influenza virus showing high virulence for mammals. Virus Evol 6:veaa077.
23. R_Development_Core_Team. 2011. R: A language and environment for statistical computing, *on* R Foundation for Statistical Computing. http://www.R-project.org/. Accessed
24. Wickham H. 2016. ggplot2 doi:10.1007/978-3-319-24277-4. Springer, Cham.
25. Milne I, Lindner D, Bayer M, Husmeier D, McGuire G, Marshall DF, Wright F. 2009. TOPALi v2: a rich graphical interface for evolutionary analyses of multiple alignments on HPC clusters and multi-core desktops. Bioinformatics 25:126-7.
26. Hennion RM, Hill G. 2015. The preparation of chicken kidney cell cultures for virus propagation. Methods Mol Biol 1282:57-62.
27. Stech J, Stech O, Herwig A, Altmeppen H, Hundt J, Gohrbandt S, Kreibich A, Weber S, Klenk HD, Mettenleiter TC. 2008. Rapid and reliable universal cloning of influenza A virus genes by target-primed plasmid amplification. Nucleic Acids Res 36:e139.
28. Alexander DJ. 2015. Avian Influenza, *on* OIE. https://www.oie.int/fileadmin/Home/eng/Health_standards/tahm/2.03.04_AI.pdf. Accessed 12.03.2021.
29. Hoffmann B, Hoffmann D, Henritzi D, Beer M, Harder TC. 2016. Riems influenza a typing array (RITA): An RT-qPCR-based low density array for subtyping avian and mammalian influenza a viruses. Sci Rep 6:27211.
30. Breithaupt A, Kalthoff D, Dale J, Bairlein F, Beer M, Teifke JP. 2011. Neurotropism in blackcaps (Sylvia atricapilla) and red-billed queleas (Quelea quelea) after highly pathogenic avian influenza virus H5N1 infection. Vet Pathol 48:924-32.
31. Li W, Moltedo B, Moran TM. 2012. Type I interferon induction during influenza virus infection increases susceptibility to secondary Streptococcus pneumoniae infection by negative regulation of gammadelta T cells. J Virol 86:12304-12.

32. Kim TS, Kang BY, Cho D, Kim SH. 2003. Induction of interleukin-12 production in mouse macrophages by berberine, a benzodioxoloquinolizine alkaloid, deviates CD4+ T cells from a Th2 to a Th1 response. Immunology 109:407-14.

33. Petersen H, Mostafa A, Tantawy MA, Iqbal AA, Hoffmann D, Tallam A, Selvakumar B, Pessler F, Beer M, Rautenschlein S, Pleschka S. 2018. NS Segment of a 1918 Influenza A Virus-Descendent Enhances Replication of H1N1pdm09 and Virus-Induced Cellular Immune Response in Mammalian and Avian Systems. Front Microbiol 9:526.

34. El-Shesheny R, Barman S, Feeroz MM, Hasan MK, Jones-Engel L, Franks J, Turner J, Seiler P, Walker D, Friedman K, Kercher L, Begum S, Akhtar S, Datta AK, Krauss S, Kayali G, McKenzie P, Webby RJ, Webster RG. 2017. Genesis of Influenza A(H5N8) Viruses. Emerg Infect Dis 23:1368-1371.

35. Youk SS, Leyson CM, Seibert BA, Jadhao S, Perez DR, Suarez DL, Pantin-Jackwood MJ. 2020. Mutations in PB1, NP, HA, and NA Contribute to Increased Virus Fitness of H5N2 Highly Pathogenic Avian Influenza Virus Clade 2.3.4.4 in Chickens. J Virol doi:10.1128/JVI.01675-20.

36. Li Z, Jiang Y, Jiao P, Wang A, Zhao F, Tian G, Wang X, Yu K, Bu Z, Chen H. 2006. The NS1 gene contributes to the virulence of H5N1 avian influenza viruses. J Virol 80:11115-23.

37. Schmolke M, Manicassamy B, Pena L, Sutton T, Hai R, Varga ZT, Hale BG, Steel J, Perez DR, Garcia-Sastre A. 2011. Differential contribution of PB1-F2 to the virulence of highly pathogenic H5N1 influenza A virus in mammalian and avian species. PLoS Pathog 7:e1002186.

38. Hulse-Post DJ, Franks J, Boyd K, Salomon R, Hoffmann E, Yen HL, Webby RJ, Walker D, Nguyen TD, Webster RG. 2007. Molecular changes in the polymerase genes (PA and PB1) associated with high pathogenicity of H5N1 influenza virus in mallard ducks. J Virol 81:8515-24.

39. Song J, Feng H, Xu J, Zhao D, Shi J, Li Y, Deng G, Jiang Y, Li X, Zhu P, Guan Y, Bu Z, Kawaoka Y, Chen H. 2011. The PA protein directly contributes to the virulence of H5N1 avian influenza viruses in domestic ducks. J Virol 85:2180-8.

40. Hu J, Hu Z, Mo Y, Wu Q, Cui Z, Duan Z, Huang J, Chen H, Chen Y, Gu M, Wang X, Hu S, Liu H, Liu W, Liu X, Liu X. 2013. The PA and HA gene-mediated high viral load and intense innate immune response in the brain contribute to the high pathogenicity of H5N1 avian influenza virus in mallard ducks. J Virol 87:11063-75.

41. Sarmento L, Wasilenko J, Pantin-Jackwood M. 2010. The effects of NS gene exchange on the pathogenicity of H5N1 HPAI viruses in ducks. Avian Dis 54:532-7.

42. Nao N, Kajihara M, Manzoor R, Maruyama J, Yoshida R, Muramatsu M, Miyamoto H, Igarashi M, Eguchi N, Sato M, Kondoh T, Okamatsu M, Sakoda Y, Kida H, Takada A. 2015. A Single Amino Acid in the M1 Protein Responsible for the Different Pathogenic Potentials of H5N1 Highly Pathogenic Avian Influenza Virus Strains. PLoS One 10:e0137989.

43. Fan S, Macken CA, Li C, Ozawa M, Goto H, Iswahyudi NF, Nidom CA, Chen H, Neumann G, Kawaoka Y. 2013. Synergistic effect of the PDZ and p85beta-binding domains of the NS1 protein on virulence of an avian H5N1 influenza A virus. J Virol 87:4861-71.

44. Ozawa M, Basnet S, Burley LM, Neumann G, Hatta M, Kawaoka Y. 2011. Impact of amino acid mutations in PB2, PB1-F2, and NS1 on the replication and pathogenicity of pandemic (H1N1) 2009 influenza viruses. J Virol 85:4596-601.

45. Wood GW, Parsons G, Alexander DJ. 1995. Replication of influenza A viruses of high and low pathogenicity for chickens at different sites in chickens and ducks following intranasal inoculation. Avian Pathol 24:545-51.

46. Short KR, Veldhuis Kroeze EJ, Reperant LA, Richard M, Kuiken T. 2014. Influenza virus and endothelial cells: a species specific relationship. Front Microbiol 5:653.
47. Schat KA, Bingham J, Butler JM, Chen LM, Lowther S, Crowley TM, Moore RJ, Donis RO, Lowenthal JW. 2012. Role of position 627 of PB2 and the multibasic cleavage site of the hemagglutinin in the virulence of H5N1 avian influenza virus in chickens and ducks. PLoS One 7:e30960.
48. Feldmann A, Schafer MK, Garten W, Klenk HD. 2000. Targeted infection of endothelial cells by avian influenza virus A/FPV/Rostock/34 (H7N1) in chicken embryos. J Virol 74:8018-27.
49. Scheibner D, Ulrich R, Fatola OI, Graaf A, Gischke M, Salaheldin AH, Harder TC, Veits J, Mettenleiter TC, Abdelwhab EM. 2019. Variable impact of the hemagglutinin polybasic cleavage site on virulence and pathogenesis of avian influenza H7N7 virus in chickens, turkeys and ducks. Sci Rep 9:11556.
50. Evseev D, Magor KE. 2019. Innate Immune Responses to Avian Influenza Viruses in Ducks and Chickens. Vet Sci 6.
51. Pantin-Jackwood MJ, Smith DM, Wasilenko JL, Cagle C, Shepherd E, Sarmento L, Kapczynski DR, Afonso CL. 2012. Effect of age on the pathogenesis and innate immune responses in Pekin ducks infected with different H5N1 highly pathogenic avian influenza viruses. Virus Res 167:196-206.
52. Saito LB, Diaz-Satizabal L, Evseev D, Fleming-Canepa X, Mao S, Webster RG, Magor KE. 2018. IFN and cytokine responses in ducks to genetically similar H5N1 influenza A viruses of varying pathogenicity. J Gen Virol 99:464-474.
53. Burggraaf S, Karpala AJ, Bingham J, Lowther S, Selleck P, Kimpton W, Bean AG. 2014. H5N1 infection causes rapid mortality and high cytokine levels in chickens compared to ducks. Virus Res 185:23-31.
54. Cornelissen JB, Vervelde L, Post J, Rebel JM. 2013. Differences in highly pathogenic avian influenza viral pathogenesis and associated early inflammatory response in chickens and ducks. Avian Pathol 42:347-64.
55. Fleming-Canepa X, Aldridge JR, Jr., Canniff L, Kobewka M, Jax E, Webster RG, Magor KE. 2019. Duck innate immune responses to high and low pathogenicity H5 avian influenza viruses. Vet Microbiol 228:101-111.

(IV) Deletion or extension of the C-terminus of non-structural protein 1 (NS1) in H5N8 clade 2.3.4.4 highly pathogenic avian influenza virus modulates induction of interferon and apoptosis in human lung cells and virulence in mice

Claudia Blaurock, Ulrike Blohm, Christine Luttermann, Julia Holzerland, David Scheibner, Alexander Schäfer, Allison Groseth, Thomas C. Mettenleiter and Elsayed M. Abdelwhab

Submitted to Emerging Microbes & Infections

Deletion or Extension of the C-Terminus of Non-Structural Protein 1 (NS1) in H5N8 Clade 2.3.4.4 Highly Pathogenic Avian Influenza Virus Modulates Induction of Interferon and Apoptosis in Human Lung Cells and Virulence in Mice

Journal:	*Emerging Microbes & Infections*
Manuscript ID	Draft
Manuscript Type:	Original Article
Date Submitted by the Author:	n/a
Complete List of Authors:	Blaurock, Claudia; Friedrich-Loeffler-Institut Bundesforschungsinstitut für Tiergesundheit, Institute for Molecular Virology and Cell Biology Blohm, U; Friedrich-Loeffler-Institut Bundesforschungsinstitut für Tiergesundheit, Institute for Immunology Luttermann, Christine ; Friedrich-Loeffler-Institut Bundesforschungsinstitut fur Tiergesundheit Holzerland, Julia; Friedrich-Loeffler-Institut Bundesforschungsinstitut für Tiergesundheit, Institute for Molecular Virology and Cell Biology Scheibner, David; Friedrich-Loeffler-Institut Bundesforschungsinstitut für Tiergesundheit, Institute for Molecular Virology and Cell Biology Schäfer, Alexander; Friedrich-Loeffler-Institut Bundesforschungsinstitut für Tiergesundheit, Institute for Immunology Groseth, Allison; Friedrich-Loeffler-Institut Bundesforschungsinstitut fur Tiergesundheit, Institute of Molecular Virology and Cell Biology Mettenleiter, Thomas; Friedrich-Loeffler-Institut Bundesforschungsinstitut für Tiergesundheit Abd El-Whab, El-Sayed; Friedrich Loeffler Inst, Institute of Molecular

	Virology and Cell Biology; Friedrich-Loeffler-Institut
Keywords:	Avian Influenza Virus, H5N8 Clade 2.3.4.4, Interspecies Transmission, Virulence Determinants, NS1
Abstract:	Avian influenza viruses (AIV) H5N8 clade 2.3.4.4 pose a public health threat but viral factors for adaptation to mammals are largely unknown. The non-structural protein 1 (NS1) of influenza viruses is an essential interferon antagonist. It commonly consists of 230 amino acids, but variations in the disordered C-terminus resulted in truncation or extension of NS1 with possible impact on virus fitness in mammals. Here, we analysed NS1 sequences from 1902 to 2020 representing human influenza viruses (hIAV) as well as AIV in birds, humans and other mammals and with an emphasis on the panzootic AIV subtype H5N8 clade 2.3.4.4A (H5N8-A) from 2013/2015 and clade 2.3.4.4B (H5N8-B) since 2016. We found a high prevalence of short NS1 sequences among hIAV, zoonotic AIV and H5N8-B, while AIV and H5N8-A had longer NS1 sequences. We assessed the fitness of recombinant H5N8-A and H5N8-B carrying NS1 with different lengths in human cells and in mice. H5N8-B with a short NS1, similar to hIAV or AIV from human and other mammal-origins, was more efficient at blocking apoptosis and interferon-induction without a significant impact on virus replication in human cells. In mice, shortening the NS1 of H5N8-A increased virulence, while the extension of NS1 of H5N8-B reduced virus virulence and replication. Taken together, we have described the biological impact of variation in the NS1 C-terminus in hIAV and AIV and shown that this affected virus fitness in vitro and in vivo.

Running Title: NS1 C-Terminus Modulates Virulence of H5N8 in Mammals

Deletion or Extension of the C-Terminus of Non-Structural Protein 1 (NS1) in H5N8 Clade 2.3.4.4 Highly Pathogenic Avian Influenza Virus Modulates Induction of Interferon and Apoptosis in Human Lung Cells and Virulence in Mice

Claudia Blaurock[a], Ulrike Blohm[b], Christine Luttermann[b], Julia Holzerland[a], David Scheibner[a], Alexander Schäfer[b], Allison Groseth[a], Thomas C. Mettenleiter[c], and Elsayed M. Abdelwhab[a*]

[a]Institute of Molecular Virology and Cell Biology, [b]Institute of Immunology, [c]Friedrich-Loeffler-Institut, Federal Research Institute for Animal Health, Südufer 10, 17493 Greifswald-Insel Riems, Germany

* Corresponding author: Elsayed M. Abdelwhab
Tel: +49 38351 7 1139;
Fax: +49 38351 7 1188
sayed.abdel-whab@fli.de

Counts:

Abstract	237 words
Text	6000 words
Figure	7
Supplementary	1

Abstract

Avian influenza viruses (AIV) H5N8 clade 2.3.4.4 pose a public health threat but viral factors for potential adaptation to mammals are largely unknown. The non-structural protein 1 (NS1) of influenza viruses is an essential interferon antagonist. It commonly consists of 230 amino acids, but variations in the disordered C-terminus resulted in truncation or extension of NS1 with possible impact on virus fitness in mammals. Here, we analysed NS1 sequences from 1902 to 2020 representing human influenza viruses (hIAV) as well as AIV in birds, humans and other mammals and with an emphasis on the panzootic AIV subtype H5N8 clade 2.3.4.4A (H5N8-A) from 2013/2015 and clade 2.3.4.4B (H5N8-B) since 2016. We found a high prevalence of short NS1 sequences among hIAV, zoonotic AIV and H5N8-B, while AIV and H5N8-A had longer NS1 sequences. We assessed the fitness of recombinant H5N8-A and H5N8-B carrying NS1 with different lengths in human cells and in mice. H5N8-B with a short NS1, similar to hIAV or AIV from human and other mammal-origins, was more efficient at blocking apoptosis and interferon-induction without a significant impact on virus replication in human cells. In mice, shortening the NS1 of H5N8-A increased virus virulence, while the extension of NS1 of H5N8-B reduced virus virulence and replication. Taken together, we have described the biological impact of variation in the NS1 C-terminus in hIAV and AIV and shown that this affected virus fitness *in vitro* and *in vivo*.

Key words

Avian Influenza Virus, H5N8 Clade 2.3.4.4, Interspecies Transmission, Mammals, NS1, Virulence, Interferon Antagonism, Apoptosis

Introduction

Avian influenza viruses (AIV) are members of the genus Influenza A Virus (IAV) in the RNA virus family *Orthomyxoviridae*. AIV infect a wide range of birds and mammals including humans. Wild birds are their natural reservoir, where the infection is usually asymptomatic with very few exceptions, while in poultry, AIV exhibit two pathotypes: low pathogenic (LP) and highly pathogenic (HP) [1, 2]. Interspecies transmission of AIV to immunologically naïve human populations can be devastating. As of 2019, there were 1096 fatalities out of 2644 (about 41.5%) laboratory-confirmed human infections with different AIV subtypes [3]. Similarly, AIV infections and mortality in different mammals have been frequently reported [4].

To date, 16 distinct hemagglutinin (HA) and 9 neuraminidase (NA) subtypes have been described in AIV. Each AIV carries one HA and one NA subtype with 144 possible HxNy combinations [5]. The genome of AIV is composed of eight gene segments, which encode at least 11 viral proteins. Mutations in the HA receptor binding domain and in the polymerase proteins are the major determinants for bird-to-human and bird-to-mammal transmission [6, 7]. However, studies have also shown that the non-structural protein 1 (NS1) plays an important role in the efficient replication and transmission of AIV in mammalian models without prior adaptation [8, 9, 10, 11].

NS1 is not incorporated into the virions but is expressed upon infection of the host cells. It consists of an RNA binding domain (RBD, residues 1 to 73) and an effector domain (ED, residues 88 to 230), which are connected by a linker (residues 74 to 87). NS1 is a multifunction protein. The best-described of its functions is the ability to antagonise the interferon (IFN) response, either through binding of the RBD with RNA-sensors or interaction of the ED domain with different cellular proteins [12, 13]. This allows the replication of influenza viruses for almost 2 days after infection before triggering a sudden burst of immune responses, including the production of IFN [14]. Although, NS1 has a typical length of 230 amino acids (aa), this is variable due to deletions in the linker region or changes in the positions of stop codons in the disordered C-terminal end (CTE) of the ED [15, 16, 17]. Sequence analysis showed that human influenza viruses from 1940-1980 possessed an NS1 of 237 aa (designated NS237), while viruses from the 1980s possessed an NS1 of 230 aa (designated NS230) [12]. Conversely, the pandemic H1N1 in 2009 has swine-origin

NS1 of 219 aa (NS219), due to an 11-aa deletion in the CTE (ΔCTE) [18]. Similarly, AIV H5Nx exhibited 15 different NS1 lengths due to changes in the CTE [19]. The role of the CTE in virulence of IAV, and particularly for AIV infection in mammals is controversial. In mice, variations in the PDZ-recognition motif (aa 227-230) of NS1 contributed to virulence of LPAIV H7N1 [20] but it did not significantly affect the virulence of an HPAIV H5N1 [21]. Similarly, the elongation of LPAIV H9N2 NS217 to NS230 or NS237 did not significantly affect virus replication in mammalian cells, virus replication or virulence in mice [22]. These paradoxical results might be explained by the use of different viruses in these experiments.

Since 1996/1997, H5Nx viruses of the Goose/Guangdong (Gs/Gd) lineage have continued to evolve in wild and domestic birds [23]. Recently, H5Nx clade 2.3.4.4 has spread in global waves to wild and domestic birds from Asia into Europe, Africa and North America [24, 25]. Two 2.3.4.4 clades were identified: clade A in 2013/2015 and clade B in 2016/2020. In contrast to clade A viruses, H5Nx viruses of clade B were also isolated from mammals including humans, pigs, mink, cats, and seals, indicating increasing risk for mammalian species [26, 27](GISAID data). As a result, there are increasing calls for vigilance, including assessing the genetic changes that might increase the zoonotic potential of clade B 2.3.4.4 viruses [28]. In our recent study [19], we have shown that H5N8 clade A and B (designated hereafter as H5N8-A and H5N8-B, respectively) have preferences for NS237 and NS217, respectively over the common NS230. NS230 reduced virus virulence, replication, transmission and/or the efficiency of H5N8 to block IFN induction in chickens and ducks; however, the impact of the variable CTE of H5N8 clade 2.3.4.4 viruses in mammals has not been studied. In this study, we (i) analysed the evolution of the NS1 CTE by analysing ~51,000 NS1 sequences from 1902 to 2020, including human influenza viruses (hIAV), mammal-origin AIV and bird-origin AIV with an emphasis on the recent H5N8 viruses, (ii) studied the impact of the NS1 CTE on the expression of type I interferon and induction of apoptosis in human lung cells and (iii) assessed the biological impact of CTE variations on the virulence of different recombinant viruses in mice.

Materials and Methods

Sequence analysis of NS1 of influenza A virus of avian, human and mammalian origin. Sequences of full-length NS1 proteins of AIV in birds, humans or mammals in addition to human H1N1 viruses from 1902 to 2020 were retrieved from GISAID (retrieval date: 28-03-2021). Ambiguous and duplicate sequences were excluded and the remaining sequences were aligned using MAFFT [29] and analysed using Geneious version 11.1. The length of the NS1 and variations in the CTE were summarized (Figure 1, Supplementary Table 1).

Recombinant viruses and cells. A/turkey/Germany-MV/AR2487/2014 (H5N8) (hereafter designated A_NS237) and A/tufted duck/Germany/8444/2016 (H5N8) (hereafter designated B_NS217), belonging to clades 2.3.4.4A and 2.3.4.4B, respectively, were kindly provided by Timm C. Harder (National Reference Laboratory for Avian Influenza Virus, Friedrich-Loeffler-Institut (FLI). Recombinant A_NS237 and B_NS217 viruses were previously generated [30]. The NS segments of these viruses were modified using site-directed mutagenesis to generate A_NS230 and A_NS217 from the A_NS237 plasmid, and similarly B_NS230 and B_NS237 were generated from B_NS217, by changing the stop codons in the CTE as described in a recent study [19] (Figure 1). All viruses were grown in 10-day old specific pathogen free (SPF) embryonated chicken eggs (ECE) according to standard protocols. Human adenocarcinomic alveolar basal epithelial (A549) cells, human embryonic kidney 293T (HEK293T) cells and Madin-Darby canine kidney type II (MDCK-II) cells were provided by the cell culture collection in veterinary medicine of the FLI. Primary turkey embryo kidney (TEK) cells were prepared according to standard protocols, as previously published [31].

Plaque assay. Standard plaque assay was used in this study to titrate the virus and assess cell-to-cell spread. Here, confluent MDCK-II cells were used for virus titration in 12-well plates. Ten-fold dilutions of the virus in phosphate-buffered saline (PBS) were incubated with the cells for 1 h at 37°C/5%CO_2. Cells were washed twice with PBS after aspirating the virus dilutions and were overlaid with Semisolid Bacto-Agar (BD, France) and minimal essential medium (MEM) containing 4% bovine serum albumin (BSA) (MP Biomedicals, USA). Cells were fixed after 3 days at 37°C, with 10% formaldehyde containing 0.1% crystal violet and kept at room temperature. 24 - 72 hours later, the overlays were discarded and the diameter of 50 - 100 plaques were measured per virus to assess cell-to-cell spread. The Nikon NIS-Elements imaging

software (Nikon, Germany) was used and the plaque diameter is shown as the mean and standard deviation.

NS1 expression in human cells. To study the impact of CTE on expression of NS1, A549 cells were transfected with different plasmids. Cloning of the six different NS genes (A_NS217, A_NS230, A_NS237, B_NS217, B_NS230, B_NS237) into pCAGGS was done after amplification of the NS genes from pHW-NS plasmids using specific primers containing NheI and SacI restriction sites (available upon request). The pCAGGS-expression plasmid was kindly provided by Stefan Finke. Besides Sanger sequencing (Eurofins, Germany) and evaluation of the sequences in Geneious prime (2021.0.1), HEK293T cells were transfected with 1µg of each pCAGGS plasmid using Lipofectamine 2000 (Fischer Scientific, Germany) according to manufactures instructions. Transfected cells as well as the supernatant were harvested after 24 h at 37°C/5%CO_2. Cells were centrifuged at 18000 xg for 5 minutes and were washed with PBS twice. Finally, pellets were resuspended in PBS and Laemmli-buffer (Serva, Germany) at a ratio of 1:1 and heated at 95°C for 5 minutes. Afterwards, standard sodium dodecyl sulfate polyacrylamide gel electrophoresis (SDS-PAGE) and Western blot procedures were performed with a 12% polyacrylamide gel, as previously described [32]. Here, a primary polyclonal anti-NS1 antibody, which was kindly provided by Daniel Marc (Infectiologie et Santé Publique, French National Institute for Agricultural Research, France), was used at a dilution of 1:5000 in Tris-buffered saline with 0.1% Tween 20 Detergent (TBST) overnight at 4°C, as well as a secondary peroxidase-conjugated rabbit IgG (Sigma, Germany) that was used at a dilution of 1:20,000 for 30 min at room temperature. Detection was performed using Clarity Western ECL Substrate (BioRad, Germany).

Replication kinetics in avian and human cells. Primary TEK cells and A549 cells were inoculated with the different viruses using a multiplicity of infection (MOI) of 0.001 for one hour at 37°C/5%CO_2. After incubation, only TEK cells were treated with citrate buffer (pH 3.0) saline (CBS) for 2 minutes to inactivate extracellular virions. After washing the cells twice with PBS (TEK cells after CBS treatment, A549 cells after 1 h of infection), cells were covered with MEM containing 0.2% BSA. Infected cells were incubated for 1, 8, 24, 48 and 72 hours at 37°C/5% CO_2. At indicated time points, cells and supernatant were harvested and were stored at - 70°C until virus titre at each time point was determined using plaque assay.

Detection of interferon response in human lung cells. The relative expression of IFN-α and IFN-β mRNAs was measured in A549 cells. Briefly, A549 cells in 24-well plates were adjusted to 4 × 10^5 cells per well. A549 cells were infected with the different viruses using an MOI of 0.1 for 24 h at 37°C/5%CO_2 in triplicates. RNA extraction was done using TRIzol Reagent (Thermo Fisher Scientific, USA) and RNeasy Kit (Qiagen, Germany) according to the manufacturers. The cDNA was transcribed from 400 ng of eluted RNA in a 20 µl reaction using Prime Script 1st Strand cDNA Synthesis Kit (TaKaRA, Germany) and Oligo dT Primers. Quantification of IFN-mRNA was done after partial amplification of IFN-α and IFN-β mRNA using generic RT-qPCR and SensiFAST SYBR Lo-ROX Kit (Bioline, USA) and the thermoprofile as previously published [33]. Relative expression of the IFN-mRNA in infected and non-infected cells was calculated using the 2^-(ΔΔct) method [34].

Detection of caspase-3 activity in human lung cells. A549 cells were infected with an MOI of 0.1 for 8 and 24 h at 37°C or treated with 20 µM (S)-(+)-Camptothecin (Sigma Aldrich, Germany) as a control. Cells and supernatants were harvested 8 and 24 hour post infection (hpi), washed once with ice-cold PBS and lysed for 45 min on ice in cell extraction buffer (CEB, Invitrogen, Germany) that was supplemented with 1x cOmplete Protease Inhibitor Cocktail (Sigma-Aldrich, Germany) and 1 mM Phenylmethylsulfonylfluoride (Sigma-Aldrich). This lysis step was followed by a 10 min 18,000 xg centrifugation step before mixing of the protein lysate with 4x SDS gel loading buffer (10% SDS (w/v), 40% glycerol (v/v), 20% β-mercaptoethanol, 0.008% Bromophenol Blue, 250 mM Tris-HCl pH 6.8). Samples were then heated at 95°C for 5 min and proteins were separated in a 12 % polyacrylamide gel by SDS-PAGE. Proteins were transferred onto a nitrocellulose membrane using a constant voltage of 15 V for 75 min (Bio-Rad) followed by a blocking step for 1 h at RT in 10% skim milk in TBST. Primary antibodies were incubated overnight at 4°C. Here, anti-NS1 (1:5000); Vinculin (1:1000, Santa Cruz Biotechnology, Germany), NP (ATCC-HB65; 1:10000) and caspase-3 (1:1000 or 1:250, Cell-Signaling Technology, USA) primary antibodies were used, whereas secondary antibodies were incubated for 1 h at RT (anti-mouse (1:20000) and anti-rabbit (1:20000 or 1:2000), Cell-Signaling Technology, USA)). Detection was performed with ECL-substrate using X-ray film (Fujifilm: Fuji Super RX-N 13x18 100 Bl).

Flow cytometry. A549 cells were infected at an MOI of 0.1 with B_NS217, B_NS230 and B_NS237. 24 hpi, supernatants and cells were transferred into a collection tube and centrifuged at 3000 xg for 5 min. Supernatant was discarded and cells were fixed with True-Nuclear-reagent (Biolegend, USA) for 30 min. Cells were washed with permeabilization buffer (Biolegend, USA) and stained with primary mouse-anti-NP antibody for 30 min followed by a secondary rat-anti-mouse IgG2a-Brilliant Violet 421 antibody (Biolegend) for 30 min. In a final staining step, the samples were incubated with an anti-active caspase-3 PE labeled antibody (Biolegend) for 30 min. After a final washing step with FACS-Buffer, cells were analyzed using the LSRFortessa Flow Cytometer (BD). The percentage of active caspase positive cells was determined in both NP-positive (infected) and NP-negative (bystander) cell populations using the DIVA software package (BD).

Luciferase assay. To determine whether the IFN-I (IFN-α and IFN-β) and/or NF-kB-induction pathway is inhibited by NS1, HEK293T cells in 6-well plates were transfected with a plasmid DNA mix of 0.5 µg of FFL reporter plasmid (i.e. p125:IFN-β-Pro-FFL, pIFNa-Pro-FFL, or p55:pNF-kB-Pro-FFL), 0.005 µg pCMV-RL (normalization), 0.2 µg (pIRF-7) or 0.5 µg (pMDA5-delta, pTrif or pMyD88) Trigger expression plasmid or 1 µg of poly(I:C) (InvivoGen, France), and 0.5 µg pCAGGS plasmid containing one of the NS1 coding sequences (or empty vector as a control) using Lipofectamine 2000 transfection reagent. IFN-β promoter induction was analyzed using p125 as reporter and poly(I:C), Trif or MyD88 as trigger. IFN-α promoter induction was analyzed using pIFNα-Pro-FFL as reporter and IRF7 as trigger. NF-kB activation was analyzed using p55 as reporter and MyD88 or Trif as trigger. 20 h post transfection cell extracts were prepared and Firefly and Renilla luciferase activities were measured using the Dual-Luciferase Reporter Assay System (Promega, Germany) according to manufacturer's instructions. Luciferase activities were measured with a TriStar² LB 942 Modular Multimode Microplate Reader (Berthold, Germany). Firefly luciferase activity was normalized to Renilla luciferase activity. Induction of the promotor by a trigger was confirmed comparing values for transfection of empty vector pCAGGS with and without trigger plasmid. Promoter induction was set as 1 (100%) for the empty pCAGGS vector control with the given stimulus.

Animal experiments

Ethic statement. Animal experiments in this study were conducted following the German Regulations for Animal Welfare after obtaining the necessary approval from the authorized ethics committee of the State Office of Agriculture, Food Safety, and Fishery in Mecklenburg – Western Pomerania (LALLF M-V: permission number 7221.3-1-060/17) and approval of the commissioner for animal welfare at the FLI representing the Institutional Animal Care and Use Committee (IACUC). All animal experiments were carried out in the BSL3 animal facilities at the FLI.

Experimental design. Five-week-old female BALB/C mice (Charles River, Sulzfeld, Germany) were allocated into groups of 3-5 mice per cage in closed ISOcage systems (Tecniplast, Buguggiate, Italy). Mice were left to acclimatize for 5 days before infection and received food and water *ad-libitum*. The light and temperature were regulated automatically. At the day of infection (d0), the bodyweight (BW) of mice was measured using digital balance and numbered on the tail. Each mouse received either 10^3 (n = 8) or 10^5 (n = 5) pfu in 50 µL MEM containing antibiotics via the intranasal (IN) route. Sham mice group (n = 8) were inoculated with 50 µL sterile MEM. All inoculation experiments were occurred under mild anaesthesia using Isoflurane (CP-Pharma, Germany). BW gain, morbidity and mortality were recorded daily for 11 days post-inoculation (dpi). BW per gram relative to the BW at d0 was calculated for each mouse. Mice that lost more than 25% of the d0-BW value were humanely killed and scored dead. At the end of the experiment, surviving mice were humanely killed using isoflurane and cervical dislocation. Mean time to death (MTD) was calculated for each group.

Replication of H5N8 viruses in mice. To detect the amounts of viral RNA in lung, spleen and brain of mice, RT-qPCR targeting the M gene was performed as described [35] using SuperScript™ III One-Step RT-PCR System with Platinum® Taq DNA Polymerase (Invitrogen, Germany) in AriaMx real-time cycler as described before [35]. Tissues were weighed and homogenized in 10% w/v 1xPBS. Homogenates were centrifuged for 10 min at 15,000 xg (tabletop centrifuge). The viral RNA was extracted using the Viral RNA/DNA Isolation Kit (NucleoMagVET) (Macherey & Nagel GmbH, Germany). Standard curves were generated by testing serial dilutions of B_NS217 (10 to 100000 pfu) in each plate. To semi-quantify the viral RNA, plotting of the Ct-value and corresponding dilution in the standard curve was automatically done. Results are shown as mean and standard deviation of positive samples.

Seroconversion. At the end of the experiment, blood samples were collected from the surviving mice after deep euthanization and decapitation. Serum samples were collected after 24 h at 4°C and centrifugation. Commercially available "ID screen Influenza A Antibody Competition Multispecies kit" enzyme-linked immunosorbent assay (ELISA) (IDvet, France) was used to detect anti-AIV nucleoprotein using Infinite® 200 PRO reader (Life Sciences, Tecan). According to the manufacturer's recommendation 55% inhibition was the cut-off-point, 45-55% were considered questionable and samples below 45% were considered as negative.

Statistics. Statistical analysis was performed with GraphPad Prism, Version 9.0.0. Plaque diameter as well as replication kinetics were analysed with non-parametric Kruskal-Wallis (Dunn's multiple comparison) test. Fold-change induction of interferons as well as caspase activity and viral load in different mice organs were statistically analysed with one-way ANOVA with post hoc Tukey's test. Variation in the survival period of the mice was statistically analysed with the Log-rank (Mantel-Cox) test. Data were considered statistically significant at p value < 0.05.

Results

In contrast to AIV of bird-origin, human H1N1, mammal-origin AIV and recent H5N8-B viruses exhibit a high prevalence for short NS1. We analysed NS1 sequences from 1902 to 2020 of human seasonal and pandemic H1N1 influenza viruses (n= 30766) and compared them to AIV of bird-origin (n=17574), avian H1N1 (n= 661), recent H5N8 clade 2.3.4.4 (n= 1070) and mammal-origin AIV in humans (zoonotic AIV) (n= 1626) and animals (n= 162) (Figure 1A-F, Supplementary Table S1). The results showed that human H1N1 viruses had three major forms NS219, NS230 and NS237 with a prevalence rate of 93.0%, 6.6% and 0.4%, respectively. However, there is a striking variation since 2009. Before the emergence of pandemic H1N1 in 2009, NS219 was less prevalent (1.9%) than NS230 (88.9%) and NS237 (9.2%). After 2009, NS219 was more prevalent (97.6%) than NS230 (2.4%) and NS237 (0.02%) (Supplementary Table S1). Conversely, we found that AIV of bird-origin have high prevalence of NS230 (70.1%) followed by NS217 (28%) and NS237 (0.6%). Similarly, avian H1N1 viruses have only two forms (NS219 and NS230) with a clear preference to NS230 (97.5%) over NS219 (2.5%) (Figure 1D, Supplementary Table

S1). These results indicate that recent hIAV prefer short NS1 (i.e. NS219) in contrast to AIV which prefer the prototypic NS230.

Surprisingly, we found that H5N8-A in 2013/2015 had NS237 (89.3%) and NS230 (10.7%), while H5N8-B in 2016/2018 had NS217 (66.2%) and NS230 (33.8%) (Figure 1E and F, Supplementary Table S1), which indicate unique clade-specific preferences. To get an insight into the association between the length of NS1 and bird-to-mammal transmission, we analysed 1788 AIV NS1 sequences detected in humans (n= 1626) and animals (n= 162) from 1956 to 2020 (Supplementary Table S1). Indeed, we found that the prevalence of short NS1 (i.e. 217) was higher (75.7%) than NS225-NS230 (23.2%) or NS237 (0.3%) (Figure 1, Supplementary Table S1). Interestingly, human-H5N8-B virus isolated in Russia in December 2020 has NS217 (accession number EPI1846965). These results indicated that transmission of AIV from birds to mammals is accompanied by high prevalence of short NS1. Recent H5N8 viruses have unique clade-specific preferences towards long (H5N8-A) or short (H5N8-B) NS1 with unknown biological function in mammals.

Recombinant H5N8 clade 2.3.4.4 A and B viruses and expression of NS1. To assess the impact of NS1 variation on increased replication efficiency of H5N8 clade 2.3.4.4 in mammals, we used six recombinant H5N8 viruses expressing NS1 of different sizes [19]: three H5N8 clade A (designated A_NS217, A_NS230 and A_NS237) and three clade B (designated B_NS217, B_NS230 and B_NS237) carrying NS1 with 217, 230 or 237 aa after changing stop codons in the CTE (Figure 1G). Viruses were propagated in ECE and virus titres were determined by plaque assay. Full genome sequences of these recombinant viruses excluded unwanted mutations. Expression of NS1 was detected in HEK293T cells at 37°C after transfection with pCAGGS-expression vector containing different NS1. As expected, the molecular mass of NS1 correlated with the length of NS217, NS230 and NS237 (Figure 1H).

Changes in the CTE significantly reduced cell-to-cell spread without impact on virus replication in human cells. Alterations of the NS1-length of H5N8-A and H5N8-B viruses reduced cell-to-cell spread as indicated by smaller plaque size in MDCK-II cells (Figure 2A -B). The parent A_NS237 and B_NS217 produced significantly larger plaques than their progeny expressing other NS1 variants ($p < 0.0001$). Viruses carrying NS230 produced the smallest plaques ($p < 0.0001$). We further compared the

replication of different viruses in primary TEK and human A549 lung cells. In TEK cells, H5N8-A virus carrying NS217 replicated to significantly higher levels than other H5N8-A viruses at 24 hpi ($p < 0.03$). The titre of B_NS237 at 72 hpi was significantly lower than B_NS230 and B_NS217 ($p < 0.03$) (Figure 2C – D). In A549, no significant differences were observed except that the titre of A_NS237 was marginally higher than that of A_NS230 at 48 hpi ($p < 0.049$) (Figure 2E - F). The replication of all viruses on human cells was significantly lower than in TEK cells. Together, NS230 significantly reduced cell-to-cell spread of both H5N8-A and H5N8-B, and extension of H5N8-B was disadvantageous for virus spread in mammalian cells with minimal impact on virus replication in human cells.

Extension of NS1 modulated the efficiency of H5N8 viruses to block IFN-α and IFN-β response in human lung cells. It has been previously reported that NS1 CTE impairs IFN-induction [36], while other reports did not find any impact [21, 22, 37]. To test whether the H5N8 NS1 CTE can affect IFN-induction, we infected A549 cells with H5N8-A and H5N8-B viruses carrying NS217, NS230 or NS237 and measured the IFN-α and IFN-β mRNA levels using generic RT-qPCR (Figure 3A-D). The results showed that viruses carrying NS217 (A_NS217 and B_NS217) had the highest efficiency to block the IFN-β response. Extension to NS230 and NS237 gradually reduced the efficiency to block IFN-response (Figure 3C-D). A_NS237 was significantly more efficient than H5N8-A carrying shorter NS1 to block IFN-α response, while B_NS217 was more efficient to block IFN-α response than H5N8-B viruses carrying longer NS1. Together, extension of the NS1 CTE reduced the efficiency of H5N8-B virus to block the induction of type I IFN response in human lung cells. Shortening of NS1 of H5N8-A reduced virus efficiency to block IFN-α response but enhanced the capacity to block IFN-β induction.

Shorter NS1 induced lower levels of active caspase-3 in human lung cells. It has been shown that H5N1 NS1 induced caspase-dependent apoptosis [38] and the PDZ domain in the CTE was associated with apoptosis induction [39]. To study the impact of NS1 CTE to control apoptosis, we infected A549 cells at 8 and 24h with B_NS217, B_NS230 or B_NS237 and detected caspase-3 using Western blot. No active (i.e. cleaved) caspase-3 (aCas3) was detected 8 hpi but all viruses induced aCas3 at 24 hpi. B_NS217 showed a weaker signal of aCas3 than B_NS230 and B_NS237 (Figure 4A). To quantify the amount of aCas3, we infected A549 cells with different H5N8-B

viruses and measured the aCas3 and influenza NP using flow cytometry in infected and non-infected bystander cells (Figure 4B-E). The results confirmed the WB findings that all viruses induced aCas3 and the shorter the NS1, the less amount of aCas3 induced regardless of the number of infected cells (Figure 4). These results indicated that shorter NS1, are more efficient in blocking H5N8-B induced apoptosis in infected cells and in uninfected bystander cells.

Changes in the NS1 CTE alone are not the main cause for the inhibition of type I IFN-induction. Some studies suggested that NS1 is unable to act as a direct inhibitor of apoptosis and IFN induction pathways which probably require the interplay or interaction of NS1 with other viral proteins (e.g. encoded by polymerase genes) [40, 41, 42, 43]. To study whether the variable efficiency of H5N8 viruses to block IFN- or apoptosis-induction was actually due to changes in the CTE, we transfected human cells with pCAGGS-NS (Figure 5A-F). We measured IFN-α, IFN-β and NF-kB promotor activity using luciferase reporter assay and different triggers for induction of IFN-β (poly IC, Trif and MDA-5delta), IFN-α (IRF-7) or activation of NF-kB (Trif and MyD88). Surprisingly, no significant differences using different NS plasmids in inhibition of IFN -induction and NF-kB activation were observed regardless of the trigger (Figure 5), the concentration of NS1 plasmids and different cells (HEK293T and A549) (data not shown). These results suggest that changes in the NS1 C-terminus are not the main driver for the efficiency of H5N8 to block type I IFN or NF-kB responses and the interaction of NS1 CTE with other gene segments is likely the reason for this variable efficiency.

H5N8 viruses carrying short NS1 CTE caused higher mortality and shorter survival period in mice. To assess the pathogenicity and impact of NS1 CTE on virus virulence in mammals, mice were inoculated IN with low- and high-dose virus preparations. Clinical examination, survival period and BW gain were assessed daily. After challenge with low-dose, H5N8-A inoculated mice did not show clinical signs and survived until the end of the experiment, except 1/5 mice inoculated with A_NS217 died suddenly at 7 dpi (Figure 6A). Conversely, all B_NS217 inoculated mice died 7 and 8 dpi with MTD of 7.5 days after showing ruffled fur and mild to moderate depression (Figure 6B). Moreover, 2/5 and 4/5 mice inoculated with B_NS230 and B_NS237 died or had to be euthanized after showing nervous signs with MTD of 8.7 and 8.8, respectively. The survival period of mice inoculated with B_NS217 was

significantly shorter than mice inoculated with B_NS230 ($p < 0.003$) or B_NS237 ($p < 0.02$). After high-dose challenge, 2/5, 4/5 and 4/5 mice died with MTD of 9, 4 and 4.5 days after inoculation with A_NS237, A_NS230 and A_NS217, respectively (Figure 6C). Mice in these groups did not show clinical signs but were humanely killed because of >25% BW loss. Conversely, all mice inoculated with B_NS217, B_NS230, and B_NS237 died with MTD of 6.4, 8.2 and 5.4 day, respectively. The survival period of mice inoculated with B_NS217 or B_NS237 was significantly shorter than mice inoculated with B_NS230 ($p < 0.03$) (Figure 6D). Mice in these groups showed severe depression and nervous signs. Taken together, H5N8-B was more virulent in mice than H5N8-A. H5N8 viruses carrying short NS1 exhibited more severe clinical signs, higher mortality rate and shorter survival periods. The only exception was that the virulence of B_NS237 was comparable to that of B_NS217 after high-dose inoculation.

H5N8 viruses carrying short NS1 CTE caused higher bodyweight loss in mice in a dose-dependent manner. To assess the impact of NS1 CTE variations on the BW gain of mice inoculated with different viruses, mice were weighed daily. The relative BW was calculated from day 0. Regardless of the infection dose, mice inoculated with B_NS217 lost significantly more BW compared to A_NS237 and shortening the NS1 of the latter increased BW gain loss. After inoculation with low dose, H5N8-A inoculated mice did not exhibit a significant reduction in BW compared to the sham group, except A_NS217 inoculated mice which showed transient reduction in BW at 1-2 dpi. Conversely, mice inoculated with B_NS217 showed the highest reduction in BW followed by mice inoculated with B_NS237 then B_NS230 (Figure 6F). After challenge with high dose, mice inoculated with A_NS217 and A_NS230 lost more BW compared to A_NS237-inoculated mice, where the reduction in BW gain was statistically significant at 3 to 5 dpi only (Figure 6G). Thereafter, surviving mice in these groups gained BW and recovered at 6 dpi (A_NS217) or 11 dpi (A_NS230 and NS237) (Figure 6G). Conversely, mice inoculated with B_NS217, B_NS230 or B_NS237 exhibited drastic reduction in BW starting 1 dpi until the day of death (Figure 6H). The highest reduction in BW was reported in mice inoculated with B_NS237 followed by mice inoculated with A_NS217 then A_NS230 (Figure 6H). Together, H5N8-B inoculated mice exhibited a severe reduction in BW compared to H5N8-A inoculated mice after low-dose challenge. H5N8-A viruses carrying short NS1 lost more BW compared to H5N8 carrying NS237. Likewise, mice inoculated with H5N8-B carrying NS217 lost

more BW compared to those inoculated with B_NS230. The impact of NS237 on BW loss after H5N8-B inoculation was dose-dependent.

Clade B virus replicated at higher levels in mice than clade A and elongation in the CTE reduced clade B virus replication. To determine the replication of different viruses in lung, spleen and brain without prior adaptation, three mice per group were euthanized 3 dpi with low-dose and the viral RNA was quantified using RT-qPCR (Figure 7A-D). H5N8-A viruses were detected only in the lungs indicating limited replication. B_NS217 replicated to 10000-fold higher titres than H5N8-A virus ($p < 0.005$) (Figure 7A-B). Extension of the NS1 of B_NS217 significantly reduced virus replication in the lungs by 1000- and 500- fold, respectively ($p < 0.005$) and abolished virus replication in the spleen (Figure 7C-D). In the brain, viral RNA was detected in only 1/3 mice inoculated with B_NS217 (data not shown). Antibodies were detected in all surviving mice, except in those inoculated with low-dose of A_NS237 (n=2/5), A_NS230 (4/5), or A_NS217 (3/5) (data not shown). Anti-NP antibodies were not detected in the sham group. Together, H5N8-B replicated at higher levels in the lungs and spleen compared to H5N8-A. Shortening the NS1 CTE did not have a significant impact on H5N8-A replication in mice, while extension of NS1 CTE reduced the replication of H5N8-B significantly.

Discussion

AIV pose a serious public health threat either by direct bird-to-human transmission or generation of pandemic influenza viruses after reassortment, exchanging gene segments with hIAV. Because the human population is immunologically naïve to AIV, AIV infections may trigger high immune response and can result in severe respiratory distress and death [44]. The continuous evolution of the panzootic H5N8 clade 2.3.4.4 viruses warrants vigilance to assess their potential zoonotic and pandemic risk [28]. Our sequence analysis revealed that the NS1 of H5N8-B virus resembles human H1N1 and zoonotic AIV with preferences for shorter NS1 protein. Conversely, AIV of bird-origin mostly possess prototypical NS1 with 230-aa. Interestingly, AIV H5N8-A and H5N8-B evolved towards NS1 with longer and shorter CTE, respectively, compared to the vast majority of AIV indicating biological advantages over NS230. We have recently shown that viruses carrying NS230 lost fitness in chickens and ducks [19]. The impact

of these deletion (NS217) and extension (NS237) in CTE of AIV on virulence and replication of HPAIV in mammals is not adequately studied. Here, we did not find a significant impact on virus replication in human lung cells, but found that NS230 significantly reduced cell-to-cell spread in both H5N8-A and H5N8-B viruses. Similar to our results, Hale et al. [18] found that increasing the length of the 2009 H1N1 NS1 protein to 230 aa did not increase virus replication in human cells and Jackson et al. [37] found that increasing the NS1 length of a laboratory WSN H1N1 increased the plaque size.

One of the well-described functions for NS1 is its ability to antagonize the interferon response. The role of CTE in the inhibition of IFN-induction is controversial. Mutations, deletions (6-aa or 10-aa) or extensions in the CTE of HPAIV H5N1, laboratory H1N1 or LPAIV H9N2 did not alter the IFN-β response in A549 cells [21, 22, 37]. Conversely, extension of the CTE in the pandemic H1N1-2009 increased the efficiency to block the IFN-β response in A549 cells [36]. Likewise, studies showed that NS1 of several AIV has pro-apoptotic activity [37], while NS1 of other viruses mediate anti-apoptotic signalling responses [45, 46]. Here, we found that NS1 with long CTE, regardless of the virus backbone, exhibited significant reduction in the efficiency of H5N8 viruses to block IFN-β induction in human lung cells. A similar pattern was obtained for the efficiency to block apoptosis induction by H5N8-B viruses in infected and non-infected bystander cells. These results suggest that apoptosis induction was interferon-dependent or both IFN-β and apoptosis were induced through a common pathway. IFN-dependent anti-apoptotic activity of laboratory IAV (PR8/H1N1) after deletion in the NS1 has been previously reported [45].

Interestingly, in contrast to the positive correlation of IFN-β induction and the length of NS1, IFN-α induction was virus-dependent and not NS1 length-dependent. Hence, increased IFN-α induction was obtained after infection with H5N8-A carrying NS217 and H5N8-B carrying NS237. These results indicate that IFN-α and IFN-β are being antagonised by different mechanisms that are influenced differently by changes in the NS1 CTE, an observation that merits further investigation. The NS1 CTE contains residues, which interact with several host proteins including poly(A)-binding protein II (PABII), PDZ domain-containing proteins, importin-α and nucleolin [13]. Changes in the CTE could affect the interaction of NS1 with these proteins which might be compensated by mutations in the NS1 or other viral proteins. Indeed, truncation of NS1

reduced the efficiency of H1N1-2009 to shut-off host mRNA transcription and trafficking including IFN mRNA. The ability of NS1 to block IFN response was restored by binding to PABII after extension of the CTE [36] or by increased binding to pre-mRNA processing protein CPSF30 via mutations in the ED [47, 48]. Similarly, recent studies have shown that interferon induction can be balanced or compensated by other viral proteins (e.g. PB2, PB1-F2 or PA-X) after changes in the NS1 [43, 49]. This might explain the discrepancy between infected and transfected cells to inhibit type I IFN or NF-kB pathways under our current experimental settings. Moreover, independent of NS1, the contribution of the polymerase genes of H5N8 clade 2.3.4.4 in the induction of IFN-β has been recently reported [50].

Compared to the low virulence and limited replication of H5N8-A in murine lungs, H5N8-B was more virulent in mice and viral RNA was detected in extrapulmonary tissues including the spleen and brain indicating better replication in mammals without prior adaptation. This is in accordance with findings of previous studies used the wild-type H5N8-B virus [51] or H5N8-A like viruses [52]. We also showed that H5N8-A and H5N8-B viruses with short NS1 CTE (NS217) exhibited increased virulence in mice as indicated by high mortality rate, rapid onset of mortality and/or shorter survival periods. Exceptionally, H5N8-B carrying NS237 was less virulent than H5N8 carrying NS217 after low-dose inoculation and exhibited comparable pathogenicity after high-dose inoculation. A possible explanation for that is the variation in the balance between immune system and virus replication. As seen from the experiment in human lung cells, H5N8-B carrying NS237 was less efficient to block induction of IFN and apoptosis. Therefore, it is likely that mice were able to clear the virus after low-dose inoculation as seen by reduced viral levels in the lungs, spleen and brain. However, high-dose inoculation of mice with H5N8-B carrying NS237 probably triggered a “cytokine storm” which caused the death of the mice similar to H5N8-B carrying NS217. This is consistent with findings of other studies describing that deletion of 11-aa in the NS1 CTE increased pathogenicity of the pandemic H1N1-2009 virus in mice [36]. Conversely, in another study, a laboratory WSN strain with truncated NS1 C-terminus (residues 227-230) showed reduced virulence and pathogenesis compared to viruses with full NS1. Variation in pathogenicity was independent of the efficiency of IFN-antagonism of NS1 [37].

In summary, we found that H5N8-B clade 2.3.4.4 viruses have preferences for a short NS1 similar to human influenza viruses and zoonotic AIV due to truncation in the C-terminus. H5N8 viruses carrying short NS1 exhibited high cell-to-cell spread capacity, were more efficient in blocking the IFN-β response and reduced the induction of apoptosis with minimal impact on virus replication in human lung cells. The truncation in the NS1 increased virulence of H5N8 in mice, regardless of the virus backbone, and therefore it should be considered as a virulence marker for similar H5N8 viruses in mammals.

Acknowledgments

Dajana Helke is highly acknowledged for expert laboratory technical assistance. Christine Fast, Marcel Gischke, Charlotte Schröder, Bärbel Hammerschmidt, Frank Klipp, Harald Manthei, Doreen Fielder, Bärbel Berger and Thomas Moeritz supported in the animal experiments. Daniel Marc provided the anti-NS1 antibodies and Stefan Finke provided the pCAGGS expression vector. Jana Schulz is thanked for help in statistical analysis. This work was partially supported by grants from Delta Flu Project, Project ID: 727922 funded by the European Union under: H2020-EU and the Deutsche Forschungsgemeinschaft (DFG; AB 567). The funders had no role in study design, data collection and analysis, decision to publish, or preparation of the manuscript.

Conflict of interests

The authors declare no conflict of interest

Figure Legends

Figure 1: Sequence analysis and expression of H5N8 2.3.4.4 carrying different NS1 in human cells

Sequences of full-length NS1 protein of human H1N1 compared to AIV in birds, humans or mammals from 1902 to 2020 were retrieved from GISAID at 28-03-2021. Sequences were cleaned from ambiguous residues and compared using Geneious version 11.1. Shown is the prevalence of NS1 of variable length in human H1N1 viruses (A), zoonotic AIV (B), AIV (C), avian H1N1 (D) and H5N8 clade 2.3.4.4A (E) and 2.3.4.4B (F). Schematic illustration for the C-terminus of recombinant viruses used in this study (G). NS1 expression in HEK293T cells transfected with 1 µg of indicated pCAGGS-NS1 plasmids for 24 h (H).

Figure 2: The impact of NS1 C-terminus variations in cell-to-cell spread and replication of recombinant H5N8 viruses in cell culture

Cell-to-cell spread was determined by measuring the diameter of 100 plaques after infection of MDCK-II cells with H5N8-A (A) and H5N8-B (B). Results are expressed as mean and standard deviation (µm). Replication kinetics in turkey embryo kidney (TEK) cells infected with H5N8-A (C) or H5N8-B (D) at MOI of 0.001 pfu at indicated time points. Replication kinetics in human lung cells (A549) infected with H5N8-A (E) or H5N8-B (F) at MOI of 0.001 pfu at indicated time points. Virus titre was determined using plaque assay in MDCK-II cells. The assay was done in duplicates and repeated twice. Asterisks indicate statistical significance at p value * < 0.05, **< 0.01, *** < 0.005, **** < 0.0005.

Figure 3: The impact of NS1 C-terminus variation on interferon-induction in human cells infected with H5N8 clade 2.3.4.4

The relative expression of IFN-α (A, B) and IFN-β (C, D) mRNAs was measured in A549 cells infected with the different viruses using an MOI of 0.1 for 24 h. Relative expression of the IFN-mRNA in infected and non-infected cells was calculated using the 2^-(ΔΔct) method of three experiments. Asterisks indicate statistical significance at p value * < 0.05, **< 0.01, *** < 0.005, **** < 0.0005.

Figure 4: The impact of NS1 C-terminus variation on apoptosis-induction in human cells infected with H5N8 clade 2.3.4.4

Active caspase-3 (i.e. cleaved caspase-3) was detected in A549 cells after the infection with an MOI of 0.1 for 8 and 24 h at 37°C. Cells treated with 20 µM Camptothecin were used as control. Detection was performed with ECL-substrate and X-ray film (A). The amount of activated caspase-3 was quantified using flow cytometry after infection of A549 cells at an MOI of 0.1 for 24 h (B-E). Cells were stained with a primary mouse-anti-NP antibody (ATCC-HB65) and a caspase-3 PE labeled antibody. Signals were analyzed via FACS with gating for either all cells (C), NP positive cells only (D), or NP negative cells only (E). Asterisks indicate statistical significance at p value * < 0.05, **< 0.01, *** < 0.005, **** < 0.0005.

Figure 5: IFN-I and NF-kB induction pathways in human cells after transfection with NS1 of H5N8 clade 2.3.4.4B

To determine which IFN-I (IFN-α and IFN-β) or NF-kB-induction pathway is inhibited by NS1, HEK293T cells in 6-well plates were transfected with a plasmid DNA mix of a FFL reporter plasmid (p125:IFN-β-Pro-FFL, pIFNα-Pro-FFL or pNF-kB-Pro-FFL), pCMV-RL, a Trigger expression plasmid or poly(I:C), and a pCAGGS plasmid containing one of the NS1 coding sequences using Lipofectamine 2000 transfection reagent. Trigger molecules used to activate the signaling cascade and analyzed promoters (reporter construct) are given above the graphs (A-F). 20 h post transfection cell extracts were prepared and luciferase activities were measured using the Dual-Luciferase Reporter Assay System (Promega) according to manufacturer's instructions. Firefly luciferase activity was normalized to Renilla luciferase activity. Promoter induction was set as 1 (100%) for the empty vector control with the given Trigger. Induction of the promotor by a trigger molecule was confirmed comparing values for transfection of empty vector pCAGGS with and without trigger plasmid. FFL: Firefly luciferase; RL: Renilla luciferase.

Figure 6: The impact of NS1 C-terminus variations on survival period and bodyweight gain in mice inoculated with H5N8 viruses

Shown are estimated survival periods of BALB/C mice inoculated intranasal with low-dose (10^3 pfu) (A, B) or high-dose (10^5 pfu) (C, D) of H5N8-A (A, C) or H5N8-B (B, D).

The relative bodyweight gains of BALB/C mice inoculated intranasal with low-dose (E, F) and high-dose (G, H) of H5N8-A (E, G) or H5N8-B (F, H) were calculated. Mock mice group were inoculated with 50 µL sterile medium. All inoculation experiments were occurred under mild anaesthesia using Isoflurane. Results are the relative mean to the bodyweight immediately before infection (d0). Mice that lost more than 25% of the d0-bodyweight value were humanely killed and scored dead. For optical reasons, standard deviations are not shown.

Figure 7: The impact of NS1 on replication of H5N8 viruses in mice

Replication of indicated viruses in mice inoculated intranasally with low-dose was assessed in 3 mice per group sacrificed 3 dpi under deep anaesthesia using isoflurane and cervical dislocation (A-D). Viral RNA was extracted from the indicated organs and was detected using RT-qPCR and standard curves of serial dilutions of B_NS217 (10 to 100000 pfu) in each plate. Results are shown as mean and standard deviation of positive samples (A-D). Asterisks indicate statistical significance at p value *** < 0.001.

References

1. Alexander DJ. An overview of the epidemiology of avian influenza. Vaccine. 2007 Jul 26;25(30):5637-44. doi: 10.1016/j.vaccine.2006.10.051. PubMed PMID: 17126960.
2. Verhagen JH, Fouchier RAM, Lewis N. Highly pathogenic avian influenza viruses at the wild–domestic bird interface in Europe: Future directions for research and surveillance. Viruses. 2021;13(2):212. PubMed PMID: doi:10.3390/v13020212.
3. Philippon DAM, Wu P, Cowling BJ, et al. Avian influenza human infections at the human-animal interface. J Infect Dis. 2020 Jul 23;222(4):528-537. doi: 10.1093/infdis/jiaa105. PubMed PMID: 32157291.
4. Reperant LA, Rimmelzwaan GF, Kuiken T. Avian influenza viruses in mammals. Rev Sci Tech. 2009 Apr;28(1):137-59. doi: 10.20506/rst.28.1.1876. PubMed PMID: 19618623; eng.
5. Fouchier RA, Munster V, Wallensten A, et al. Characterization of a novel influenza A virus hemagglutinin subtype (H16) obtained from black-headed gulls. J Virol. 2005 Mar;79(5):2814-22. doi: 10.1128/JVI.79.5.2814-2822.2005. PubMed PMID: 15709000; PubMed Central PMCID: PMCPMC548452.
6. Lloren KKS, Lee T, Kwon JJ, et al. Molecular markers for interspecies transmission of avian influenza viruses in mammalian hosts. Int J Mol Sci. 2017 Dec 13;18(12):2706. doi: 10.3390/ijms18122706. PubMed PMID: 29236050; PubMed Central PMCID: PMCPMC5751307.
7. Herfst S, Imai M, Kawaoka Y, et al. Avian influenza virus transmission to mammals. Curr Top Microbiol Immunol. 2014;385:137-55. doi: 10.1007/82_2014_387. PubMed PMID: 25048542; eng.
8. Zanin M, Wong SS, Barman S, et al. Molecular basis of mammalian transmissibility of avian H1N1 influenza viruses and their pandemic potential. Proc Natl Acad Sci U S A. 2017 Oct 17;114(42):11217-11222. doi: 10.1073/pnas.1713974114. PubMed PMID: 28874549; PubMed Central PMCID: PMCPMC5651783.
9. Li Z, Jiang Y, Jiao P, et al. The NS1 gene contributes to the virulence of H5N1 avian influenza viruses. J Virol. 2006 Nov;80(22):11115-23. doi: 10.1128/JVI.00993-06. PubMed PMID: 16971424; PubMed Central PMCID: PMC1642184.
10. Ayllon J, Domingues P, Rajsbaum R, et al. A single amino acid substitution in the novel H7N9 influenza A virus NS1 protein increases CPSF30 binding and virulence. J Virol. 2014 Oct;88(20):12146-51. doi: 10.1128/JVI.01567-14. PubMed PMID: 25078692; PubMed Central PMCID: PMC4178744.
11. Long JX, Peng DX, Liu YL, et al. Virulence of H5N1 avian influenza virus enhanced by a 15-nucleotide deletion in the viral nonstructural gene. Virus genes. 2008 Jun;36(3):471-8. doi: 10.1007/s11262-007-0187-8. PubMed PMID: 18317917.
12. Hale BG, Randall RE, Ortin J, et al. The multifunctional NS1 protein of influenza A viruses. J Gen Virol. 2008 Oct;89(Pt 10):2359-2376. doi: 10.1099/vir.0.2008/004606-0. PubMed PMID: 18796704; eng.
13. Marc D. Influenza virus non-structural protein NS1: interferon antagonism and beyond. J Gen Virol. 2014 Dec;95(Pt 12):2594-2611. doi: 10.1099/vir.0.069542-0. PubMed PMID: 25182164.
14. Moltedo B, López CB, Pazos M, et al. Cutting edge: stealth influenza virus replication precedes the initiation of adaptive immunity. J Immunol. 2009 Sep

15;183(6):3569-73. doi: 10.4049/jimmunol.0900091. PubMed PMID: 19717515; eng.

15. Dundon WG, Milani A, Cattoli G, et al. Progressive truncation of the Non-Structural 1 gene of H7N1 avian influenza viruses following extensive circulation in poultry. Virus research. 2006 Aug;119(2):171-6. doi: 10.1016/j.virusres.2006.01.005. PubMed PMID: 16464514.
16. Suarez DL, Perdue ML. Multiple alignment comparison of the non-structural genes of influenza A viruses. Virus research. 1998 Mar;54(1):59-69. PubMed PMID: 9660072.
17. Abdelwhab el SM, Veits J, Breithaupt A, et al. Prevalence of the C-terminal truncations of NS1 in avian influenza A viruses and effect on virulence and replication of a highly pathogenic H7N1 virus in chickens. Virulence. 2016 Jul 03;7(5):546-57. doi: 10.1080/21505594.2016.1159367. PubMed PMID: 26981790; PubMed Central PMCID: PMCPMC5026787.
18. Hale BG, Steel J, Manicassamy B, et al. Mutations in the NS1 C-terminal tail do not enhance replication or virulence of the 2009 pandemic H1N1 influenza A virus. J Gen Virol. 2010 Jul;91(Pt 7):1737-42. doi: 10.1099/vir.0.020925-0. PubMed PMID: 20237225; PubMed Central PMCID: PMCPMC3052525. eng.
19. Blaurock C, Breithaupt A, Scheibner D, et al. Preferential selection and contribution of non-structural protein 1 (NS1) to the efficient transmission of the panzootic avian influenza H5N8 2.3.4.4 clades A and B viruses in chickens and ducks. bioRxiv. 2021:2021.03.14.435362. doi: 10.1101/2021.03.14.435362.
20. Soubies SM, Volmer C, Croville G, et al. Species-specific contribution of the four C-terminal amino acids of influenza A virus NS1 protein to virulence. J Virol. 2010 Jul;84(13):6733-47. doi: 10.1128/JVI.02427-09. PubMed PMID: 20410267; PubMed Central PMCID: PMC2903243.
21. Zielecki F, Semmler I, Kalthoff D, et al. Virulence determinants of avian H5N1 influenza A virus in mammalian and avian hosts: role of the C-terminal ESEV motif in the viral NS1 protein. J Virol. 2010 Oct;84(20):10708-18. doi: 10.1128/JVI.00610-10. PubMed PMID: 20686040; PubMed Central PMCID: PMC2950580.
22. Kong W, Liu L, Wang Y, et al. C-terminal elongation of NS1 of H9N2 influenza virus induces a high level of inflammatory cytokines and increases transmission. J Gen Virol. 2015 Feb;96(Pt 2):259-268. doi: 10.1099/vir.0.071001-0. PubMed PMID: 25326314; eng.
23. Guan Y, Smith GJ. The emergence and diversification of panzootic H5N1 influenza viruses. Virus research. 2013 Dec 5;178(1):35-43. doi: 10.1016/j.virusres.2013.05.012. PubMed PMID: 23735533; PubMed Central PMCID: PMCPMC4017639.
24. Ip HS, Torchetti MK, Crespo R, et al. Novel Eurasian highly pathogenic avian influenza A H5 viruses in wild birds, Washington, USA, 2014. Emerg Infect Dis. 2015 May;21(5):886-90. doi: 10.3201/eid2105.142020. PubMed PMID: 25898265; PubMed Central PMCID: PMCPMC4412248.
25. Pasick J, Berhane Y, Joseph T, et al. Reassortant highly pathogenic influenza A H5N2 virus containing gene segments related to Eurasian H5N8 in British Columbia, Canada, 2014. Sci Rep. 2015 Mar 25;5:9484. doi: 10.1038/srep09484. PubMed PMID: 25804829; PubMed Central PMCID: PMCPMC4372658.

26. WHO. Human infection with avian influenza A (H5N8) – the Russian Federation. Available online at: https://www.who.int/csr/don/26-feb-2021-influenza-a-russian-federation/en/ (Accessed 26-03-2021). 2021.
27. Shin DL, Siebert U, Lakemeyer J, et al. Highly pathogenic avian influenza A(H5N8) virus in Gray Seals, Baltic Sea. Emerg Infect Dis. 2019 Dec;25(12):2295-2298. doi: 10.3201/eid2512.181472. PubMed PMID: 31742519; PubMed Central PMCID: PMCPMC6874272. eng.
28. Yamaji R, Saad MD, Davis CT, et al. Pandemic potential of highly pathogenic avian influenza clade 2.3.4.4 A(H5) viruses. Rev Med Virol. 2020 May;30(3):e2099. doi: 10.1002/rmv.2099. PubMed PMID: 32135031; eng.
29. Katoh K, Standley DM. MAFFT multiple sequence alignment software version 7: improvements in performance and usability. Mol Biol Evol. 2013 Apr;30(4):772-80. doi: 10.1093/molbev/mst010. PubMed PMID: 23329690; PubMed Central PMCID: PMCPMC3603318.
30. Mostafa A, Blaurock C, Scheibner D, et al. Genetic incompatibilities and reduced transmission in chickens may limit the evolution of reassortants between H9N2 and panzootic H5N8 clade 2.3.4.4 avian influenza virus showing high virulence for mammals. Virus Evol. 2020 Jul;6(2):veaa077. doi: 10.1093/ve/veaa077. PubMed PMID: 33343923; PubMed Central PMCID: PMCPMC7733613.
31. Hennion RM, Hill G. The preparation of chicken kidney cell cultures for virus propagation. Methods Mol Biol. 2015;1282:57-62. doi: 10.1007/978-1-4939-2438-7_6. PubMed PMID: 25720471; PubMed Central PMCID: PMCPMC7122669.
32. Blaurock C, Scheibner D, Landmann M, et al. Non-basic amino acids in the hemagglutinin proteolytic cleavage site of a European H9N2 avian influenza virus modulate virulence in turkeys. Sci Rep. 2020 Dec 4;10(1):21226. doi: 10.1038/s41598-020-78210-8. PubMed PMID: 33277593; PubMed Central PMCID: PMCPMC7718272.
33. Petersen H, Mostafa A, Tantawy MA, et al. NS segment of a 1918 influenza A virus-descendent enhances replication of H1N1pdm09 and virus-induced cellular immune response in mammalian and avian systems. Front Microbiol. 2018;9:526. doi: 10.3389/fmicb.2018.00526. PubMed PMID: 29623073; PubMed Central PMCID: PMCPMC5874506.
34. Livak KJ, Schmittgen TD. Analysis of relative gene expression data using real-time quantitative PCR and the 2(-Delta Delta C(T)) Method. Methods. 2001 Dec;25(4):402-8. doi: 10.1006/meth.2001.1262. PubMed PMID: 11846609.
35. Hoffmann B, Hoffmann D, Henritzi D, et al. Riems influenza a typing array (RITA): An RT-qPCR-based low density array for subtyping avian and mammalian influenza a viruses. Sci Rep. 2016 Jun 3;6:27211. doi: 10.1038/srep27211. PubMed PMID: 27256976; PubMed Central PMCID: PMCPMC4891686.
36. Tu J, Guo J, Zhang A, et al. Effects of the C-terminal truncation in NS1 protein of the 2009 pandemic H1N1 influenza virus on host gene expression. PloS one. 2011;6(10):e26175. doi: 10.1371/journal.pone.0026175. PubMed PMID: 22022552; PubMed Central PMCID: PMCPMC3192165. eng.
37. Jackson D, Hossain MJ, Hickman D, et al. A new influenza virus virulence determinant: the NS1 protein four C-terminal residues modulate pathogenicity. Proc Natl Acad Sci U S A. 2008 Mar 18;105(11):4381-6. doi: 10.1073/pnas.0800482105. PubMed PMID: 18334632; PubMed Central PMCID: PMCPMC2393797.

38. Lam WY, Tang JW, Yeung AC, et al. Avian influenza virus A/HK/483/97(H5N1) NS1 protein induces apoptosis in human airway epithelial cells. J Virol. 2008 Mar;82(6):2741-51. doi: 10.1128/JVI.01712-07. PubMed PMID: 18199656; PubMed Central PMCID: PMCPMC2258969.

39. Liu H, Golebiewski L, Dow EC, et al. The ESEV PDZ-binding motif of the avian influenza A virus NS1 protein protects infected cells from apoptosis by directly targeting Scribble. J Virol. 2010 Nov;84(21):11164-74. doi: 10.1128/JVI.01278-10. PubMed PMID: 20702615; PubMed Central PMCID: PMCPMC2953166.

40. Jackson D, Killip MJ, Galloway CS, et al. Loss of function of the influenza A virus NS1 protein promotes apoptosis but this is not due to a failure to activate phosphatidylinositol 3-kinase (PI3K). Virology. 2010 2010/01/05/;396(1):94-105. doi: https://doi.org/10.1016/j.virol.2009.10.004.

41. Nogales A, Martinez-Sobrido L, Topham DJ, et al. Modulation of innate immune responses by the influenza A NS1 and PA-X proteins. Viruses. 2018;10(12):708. doi: 10.3390/v10120708. PubMed PMID: 30545063; eng.

42. Liedmann S, Hrincius ER, Anhlan D, et al. New virulence determinants contribute to the enhanced immune response and reduced virulence of an influenza A virus A/PR8/34 variant. J Infect Dis. 2014 Feb 15;209(4):532-41. doi: 10.1093/infdis/jit463. PubMed PMID: 23983213; eng.

43. Ozawa M, Basnet S, Burley LM, et al. Impact of amino acid mutations in PB2, PB1-F2, and NS1 on the replication and pathogenicity of pandemic (H1N1) 2009 influenza viruses. J Virol. 2011 May;85(9):4596-601. doi: 10.1128/jvi.00029-11. PubMed PMID: 21325408; PubMed Central PMCID: PMCPMC3126221. eng.

44. Reperant LA, Kuiken T, Osterhaus AD. Adaptive pathways of zoonotic influenza viruses: from exposure to establishment in humans. Vaccine. 2012 Jun 22;30(30):4419-34. doi: 10.1016/j.vaccine.2012.04.049. PubMed PMID: 22537992.

45. Zhirnov OP, Konakova TE, Wolff T, et al. NS1 protein of influenza A virus down-regulates apoptosis. J Virol. 2002 Feb;76(4):1617-25. doi: 10.1128/jvi.76.4.1617-1625.2002. PubMed PMID: 11799156; PubMed Central PMCID: PMCPMC135891.

46. Ehrhardt C, Wolff T, Pleschka S, et al. Influenza A virus NS1 protein activates the PI3K/Akt pathway to mediate antiapoptotic signaling responses. J Virol. 2007 Apr;81(7):3058-67. doi: 10.1128/JVI.02082-06. PubMed PMID: 17229704; PubMed Central PMCID: PMCPMC1866065.

47. Hale BG, Steel J, Medina RA, et al. Inefficient control of host gene expression by the 2009 pandemic H1N1 influenza A virus NS1 protein. J Virol. 2010 Jul;84(14):6909-22. doi: 10.1128/jvi.00081-10. PubMed PMID: 20444891; PubMed Central PMCID: PMCPMC2898253. eng.

48. Clark AM, Nogales A, Martinez-Sobrido L, et al. Functional evolution of influenza virus NS1 protein in currently circulating human 2009 pandemic H1N1 viruses. J Virol. 2017 Sep 1;91(17). doi: 10.1128/jvi.00721-17. PubMed PMID: 28637754; PubMed Central PMCID: PMCPMC5553169. eng.

49. Nogales A, Martinez-Sobrido L, Chiem K, et al. Functional evolution of the 2009 pandemic H1N1 influenza virus NS1 and PA in humans. J Virol. 2018 Oct 1;92(19). doi: 10.1128/jvi.01206-18. PubMed PMID: 30021892; PubMed Central PMCID: PMCPMC6146824.

50. Vigeveno RM, Poen MJ, Parker E, et al. Outbreak severity of highly pathogenic avian influenza A(H5N8) viruses is inversely correlated to

polymerase complex activity and interferon induction. Journal of Virology. 2020;94(11):e00375-20. doi: 10.1128/JVI.00375-20.

51. Grund C, Hoffmann D, Ulrich R, et al. A novel European H5N8 influenza A virus has increased virulence in ducks but low zoonotic potential. Emerg Microbes Infect. 2018 Jul 19;7(1):132. doi: 10.1038/s41426-018-0130-1. PubMed PMID: 30026505; PubMed Central PMCID: PMCPMC6053424.

52. Kim YI, Pascua PN, Kwon HI, et al. Pathobiological features of a novel, highly pathogenic avian influenza A(H5N8) virus. Emerg Microbes Infect. 2014 Oct;3(10):e75. doi: 10.1038/emi.2014.75. PubMed PMID: 26038499; PubMed Central PMCID: PMCPMC4217095. eng.

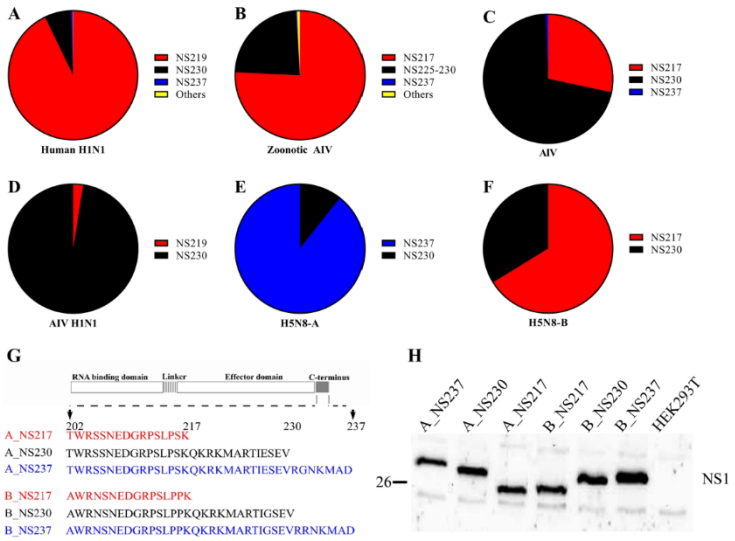

Figure 1: Sequence analysis and expression of H5N8 2.3.4.4 carrying different NS1 in human cells Sequences of full-length NS1 protein of human H1N1 compared to AIV in birds, humans or mammals from 1902 to 2020 were retrieved from GISAID at 28-03-2021. Sequences were cleaned from ambiguous residues and compared using Geneious version 11.1. Shown is the prevalence of NS1 of variable length in human H1N1 viruses (A), zoonotic AIV (B), AIV (C), avian H1N1 (D) and H5N8 clade 2.3.4.4A (E) and 2.3.4.4B (F). Schematic illustration for the C-terminus of recombinant viruses used in this study (G). NS1 expression in HEK293T cells transfected with 1 µg of indicated pCAGGS-NS1 plasmids for 24 h (H).

206x150mm (300 x 300 DPI)

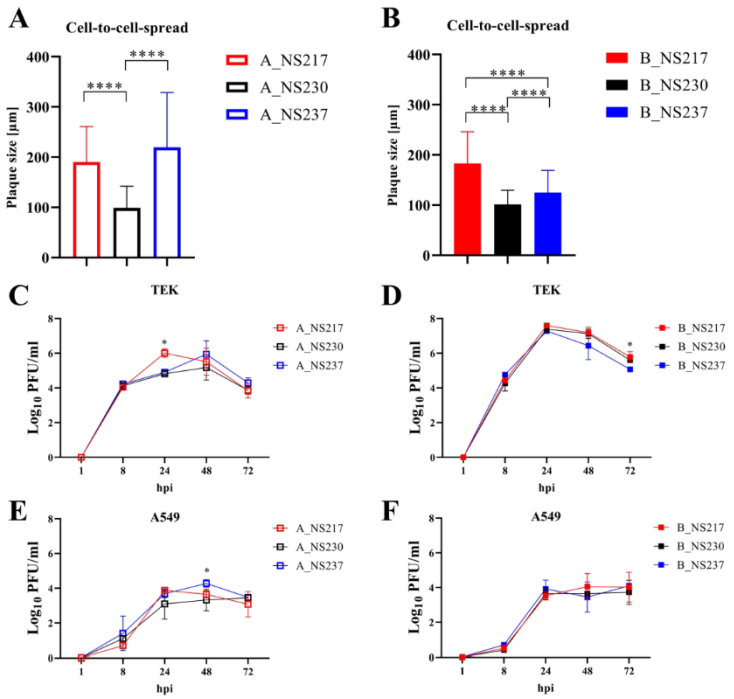

Figure 2: The impact of NS1 C-terminus variations in cell-to-cell spread and replication of recombinant H5N8 viruses in cell culture

Cell-to-cell spread was determined by measuring the diameter of 100 plaques after infection of MDCK-II cells with H5N8-A (A) and H5N8-B (B). Results are expressed as mean and standard deviation (µm). Replication kinetics in turkey embryo kidney (TEK) cells infected with H5N8-A (C) or H5N8-B (D) at MOI of 0.001 pfu at indicated time points. Replication kinetics in human lung cells (A549) infected with H5N8-A (E) or H5N8-B (F) at MOI of 0.001 pfu at indicated time points. Virus titre was determined using plaque assay in MDCK-II cells. The assay was done in duplicates and repeated twice. Asterisks indicate statistical significance at p value * < 0.05, **< 0.01, *** < 0.005, **** < 0.0005.

175x167mm (300 x 300 DPI)

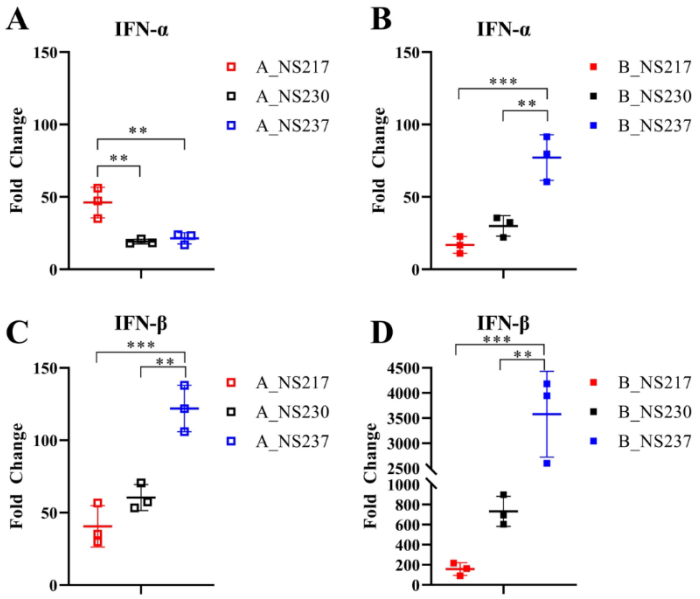

Figure 3: The impact of NS1 C-terminus variation on interferon-induction in human cells infected with H5N8 clade 2.3.4.4

The relative expression of IFN-α (A, B) and IFN-β (C, D) mRNAs was measured in A549 cells infected with the different viruses using an MOI of 0.1 for 24 h. Relative expression of the IFN-mRNA in infected and non-infected cells was calculated using the 2^-(ΔΔct) method of three experiments. Asterisks indicate statistical significance at p value * < 0.05, **< 0.01, *** < 0.005, **** < 0.0005.

155x129mm (300 x 300 DPI)

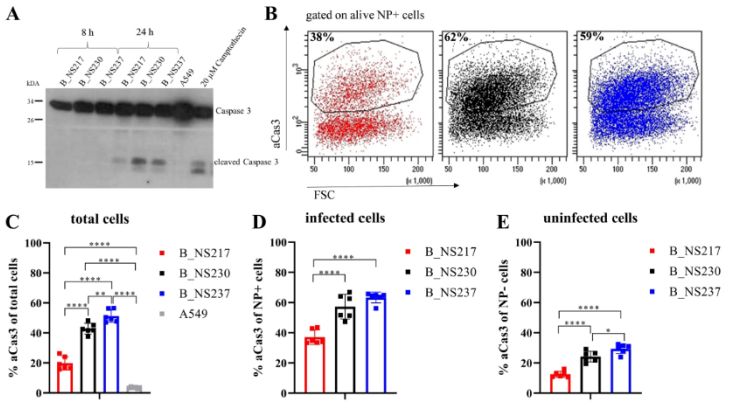

Figure 4: The impact of NS1 C-terminus variation on apoptosis-induction in human cells infected with H5N8 clade 2.3.4.4

Active caspase-3 (i.e. cleaved caspase-3) was detected in A549 cells after the infection with an MOI of 0.1 for 8 and 24 h at 37°C. Cells treated with 20 µM Camptothecin were used as control. Detection was performed with ECL-substrate and X-ray film (A). The amount of activated caspase-3 was quantified using flow cytometry after infection of A549 cells at an MOI of 0.1 for 24 h (B-E). Cells were stained with a primary mouse-anti-NP antibody (ATCC-HB65) and a caspase-3 PE labeled antibody. Signals were analyzed via FACS with gating for either all cells (C), NP positive cells only (D), or NP negative cells only (E). Asterisks indicate statistical significance at p value * < 0.05, **< 0.01, *** < 0.005, **** < 0.0005.

179x100mm (600 x 600 DPI)

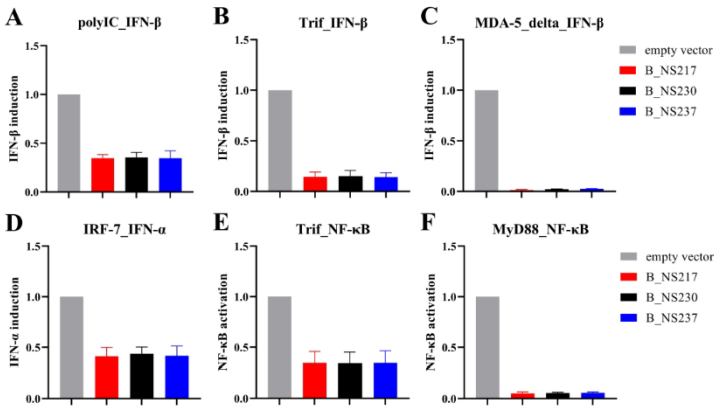

Figure 5: IFN-I and NF-kB induction pathways in human cells after transfection with NS1 of H5N8 clade 2.3.4.4B

To determine which IFN-I (IFN-α and IFN-β) or NF-kB-induction pathway is inhibited by NS1, HEK293T cells in 6-well plates were transfected with a plasmid DNA mix of a FFL reporter plasmid (p125:IFN-β-Pro-FFL, pIFNα-Pro-FFL or pNF-kB-Pro-FFL), pCMV-RL, a Trigger expression plasmid or poly(I:C), and a pCAGGS plasmid containing one of the NS1 coding sequences using Lipofectamine 2000 transfection reagent. Trigger molecules used to activate the signaling cascade and analyzed promoters (reporter construct) are given above the graphs (A-F). 20 h post transfection cell extracts were prepared and luciferase activities were measured using the Dual-Luciferase Reporter Assay System (Promega) according to manufacturer's instructions. Firefly luciferase activity was normalized to Renilla luciferase activity. Promoter induction was set as 1 (100%) for the empty vector control with the given Trigger. Induction of the promotor by a trigger molecule was confirmed comparing values for transfection of empty vector pCAGGS with and without trigger plasmid. FFL: Firefly luciferase; RL: Renilla luciferase.

143x83mm (600 x 600 DPI)

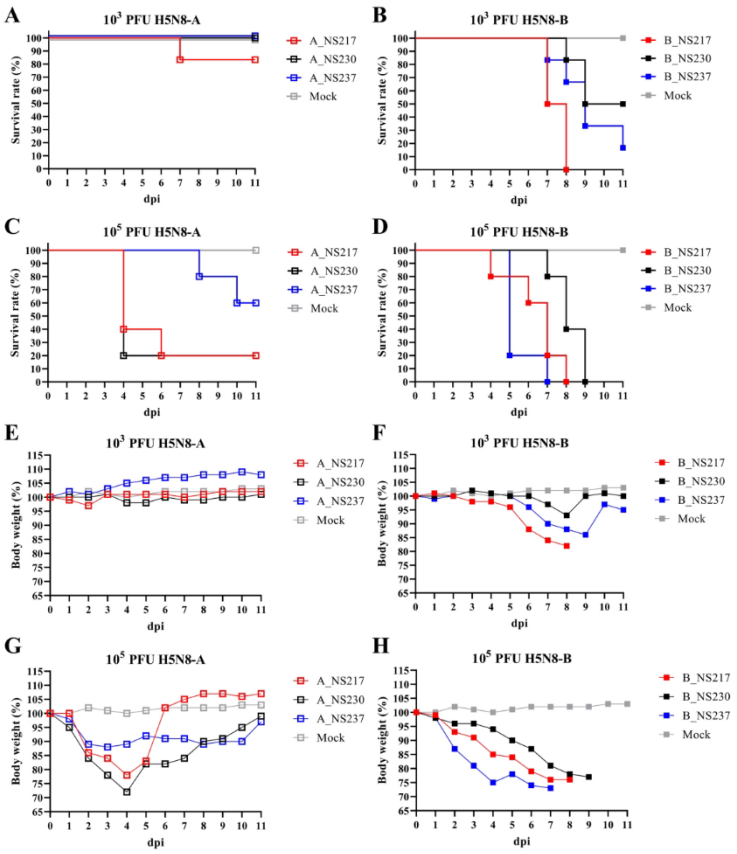

Figure 6: The impact of NS1 C-terminus variations on survival period and bodyweight gain in mice inoculated with H5N8 viruses

Shown are estimated survival periods of BALB/C mice inoculated intranasal with low-dose (103 pfu) (A, B) or high-dose (105 pfu) (C, D) of H5N8-A (A, C) or H5N8-B (B, D). The relative bodyweight gains of BALB/C mice inoculated intranasal with low-dose (E, F) and high-dose (G, H) of H5N8-A (E, G) or H5N8-B (F, H) were calculated. Mock mice group were inoculated with 50 µL sterile medium. All inoculation experiments were occurred under mild anaesthesia using Isoflurane. Results are the relative mean to the bodyweight immediately before infection (d0). Mice that lost more than 25% of the d0-bodyweight value were humanely killed and scored dead. For optical reasons, standard deviations are not shown.

182x212mm (300 x 300 DPI)

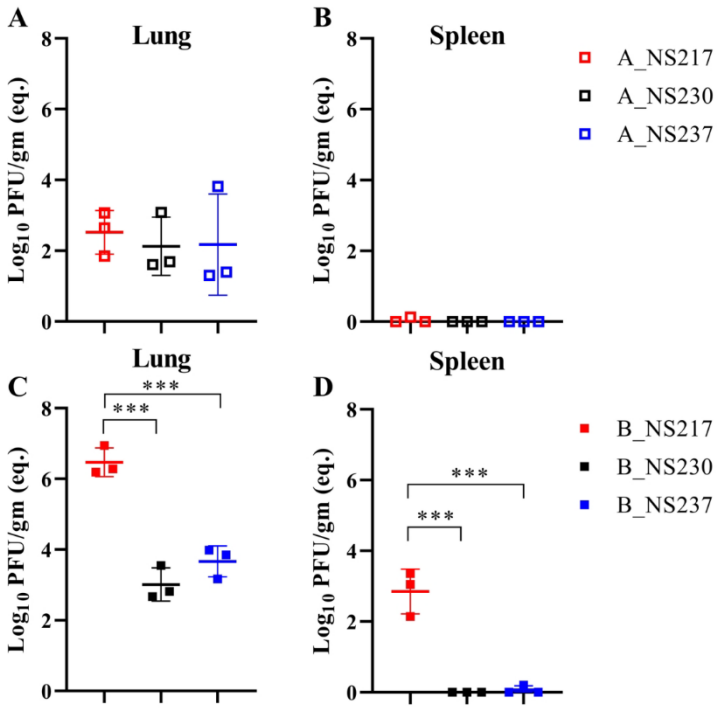

Figure 7: The impact of NS1 on replication of H5N8 viruses in mice
Replication of indicated viruses in mice inoculated intranasally with low-dose was assessed in 3 mice per group sacrificed 3 dpi under deep anaesthesia using isoflurane and cervical dislocation (A-D). Viral RNA was extracted from the indicated organs and was detected using RT-qPCR and standard curves of serial dilutions of B_NS217 (10 to 100000 pfu) in each plate. Results are shown as mean and standard deviation of positive samples (A-D). Asterisks indicate statistical significance at p value *** < 0.001.

145x143mm (300 x 300 DPI)

Deletion or Extension of the C-Terminus of Non-Structural Protein 1 (NS1) in H5N8 Clade 2.3.4.4 Highly Pathogenic Avian Influenza Virus Modulates Induction of Interferon and Apoptosis in Human Lung Cells and Virulence in Mice

Claudia Blaurock[a], Ulrike Blohm[b], Christine Luttermann[b], Julia Holzerland[a], David Scheibner[a], Alexander Schäfer[b], Allison Groseth[a], Thomas C. Mettenleiter[c], and Elsayed M. Abdelwhab[a*]

[a]Institute of Molecular Virology and Cell Biology, [b]Institute of Immunology, [c]Friedrich-Loeffler-Institut, Federal Research Institute for Animal Health, Südufer 10, 17493 Greifswald-Insel Riems, Germany

* Corresponding author: Elsayed M. Abdelwhab
Tel: +49 38351 7 1139;
Fax: +49 38351 7 1188
sayed.abdel-whab@fli.de

Supplementary Table S1. Prevalence of NS1 size of influenza A viruses from different hosts from 1902 to 2020

	Host	NS1 amino acid length						Total
		217	**219**	**225**	**230**	**237**	Others	
AIV	**H1**		2		299			301
	H2	1		1	556		NS228 (1)	559
	H3	4	24	5	2218		NS224 (1), NS228 (1)	2253
	H4	2	4	1	2140	6	NS202 (1)	2154
	H6	920		15	1227	1	NS202 (2), NS227 (1), NS228 (1)	2167
	H7	818	1	5	1625	2	NS214 (1), NS216 (2), NS220 (24), NS224 (63), NS228 (1)	2574
	H8				194			194
	H9	3091	12	53	917	93	NS202 (1), NS212 (1), NS214 (2), NS220 (4), NS228 (5), NS229 (2), NS234 (2)	4178
	H10	73			1226		NS207 (1)	1300
	H11	1	5	1	763			770
	H12			1	340			341
	H13				466	2		468
	H14				42			42
	H15				18			18
	H16		3		252			255
	Total	**4910**	**51**	**82**	**12310**	**104**	**117**	**17574**
	%	28.0	0.3	0.5	70.1	0.6	≈ 0.7	100%
Human-Influenza	**Zoonotic AIV**	1231		343	35	5	NS202 (2), NS212 (1), NS215 (8), NS224 (1)	1626
	hH1N1 (1918-2008)		24		1145	119		1288
	hH1N1 (2009)		4264		295	1		4560
	hH1N1 (2010-2020)		24309		604	5		24918

	Total	1231	28597	343	2079	130	12	32392
Mammal-origin AIV	bat		1					1
	feline	2		16	6		NS223 (1)	25
	dog			3				3
	equine	1			17			18
	ferret			6	4			10
	meerkat			1				1
	mink	9	1	8	4	1		23
	rat				1			1
	pika	1		5				6
	stone martin			1				1
	seal	1			6			7
	swine	29		22	13		NS220 (1), NS228 (1)	66
	Total	43	2	62	51	1	3	162
AIV	H1N1		16		645			661
	H5N8-A				51	427		478
	H5N8-B		392		200			592

Sequences were retrieved from GISAID and analyzed using Geneious. They represent all sequences in the GISAID to 28-03-2021
NS225 and NS230 have a full CTE. Variation in length is due to deletion in the linker region

4 Own contributions to publications

Paper I

Non-basic amino acids in the hemagglutinin proteolytic cleavage site of a European H9N2 avian influenza virus modulate virulence in turkeys

Claudia Blaurock, David Scheibner, Maria Landmann, Melina Vallbracht, Reiner Ulrich, Eva Böttcher-Friebertshäuser, Thomas C. Mettenleiter & Elsayed M. Abdelwhab

Scientific Reports, Sci Rep 10, 21226 (2020), doi: 10.1038/s41598-020-78210-8

Claudia Blaurock: generated recombinant viruses, performed the in vitro characterization and statistical analysis, conducted the animal experiments, wrote the draft of the manuscript, discussed the results, commented on the manuscript, and approved the final version.

David Scheibner: conducted the animal experiments, discussed the results, commented on the manuscript, and approved the final version.

Maria Landmann: conducted the histopathological examination, discussed the results, commented on the manuscript, and approved the final version.

Melina Vallbracht: conducted the fusion assay, discussed the results, commented on the manuscript, and approved the final version.

Reiner Ulrich: analyzed the histopathological data, discussed the results, commented on the manuscript, and approved the final version.

Eva Böttcher-Friebertshäuser: conceived and designed the experiment, provided materials, discussed the results, commented on the manuscript, and approved the final version.

Thomas C. Mettenleiter: conceived and designed the experiment, financial support, discussed the results, commented on the manuscript, and approved the final version.

Elsayed M. Abdelwhab: conceived and designed the experiment, financial support, analysed the sequences, conducted the animal experiments, wrote the draft of the manuscript, discussed the results, commented on the manuscript, and approved the final version.

Paper II

Genetic incompatibilities and reduced transmission in chickens may limit the evolution of reassortants between H9N2 and panzootic H5N8 clade 2.3.4.4 avian influenza virus showing high virulence for mammals

Ahmed Mostafa*, Claudia Blaurock*, David Scheibner, Christin Müller, Ulrike Blohm, Alexander Schäfer, Marcel Gischke, Ahmed H. Salaheldin, Hanaa Z. Nooh, Mohamed A. Ali, Angele Breithaupt, Thomas C. Mettenleiter, Stephan Pleschka, and Elsayed M. Abdelwhab

* Ahmed Mostafa and Claudia Blaurock contributed equally to this work. Author order was determined both alphabetically and in order of seniority.

Virus Evolution, Virus Evol 6 (2), veaa077 (2020), doi: 10.1093/ve/veaa077

Ahmed Mostafa: conceived and designed the experiment**,** generation of recombinant viruses, virus characterisation in human cells, interferon induction and polymerase activity assay *in vitro*, financial support, discussed the results, commented on the manuscript and approved the final version.

Claudia Blaurock: generated recombinant viruses, Flow cytometry of infected A549 cells, conducted the animal experiments, titration of chicken samples, detection of IFN-β response in mice, ELISA, commented on the manuscript and approved the final version.

David Scheibner: performed the growth kinetic in CEK, conducted the animal experiments; commented on the manuscript, and approved the final version.

Christin Müller: prepared and infected the primary human bronchial epithelial cells.

Ulrike Blohm: FACS-Analysis, commented on the manuscript, and approved the final version.

Alexander Schäfer: FACS-Analysis for cell-mediated immunity, commented on the manuscript, and approved the final version.

Marcel Gischke: performed the growth kinetic in CEK, conducted the animal experiments; commented on the manuscript, and approved the final version.

Ahmed H. Salaheldin: generation of recombinant viruses, conducted the animal experiments, commented on the manuscript and approved the final version.

Hanaa Z. Nooh: in vitro characterization for recombinant viruses in JLU-Gießen, commented on the manuscript and approved the final version.

Mohamed A. Ali: conceived and designed the experiment, financial support, discussed the results, commented on the manuscript and approved the final version

Angele Breithaupt: conducted the histopathological examination, discussed the results, commented on the manuscript, and approved the final version.

Thomas C. Mettenleiter: conceived and designed the experiment, financial support, discussed the results, commented on the manuscript, and approved the final version.

Stephan Pleschka: conceived and designed the experiment, financial support, discussed the results, commented on the manuscript, and approved the final version.

Elsayed M. Abdelwhab: conceived and designed the experiment, financial support, conducted the animal experiments, analysed the sequences, wrote the draft of the manuscript; discussed the results, commented on the manuscript, and approved the final version.

Paper III

Preferential selection and contribution of non-structural protein 1 (NS1) to the efficient transmission of the panzootic avian influenza H5N8 2.3.4.4 clades A and B viruses in chickens and ducks

Claudia Blaurock, Angele Breithaupt, David Scheibner, Ola Bagato, Axel Karger, Thomas C. Mettenleiter and Elsayed M. Abdelwhab

Submitted to Journal of Virology

Claudia Blaurock: generated recombinant viruses, conducted the animal experiments, in vitro characterization, titration of samples, wrote the draft of the manuscript and approved the final version.

Angele Breithaupt: conducted the histopathological examination, discussed the results, commented on the manuscript and approved the final version.

David Scheibner: conducted the animal experiments, commented on the manuscript and approved the final version.

Ola Bagato: extraction, amplification and sequence of viral RNA from plaque samples in the competitive experiments and approved the final version.

Thomas C. Mettenleiter: conceived and designed the experiment, financial support, discussed the results, commented on the manuscript, and approved the final version.

Elsayed M. Abdelwhab: conceived and designed the experiment, financial support, conducted the animal experiments, analysed the sequences, wrote the draft of the manuscript; discussed the results, commented on the manuscript, and approved the final version.

Paper IV

Deletion or extension of the C-terminus of non-structural protein 1 (NS1) in H5N8 clade 2.3.4.4 highly pathogenic avian influenza virus modulates induction of interferon and apoptosis in human lung cells and virulence in mice

Claudia Blaurock, Ulrike Blohm, Christine Luttermann, Julia Holzerland, David Scheibner, Alexander Schäfer, Allison Groseth, Thomas C. Mettenleiter and Elsayed M. Abdelwhab

Submitted to Emerging Microbes & Infections

Claudia Blaurock: propagation and titration of recombinant viruses, conducted the animal experiment, in vitro characterization, wrote the draft of the manuscript and approved the final version.

Ulrike Blohm: FACS-Analysis, commented on the manuscript, and approved the final version.

Christine Luttermann: in vitro determination of IFN- or NF-kB-induction pathway, commented on the manuscript and approved the final version.

Julia Holzerland: conducted the caspase-induction with Claudia Blaurock, commented on the manuscript and approved the final version.

David Scheibner: conducted the animal experiment, commented on the manuscript and approved the final version.

Alexander Schäfer: FACS analysis, commented on the manuscript, and approved the final version.

Allison Groseth: induction of caspase, commented on the manuscript, and approved the final version.

Thomas C. Mettenleiter: conceived and designed the experiment, financial support, discussed the results, commented on the manuscript, and approved the final version.

Elsayed M. Abdelwhab: conceived and designed the experiment, financial support, conducted the animal experiment, analysed the sequences, wrote the draft of the manuscript; discussed the results, commented on the manuscript, and approved the final version.

In agreement (Paper I to IV):

……..

Place, Date

……..	……
Prof. Dr. Dr. h.c. Thomas C. Mettenleiter	Claudia Blaurock

5 Discussion

Avian influenza viruses (AIV), particularly H5N8 and H9N2 subtypes, are a significant threat for poultry worldwide and pose a serious public health risk. AIV, including H5N8 and H9N2, disrupt the protein supply particularly in developing countries. Since, AIV H9N2 is not a notifiable disease and therefore infected birds are not culled, it is now endemic in poultry in many countries (Carnaccini and Perez, 2020; Pusch and Suarez, 2018). It causes severe losses in meat and egg production and the burden of H9N2 is high due to the costs for vaccination (Gu et al., 2017; Peacock et al., 2017). AIV H9N2 is a risk for human health due to the widespread "silent" circulation in (vaccinated) poultry (Gu et al., 2017; Peacock et al., 2017) coupled with the plasticity of the viral genome for mutations that enable efficient replication in mammals (Arai et al., 2019b; Obadan et al., 2019) and the high rate of reassortment yielding zoonotic influenza viruses associated with increased case fatality rates in humans (e.g. H5N1, H7N9) (Guan et al., 1999; Liu et al., 2013; Pu et al., 2021). To date, about 50 laboratory-confirmed H9N2 infections in humans have been reported to the WHO (Carnaccini and Perez, 2020; Freidl et al., 2014; WHO, 2021c) and thousands of subclinically individuals have been discovered worldwide (Carnaccini and Perez, 2020; Khan et al., 2015; Li et al., 2017; Peacock et al., 2019) including poultry workers in Europe (Coman et al., 2013). Therefore, vigilance is of utmost importance to study the impact of genetic changes in H9N2 on virus adaptation and to assess their zoonotic potentials particularly after a long-term circulation in poultry within a country where other avian or swine influenza viruses are also co-circulating. The second most commonly spread AIV in birds worldwide is the H5Nx Gs/Gd96 lineage, especially H5N8 clade 2.3.4.4. Since 2013, the infection with H5N8 virus resulted in the death or culling of 100s of millions of wild and domestic birds worldwide (Swayne et al., 2017) and vaccination failure in poultry has been reported due to the antigenic drift from vaccine-induced antibodies (Li et al., 2020). A global concern on the zoonotic and pandemic potentials of H5N8 clade 2.3.4.4 has been raised (Yamaji et al., 2020). In December 2020, seven poultry farm workers in Russia were infected with H5N8 clade 2.3.4.4 (WHO, 2021a). Therefore, in this dissertation we focused on the recent German H9N2 and H5N8 viruses to assess their virulence and transmission in birds and potential adaptation to mammals using broad *in vitro* and *in vivo* experimental approaches.

In the first study in this dissertation **(Paper I)**, European and non-European sequences of H9N2 AIV from 1966 to 2020 were analysed and the polymorphism in positions P4 to P1 in the hemagglutinin cleavage site (HACS) was described. Strikingly, polymorphism of non-basic amino acids (aa) (G, A, N, S, D) was observed at P2 in European H9N2 viruses, particularly in turkeys, the second most common poultry species in Europe and the US which is more vulnerable than chickens to AIV infections (FAOSTAT., 2019; Spackman et al., 2010; Swayne and Slemons, 2008; Tumpey et al., 2004). It is well established that the insertion of basic aa into the HACS increased the virulence of H5 and H7 (Abdelwhab et al., 2016b; Scheibner et al., 2019b). However, not all H5 and H7 viruses with a polybasic HACS were highly virulent in chickens (Lee et al., 2006; Londt et al., 2007). To date, in all outbreaks,

the HPAIV acquired a unique polybasic HACS and several studies showed that specific composition and the number of polybasic aa in the HACS affected the clinical outcomes of H5 and H7 HPAIV infection in chickens (Abdelwhab et al., 2016b; Gischke et al., 2020; Kawaoka, 1991; Kawaoka and Webster, 1989; Scheibner et al., 2019b). Similarly, the insertion of polybasic HACS in non-H5/H7 viruses including H9N2 resulted in increased virulence of some strains in chickens (Gischke et al., 2020; Gohrbandt et al., 2011; Stech et al., 2009; Veits et al., 2012). However, little is known about the impact of non-basic aa in the HACS on virus fitness in poultry. Studies on mice using a laboratory H1N1 virus showed that non-basic aa in P2 in the HACS are virulence determinants and caused neurotropism conferred mainly by the HA cleavage-activation using plasmin (Sun et al., 2010). In **Paper I**, I was able to show that the non-basic aa in the HACS affected replication in turkey cells *in vitro* and modulated virulence in turkeys but not in chickens *in vivo*. Our sequence analysis indicated that most of H9N2 sequences in Europe are from turkeys, which may explain that these mutations are important for H9N2-adaptation in turkeys. The underlying mechanism behind this species variation merits further investigation. However, I found that the optimal pH fusion-activation of G, A and S, which exhibited the lowest virulence, was lower than the wild type virus with basic aa (K) at P2. The correlation between pH-fusion activation and virulence of AIV in poultry has been described (Okamatsu et al., 2016). The replication of H9N2 in turkeys and chickens was limited to the upper respiratory tract, which is in accordance with the majority of studies on H9N2 (Bonfante et al., 2013; Sun et al., 2019; Swieton et al., 2020). However, I could find viral RNA in the brain of turkeys. In some studies, H9N2 virus could be isolated from the brain of experimental infected chickens and/or finches (Lenny et al., 2015; Song et al., 2019). Furthermore, one of the interesting results in **Paper I** is the ability of H9N2 to replicate in brain cells of cats and pigs, although at lower levels compared to virus replication in primary turkey brain cells. Polymorphism in P2 enabled the neurovirulence of H1N1 in mice after intracranial inoculation (Sun et al., 2010). The demonstration of virus replication in brain of mammals and replication in birds without showing severe clinical signs prompted us to assess the replication of H9N2 in human cells and to assess virus virulence in mice.

In the second paper in this thesis **(Paper II)**, I found that H9N2 was able to infect human cell lines, although at lower levels compared to H5N8 virus. In mice, H9N2 caused bodyweight loss and mortality after intranasal inoculation with high-dose and it replicated at comparable high levels to HPAIV H5N8 in the lungs. Previous studies showed that some H9N2 strains of avian origin are able to replicate in mice and cause mortality without prior adaptation (Li et al., 2014a; Zhang et al., 2021). The avirulent nature and high replication levels of H9N2 in poultry and the wide spectrum of host species infected with the virus warrant vigilance to protect both animal and human health which is an excellent example for the one-health concept (Kim, 2018). Co-circulation of H9N2 with other AIV subtypes including H5Nx viruses has been previously reported in several Asian and African countries and the emergence of H9N2/H5 clade 2.3.4 reassortants has been frequently documented under natural or experimental

settings (El-Shesheny et al., 2020; Hao et al., 2017; Hassan et al., 2020; Venkatesh et al., 2020). Some of these reassortants exhibited higher virulence in mammals and were transmissible by air in mammalian models, while others exhibited low or no virulence in mice and chickens (El-Shesheny et al., 2020; Hao et al., 2017). Since 2014, the intercontinental transmission and the swarm incursions of H5N8 in poultry and wild birds in Germany was unprecedented. Notably, compared to previous Gs/GD96 lineages, clade 2.3.4.4 H5 viruses have an unusual ability to reassort with other AIV (Claes et al., 2016; King et al., 2020a; Pohlmann et al., 2019; Pohlmann et al., 2018). Clade B H5N8 in Germany was highly virulent in mice, although it did not transmit from ferret to ferret (Grund et al., 2018). Due to these facts, collectively, we aimed in **Paper II** to assess the virulence of H5N8 in mice and study the risk for evolution and impact of recent German H5N8/H9N2 reassortants in birds and mammals.

I successfully generated H5N8 carrying single gene segments from H9N2. However, several attempts to rescue infectious H5N8 carrying PB1 or NP from H9N2 failed. Little is known about the contributing factors to the efficiency of reassortment in AIV compared to human or bat influenza viruses (Ciminski et al., 2017; Marshall et al., 2013). Generally, the segmentation of the influenza virus genome complicates the selective packaging of eight unique vRNPs into one particle which necessitates sophisticated compatibility of the protein and RNA interactions (Gerber et al., 2014; Lowen, 2017). Previous studies showed that mutations in the packaging regions are major determinants for reassortment of different influenza viruses (Essere et al., 2013). I found that mutations outside the packaging region were the reason for the incompatibility between PB1 and NP segments of H9N2 to replace their H5N8 analogues. The compatibility between the polymerase subunits on protein-protein interaction levels was essential for reassortment between different human influenza viruses (Hara et al., 2013; Li et al., 2008). It remains to pin-point the mutations in the H9N2 PB1 and NP proteins and the underlying mechanism for this incompatibility.

Our experiments clearly showed that H9N2 PB2, PA and NS gene segments (i) increased replication of H5N8 in primary cells or cell lines obtained from the respiratory tract of humans, (ii) affected the efficiency to block IFN-β response and (iii) increased virulence in mice. This is in accordance with previous reports that H9N2-PB2, PB1, PA, NS or NP are able to reassort with multiple viruses (e.g. H7N9, H7N7, H5N6, H5N1) and can enhance the pathogenesis and lethality in mice (Arai et al., 2019a; Lam et al., 2013; Shen et al., 2016; Su et al., 2015). Interestingly, the reassortment of H5N8 with H9N2 PB2, PA and NS reduced virus fitness in chickens and NS clearly impaired virus transmission to contact chickens. Firstly, these results further confirm previous findings that adaptation of some AIV in poultry might decrease the replication in mammals (Long et al., 2015) and *vice versa*. Secondly, the lower fitness, particularly of H5N8 carrying H9N2-NS, lowers the possibility for the emergence of these reassortants in chickens, but does not exclude the possibility for reassortment in e.g. turkeys or ducks, which remains to be determined. Thirdly, these results indicate that the NS segment of H5N8 plays a role in the efficient transmission of H5N8 in chickens, which has been studied in **Paper III**.

In **Paper III**, we had a closer look on the NS1 protein of H5N8 clade 2.3.4.4 viruses. Typically, the NS1 protein is composed of 230 aa (NS230), which is also true for the parental Gs/Gd96 H5N1 and the German H9N2 used in this dissertation. However, the NS1 varies in length mostly due to truncations in the carboxyl terminal end (ΔCTE) (Abdelwhab et al., 2016a). In this paper, we analysed 8185 H5Nx NS1 protein sequences and found 15 different forms of NS1, ranging from 202 to 238 aa, with a majority of 230 aa. We further analysed the sequence of NS1 in H5N8 viruses from 2013-2019 (n= 1068 sequences) which showed (i) a preferential selection for H5N8 clade A viruses to NS1 with 237 aa, while clade B viruses prefer NS1 with 217 aa, (ii) a temporal pattern for distribution of NS1 where NS217 was not observed in the first wave caused by clade A in 2014/2015 and NS237 was not observed in the second wave caused by clade B in 2016/2017 and (iii) NS1 of clade B viruses with NS217 was only observed in wild and domestic birds in Europe which is in line with previous reports describing the local amplification of H5N8 in birds in Europe (Lycett et al., 2020; Poen et al., 2018). We further confirmed our findings for the preferential selection of clade A and B viruses to NS237 or NS217, respectively over the common NS1 length with 230 aa. Using co-transfection experiments, where NS1 with different length compete to be included in infectious viruses in cell culture and embryonated eggs, we found no single plaque containing NS217 in clade A virus, and no single plaque with NS237 in clade B virus. Furthermore, NS237 or NS217 were preferential selected in a clade-specific pattern over the NS1 with 230 aa as seen in the sequence analysis. A previous study has shown that long-term circulation of H9N2 in poultry in China from 1996 to 2014 resulted in the selection of NS1 with 217-aa over NS1 with 230-aa (Kong et al., 2015).

NS1 is a multifunction protein and a virulence factor for IAV, particularly in mammals (Ayllon and Garcia-Sastre, 2015). It interacts with more than 560 cellular factors in a strain-dependent manner (de Chassey et al., 2013; Nogales et al., 2018b). The interaction of NS1 with the cell host machinery is of great benefit for virus replication by e.g. antagonizing the interferon response, controlling programmed cell death (apoptosis), host protein shut-off and increasing viral RNA synthesis (Ayllon and Garcia-Sastre, 2015; Hale et al., 2008b; Krug, 2015; Nogales et al., 2018b). Therefore, IAV lacking full NS1 or with severe truncated forms can grow only in IFN-deficient cells (e.g. Vero cells) (Garcia-Sastre et al., 1998). The CTE of NS1 has important structures which play diverse roles in subcellular localization (via NLS and NoLS), inhibition of interferon response and regulation of apoptosis (Ayllon and Garcia-Sastre, 2015; Hale et al., 2008b; Krug, 2015; Nogales et al., 2018b). Most information on the role of CTE on virus fitness is driven by research on human influenza viruses and little is known about AIV. Therefore, in **Paper III** we focused on the NS1 CTE to understand this striking preferential NS1 selection in clade A and clade B viruses.

To elucidate the biological advantages of NS1 CTE, I generated three recombinant H5N8-A and three H5N8-B viruses with NS217, NS230 or NS237. I compared the replication of these viruses in primary chicken and duck cells *in vitro* and determined the impact on virus virulence, replication, IFN-response

and transmission to contact chickens or ducks *in vivo*. Collectively, NS230 had negative impact on virus fitness *in vitro* and/or *in vivo* which may explain the preferential selection of H5N8 clade 2.3.4.4 for a certain length of the NS1 protein. Shortening of NS237 of clade A to 230-aa or 217-aa reduced the efficiency of NS1 to block IFN-α response in the lungs of chickens. Conversely, the elongation of NS217 of clade B virus to 230-aa or 237-aa reduced virus replication in duck cells and virulence, transmission, excretion and replication in different organs of inoculated chickens and ducks. These results indicated that the NS1 CTE is important for virus fitness in a strain-specific manner. This explains the controversial results in other studies where mutations in the NS1 CTE of an HPAIV H5N1 had no impact on virus virulence or replication in chickens and ducks (Soubies et al., 2013; Zielecki et al., 2010), while others found that NS1 ΔCTE was advantageous for replication of HPAIV H7N1 NS1 in chickens (Abdelwhab et al., 2016a) but reduced virus replication and transmission of H9N2 in chickens (Kong et al., 2015). Our findings also clearly showed that the NS1 of clade A and clade B viruses evolved toward high fitness, regardless of the NS1 length. This can be achieved by the synergism (or biological compensation) between the CTE and residues in other NS1 domains or may be other gene segments. For example, NS1 has two NLS (NLS1 and NLS2) and one NES in the ED. These signals are important to mediate (i) the early localization of NS1 in the nucleus (e.g. to block host mRNA synthesis) and (ii) the export to cytoplasm (e.g. to block the intracytoplasmic viral sensors like RIG-I). Some studies have shown that there is a synergism between the NLS2, which is absent in many AIV including clade B H5N8, and mutations in NS1 ED. Keiner et al. found that D139N mutation in the NES (similar to H5N8-B virus in this study) can compensate the subcellular localization of an H7N1 virus lacking the NLS2 due to a 6-aa-deletion in the NS1 CTE (Keiner et al., 2010). Similarly, a functional interplay was described between the mutations at residue 138 and CTE that results in a synergistic effect on AIV H5N1 virulence in mice (Fan et al., 2013). Likewise, co-mutations in residue 127 in the ED and CTE conferred high virulence of AIV H3N8 in mice when combined (Pu et al., 2010).

Furthermore, the results of animal experiments in **Paper III** indicated that NS1 modulates virulence and transmission of H5N8 in chickens and ducks. Firstly, our results confirmed that H5N8-A and H5N8-B are highly virulent in chickens, while in ducks only H5N8-B was highly virulent. This is in accordance with the results of Grund et al. using wild type H5N8-viruses (Grund et al., 2018), which were used for the generation of recombinant viruses in my study. The death of chickens and ducks was due to the extensive systemic replication and multiple organ dysfunction, which is characteristic for HPAIV infection in poultry (Pantin-Jackwood and Swayne, 2007; Perkins and Swayne, 2001; Swayne and Suarez, 2000). Secondly, we confirmed our results in **Paper II** and the recent results of Scheibner et al. (in preparation) that NS plays a role in the transmission of H5N8-B in chickens and ducks. Thirdly, we found that mutations in the NS1 CTE can reduce H5N8-B tissue distribution and endotheliotropism, a role for the NS1 which merits further investigation.

In **Paper IV,** we explored the prevalence of NS1 CTE variations in all human influenza viruses (hIAV), AIV of human-, other mammal- and bird-origin compared to all AIV sequences from 1902 to 2020. We found that H5N8-B viruses are similar to hIAV and zoonotic AIV in their preferences to short NS1, which encouraged us to determine the replication efficiency in human cells and the virulence in mice after infection with recombinant viruses generated in Paper III. In human lung cells, the shorter the NS1 of H5N8-B, the higher efficiency to (i) block type I IFN induction and (ii) reduce interferon-dependent apoptosis. These results are similar to findings obtained by Zhirnov et al. (2002) using laboratory strain PR8/H1N1 containing a deletion in NS1. Interestingly, the efficiency of H5N8 viruses to block IFN or apoptosis induction was not directly attributable to the NS1 CTE and most likely the interplay or interaction with other residues in the NS1 (e.g. RBD or ED) or in other gene segments (e.g. PB1, PA) were important (Clark et al., 2017; Hale et al., 2010b; Nogales et al., 2018a; Ozawa et al., 2011). In mice, H5N8 viruses carrying short NS1 CTE, regardless of the virus background, caused higher mortality, shorter survival period and higher bodyweight loss in a dose-dependent manner. In addition, NS1 CTE affected virus replication in the lungs and extrapulmonary tissues including the spleen and brain. Results of experiments in Paper IV confirmed my results in Paper II that NS segment modulates virulence of H5N8 in mice. Also, these results confirmed that adaptation markers in birds and mammals can be different, since changes in the NS1 did not affect virulence or transmission of H5N8-A in chickens (**Paper II**), however, shortening of H5N8-A NS1 increased virulence in mice. Nevertheless, our results also confirmed that some influenza viruses, e.g. H5N8-B, can be highly virulent in chickens, ducks and mice and the changes in the NS1 decreased virus fitness in the three species. Therefore, it is important to understand virus-dependent properties and host-variation when studying influenza viruses.

The overall conclusion of this thesis is that European H9N2 viruses have preferences for non-basic amino acids in the HACS and these residues affect virus fitness in turkeys. Since H9N2 viruses replicated in mammalian brain cells without showing clinical signs in poultry, the zoonotic risk of H9N2 should not be neglected (**Paper I**). H9N2 is able to reassort with H5N8 clade 2.3.4.4 B viruses, but there is a genetic incompatibility for PB1 and NP. H5N8/H9N2 reassortants exhibited increased virulence in mice, but conversely resulted in reduced transmission in chickens. This was mainly achieved by the NS segment (**Paper II**). There is a preferential selection for NS1 in H5N8 clade 2.3.4.4. A and B viruses and the C-terminus of H5N8-B was important for virulence, transmission and replication in chickens and in ducks. The NS1 of H5N8-A and H5N8-B viruses, regardless of the CTE length evolved toward efficient inhibition to IFN-α induction (**Paper III**). Conversely, shortening the NS1, regardless of virus background, increased the efficiency to block IFN-induction in human cells and virus virulence in mice after infection with H5N8-A and H5N8-B viruses. The latter was highly virulent in mice as a model to study the pathogenicity of influenza viruses in mammals (**Paper IV**). Therefore, studies should continue to understand the molecular basis for adaptation of AIV in poultry and assess the potential zoonotic risk.

6 Summary

LPAIV H9N2 and HPAIV H5N8 clade 2.3.4.4 viruses have been frequently isolated from domestic and wild birds in Germany and they are endemic in poultry worldwide. H9N2 is known to donate gene segments to other AIV with high case fatality rate in humans (e.g. H5N1, H7N9). Similarly, H5N8 devastated poultry worldwide since 2014 and has been recently isolated from humans. Therefore, it is important to understand the genetic predisposition for adaptation of H9N2 and H5N8 AIV in poultry and mammals.

In the first publication, we focused on the variable hemagglutinin cleavage site (HACS) of European and Non-European H9N2 viruses, since the HACS is a main virulence determinant of AIV in birds. We found a preferential substitution of non-basic amino acids (G, A, N, S, D, K) in the HACS at position 319 of European H9N2 viruses compared to non-European H9N2 viruses. Recombinant viruses carrying different non-basic amino acids in the HACS modulated replication in *vitro*. While these non-basic amino acids did not affect virulence or transmission in chickens, they modulated virulence and replication in turkeys. Moreover, H9N2 viruses with non-basic amino acids in the HACS were able to replicate in mammalian brain cells for multiple cycles even without trypsin.

In the second publication, we addressed the question whether reassortment between two recent German H9N2 and H5N8 clade 2.3.4.4. B viruses is possible and analysed the impact on virus fitness in mammals and birds. We found that H9N2 PB1 and NP segments were not compatible to generate infectious H5N8 viruses and this incompatibility was due to mutations outside the packaging region. However, H9N2 NS alone or in combination with PB2 and PA significantly increased replication of H5N8 in human cells. Moreover, H9N2 PB2, PA and/or NS segments increased virulence of H5N8 in mice. Interestingly, in chickens, reassortment with H9N2 gene segments, particularly NS, partially or fully impaired chicken-to-chicken transmission. These results indicate that the evolution of H9N2/H5N8 reassortants showing high virulence for mammals is unlikely to occur in chickens.

In the third publication, we focused on the NS1 protein of different HPAIV H5N8 clade 2.3.4.4 viruses from 2013 to 2019 and studied the impact of its C-terminus (CTE) variation on virus fitness in chickens and ducks. Our findings revealed a preferential selection for a certain NS1 CTE length in 2.3.4.4. H5N8 clade A (237 aa) and B (217 aa) viruses over the common length of 230 aa. Indeed, the NS1 CTE can affect virus virulence and pathogenesis in a species and virus clade dependent manner. In chickens, although there was no impact on virulence, NS1 CTE of H5N8-A and H5N8-B, regardless of the length, have evolved towards higher efficiency to block the IFN response. In ducks, NS1 CTE contributed to efficient transmission, replication and high virulence of H5N8-B.

In the fourth publication, we assessed the impact of variable length of NS1 on H5N8 virus replication in human cells and virulence in mice. We showed that NS1 of H5N8-B virus unlike the vast majority of

NS1 of AIV, shared preferences for short NS1 similar to human and zoonotic influenza viruses. This virus (i) was able to efficiently block IFN and apoptosis induction which might be the first steps for efficient adaptation to human cells and (ii) without prior adaptation replicated at higher levels and was more virulent in mice than H5N8-A. The virulence of the latter virus increased after shortening the NS1 similar to H5N8-B virus. Therefore, it is conceivable that truncation in NS1 is a determinant for adaptation of H5N8 in mammals irrespective of its impact on virus fitness in poultry.

Findings in this dissertation indicated that HA mutations in the European H9N2 and NS1 variations in H5N8 viruses play a role in virus fitness in poultry and/or mammals. These results improve our current understanding for AIV adaptation and are useful to assess the potential of these viruses to infect mammals.

7 References

Abdelwhab, E.-S.M., Veits, J., Breithaupt, A., Gohrbandt, S., Ziller, M., Teifke, J.P., Stech, J., Mettenleiter, T.C., 2016a. Prevalence of the C-terminal truncations of NS1 in avian influenza A viruses and effect on virulence and replication of a highly pathogenic H7N1 virus in chickens. Virulence 7, 546-557.

Abdelwhab, E.M., Veits, J., Mettenleiter, T.C., 2014. Prevalence and control of H7 avian influenza viruses in birds and humans. Epidemiol Infect 142, 896-920.

Abdelwhab, E.M., Veits, J., Ulrich, R., Kasbohm, E., Teifke, J.P., Mettenleiter, T.C., 2016b. Composition of the hemagglutinin polybasic proteolytic cleavage motif ediates variable virulence of H7N7 avian influenza viruses. Sci Rep 6, 39505.

Air, G.M., 1981. Sequence relationships among the hemagglutinin genes of 12 subtypes of influenza A virus. Proc Natl Acad Sci U S A 78, 7639-7643.

Alexander, D.J., 2000. A review of avian influenza in different bird species. Vet Microbiol 74, 3-13.

Alexander, D.J., Allan, W.H., Parsons, D.G., Parsons, G., 1978. The pathogenicity of four avian influenza viruses for fowls, turkeys and ducks. Res Vet Sci 24, 242-247.

Alexander, D.J., Parsons, G., Manvell, R.J., 1986. Experimental assessment of the pathogenicity of eight avian influenza A viruses of H5 subtype for chickens, turkeys, ducks and quail. Avian Pathol 15, 647-662.

Altman, M.O., Angel, M., Kosik, I., Trovao, N.S., Zost, S.J., Gibbs, J.S., Casalino, L., Amaro, R.E., Hensley, S.E., Nelson, M.I., Yewdell, J.W., 2019. Human influenza A virus hemagglutinin glycan evolution follows a temporal pattern to a glycan limit. mBio 10, e00204-00219.

Arai, Y., Elgendy, E.M., Daidoji, T., Ibrahim, M.S., Ono, T., Sriwilaijaroen, N., Suzuki, Y., Nakaya, T., Matsumoto, K., Watanabe, Y., 2020. H9N2 influenza virus infections in human cells require a balance between neuraminidase sialidase activity and hemagglutinin receptor affinity. J Virol 94, e01210-01220.

Arai, Y., Ibrahim, M.S., Elgendy, E.M., Daidoji, T., Ono, T., Suzuki, Y., Nakaya, T., Matsumoto, K., Watanabe, Y., 2019a. Genetic compatibility of reassortants between avian H5N1 and H9N2 influenza viruses with higher pathogenicity in mammals. J Virol 93, e01969-01918.

Arai, Y., Kawashita, N., Ibrahim, M.S., Elgendy, E.M., Daidoji, T., Ono, T., Takagi, T., Nakaya, T., Matsumoto, K., Watanabe, Y., 2019b. PB2 mutations arising during H9N2 influenza evolution in the Middle East confer enhanced replication and growth in mammals. PLoS Pathog 15, e1007919.

Ayllon, J., Garcia-Sastre, A., 2015. The NS1 protein: a multitasking virulence factor. Curr Top Microbiol Immunol 386, 73-107.

Banks, J., Speidel, E.S., Moore, E., Plowright, L., Piccirillo, A., Capua, I., Cordioli, P., Fioretti, A., Alexander, D.J., 2001. Changes in the haemagglutinin and the neuraminidase genes prior to the emergence of highly pathogenic H7N1 avian influenza viruses in Italy. Arch Virol 146, 963-973.

Bano, S., Naeem, K., Malik, S.A., 2003. Evaluation of pathogenic potential of avian influenza virus serotype H9N2 in chickens. Avian Dis 47, 817-822.

Barber, M.R., Aldridge, J.R., Jr., Webster, R.G., Magor, K.E., 2010. Association of RIG-I with innate immunity of ducks to influenza. Proc Natl Acad Sci U S A 107, 5913-5918.

Baron, J., Tarnow, C., Mayoli-Nussle, D., Schilling, E., Meyer, D., Hammami, M., Schwalm, F., Steinmetzer, T., Guan, Y., Garten, W., Klenk, H.D., Bottcher-Friebertshauser, E., 2013. Matriptase, HAT, and TMPRSS2 activate the hemagglutinin of H9N2 influenza A viruses. J Virol 87, 1811-1820.

Becker, W.B., 1966. The isolation and classification of Tern virus: influenza A-Tern South Africa--1961. J Hyg (Lond) 64, 309-320.

Belkasmi, S.F.Z., Fellahi, S., Touzani, C.D., Faraji, F.Z., Maaroufi, I., Delverdier, M., Guerin, J.L., Fihri, O.F., El Houadfi, M., Ducatez, M.F., 2020. Co-infections of chickens with avian influenza virus H9N2 and Moroccan Italy 02 infectious bronchitis virus: effect on pathogenesis and protection conferred by different vaccination programmes. Avian Pathol 49, 21-28.

Bodewes, R., Kuiken, T., 2018. Changing role of wild birds in the epidemiology of avian influenza A viruses. Adv Virus Res 100, 279-307.

Bonfante, F., Patrono, L.V., Aiello, R., Beato, M.S., Terregino, C., Capua, I., 2013. Susceptibility and intra-species transmission of the H9N2 G1 prototype lineage virus in Japanese quail and turkeys. Vet Microbiol 165, 177-183.
Bottcher, E., Matrosovich, T., Beyerle, M., Klenk, H.D., Garten, W., Matrosovich, M., 2006. Proteolytic activation of influenza viruses by serine proteases TMPRSS2 and HAT from human airway epithelium. J Virol 80, 9896-9898.
Bouvier, N.M., Palese, P., 2008. The biology of influenza viruses. Vaccine 26 Suppl 4, D49-53.
Brisse, M., Ly, H., 2019. Comparative structure and function analysis of the RIG-I-like receptors: RIG-I and MDA5. Front Immunol 10, 1586.
Bui, M., Whittaker, G., Helenius, A., 1996. Effect of M1 protein and low pH on nuclear transport of influenza virus ribonucleoproteins. J Virol 70, 8391-8401.
Burgui, I., Aragon, T., Ortin, J., Nieto, A., 2003. PABP1 and eIF4GI associate with influenza virus NS1 protein in viral mRNA translation initiation complexes. J Gen Virol 84, 3263-3274.
Byrd-Leotis, L., Cummings, R.D., Steinhauer, D.A., 2017. The interplay between the host receptor and influenza virus hemagglutinin and neuraminidase. Int J Mol Sci 18, 1541.
Cagle, C., To, T.L., Nguyen, T., Wasilenko, J., Adams, S.C., Cardona, C.J., Spackman, E., Suarez, D.L., Pantin-Jackwood, M.J., 2011. Pekin and Muscovy ducks respond differently to vaccination with a H5N1 highly pathogenic avian influenza (HPAI) commercial inactivated vaccine. Vaccine 29, 6549-6557.
Cagle, C., Wasilenko, J., Adams, S.C., Cardona, C.J., To, T.L., Nguyen, T., Spackman, E., Suarez, D.L., Smith, D., Shepherd, E., Roth, J., Pantin-Jackwood, M.J., 2012. Differences in pathogenicity, response to vaccination, and innate immune responses in different types of ducks infected with a virulent H5N1 highly pathogenic avian influenza virus from Vietnam. Avian Dis 56, 479-487.
Campbell, L.K., Magor, K.E., 2020. Pattern recognition receptor signaling and innate responses to influenza A viruses in the Mallard duck, compared to humans and chickens. Front Cell Infect Microbiol 10, 209.
Cao, S., Liu, X., Yu, M., Li, J., Jia, X., Bi, Y., Sun, L., Gao, G.F., Liu, W., 2012. A nuclear export signal in the matrix protein of Influenza A virus is required for efficient virus replication. J Virol 86, 4883-4891.
Capua, I., Mutinelli, F., 2001. Mortality in Muscovy ducks (Cairina moschata) and domestic geese (Anser anser var. domestica) associated with natural infection with a highly pathogenic avian influenza virus of H7N1 subtype. Avian Pathol 30, 179-183.
Carnaccini, S., Perez, D.R., 2020. H9 influenza viruses: an emerging challenge. Cold Spring Harb Perspect Med 10, a038588.
Chen, C.-J., Chen, G.-W., Wang, C.-H., Huang, C.-H., Wang, Y.-C., Shih, S.-R., 2010. Differential localization and function of PB1-F2 derived from different strains of influenza A virus. J Virol 84, 10051-10062.
Chen, H., Yuan, H., Gao, R., Zhang, J., Wang, D., Xiong, Y., Fan, G., Yang, F., Li, X., Zhou, J., Zou, S., Yang, L., Chen, T., Dong, L., Bo, H., Zhao, X., Zhang, Y., Lan, Y., Bai, T., Dong, J., Li, Q., Wang, S., Zhang, Y., Li, H., Gong, T., Shi, Y., Ni, X., Li, J., Zhou, J., Fan, J., Wu, J., Zhou, X., Hu, M., Wan, J., Yang, W., Li, D., Wu, G., Feng, Z., Gao, G.F., Wang, Y., Jin, Q., Liu, M., Shu, Y., 2014. Clinical and epidemiological characteristics of a fatal case of avian influenza A H10N8 virus infection: a descriptive study. Lancet 383, 714-721.
Chen, J., Lee, K.H., Steinhauer, D.A., Stevens, D.J., Skehel, J.J., Wiley, D.C., 1998. Structure of the hemagglutinin precursor cleavage site, a determinant of influenza pathogenicity and the origin of the labile conformation. Cell 95, 409-417.
Chen, S., Cheng, A., Wang, M., 2013. Innate sensing of viruses by pattern recognition receptors in birds. Vet Res 44, 82.
Chen, S., Quan, K., Wang, D., Du, Y., Qin, T., Peng, D., Liu, X., 2020. Truncation or deglycosylation of the neuraminidase stalk enhances the pathogenicity of the H5N1 subtype avian influenza virus in Mallard ducks. Front Microbiol 11, 583588.
Chen, W., Calvo, P.A., Malide, D., Gibbs, J., Schubert, U., Bacik, I., Basta, S., O'Neill, R., Schickli, J., Palese, P., Henklein, P., Bennink, J.R., Yewdell, J.W., 2001. A novel influenza A virus mitochondrial protein that induces cell death. Nat Med 7, 1306-1312.

Chien, C.Y., Tejero, R., Huang, Y., Zimmerman, D.E., Rios, C.B., Krug, R.M., Montelione, G.T., 1997. A novel RNA-binding motif in influenza A virus non-structural protein 1. Nat Struct Biol 4, 891-895.
Chlanda, P., Zimmerberg, J., 2016. Protein-lipid interactions critical to replication of the influenza A virus. FEBS Lett 590, 1940-1954.
Chou, Y.Y., Vafabakhsh, R., Doganay, S., Gao, Q., Ha, T., Palese, P., 2012. One influenza virus particle packages eight unique viral RNAs as shown by FISH analysis. Proc Natl Acad Sci U S A 109, 9101-9106.
Chuang, Y.C., Tseng, J.C., Yang, J.X., Liu, Y.L., Yeh, D.W., Lai, C.Y., Yu, G.Y., Hsu, L.C., Huang, C.M., Chuang, T.H., 2020. Toll-like receptor 21 of chicken and duck recognize a broad array of immunostimulatory CpG-oligodeoxynucleotide sequences. Vaccines (Basel) 8, 639.
Ciminski, K., Thamamongood, T., Zimmer, G., Schwemmle, M., 2017. Novel insights into bat influenza A viruses. J Gen Virol 98, 2393-2400.
Claes, F., Morzaria, S.P., Donis, R.O., 2016. Emergence and dissemination of clade 2.3.4.4 H5Nx influenza viruses-how is the Asian HPAI H5 lineage maintained. Curr Opin Virol 16, 158-163.
Clark, A.M., Nogales, A., Martinez-Sobrido, L., Topham, D.J., DeDiego, M.L., 2017. Functional evolution of influenza virus NS1 protein in currently circulating human 2009 pandemic H1N1 viruses. J Virol 91, e00721-00717.
Colman, P.M., 1994. Influenza virus neuraminidase: structure, antibodies, and inhibitors. Protein Sci 3, 1687-1696.
Coman, A., Maftei, D.N., Krueger, W.S., Heil, G.L., Friary, J.A., Chereches, R.M., Sirlincan, E., Bria, P., Dragnea, C., Kasler, I., Gray, G.C., 2013. Serological evidence for avian H9N2 influenza virus infections among Romanian agriculture workers. J Infect Public Health 6, 438-447.
Conenello, G.M., Tisoncik, J.R., Rosenzweig, E., Varga, Z.T., Palese, P., Katze, M.G., 2011. A single N66S mutation in the PB1-F2 protein of influenza A virus increases virulence by inhibiting the early interferon response in vivo. J Virol 85, 652-662.
Connor, R.J., Kawaoka, Y., Webster, R.G., Paulson, J.C., 1994. Receptor specificity in human, avian, and equine H2 and H3 influenza virus isolates. Virology 205, 17-23.
Cornelissen, J.B., Post, J., Peeters, B., Vervelde, L., Rebel, J.M., 2012. Differential innate responses of chickens and ducks to low-pathogenic avian influenza. Avian Pathol 41, 519-529.
Cornelissen, J.B., Vervelde, L., Post, J., Rebel, J.M., 2013. Differences in highly pathogenic avian influenza viral pathogenesis and associated early inflammatory response in chickens and ducks. Avian Pathol 42, 347-364.
Czudai-Matwich, V., Otte, A., Matrosovich, M., Gabriel, G., Klenk, H.D., 2014. PB2 mutations D701N and S714R promote adaptation of an influenza H5N1 virus to a mammalian host. J Virol 88, 8735-8742.
Dawson, A.R., Mehle, A., 2018. Flu's cues: Exploiting host post-translational modifications to direct the influenza virus replication cycle. PLoS Pathog 14, e1007205.
Dawson, A.R., Wilson, G.M., Coon, J.J., Mehle, A., 2020. Post-translation regulation of influenza virus replication. Annu Rev Virol 7, 167-187.
de Chassey, B., Aublin-Gex, A., Ruggieri, A., Meyniel-Schicklin, L., Pradezynski, F., Davoust, N., Chantier, T., Tafforeau, L., Mangeot, P.E., Ciancia, C., Perrin-Cocon, L., Bartenschlager, R., Andre, P., Lotteau, V., 2013. The interactomes of influenza virus NS1 and NS2 proteins identify new host factors and provide insights for ADAR1 playing a supportive role in virus replication. PLoS Pathog 9, e1003440.
Desselberger, U., Racaniello, V.R., Zazra, J.J., Palese, P., 1980. The 3' and 5'-terminal sequences of influenza A, B and C virus RNA segments are highly conserved and show partial inverted complementarity. Gene 8, 315-328.
Dias, A., Bouvier, D., Crepin, T., McCarthy, A.A., Hart, D.J., Baudin, F., Cusack, S., Ruigrok, R.W., 2009. The cap-snatching endonuclease of influenza virus polymerase resides in the PA subunit. Nature 458, 914-918.
Diebold, S.S., Kaisho, T., Hemmi, H., Akira, S., Reis e Sousa, C., 2004. Innate antiviral responses by means of TLR7-mediated recognition of single-stranded RNA. Science 303, 1529-1531.

Dittrich, A., Scheibner, D., Salaheldin, A.H., Veits, J., Gischke, M., Mettenleiter, T.C., Abdelwhab, E.M., 2018. Impact of mutations in the hemagglutinin of H10N7 viruses isolated from seals on virus replication in avian and human cells. Viruses 10, 83.
Dou, D., Revol, R., Ostbye, H., Wang, H., Daniels, R., 2018. Influenza A virus cell entry, replication, virion assembly and movement. Front Immunol 9, 1581.
Drake, J.W., 1993. Rates of spontaneous mutation among RNA viruses. Proc Natl Acad Sci U S A 90, 4171-4175.
DuBois, R.M., Zaraket, H., Reddivari, M., Heath, R.J., White, S.W., Russell, C.J., 2011. Acid stability of the hemagglutinin protein regulates H5N1 influenza virus pathogenicity. PLoS Pathog 7, e1002398.
EFSA, 2021. European Food Safety Authority: Avian influenza overview December 2020 – February 2021. Available online at: https://www.ecdc.europa.eu/sites/default/files/documents/avian-influenza-overview-december-2020%E2%80%93february-2021.pdf (last accessed 06-04-2021).
Eisfeld, A.J., Neumann, G., Kawaoka, Y., 2015. At the centre: influenza A virus ribonucleoproteins. Nat Rev Microbiol 13, 28-41.
El-Shesheny, R., Franks, J., Turner, J., Seiler, P., Walker, D., Friedman, K., Mukherjee, N., Kercher, L., Hasan, M.K., Feeroz, M.M., Krauss, S., Vogel, P., McKenzie, P., Barman, S., Webby, R.J., Webster, R.G., 2020. Continued evolution of H5Nx avian influenza viruses in Bangladeshi live poultry markets: pathogenic potential in poultry and mammalian models. J Virol 94, e01141-01120.
Essere, B., Yver, M., Gavazzi, C., Terrier, O., Isel, C., Fournier, E., Giroux, F., Textoris, J., Julien, T., Socratous, C., Rosa-Calatrava, M., Lina, B., Marquet, R., Moules, V., 2013. Critical role of segment-specific packaging signals in genetic reassortment of influenza A viruses. Proc Natl Acad Sci U S A 110, E3840-3848.
Evseev, D., Magor, K.E., 2019. Innate immune responses to avian influenza viruses in ducks and chickens. Vet Sci 6, 5.
Fan, S., Macken, C.A., Li, C., Ozawa, M., Goto, H., Iswahyudi, N.F., Nidom, C.A., Chen, H., Neumann, G., Kawaoka, Y., 2013. Synergistic effect of the PDZ and p85beta-binding domains of the NS1 protein on virulence of an avian H5N1 influenza A virus. J Virol 87, 4861-4871.
FAOSTAT., 2019. Food and Agriculture Organization of the United Nations. Livestock Processed. Access 17.03.2021. http://www.fao.org/faostat/en/#data.
Fleming-Canepa, X., Aldridge, J.R., Jr., Canniff, L., Kobewka, M., Jax, E., Webster, R.G., Magor, K.E., 2019. Duck innate immune responses to high and low pathogenicity H5 avian influenza viruses. Vet Microbiol 228, 101-111.
FLI, 2020. HPAI in Norddeutschland vom 01.07.2020 bis 12.11.2020 (https://www.openagrar.de/rsc/viewer/openagrar_derivate_00034778/Map_AI_ND_2020-11-12.jpg).
FLI, 2021a. HPAI in Deutschland vom 01.10.2020 bis 01.04.2021 (https://www.fli.de/fileadmin/FLI/Images/Tierseuchengeschehen/H5N8/Karten_D/2021/Map_AI_D_2021-04-01.jpg).
FLI, 2021b. Risikoeinschätzung zum Auftreten von HPAIV H5 in Deutschland (https://www.openagrar.de/servlets/MCRFileNodeServlet/openagrar_derivate_00036488/FLI-Risikoeinschaetzung_HPAIV_H5N8_2021-03-25-bf.pdf).
Forgac, M., 2007. Vacuolar ATPases: rotary proton pumps in physiology and pathophysiology. Nat Rev Mol Cell Biol 8, 917-929.
Fouchier, R.A., 2015. Studies on influenza virus transmission between ferrets: the public health risks revisited. mBio 6, e02560-02514.
Fouchier, R.A., Munster, V., Wallensten, A., Bestebroer, T.M., Herfst, S., Smith, D., Rimmelzwaan, G.F., Olsen, B., Osterhaus, A.D., 2005. Characterization of a novel influenza A virus hemagglutinin subtype (H16) obtained from black-headed gulls. J Virol 79, 2814-2822.
Fouchier, R.A., Schneeberger, P.M., Rozendaal, F.W., Broekman, J.M., Kemink, S.A., Munster, V., Kuiken, T., Rimmelzwaan, G.F., Schutten, M., Van Doornum, G.J., Koch, G., Bosman, A., Koopmans, M., Osterhaus, A.D., 2004. Avian influenza A virus (H7N7) associated with human conjunctivitis and a fatal case of acute respiratory distress syndrome. Proc Natl Acad Sci U S A 101, 1356-1361.

Franca, M., Stallknecht, D.E., Howerth, E.W., 2013. Expression and distribution of sialic acid influenza virus receptors in wild birds. Avian Pathol 42, 60-71.
Freidl, G.S., Meijer, A., de Bruin, E., de Nardi, M., Munoz, O., Capua, I., Breed, A.C., Harris, K., Hill, A., Kosmider, R., Banks, J., von Dobschuetz, S., Stark, K., Wieland, B., Stevens, K., van der Werf, S., Enouf, V., van der Meulen, K., Van Reeth, K., Dauphin, G., Koopmans, M., Consortium, F., 2014. Influenza at the animal-human interface: a review of the literature for virological evidence of human infection with swine or avian influenza viruses other than A(H5N1). Euro Surveill 19, 20793.
Fu, B., Wang, L., Ding, H., Schwamborn, J.C., Li, S., Dorf, M.E., 2015. TRIM32 senses and restricts influenza A virus by ubiquitination of PB1 polymerase. PLoS Pathog 11, e1004960.
Gadalla, M.R., Morrison, E., Serebryakova, M.V., Han, X., Wolff, T., Freund, C., Kordyukova, L., Veit, M., 2021. NS1-mediated upregulation of ZDHHC22 acyltransferase in influenza a virus infected cells. Cell Microbiol, e13322.
Gales, J.P., Kubina, J., Geldreich, A., Dimitrova, M., 2020. Strength in diversity: nuclear export of viral RNAs. Viruses 12, 1014.
Gamblin, S.J., Haire, L.F., Russell, R.J., Stevens, D.J., Xiao, B., Ha, Y., Vasisht, N., Steinhauer, D.A., Daniels, R.S., Elliot, A., Wiley, D.C., Skehel, J.J., 2004. The structure and receptor binding properties of the 1918 influenza hemagglutinin. Science 303, 1838-1842.
Gamblin, S.J., Skehel, J.J., 2010. Influenza hemagglutinin and neuraminidase membrane glycoproteins. J Biol Chem 285, 28403-28409.
Gao, R., Cao, B., Hu, Y., Feng, Z., Wang, D., Hu, W., Chen, J., Jie, Z., Qiu, H., Xu, K., Xu, X., Lu, H., Zhu, W., Gao, Z., Xiang, N., Shen, Y., He, Z., Gu, Y., Zhang, Z., Yang, Y., Zhao, X., Zhou, L., Li, X., Zou, S., Zhang, Y., Li, X., Yang, L., Guo, J., Dong, J., Li, Q., Dong, L., Zhu, Y., Bai, T., Wang, S., Hao, P., Yang, W., Zhang, Y., Han, J., Yu, H., Li, D., Gao, G.F., Wu, G., Wang, Y., Yuan, Z., Shu, Y., 2013. Human infection with a novel avian-origin influenza A (H7N9) virus. N Engl J Med 368, 1888-1897.
Gao, S., Wu, J., Liu, R.Y., Li, J., Song, L., Teng, Y., Sheng, C., Liu, D., Yao, C., Chen, H., Jiang, W., Chen, S., Huang, W., 2015. Interaction of NS2 with AIMP2 facilitates the switch from ubiquitination to SUMOylation of M1 in influenza A virus-infected cells. J Virol 89, 300-311.
Garcia-Sastre, A., Egorov, A., Matassov, D., Brandt, S., Levy, D.E., Durbin, J.E., Palese, P., Muster, T., 1998. Influenza A virus lacking the NS1 gene replicates in interferon-deficient systems. Virology 252, 324-330.
Garten, R.J., Davis, C.T., Russell, C.A., Shu, B., Lindstrom, S., Balish, A., Sessions, W.M., Xu, X., Skepner, E., Deyde, V., Okomo-Adhiambo, M., Gubareva, L., Barnes, J., Smith, C.B., Emery, S.L., Hillman, M.J., Rivailler, P., Smagala, J., de Graaf, M., Burke, D.F., Fouchier, R.A., Pappas, C., Alpuche-Aranda, C.M., Lopez-Gatell, H., Olivera, H., Lopez, I., Myers, C.A., Faix, D., Blair, P.J., Yu, C., Keene, K.M., Dotson, P.D., Jr., Boxrud, D., Sambol, A.R., Abid, S.H., St George, K., Bannerman, T., Moore, A.L., Stringer, D.J., Blevins, P., Demmler-Harrison, G.J., Ginsberg, M., Kriner, P., Waterman, S., Smole, S., Guevara, H.F., Belongia, E.A., Clark, P.A., Beatrice, S.T., Donis, R., Katz, J., Finelli, L., Bridges, C.B., Shaw, M., Jernigan, D.B., Uyeki, T.M., Smith, D.J., Klimov, A.I., Cox, N.J., 2009. Antigenic and genetic characteristics of swine-origin 2009 A(H1N1) influenza viruses circulating in humans. Science 325, 197-201.
Gerber, M., Isel, C., Moules, V., Marquet, R., 2014. Selective packaging of the influenza A genome and consequences for genetic reassortment. Trends Microbiol 22, 446-455.
Gerlach, T., Hensen, L., Matrosovich, T., Bergmann, J., Winkler, M., Peteranderl, C., Klenk, H.D., Weber, F., Herold, S., Pohlmann, S., Matrosovich, M., 2017. pH optimum of hemagglutinin-mediated membrane fusion determines sensitivity of influenza A viruses to the interferon-induced antiviral state and IFITMs. J Virol 91.
Gischke, M., Ulrich, R., O, I.F., Scheibner, D., Salaheldin, A.H., Crossley, B., Bottcher-Friebertshauser, E., Veits, J., Mettenleiter, T.C., Abdelwhab, E.M., 2020. Insertion of basic amino acids in the hemagglutinin cleavage site of H4N2 avian influenza virus (AIV)-reduced virus fitness in chickens is restored by reassortment with highly pathogenic H5N1 AIV. Int J Mol Sci 21, 2353.
Glezen, W.P., 1996. Emerging infections: pandemic influenza. Epidemiol Rev 18, 64-76.

Global Consortium for, H.N., Related Influenza, V., 2016. Role for migratory wild birds in the global spread of avian influenza H5N8. Science 354, 213-217.
Globig, A., Staubach, C., Sauter-Louis, C., Dietze, K., Homeier-Bachmann, T., Probst, C., Gethmann, J., Depner, K.R., Grund, C., Harder, T.C., Starick, E., Pohlmann, A., Hoper, D., Beer, M., Mettenleiter, T.C., Conraths, F.J., 2017. Highly pathogenic avian influenza H5N8 clade 2.3.4.4b in Germany in 2016/2017. Front Vet Sci 4, 240.
Gohrbandt, S., Veits, J., Breithaupt, A., Hundt, J., Teifke, J.P., Stech, O., Mettenleiter, T.C., Stech, J., 2011. H9 avian influenza reassortant with engineered polybasic cleavage site displays a highly pathogenic phenotype in chicken. J Gen Virol 92, 1843-1853.
Goto, H., Muramoto, Y., Noda, T., Kawaoka, Y., 2013. The genome-packaging signal of the influenza A virus genome comprises a genome incorporation signal and a genome-bundling signal. J Virol 87, 11316-11322.
Greenspan, D., Palese, P., Krystal, M., 1988. Two nuclear location signals in the influenza virus NS1 nonstructural protein. J Virol 62, 3020-3026.
Grund, C., Abdelwhab el, S.M., Arafa, A.S., Ziller, M., Hassan, M.K., Aly, M.M., Hafez, H.M., Harder, T.C., Beer, M., 2011. Highly pathogenic avian influenza virus H5N1 from Egypt escapes vaccine-induced immunity but confers clinical protection against a heterologous clade 2.2.1 Egyptian isolate. Vaccine 29, 5567-5573.
Grund, C., Hoffmann, D., Ulrich, R., Naguib, M., Schinkothe, J., Hoffmann, B., Harder, T., Saenger, S., Zscheppang, K., Tonnies, M., Hippenstiel, S., Hocke, A., Wolff, T., Beer, M., 2018. A novel European H5N8 influenza A virus has increased virulence in ducks but low zoonotic potential. Emerg Microbes Infect 7, 132.
Gu, M., Xu, L., Wang, X., Liu, X., 2017. Current situation of H9N2 subtype avian influenza in China. Vet Res 48, 49.
Guan, Y., Shortridge, K.F., Krauss, S., Webster, R.G., 1999. Molecular characterization of H9N2 influenza viruses: Were they the donors of the “internal” genes of H5N1 viruses in Hong Kong? Proc Natl Acad Sci U S A 96, 9363-9367.
Gultyaev, A.P., Spronken, M.I., Funk, M., Fouchier, R.A.M., Richard, M., 2021. Insertions of codons encoding basic amino acids in H7 hemagglutinins of influenza A viruses occur by recombination with RNA at hotspots near snoRNA binding sites. RNA (New York, N.Y.) 27, 123-132.
Guo, Y.J., Jin, F.G., Wang, P., Wang, M., Zhu, J.M., 1983. Isolation of influenza C virus from pigs and experimental infection of pigs with influenza C virus. J Gen Virol 64 (Pt 1), 177-182.
Hale, B.G., Barclay, W.S., Randall, R.E., Russell, R.J., 2008a. Structure of an avian influenza A virus NS1 protein effector domain. Virology 378, 1-5.
Hale, B.G., Randall, R.E., Ortin, J., Jackson, D., 2008b. The multifunctional NS1 protein of influenza A viruses. J Gen Virol 89, 2359-2376.
Hale, B.G., Steel, J., Manicassamy, B., Medina, R.A., Ye, J., Hickman, D., Lowen, A.C., Perez, D.R., García-Sastre, A., 2010a. Mutations in the NS1 C-terminal tail do not enhance replication or virulence of the 2009 pandemic H1N1 influenza A virus. J Gen Virol 91, 1737-1742.
Hale, B.G., Steel, J., Medina, R.A., Manicassamy, B., Ye, J., Hickman, D., Hai, R., Schmolke, M., Lowen, A.C., Perez, D.R., Garcia-Sastre, A., 2010b. Inefficient control of host gene expression by the 2009 pandemic H1N1 influenza A virus NS1 protein. J Virol 84, 6909-6922.
Han, Q., Chang, C., Li, L., Klenk, C., Cheng, J., Chen, Y., Xia, N., Shu, Y., Chen, Z., Gabriel, G., Sun, B., Xu, K., 2014. Sumoylation of influenza A virus nucleoprotein is essential for intracellular trafficking and virus growth. J Virol 88, 9379-9390.
Hao, W., Wang, L., Li, S., 2020. Roles of the non-structural proteins of influenza A virus. Pathogens 9, 812.
Hao, X., Wang, J., Hu, J., Lu, X., Gao, Z., Liu, D., Li, J., Wang, X., Gu, M., Hu, Z., Liu, X., Hu, S., Xu, X., Peng, D., Jiao, X., Liu, X., 2017. Internal gene cassette from a genotype S H9N2 avian influenza virus attenuates the pathogenicity of H5 viruses in chickens and mice. Front Microbiol 8, 1978.
Hara, K., Nakazono, Y., Kashiwagi, T., Hamada, N., Watanabe, H., 2013. Co-incorporation of the PB2 and PA polymerase subunits from human H3N2 influenza virus is a critical determinant of the replication of reassortant ribonucleoprotein complexes. J Gen Virol 94, 2406-2416.

Harder, T., Maurer-Stroh, S., Pohlmann, A., Starick, E., Horeth-Bontgen, D., Albrecht, K., Pannwitz, G., Teifke, J., Gunalan, V., Lee, R.T., Sauter-Louis, C., Homeier, T., Staubach, C., Wolf, C., Strebelow, G., Hoper, D., Grund, C., Conraths, F.J., Mettenleiter, T.C., Beer, M., 2015. Influenza A(H5N8) virus similar to strain in Korea causing highly pathogenic avian influenza in Germany. Emerg Infect Dis 21, 860-863.

Hassan, K.E., King, J., El-Kady, M., Afifi, M., Abozeid, H.H., Pohlmann, A., Beer, M., Harder, T., 2020. Novel reassortant highly pathogenic avian influenza A(H5N2) virus in broiler chickens, Egypt. Emerg Infect Dis 26, 129-133.

Hause, B.M., Collin, E.A., Liu, R., Huang, B., Sheng, Z., Lu, W., Wang, D., Nelson, E.A., Li, F., 2014. Characterization of a novel influenza virus in cattle and Swine: proposal for a new genus in the Orthomyxoviridae family. mBio 5, e00031-00014.

Hause, B.M., Ducatez, M., Collin, E.A., Ran, Z., Liu, R., Sheng, Z., Armien, A., Kaplan, B., Chakravarty, S., Hoppe, A.D., Webby, R.J., Simonson, R.R., Li, F., 2013. Isolation of a novel swine influenza virus from Oklahoma in 2011 which is distantly related to human influenza C viruses. PLoS Pathog 9, e1003176.

Hoffmann, T.W., Munier, S., Larcher, T., Soubieux, D., Ledevin, M., Esnault, E., Tourdes, A., Croville, G., Guerin, J.L., Quere, P., Volmer, R., Naffakh, N., Marc, D., 2012. Length variations in the NA stalk of an H7N1 influenza virus have opposite effects on viral excretion in chickens and ducks. J Virol 86, 584-588.

Holland, J., Spindler, K., Horodyski, F., Grabau, E., Nichol, S., VandePol, S., 1982. Rapid evolution of RNA genomes. Science 215, 1577-1585.

Homme, P.J., Easterday, B.C., 1970. Avian influenza virus infections. I. Characteristics of influenza A-turkey-Wisconsin-1966 virus. Avian Dis 14, 66-74.

Hu, J., Hu, Z., Mo, Y., Wu, Q., Cui, Z., Duan, Z., Huang, J., Chen, H., Chen, Y., Gu, M., Wang, X., Hu, S., Liu, H., Liu, W., Liu, X., Liu, X., 2013. The PA and HA gene-mediated high viral load and intense innate immune response in the brain contribute to the high pathogenicity of H5N1 avian influenza virus in mallard ducks. J Virol 87, 11063-11075.

Hu, Y., Sneyd, H., Dekant, R., Wang, J., 2017. Influenza A virus nucleoprotein: A highly conserved multi-functional viral protein as a hot antiviral drug target. Curr Top Med Chem 17, 2271-2285.

Huang, S., Chen, J., Chen, Q., Wang, H., Yao, Y., Chen, J., Chen, Z., 2013. A second CRM1-dependent nuclear export signal in the influenza A virus NS2 protein contributes to the nuclear export of viral ribonucleoproteins. J Virol 87, 767-778.

Hutchinson, E.C., Charles, P.D., Hester, S.S., Thomas, B., Trudgian, D., Martinez-Alonso, M., Fodor, E., 2015. Erratum: Conserved and host-specific features of influenza virion architecture. Nat Commun 6, 6446.

Hutchinson, E.C., Denham, E.M., Thomas, B., Trudgian, D.C., Hester, S.S., Ridlova, G., York, A., Turrell, L., Fodor, E., 2012. Mapping the phosphoproteome of influenza A and B viruses by mass spectrometry. PLoS Pathog 8, e1002993.

Hutchinson, E.C., von Kirchbach, J.C., Gog, J.R., Digard, P., 2010. Genome packaging in influenza A virus. J Gen Virol 91, 313-328.

Iba, Y., Fujii, Y., Ohshima, N., Sumida, T., Kubota-Koketsu, R., Ikeda, M., Wakiyama, M., Shirouzu, M., Okada, J., Okuno, Y., Kurosawa, Y., Yokoyama, S., 2014. Conserved neutralizing epitope at globular head of hemagglutinin in H3N2 influenza viruses. J Virol 88, 7130-7144.

ICTV, 2019. International Committee on Taxonomy of Viruses: Orthomyxoviridae. Available online at: https://talk.ictvonline.org/ictv-reports/ictv_9th_report/negative-sense-rna-viruses-2011/w/negrna_viruses/209/orthomyxoviridae (last accessed 28-03-2021).

Imai, M., Watanabe, T., Hatta, M., Das, S.C., Ozawa, M., Shinya, K., Zhong, G., Hanson, A., Katsura, H., Watanabe, S., Li, C., Kawakami, E., Yamada, S., Kiso, M., Suzuki, Y., Maher, E.A., Neumann, G., Kawaoka, Y., 2012. Experimental adaptation of an influenza H5 HA confers respiratory droplet transmission to a reassortant H5 HA/H1N1 virus in ferrets. Nature 486, 420-428.

Ito, T., Couceiro, J.N., Kelm, S., Baum, L.G., Krauss, S., Castrucci, M.R., Donatelli, I., Kida, H., Paulson, J.C., Webster, R.G., Kawaoka, Y., 1998. Molecular basis for the generation in pigs of influenza A viruses with pandemic potential. J Virol 72, 7367-7373.

Ito, T., Suzuki, Y., Mitnaul, L., Vines, A., Kida, H., Kawaoka, Y., 1997. Receptor specificity of influenza A viruses correlates with the agglutination of erythrocytes from different animal species. Virology 227, 493-499.
Jagger, B.W., Wise, H.M., Kash, J.C., Walters, K.A., Wills, N.M., Xiao, Y.L., Dunfee, R.L., Schwartzman, L.M., Ozinsky, A., Bell, G.L., Dalton, R.M., Lo, A., Efstathiou, S., Atkins, J.F., Firth, A.E., Taubenberger, J.K., Digard, P., 2012. An overlapping protein-coding region in influenza A virus segment 3 modulates the host response. Science 337, 199-204.
Jiao, P., Tian, G., Li, Y., Deng, G., Jiang, Y., Liu, C., Liu, W., Bu, Z., Kawaoka, Y., Chen, H., 2008. A single-amino-acid substitution in the NS1 protein changes the pathogenicity of H5N1 avian influenza viruses in mice. J Virol 82, 1146-1154.
Kaiser, P., 2010. Advances in avian immunology--prospects for disease control: a review. Avian Pathol 39, 309-324.
Kajihara, M., Sakoda, Y., Soda, K., Minari, K., Okamatsu, M., Takada, A., Kida, H., 2013. The PB2, PA, HA, NP, and NS genes of a highly pathogenic avian influenza virus A/whooper swan/Mongolia/3/2005 (H5N1) are responsible for pathogenicity in ducks. Virol J 10, 45.
Kalthoff, D., Globig, A., Beer, M., 2010. (Highly pathogenic) avian influenza as a zoonotic agent. Vet Microbiol 140, 237-245.
Kalthoff, D., Rohrs, S., Hoper, D., Hoffmann, B., Bogs, J., Stech, J., Beer, M., 2013. Truncation and sequence shuffling of segment 6 generate replication-competent neuraminidase-negative influenza H5N1 viruses. J Virol 87, 13556-13568.
Kaplan, B.S., Falkenberg, S., Dassanayake, R., Neill, J., Velayudhan, B., Li, F., Vincent, A.L., 2020. Virus strain influenced the interspecies transmission of influenza D virus between calves and pigs. Transbound Emerg Dis, 13943.
Kaverin, N.V., Rudneva, I.A., Govorkova, E.A., Timofeeva, T.A., Shilov, A.A., Kochergin-Nikitsky, K.S., Krylov, P.S., Webster, R.G., 2007. Epitope mapping of the hemagglutinin molecule of a highly pathogenic H5N1 influenza virus by using monoclonal antibodies. J Virol 81, 12911-12917.
Kawaoka, Y., 1991. Structural features influencing hemagglutinin cleavability in a human influenza A virus. J Virol 65, 1195-1201.
Kawaoka, Y., Gorman, O.T., Ito, T., Wells, K., Donis, R.O., Castrucci, M.R., Donatelli, I., Webster, R.G., 1998. Influence of host species on the evolution of the nonstructural (NS) gene of influenza A viruses. Virus Res 55, 143-156.
Kawaoka, Y., Webster, R.G., 1989. Interplay between carbohydrate in the stalk and the length of the connecting peptide determines the cleavability of influenza virus hemagglutinin. J Virol 63, 3296-3300.
Keiner, B., Maenz, B., Wagner, R., Cattoli, G., Capua, I., Klenk, H.D., 2010. Intracellular distribution of NS1 correlates with the infectivity and interferon antagonism of an avian influenza virus (H7N1). J Virol 84, 11858-11865.
Khan, S.U., Anderson, B.D., Heil, G.L., Liang, S., Gray, G.C., 2015. A systematic review and meta-analysis of the seroprevalence of influenza A(H9N2) infection among humans. J Infect Dis 212, 562-569.
Kilbourne, E.D., 2006. Influenza pandemics of the 20th century. Emerg Infect Dis 12, 9-14.
Kim, J.K., Negovetich, N.J., Forrest, H.L., Webster, R.G., 2009. Ducks: the "Trojan horses" of H5N1 influenza. Influenza Other Respir Viruses 3, 121-128.
Kim, S.H., 2018. Challenge for One Health: co-circulation of zoonotic H5N1 and H9N2 avian influenza viruses in Egypt. Viruses 10, 121.
King, J., Harder, T., Conraths, F.J., Beer, M., Pohlmann, A., 2020a. The genetics of highly pathogenic avian influenza viruses of subtype H5 in Germany, 2006-2020. Transbound Emerg Dis, 13843.
King, J., Schulze, C., Engelhardt, A., Hlinak, A., Lennermann, S.L., Rigbers, K., Skuballa, J., Staubach, C., Mettenleiter, T.C., Harder, T., Beer, M., Pohlmann, A., 2020b. Novel HPAIV H5N8 reassortant (clade 2.3.4.4b) detected in Germany. Viruses 12, 281.
Kirui, J., Mondal, A., Mehle, A., 2016. Ubiquitination upregulates influenza virus polymerase function. J Virol 90, 10906-10914.

Kobayashi, Y., Horimoto, T., Kawaoka, Y., Alexander, D.J., Itakura, C., 1996. Pathological studies of chickens experimentally infected with two highly pathogenic avian influenza viruses. Avian Pathol 25, 285-304.
Koerner, I., Kochs, G., Kalinke, U., Weiss, S., Staeheli, P., 2007. Protective role of beta interferon in host defense against influenza A virus. J Virol 81, 2025-2030.
Kong, W., Liu, L., Wang, Y., He, Q., Wu, S., Qin, Z., Wang, J., Sun, H., Sun, Y., Zhang, R., Pu, J., Liu, J., 2015. C-terminal elongation of NS1 of H9N2 influenza virus induces a high level of inflammatory cytokines and increases transmission. J Gen Virol 96, 259-268.
Krog, J.S., Hansen, M.S., Holm, E., Hjulsager, C.K., Chriel, M., Pedersen, K., Andresen, L.O., Abildstrom, M., Jensen, T.H., Larsen, L.E., 2015. Influenza A(H10N7) virus in dead harbor seals, Denmark. Emerg Infect Dis 21, 684-687.
Krug, R.M., 2015. Functions of the influenza A virus NS1 protein in antiviral defense. Curr Opin Virol 12, 1-6.
Krug, R.M., Etkind, P.R., 1973. Cytoplasmic and nuclear virus-specific proteins in influenza virus-infected MDCK cells. Virology 56, 334-348.
Kumlin, U., Olofsson, S., Dimock, K., Arnberg, N., 2008. Sialic acid tissue distribution and influenza virus tropism. Influenza Other Respir Viruses 2, 147-154.
Lam, T.T., Wang, J., Shen, Y., Zhou, B., Duan, L., Cheung, C.L., Ma, C., Lycett, S.J., Leung, C.Y., Chen, X., Li, L., Hong, W., Chai, Y., Zhou, L., Liang, H., Ou, Z., Liu, Y., Farooqui, A., Kelvin, D.J., Poon, L.L., Smith, D.K., Pybus, O.G., Leung, G.M., Shu, Y., Webster, R.G., Webby, R.J., Peiris, J.S., Rambaut, A., Zhu, H., Guan, Y., 2013. The genesis and source of the H7N9 influenza viruses causing human infections in China. Nature 502, 241-244.
Lamb, R.A., Zebedee, S.L., Richardson, C.D., 1985. Influenza virus M2 protein is an integral membrane protein expressed on the infected-cell surface. Cell 40, 627-633.
Laporte, M., Naesens, L., 2017. Airway proteases: an emerging drug target for influenza and other respiratory virus infections. Curr Opin Virol 24, 16-24.
Lazear, H.M., Schoggins, J.W., Diamond, M.S., 2019. Shared and distinct functions of type I and type III interferons. Immunity 50, 907-923.
Lee, C.C., Wu, C.C., Lin, T.L., 2012. Characterization of chicken melanoma differentiation-associated gene 5 (MDA5) from alternative translation initiation. Comp Immunol Microbiol Infect Dis 35, 335-343.
Lee, C.W., Lee, Y.J., Senne, D.A., Suarez, D.L., 2006. Pathogenic potential of North American H7N2 avian influenza virus: a mutagenesis study using reverse genetics. Virology 353, 388-395.
Lee, D.H., Bertran, K., Kwon, J.H., Swayne, D.E., 2017. Evolution, global spread, and pathogenicity of highly pathogenic avian influenza H5Nx clade 2.3.4.4. J Vet Sci 18, 269-280.
Lenny, B.J., Shanmuganatham, K., Sonnberg, S., Feeroz, M.M., Alam, S.M., Hasan, M.K., Jones-Engel, L., McKenzie, P., Krauss, S., Webster, R.G., Jones, J.C., 2015. Replication capacity of avian influenza A(H9N2) virus in pet birds and mammals, Bangladesh. Emerg Infect Dis 21, 2174-2177.
Li, C.J., Hatta, M., Watanabe, S., Neumann, G., Kawaoka, Y., 2008. Compatibility among polymerase subunit proteins is a restricting factor in reassortment between equine H7N7 and human H3N2 influenza viruses. J Virol 82, 11880-11888.
Li, J., Gu, M., Liu, K., Gao, R., Sun, W., Liu, D., Jiang, K., Zhong, L., Wang, X., Hu, J., Hu, S., Liu, X., Shi, W., Ren, H., Peng, D., Jiao, X., Liu, X., 2020. Amino acid substitutions in antigenic region B of hemagglutinin play a critical role in the antigenic drift of subclade 2.3.4.4 highly pathogenic H5NX influenza viruses. Transbound Emerg Dis 67, 263-275.
Li, J., Zu Dohna, H., Cardona, C.J., Miller, J., Carpenter, T.E., 2011. Emergence and genetic variation of neuraminidase stalk deletions in avian influenza viruses. PLoS One 6, e14722.
Li, X., Shi, J., Guo, J., Deng, G., Zhang, Q., Wang, J., He, X., Wang, K., Chen, J., Li, Y., Fan, J., Kong, H., Gu, C., Guan, Y., Suzuki, Y., Kawaoka, Y., Liu, L., Jiang, Y., Tian, G., Li, Y., Bu, Z., Chen, H., 2014a. Genetics, receptor binding property, and transmissibility in mammals of naturally isolated H9N2 Avian Influenza viruses. PLoS Pathog 10, e1004508.
Li, X., Tian, B., Jianfang, Z., Yongkun, C., Xiaodan, L., Wenfei, Z., Yan, L., Jing, T., Junfeng, G., Tao, C., Rongbao, G., Dayan, W., Shu, Y., 2017. A comprehensive retrospective study of the seroprevalence of H9N2 avian influenza viruses in occupationally exposed populations in China. PLoS One 12, e0178328.

Li, Y., Chen, S., Zhang, X., Fu, Q., Zhang, Z., Shi, S., Zhu, Y., Gu, M., Peng, D., Liu, X., 2014b. A 20-amino-acid deletion in the neuraminidase stalk and a five-amino-acid deletion in the NS1 protein both contribute to the pathogenicity of H5N1 avian influenza viruses in Mallard ducks. PLoS One 9, e95539.
Li, Z., Jiang, Y., Jiao, P., Wang, A., Zhao, F., Tian, G., Wang, X., Yu, K., Bu, Z., Chen, H., 2006. The NS1 gene contributes to the virulence of H5N1 avian influenza viruses. J Virol 80, 11115-11123.
Liao, T.L., Wu, C.Y., Su, W.C., Jeng, K.S., Lai, M.M., 2010. Ubiquitination and deubiquitination of NP protein regulates influenza A virus RNA replication. EMBO J 29, 3879-3890.
Lindh, E., Ek-Kommonen, C., Vaananen, V.M., Vaheri, A., Vapalahti, O., Huovilainen, A., 2014. Molecular epidemiology of H9N2 influenza viruses in Northern Europe. Vet Microbiol 172, 548-554.
Liu, D., Shi, W., Shi, Y., Wang, D., Xiao, H., Li, W., Bi, Y., Wu, Y., Li, X., Yan, J., Liu, W., Zhao, G., Yang, W., Wang, Y., Ma, J., Shu, Y., Lei, F., Gao, G.F., 2013. Origin and diversity of novel avian influenza A H7N9 viruses causing human infection: phylogenetic, structural, and coalescent analyses. Lancet 381, 1926-1932.
Liu, Q., Qiao, C., Marjuki, H., Bawa, B., Ma, J., Guillossou, S., Webby, R.J., Richt, J.A., Ma, W., 2012. Combination of PB2 271A and SR polymorphism at positions 590/591 is critical for viral replication and virulence of swine influenza virus in cultured cells and in vivo. J Virol 86, 1233-1237.
Londt, B.Z., Banks, J., Alexander, D.J., 2007. Highly pathogenic avian influenza viruses with low virulence for chickens in in vivo tests. Avian Pathol 36, 347-350.
Long, J.S., Benfield, C.T., Barclay, W.S., 2015. One-way trip: influenza virus' adaptation to gallinaceous poultry may limit its pandemic potential. Bioessays 37, 204-212.
Long, J.X., Peng, D.X., Liu, Y.L., Wu, Y.T., Liu, X.F., 2008. Virulence of H5N1 avian influenza virus enhanced by a 15-nucleotide deletion in the viral nonstructural gene. Virus genes 36, 471-478.
Lowen, A.C., 2017. Constraints, drivers, and implications of influenza A virus reassortment. Annu Rev Virol 4, 105-121.
Luczo, J.M., Stambas, J., Durr, P.A., Michalski, W.P., Bingham, J., 2015. Molecular pathogenesis of H5 highly pathogenic avian influenza: the role of the haemagglutinin cleavage site motif. Rev Med Virol 25, 406-430.
Lycett, S.J., Pohlmann, A., Staubach, C., Caliendo, V., Woolhouse, M., Beer, M., Kuiken, T., Global Consortium for, H.N., Related Influenza, V., 2020. Genesis and spread of multiple reassortants during the 2016/2017 H5 avian influenza epidemic in Eurasia. Proc Natl Acad Sci U S A 117, 20814-20825.
Lycett, S.J., Ward, M.J., Lewis, F.I., Poon, A.F., Kosakovsky Pond, S.L., Brown, A.J., 2009. Detection of mammalian virulence determinants in highly pathogenic avian influenza H5N1 viruses: multivariate analysis of published data. J Virol 83, 9901-9910.
Mair, C.M., Ludwig, K., Herrmann, A., Sieben, C., 2014. Receptor binding and pH stability - how influenza A virus hemagglutinin affects host-specific virus infection. Biochim Biophys Acta 1838, 1153-1168.
Marc, D., 2014. Influenza virus non-structural protein NS1: interferon antagonism and beyond. J Gen Virol 95, 2594-2611.
Marshall, N., Priyamvada, L., Ende, Z., Steel, J., Lowen, A.C., 2013. Influenza virus reassortment occurs with high frequency in the absence of segment mismatch. PLoS Pathog 9, e1003421.
Martin, K., Helenius, A., 1991. Transport of incoming influenza virus nucleocapsids into the nucleus. J Virol 65, 232-244.
Matlin, K.S., Reggio, H., Helenius, A., Simons, K., 1981. Infectious entry pathway of influenza virus in a canine kidney cell line. J Cell Biol 91, 601-613.
Matsuoka, Y., Swayne, D.E., Thomas, C., Rameix-Welti, M.A., Naffakh, N., Warnes, C., Altholtz, M., Donis, R., Subbarao, K., 2009. Neuraminidase stalk length and additional glycosylation of the hemagglutinin influence the virulence of influenza H5N1 viruses for mice. J Virol 83, 4704-4708.
Maurer-Stroh, S., Lee, R.T., Gunalan, V., Eisenhaber, F., 2013. The highly pathogenic H7N3 avian influenza strain from July 2012 in Mexico acquired an extended cleavage site through recombination with host 28S rRNA. Virol J 10, 139.

McAuley, J.L., Gilbertson, B.P., Trifkovic, S., Brown, L.E., McKimm-Breschkin, J.L., 2019. Influenza virus neuraminidase structure and functions. Front Microbiol 10, 39.
McAuley, J.L., Zhang, K., McCullers, J.A., 2010. The effects of influenza A virus PB1-F2 protein on polymerase activity are strain specific and do not impact pathogenesis. J Virol 84, 558-564.
McGeoch, D., Fellner, P., Newton, C., 1976. Influenza virus genome consists of eight distinct RNA species. Proc Natl Acad Sci U S A 73, 3045-3049.
Melen, K., Kinnunen, L., Fagerlund, R., Ikonen, N., Twu, K.Y., Krug, R.M., Julkunen, I., 2007. Nuclear and nucleolar targeting of influenza A virus NS1 protein: striking differences between different virus subtypes. J Virol 81, 5995-6006.
Meseko, C., Globig, A., Ijomanta, J., Joannis, T., Nwosuh, C., Shamaki, D., Harder, T., Hoffman, D., Pohlmann, A., Beer, M., Mettenleiter, T., Starick, E., 2018. Evidence of exposure of domestic pigs to highly pathogenic avian influenza H5N1 in Nigeria. Sci Rep 8, 5900.
Moeller, A., Kirchdoerfer, R.N., Potter, C.S., Carragher, B., Wilson, I.A., 2012. Organization of the influenza virus replication machinery. Science 338, 1631-1634.
Mok, B.W., Liu, H., Chen, P., Liu, S., Lau, S.Y., Huang, X., Liu, Y.C., Wang, P., Yuen, K.Y., Chen, H., 2017. The role of nuclear NS1 protein in highly pathogenic H5N1 influenza viruses. Microbes Infect 19, 587-596.
Mok, C.K., Yen, H.L., Yu, M.Y., Yuen, K.M., Sia, S.F., Chan, M.C., Qin, G., Tu, W.W., Peiris, J.S., 2011. Amino acid residues 253 and 591 of the PB2 protein of avian influenza virus A H9N2 contribute to mammalian pathogenesis. J Virol 85, 9641-9645.
Mondal, S., Xing, Z., Cardona, C., 2013. A comparison of virulence of influenza A virus isolates from mallards in experimentally inoculated turkeys. Avian Dis 57, 790-796.
Monne, I., Hussein, H.A., Fusaro, A., Valastro, V., Hamoud, M.M., Khalefa, R.A., Dardir, S.N., Radwan, M.I., Capua, I., Cattoli, G., 2013. H9N2 influenza A virus circulates in H5N1 endemically infected poultry population in Egypt. Influenza Other Respir Viruses 7, 240-243.
Monto, A.S., Fukuda, K., 2020. Lessons from influenza pandemics of the last 100 Years. Clin Infect Dis 70, 951-957.
Morales, A.C., Jr., Hilt, D.A., Williams, S.M., Pantin-Jackwood, M.J., Suarez, D.L., Spackman, E., Stallknecht, D.E., Jackwood, M.W., 2009. Biologic characterization of H4, H6, and H9 type low pathogenicity avian influenza viruses from wild birds in chickens and turkeys. Avian Dis 53, 552-562.
Mostafa, A., Abdelwhab, E.M., Mettenleiter, T.C., Pleschka, S., 2018. Zoonotic potential of influenza A viruses: a comprehensive overview. Viruses 10, 497.
Munoz, E.T., Deem, M.W., 2005. Epitope analysis for influenza vaccine design. Vaccine 23, 1144-1148.
Munster, V.J., Schrauwen, E.J., de Wit, E., van den Brand, J.M., Bestebroer, T.M., Herfst, S., Rimmelzwaan, G.F., Osterhaus, A.D., Fouchier, R.A., 2010. Insertion of a multibasic cleavage motif into the hemagglutinin of a low-pathogenic avian influenza H6N1 virus induces a highly pathogenic phenotype. J Virol 84, 7953-7960.
Muramoto, Y., Noda, T., Kawakami, E., Akkina, R., Kawaoka, Y., 2013. Identification of novel influenza A virus proteins translated from PA mRNA. J Virol 87, 2455-2462.
Muramoto, Y., Takada, A., Fujii, K., Noda, T., Iwatsuki-Horimoto, K., Watanabe, S., Horimoto, T., Kida, H., Kawaoka, Y., 2006. Hierarchy among viral RNA (vRNA) segments in their role in vRNA incorporation into influenza A virions. J Virol 80, 2318-2325.
Nan, Y., Wu, C., Zhang, Y.J., 2017. Interplay between Janus kinase/signal transducer and activator of transcription signaling activated by type I interferons and viral antagonism. Front Immunol 8, 1758.
Narayan, O., Lang, G., Rouse, B.T., 1969. A new influenza A virus infection in turkeys. IV. Experimental susceptibility of domestic birds to virus strain turkey-Ontario 7732-1966. Arch Gesamte Virusforsch 26, 149-165.
Neumann, G., Castrucci, M.R., Kawaoka, Y., 1997. Nuclear import and export of influenza virus nucleoprotein. J Virol 71, 9690-9700.
Neumann, G., Hughes, M.T., Kawaoka, Y., 2000. Influenza A virus NS2 protein mediates vRNP nuclear export through NES-independent interaction with hCRM1. EMBO J 19, 6751-6758.
Nishi, H., Shaytan, A., Panchenko, A.R., 2014. Physicochemical mechanisms of protein regulation by phosphorylation. Front Genet 5, 270.

Noah, D.L., Krug, R.M., 2005. Influenza virus virulence and its molecular determinants. Adv Virus Res 65, 121-145.
Nobusawa, E., Aoyama, T., Kato, H., Suzuki, Y., Tateno, Y., Nakajima, K., 1991. Comparison of complete amino acid sequences and receptor-binding properties among 13 serotypes of hemagglutinins of influenza A viruses. Virology 182, 475-485.
Noda, T., 2011. Native morphology of influenza virions. Front Microbiol 2, 269.
Nogales, A., Martinez-Sobrido, L., Chiem, K., Topham, D.J., DeDiego, M.L., 2018a. Functional evolution of the 2009 pandemic H1N1 influenza virus NS1 and PA in humans. J Virol 92, e01206-01218.
Nogales, A., Martinez-Sobrido, L., Topham, D.J., DeDiego, M.L., 2018b. Modulation of innate immune responses by the influenza a NS1 and PA-X proteins. Viruses 10, 708.
Obadan, A.O., Santos, J., Ferreri, L., Thompson, A.J., Carnaccini, S., Geiger, G., Gonzalez Reiche, A.S., Rajao, D.S., Paulson, J.C., Perez, D.R., 2019. Flexibility in vitro of amino acid 226 in the receptor-binding site of an H9 subtype influenza A virus and its effect in vivo on virus replication, tropism, and transmission. J Virol 93, e02011-02018.
Obenauer, J.C., Denson, J., Mehta, P.K., Su, X., Mukatira, S., Finkelstein, D.B., Xu, X., Wang, J., Ma, J., Fan, Y., Rakestraw, K.M., Webster, R.G., Hoffmann, E., Krauss, S., Zheng, J., Zhang, Z., Naeve, C.W., 2006. Large-scale sequence analysis of avian influenza isolates. Science 311, 1576-1580.
OIE, 2008. Chapter 3.3.4 - Avian Influenza (Infection with Avian Influenza Viruses). OIE Terrestrial Manual.
OIE, 2021. World Animal Health Information System. Available online at: https://wahis.oie.int/#/home (last accessed 06-04-2021).
Okamatsu, M., Motohashi, Y., Hiono, T., Tamura, T., Nagaya, K., Matsuno, K., Sakoda, Y., Kida, H., 2016. Is the optimal pH for membrane fusion in host cells by avian influenza viruses related to host range and pathogenicity? Arch Virol 161, 2235-2242.
Olsen, B., Munster, V.J., Wallensten, A., Waldenstrom, J., Osterhaus, A.D., Fouchier, R.A., 2006. Global patterns of influenza a virus in wild birds. Science 312, 384-388.
Opitz, B., Rejaibi, A., Dauber, B., Eckhard, J., Vinzing, M., Schmeck, B., Hippenstiel, S., Suttorp, N., Wolff, T., 2007. IFNbeta induction by influenza A virus is mediated by RIG-I which is regulated by the viral NS1 protein. Cell Microbiol 9, 930-938.
Oritani, K., Medina, K.L., Tomiyama, Y., Ishikawa, J., Okajima, Y., Ogawa, M., Yokota, T., Aoyama, K., Takahashi, I., Kincade, P.W., Matsuzawa, Y., 2000. Limitin: An interferon-like cytokine that preferentially influences B-lymphocyte precursors. Nat Med 6, 659-666.
Osterhaus, A.D., Rimmelzwaan, G.F., Martina, B.E., Bestebroer, T.M., Fouchier, R.A., 2000. Influenza B virus in seals. Science 288, 1051-1053.
Ozawa, M., Basnet, S., Burley, L.M., Neumann, G., Hatta, M., Kawaoka, Y., 2011. Impact of amino acid mutations in PB2, PB1-F2, and NS1 on the replication and pathogenicity of pandemic (H1N1) 2009 influenza viruses. J Virol 85, 4596-4601.
Ozawa, M., Fujii, K., Muramoto, Y., Yamada, S., Yamayoshi, S., Takada, A., Goto, H., Horimoto, T., Kawaoka, Y., 2007. Contributions of two nuclear localization signals of influenza A virus nucleoprotein to viral replication. J Virol 81, 30-41.
Pantin-Jackwood, M., Swayne, D.E., Smith, D., Shepherd, E., 2013. Effect of species, breed and route of virus inoculation on the pathogenicity of H5N1 highly pathogenic influenza (HPAI) viruses in domestic ducks. Vet Res 44, 62.
Pantin-Jackwood, M.J., Smith, D.M., Wasilenko, J.L., Cagle, C., Shepherd, E., Sarmento, L., Kapczynski, D.R., Afonso, C.L., 2012. Effect of age on the pathogenesis and innate immune responses in Pekin ducks infected with different H5N1 highly pathogenic avian influenza viruses. Virus Res 167, 196-206.
Pantin-Jackwood, M.J., Swayne, D.E., 2007. Pathobiology of Asian highly pathogenic avian influenza H5N1 virus infections in ducks. Avian Dis 51, 250-259.
Pantin-Jackwood, M.J., Swayne, D.E., 2009. Pathogenesis and pathobiology of avian influenza virus infection in birds. Rev Sci Tech 28, 113-136.
Parvin, R., Schinkoethe, J., Grund, C., Ulrich, R., Bonte, F., Behr, K.P., Voss, M., Samad, M.A., Hassan, K.E., Luttermann, C., Beer, M., Harder, T., 2020. Comparison of pathogenicity of

subtype H9 avian influenza wild-type viruses from a wide geographic origin expressing mono-, di-, or tri-basic hemagglutinin cleavage sites. Vet Res 51, 48.
Pasick, J., Handel, K., Robinson, J., Copps, J., Ridd, D., Hills, K., Kehler, H., Cottam-Birt, C., Neufeld, J., Berhane, Y., Czub, S., 2005. Intersegmental recombination between the haemagglutinin and matrix genes was responsible for the emergence of a highly pathogenic H7N3 avian influenza virus in British Columbia. J Gen Virol 86, 727-731.
Peacock, T.H.P., James, J., Sealy, J.E., Iqbal, M., 2019. A global perspective on H9N2 avian influenza virus. Viruses 11, 620.
Peacock, T.P., Benton, D.J., James, J., Sadeyen, J.-R., Chang, P., Sealy, J.E., Bryant, J.E., Martin, S.R., Shelton, H., Barclay, W.S., Iqbal, M., 2017. Immune escape variants of H9N2 influenza viruses containing deletions at the hemagglutinin receptor binding site retain fitness in vivo and display enhanced zoonotic characteristics. J Virol 91, e00218-00217.
Peacock, T.P., Sealy, J.E., Harvey, W.T., Benton, D.J., Reeve, R., Iqbal, M., 2020. Genetic determinants of receptor-binding preference and zoonotic potential of H9N2 avian influenza viruses. J Virol 95, e01651-01620.
Peck, K.M., Lauring, A.S., 2018. Complexities of viral mutation rates. J Virol 92, e01031-01017.
Perkins, L.E., Swayne, D.E., 2001. Pathobiology of A/chicken/Hong Kong/220/97 (H5N1) avian influenza virus in seven gallinaceous species. Vet Pathol 38, 149-164.
Pillai, S.P., Lee, C.W., 2010. Species and age related differences in the type and distribution of influenza virus receptors in different tissues of chickens, ducks and turkeys. Virol J 7, 5.
Poen, M.J., Bestebroer, T.M., Vuong, O., Scheuer, R.D., van der Jeugd, H.P., Kleyheeg, E., Eggink, D., Lexmond, P., van den Brand, J.M.A., Begeman, L., van der Vliet, S., Muskens, G., Majoor, F.A., Koopmans, M.P.G., Kuiken, T., Fouchier, R.A.M., 2018. Local amplification of highly pathogenic avian influenza H5N8 viruses in wild birds in the Netherlands, 2016 to 2017. Euro Surveill 23, 17-00449.
Pohlmann, A., Hoffmann, D., Grund, C., Koethe, S., Hussy, D., Meier, S.M., King, J., Schinkothe, J., Ulrich, R., Harder, T., Beer, M., 2019. Genetic characterization and zoonotic potential of highly pathogenic avian influenza virus A(H5N6/H5N5), Germany, 2017-2018. Emerg Infect Dis 25, 1973-1976.
Pohlmann, A., Starick, E., Grund, C., Hoper, D., Strebelow, G., Globig, A., Staubach, C., Conraths, F.J., Mettenleiter, T.C., Harder, T., Beer, M., 2018. Swarm incursions of reassortants of highly pathogenic avian influenza virus strains H5N8 and H5N5, clade 2.3.4.4b, Germany, winter 2016/17. Sci Rep 8, 15.
Pohlmann, A., Starick, E., Harder, T., Grund, C., Hoper, D., Globig, A., Staubach, C., Dietze, K., Strebelow, G., Ulrich, R.G., Schinkothe, J., Teifke, J.P., Conraths, F.J., Mettenleiter, T.C., Beer, M., 2017. Outbreaks among wild birds and domestic poultry caused by reassorted influenza A(H5N8) clade 2.3.4.4 viruses, Germany, 2016. Emerg Infect Dis 23, 633-636.
Poon, L.L., Pritlove, D.C., Fodor, E., Brownlee, G.G., 1999. Direct evidence that the poly(A) tail of influenza A virus mRNA is synthesized by reiterative copying of a U track in the virion RNA template. J Virol 73, 3473-3476.
Portela, A., Digard, P., 2002. The influenza virus nucleoprotein: a multifunctional RNA-binding protein pivotal to virus replication. J Gen Virol 83, 723-734.
Pu, J., Wang, J., Zhang, Y., Fu, G., Bi, Y., Sun, Y., Liu, J., 2010. Synergism of co-mutation of two amino acid residues in NS1 protein increases the pathogenicity of influenza virus in mice. Virus Res 151, 200-204.
Pu, J., Yin, Y., Liu, J., Wang, X., Zhou, Y., Wang, Z., Sun, Y., Sun, H., Li, F., Song, J., Qu, R., Gao, W., Wang, D., Wang, Z., Yan, S., Chen, M., Zeng, J., Jiang, Z., Sun, H., Zong, Y., Wang, C., Tong, Q., Bi, Y., Huang, Y., Du, X., Chang, K.C., Liu, J., 2021. Reassortment with dominant chicken H9N2 influenza virus contributed to the fifth H7N9 virus human epidemic. J Virol, JVI.01578-01520.
Pu, Z., Xiang, D., Li, X., Luo, T., Shen, X., Murphy, R.W., Liao, M., Shen, Y., 2018. Potential pandemic of H7N9 avian influenza A virus in human. Front Cell Infect Microbiol 8, 414.
Pusch, E.A., Suarez, D.L., 2018. The multifaceted zoonotic risk of H9N2 avian influenza. Vet Sci 5, 82.
Reid, A.H., Taubenberger, J.K., 2003. The origin of the 1918 pandemic influenza virus: a continuing enigma. J Gen Virol 84, 2285-2292.

Reid, S.M., Banks, J., Ceeraz, V., Seekings, A., Howard, W.A., Puranik, A., Collins, S., Manvell, R., Irvine, R.M., Brown, I.H., 2016. The detection of a low pathogenicity avian influenza virus subtype H9 infection in a turkey breeder flock in the United Kingdom. Avian Dis 60, 126-131.
Reperant, L.A., Kuiken, T., Osterhaus, A.D., 2012. Adaptive pathways of zoonotic influenza viruses: from exposure to establishment in humans. Vaccine 30, 4419-4434.
Robb, N.C., Chase, G., Bier, K., Vreede, F.T., Shaw, P.C., Naffakh, N., Schwemmle, M., Fodor, E., 2011. The influenza A virus NS1 protein interacts with the nucleoprotein of viral ribonucleoprotein complexes. J Virol 85, 5228-5231.
Robertson, J.S., 1979. 5' and 3' terminal nucleotide sequences of the RNA genome segments of influenza virus. Nucleic Acids Res 6, 3745-3757.
Robertson, J.S., Schubert, M., Lazzarini, R.A., 1981. Polyadenylation sites for influenza virus mRNA. J Virol 38, 157-163.
Rosario-Ferreira, N., Preto, A.J., Melo, R., Moreira, I.S., Brito, R.M.M., 2020. The central role of non-structural protein 1 (NS1) in influenza biology and infection. Int J Mol Sci 21, 1511.
Ruigrok, R.W., Barge, A., Durrer, P., Brunner, J., Ma, K., Whittaker, G.R., 2000. Membrane interaction of influenza virus M1 protein. Virology 267, 289-298.
Russell, R.J., Haire, L.F., Stevens, D.J., Collins, P.J., Lin, Y.P., Blackburn, G.M., Hay, A.J., Gamblin, S.J., Skehel, J.J., 2006a. The structure of H5N1 avian influenza neuraminidase suggests new opportunities for drug design. Nature 443, 45-49.
Russell, R.J., Stevens, D.J., Haire, L.F., Gamblin, S.J., Skehel, J.J., 2006b. Avian and human receptor binding by hemagglutinins of influenza A viruses. Glycoconj J 23, 85-92.
Saito, L.B., Diaz-Satizabal, L., Evseev, D., Fleming-Canepa, X., Mao, S., Webster, R.G., Magor, K.E., 2018. IFN and cytokine responses in ducks to genetically similar H5N1 influenza A viruses of varying pathogenicity. J Gen Virol 99, 464-474.
Santhakumar, D., Rubbenstroth, D., Martinez-Sobrido, L., Munir, M., 2017. Avian interferons and their antiviral effectors. Front Immunol 8, 49.
Santos, A., Pal, S., Chacon, J., Meraz, K., Gonzalez, J., Prieto, K., Rosas-Acosta, G., 2013. SUMOylation affects the interferon blocking activity of the influenza A nonstructural protein NS1 without affecting its stability or cellular localization. J Virol 87, 5602-5620.
Scheibner, D., Blaurock, C., Mettenleiter, T.C., Abdelwhab, E.M., 2019a. Virulence of three European highly pathogenic H7N1 and H7N7 avian influenza viruses in Pekin and Muscovy ducks. BMC Vet Res 15, 142.
Scheibner, D., Ulrich, R., Fatola, O.I., Graaf, A., Gischke, M., Salaheldin, A.H., Harder, T.C., Veits, J., Mettenleiter, T.C., Abdelwhab, E.M., 2019b. Variable impact of the hemagglutinin polybasic cleavage site on virulence and pathogenesis of avian influenza H7N7 virus in chickens, turkeys and ducks. Sci Rep 9, 11556.
Schmitt, A.P., Lamb, R.A., 2005. Influenza virus assembly and budding at the viral budozone. Adv Virus Res 64, 383-416.
Schrauwen, E.J.A., Bestebroer, T.M., Munster, V.J., de Wit, E., Herfst, S., Rimmelzwaan, G.F., Osterhaus, A., Fouchier, R.A.M., 2011. Insertion of a multibasic cleavage site in the haemagglutinin of human influenza H3N2 virus does not increase pathogenicity in ferrets. J Gen Virol 92, 1410-1415.
Schroder, K., Hertzog, P.J., Ravasi, T., Hume, D.A., 2004. Interferon-gamma: an overview of signals, mechanisms and functions. J Leukoc Biol 75, 163-189.
Schulman, J.L., Kilbourne, E.D., 1969. Independent variation in nature of hemagglutinin and neuraminidase antigens of influenza virus: distinctiveness of hemagglutinin antigen of Hong Kong-68 virus. Proc Natl Acad Sci U S A 63, 326-333.
Selman, M., Dankar, S.K., Forbes, N.E., Jia, J.J., Brown, E.G., 2012. Adaptive mutation in influenza A virus non-structural gene is linked to host switching and induces a novel protein by alternative splicing. Emerg Microbes Infect 1, e42.
Shao, W., Li, X., Goraya, M.U., Wang, S., Chen, J.L., 2017. Evolution of influenza A virus by mutation and re-assortment. Int J Mol Sci 18, 1650.
Shaw, M.L., Stone, K.L., Colangelo, C.M., Gulcicek, E.E., Palese, P., 2008. Cellular proteins in influenza virus particles. PLoS Pathog 4, e1000085.

Shelton, H., Ayora-Talavera, G., Ren, J., Loureiro, S., Pickles, R.J., Barclay, W.S., Jones, I.M., 2011. Receptor binding profiles of avian influenza virus hemagglutinin subtypes on human cells as a predictor of pandemic potential. J Virol 85, 1875-1880.
Shen, Y.Y., Ke, C.W., Li, Q., Yuan, R.Y., Xiang, D., Jia, W.X., Yu, Y.D., Liu, L., Huang, C., Qi, W.B., Sikkema, R., Wu, J., Koopmans, M., Liao, M., 2016. Novel reassortant avian influenza A(H5N6) viruses in humans, Guangdong, China, 2015. Emerg Infect Dis 22, 1507-1509.
Shi, L., Summers, D.F., Peng, Q., Galarz, J.M., 1995. Influenza A virus RNA polymerase subunit PB2 is the endonuclease which cleaves host cell mRNA and functions only as the trimeric enzyme. Virology 208, 38-47.
Skehel, J.J., Wiley, D.C., 2000. Receptor binding and membrane fusion in virus entry: the influenza hemagglutinin. Annu Rev Biochem 69, 531-569.
Smith, G.J., Donis, R.O., World Health Organization/World Organisation for Animal, H.F., Agriculture Organization, H.E.W.G., 2015. Nomenclature updates resulting from the evolution of avian influenza A(H5) virus clades 2.1.3.2a, 2.2.1, and 2.3.4 during 2013-2014. Influenza Other Respir Viruses 9, 271-276.
Soda, K., Asakura, S., Okamatsu, M., Sakoda, Y., Kida, H., 2011. H9N2 influenza virus acquires intravenous pathogenicity on the introduction of a pair of di-basic amino acid residues at the cleavage site of the hemagglutinin and consecutive passages in chickens. Virol J 8, 64.
Song, W., Wang, P., Mok, B.W., Lau, S.Y., Huang, X., Wu, W.L., Zheng, M., Wen, X., Yang, S., Chen, Y., Li, L., Yuen, K.Y., Chen, H., 2014. The K526R substitution in viral protein PB2 enhances the effects of E627K on influenza virus replication. Nat Commun 5, 5509.
Song, Y., Zhang, Y., Chen, L., Zhang, B., Zhang, M., Wang, J., Jiang, Y., Yang, C., Jiang, T., 2019. Genetic characteristics and pathogenicity analysis in chickens and mice of three H9N2 avian influenza viruses. Viruses 11, 1127.
Sorrell, E.M., Song, H., Pena, L., Perez, D.R., 2010. A 27-amino-acid deletion in the neuraminidase stalk supports replication of an avian H2N2 influenza A virus in the respiratory tract of chickens. J Virol 84, 11831-11840.
Soubies, S.M., Hoffmann, T.W., Croville, G., Larcher, T., Ledevin, M., Soubieux, D., Quere, P., Guerin, J.L., Marc, D., Volmer, R., 2013. Deletion of the C-terminal ESEV domain of NS1 does not affect the replication of a low-pathogenic avian influenza virus H7N1 in ducks and chickens. J Gen Virol 94, 50-58.
Spackman, E., 2009. The ecology of avian influenza virus in wild birds: what does this mean for poultry? Poult Sci 88, 847-850.
Spackman, E., Gelb, J., Jr., Preskenis, L.A., Ladman, B.S., Pope, C.R., Pantin-Jackwood, M.J., McKinley, E.T., 2010. The pathogenesis of low pathogenicity H7 avian influenza viruses in chickens, ducks and turkeys. Virol J 7, 331.
Spickler, A.R., Trampel, D.W., Roth, J.A., 2008. The onset of virus shedding and clinical signs in chickens infected with high-pathogenicity and low-pathogenicity avian influenza viruses. Avian Pathol 37, 555-577.
Stanifer, M.L., Pervolaraki, K., Boulant, S., 2019. Differential regulation of type I and type III interferon signaling. Int J Mol Sci 20, 1445.
Stech, O., Veits, J., Abdelwhab, E.M., Wessels, U., Mettenleiter, T.C., Stech, J., 2015. The neuraminidase stalk deletion serves as major virulence determinant of H5N1 highly pathogenic avian influenza viruses in chicken. Sci Rep 5, 13493.
Stech, O., Veits, J., Weber, S., Deckers, D., Schroer, D., Vahlenkamp, T.W., Breithaupt, A., Teifke, J., Mettenleiter, T.C., Stech, J., 2009. Acquisition of a polybasic hemagglutinin cleavage site by a low-pathogenic avian influenza virus is not sufficient for immediate transformation into a highly pathogenic strain. J Virol 83, 5864-5868.
Steel, J., Lowen, A.C., Mubareka, S., Palese, P., 2009. Transmission of influenza virus in a mammalian host is increased by PB2 amino acids 627K or 627E/701N. PLoS Pathog 5, e1000252.
Steinhauer, D.A., 1999. Role of hemagglutinin cleavage for the pathogenicity of influenza virus. Virology 258, 1-20.
Stieneke-Grober, A., Vey, M., Angliker, H., Shaw, E., Thomas, G., Roberts, C., Klenk, H.D., Garten, W., 1992. Influenza virus hemagglutinin with multibasic cleavage site is activated by furin, a subtilisin-like endoprotease. EMBO J 11, 2407-2414.

Su, W., Wang, C., Luo, J., Zhao, Y., Wu, Y., Chen, L., Zhao, N., Li, M., Xing, C., Liu, H., Zhang, H., Chang, Y.F., Li, T., Ding, H., Wan, X., He, H., 2015. Testing the effect of internal genes derived from a wild-bird-origin H9N2 influenza A virus on the pathogenicity of an A/H7N9 virus. Cell Rep 13, 1283.

Su, W.C., Yu, W.Y., Huang, S.H., Lai, M.M.C., 2018. Ubiquitination of the cytoplasmic domain of influenza A virus M2 protein is crucial for production of infectious virus particles. J Virol 92, e01972-01917.

Suarez, D.L., Perdue, M.L., 1998. Multiple alignment comparison of the non-structural genes of influenza A viruses. Virus Res 54, 59-69.

Suarez, D.L., Senne, D.A., Banks, J., Brown, I.H., Essen, S.C., Lee, C.W., Manvell, R.J., Mathieu-Benson, C., Moreno, V., Pedersen, J.C., Panigrahy, B., Rojas, H., Spackman, E., Alexander, D.J., 2004. Recombination resulting in virulence shift in avian influenza outbreak, Chile. Emerg Infect Dis 10, 693-699.

Subbarao, E.K., London, W., Murphy, B.R., 1993. A single amino acid in the PB2 gene of influenza A virus is a determinant of host range. J Virol 67, 1761-1764.

Sugrue, R.J., Hay, A.J., 1991. Structural characteristics of the M2 protein of influenza-a viruses - evidence that it forms a tetrameric channel. Virology 180, 617-624.

Sun, H., Wang, K., Yao, W., Liu, Q., Yang, J., Teng, Q., Li, X., Li, Z., Chen, H., 2019. H9N2 viruses isolated from mammals replicated in mice at higher levels than avian-origin viruses. Front Microbiol 10, 416.

Sun, X., Tse, L.V., Ferguson, A.D., Whittaker, G.R., 2010. Modifications to the hemagglutinin cleavage site control the virulence of a neurotropic H1N1 influenza virus. J Virol 84, 8683-8690.

Sun, Y., Hu, Z., Zhang, X., Chen, M., Wang, Z., Xu, G., Bi, Y., Tong, Q., Wang, M., Sun, H., Pu, J., Iqbal, M., Liu, J., 2020. An R195K mutation in the PA-X protein increases the virulence and transmission of influenza A virus in mammalian hosts. J Virol 94, e01817-01819.

Sun, Y., Tan, Y., Wei, K., Sun, H., Shi, Y., Pu, J., Yang, H., Gao, G.F., Yin, Y., Feng, W., Perez, D.R., Liu, J., 2013. Amino acid 316 of hemagglutinin and the neuraminidase stalk length influence virulence of H9N2 influenza virus in chickens and mice. J Virol 87, 2963-2968.

Sun, Y., Xu, Q., Shen, Y., Liu, L., Wei, K., Sun, H., Pu, J., Chang, K.C., Liu, J., 2014. Naturally occurring mutations in the PA gene are key contributors to increased virulence of pandemic H1N1/09 influenza virus in mice. J Virol 88, 4600-4604.

Swayne, D.E., Hill, R.E., Clifford, J., 2017. Safe application of regionalization for trade in poultry and poultry products during highly pathogenic avian influenza outbreaks in the USA. Avian Pathol 46, 125-130.

Swayne, D.E., Slemons, R.D., 2008. Using mean infectious dose of high- and low-pathogenicity avian influenza viruses originating from wild duck and poultry as one measure of infectivity and adaptation to poultry. Avian Dis 52, 455-460.

Swayne, D.E., Suarez, D.L., 2000. Highly pathogenic avian influenza. Rev Sci Tech 19, 463-482.

Swieton, E., Jozwiak, M., Minta, Z., Smietanka, K., 2018. Genetic characterization of H9N2 avian influenza viruses isolated from poultry in Poland during 2013/2014. Virus genes 54, 67-76.

Swieton, E., Tarasiuk, K., Olszewska-Tomczyk, M., Iwan, E., Smietanka, K., 2020. A turkey-origin H9N2 avian influenza virus shows low pathogenicity but different within-host diversity in experimentally infected turkeys, quail and ducks. Viruses 12, 319.

Sylte, M.J., Hubby, B., Suarez, D.L., 2007. Influenza neuraminidase antibodies provide partial protection for chickens against high pathogenic avian influenza infection. Vaccine 25, 3763-3772.

Tada, T., Suzuki, K., Sakurai, Y., Kubo, M., Okada, H., Itoh, T., Tsukamoto, K., 2011. NP body domain and PB2 contribute to increased virulence of H5N1 highly pathogenic avian influenza viruses in chickens. J Virol 85, 1834-1846.

Takizawa, N., Ogura, Y., Fujita, Y., Noda, T., Shigematsu, H., Hayashi, T., Kurokawa, K., 2019. Local structural changes of the influenza A virus ribonucleoprotein complex by single mutations in the specific residues involved in efficient genome packaging. Virol J 531, 126-140.

Tate, M.D., Job, E.R., Deng, Y.M., Gunalan, V., Maurer-Stroh, S., Reading, P.C., 2014. Playing hide and seek: how glycosylation of the influenza virus hemagglutinin can modulate the immune response to infection. Viruses 6, 1294-1316.
Taubenberger, J.K., Morens, D.M., 2006. 1918 Influenza: the mother of all pandemics. Emerg Infect Dis 12, 15-22.
Taubenberger, J.K., Reid, A.H., Lourens, R.M., Wang, R., Jin, G., Fanning, T.G., 2005. Characterization of the 1918 influenza virus polymerase genes. Nature 437, 889-893.
Temperley, N.D., Berlin, S., Paton, I.R., Griffin, D.K., Burt, D.W., 2008. Evolution of the chicken Toll-like receptor gene family: a story of gene gain and gene loss. BMC Genomics 9, 62.
Tong, S., Li, Y., Rivailler, P., Conrardy, C., Castillo, D.A., Chen, L.M., Recuenco, S., Ellison, J.A., Davis, C.T., York, I.A., Turmelle, A.S., Moran, D., Rogers, S., Shi, M., Tao, Y., Weil, M.R., Tang, K., Rowe, L.A., Sammons, S., Xu, X., Frace, M., Lindblade, K.A., Cox, N.J., Anderson, L.J., Rupprecht, C.E., Donis, R.O., 2012. A distinct lineage of influenza A virus from bats. Proc Natl Acad Sci U S A 109, 4269-4274.
Tong, S., Zhu, X., Li, Y., Shi, M., Zhang, J., Bourgeois, M., Yang, H., Chen, X., Recuenco, S., Gomez, J., Chen, L.M., Johnson, A., Tao, Y., Dreyfus, C., Yu, W., McBride, R., Carney, P.J., Gilbert, A.T., Chang, J., Guo, Z., Davis, C.T., Paulson, J.C., Stevens, J., Rupprecht, C.E., Holmes, E.C., Wilson, I.A., Donis, R.O., 2013. New world bats harbor diverse influenza A viruses. PLoS Pathog 9, e1003657.
Tumpey, T.M., Kapczynski, D.R., Swayne, D.E., 2004. Comparative susceptibility of chickens and turkeys to avian influenza A H7N2 virus infection and protective efficacy of a commercial avian influenza H7N2 virus vaccine. Avian Dis 48, 167-176.
Turrell, L., Lyall, J.W., Tiley, L.S., Fodor, E., Vreede, F.T., 2013. The role and assembly mechanism of nucleoprotein in influenza A virus ribonucleoprotein complexes. Nat Commun 4, 1591.
Umar, S., Delverdier, M., Delpont, M., Belkasmi, S.F.Z., Teillaud, A., Bleuart, C., Pardo, I., El Houadfi, M., Guerin, J.L., Ducatez, M.F., 2018. Co-infection of turkeys with Escherichia coli (O78) and H6N1 avian influenza virus. Avian Pathol 47, 314-324.
van der Kolk, J.H., 2019. Role for migratory domestic poultry and/or wild birds in the global spread of avian influenza? Vet Q 39, 161-167.
Varga, Z.T., Ramos, I., Hai, R., Schmolke, M., Garcia-Sastre, A., Fernandez-Sesma, A., Palese, P., 2011. The influenza virus protein PB1-F2 inhibits the induction of type I interferon at the level of the MAVS adaptor protein. PLoS Pathog 7, e1002067.
Vasin, A.V., Temkina, O.A., Egorov, V.V., Klotchenko, S.A., Plotnikova, M.A., Kiselev, O.I., 2014. Molecular mechanisms enhancing the proteome of influenza A viruses: an overview of recently discovered proteins. Virus Res 185, 53-63.
Veit, M., 2012. Palmitoylation of virus proteins. Biol Cell 104, 493-515.
Veit, M., Schmidt, M.F., 1993. Timing of palmitoylation of influenza virus hemagglutinin. FEBS Lett 336, 243-247.
Veits, J., Weber, S., Stech, O., Breithaupt, A., Graber, M., Gohrbandt, S., Bogs, J., Hundt, J., Teifke, J.P., Mettenleiter, T.C., Stech, J., 2012. Avian influenza virus hemagglutinins H2, H4, H8, and H14 support a highly pathogenic phenotype. Proc Natl Acad Sci U S A 109, 2579-2584.
Venkatesh, D., Brouwer, A., Goujgoulova, G., Ellis, R., Seekings, J., Brown, I.H., Lewis, N.S., 2020. Regional transmission and reassortment of 2.3.4.4b highly pathogenic avian influenza (HPAI) viruses in Bulgarian poultry 2017/18. Viruses 12, 605.
Verhagen, J.H., Fouchier, R.A.M., Lewis, N., 2021. Highly pathogenic avian influenza viruses at the wild-domestic bird interface in Europe: Future directions for research and surveillance. Viruses 13.
Verhagen, J.H., Lexmond, P., Vuong, O., Schutten, M., Guldemeester, J., Osterhaus, A.D., Elbers, A.R., Slaterus, R., Hornman, M., Koch, G., Fouchier, R.A., 2017. Discordant detection of avian influenza virus subtypes in time and space between poultry and wild birds; Towards improvement of surveillance programs. PLoS One 12, e0173470.
Vines, A., Wells, K., Matrosovich, M., Castrucci, M.R., Ito, T., Kawaoka, Y., 1998. The role of influenza A virus hemagglutinin residues 226 and 228 in receptor specificity and host range restriction. J Virol 72, 7626-7631.
Volmer, R., Mazel-Sanchez, B., Volmer, C., Soubies, S.M., Guerin, J.L., 2010. Nucleolar localization of influenza A NS1: striking differences between mammalian and avian cells. Virol J 7, 63.

Wacquiez, A., Coste, F., Kut, E., Gaudon, V., Trapp, S., Castaing, B., Marc, D., 2020. Structure and sequence determinants governing the interactions of RNAs with influenza A virus non-structural protein NS1. Viruses 12, 947.
Wagner, R., Matrosovich, M., Klenk, H.D., 2002. Functional balance between haemagglutinin and neuraminidase in influenza virus infections. Rev Med Virol 12, 159-166.
Watanabe, Y., Ibrahim, M.S., Ellakany, H.F., Kawashita, N., Mizuike, R., Hiramatsu, H., Sriwilaijaroen, N., Takagi, T., Suzuki, Y., Ikuta, K., 2011. Acquisition of human-type receptor binding specificity by new H5N1 influenza virus sublineages during their emergence in birds in Egypt. PLoS Pathog 7, e1002068.
Weber-Gerlach, M., Weber, F., 2016a. Standing on three legs: antiviral activities of RIG-I against influenza viruses. Curr Opin Immunol 42, 71-75.
Weber-Gerlach, M., Weber, F., 2016b. To conquer the host, influenza virus is packing it in: Interferon-antagonistic strategies beyond ns1. J Virol 90, 8389-8394.
Weber, M., Sediri, H., Felgenhauer, U., Binzen, I., Banfer, S., Jacob, R., Brunotte, L., Garcia-Sastre, A., Schmid-Burgk, J.L., Schmidt, T., Hornung, V., Kochs, G., Schwemmle, M., Klenk, H.D., Weber, F., 2015. Influenza virus adaptation PB2-627K modulates nucleocapsid inhibition by the pathogen sensor RIG-I. Cell Host Microbe 17, 309-319.
Webster, R.G., Bean, W.J., Gorman, O.T., Chambers, T.M., Kawaoka, Y., 1992. Evolution and ecology of influenza A viruses. Microbiol Rev 56, 152-179.
Webster, R.G., Laver, W.G., Kilbourne, E.D., 1968. Reactions of antibodies with surface antigens of influenza virus. J Gen Virol 3, 315-326.
Webster, R.G., Yakhno, M., Hinshaw, V.S., Bean, W.J., Murti, K.G., 1978. Intestinal influenza: replication and characterization of influenza viruses in ducks. Virology 84, 268-278.
Wei, L., Cui, J., Song, Y., Zhang, S., Han, F., Yuan, R., Gong, L., Jiao, P., Liao, M., 2014. Duck MDA5 functions in innate immunity against H5N1 highly pathogenic avian influenza virus infections. Vet Res 45, 66.
Wen, S., Wu, Z., Zhong, S., Li, M., Shu, Y., 2021. Factors influencing the immunogenicity of influenza vaccines. Hum Vaccin Immunother, 1-13.
WHO, 1980. A revision of the system of nomenclature for influenza viruses: a WHO memorandum. Bull World Health Organ 58, 585-591.
WHO, 2021a. Human infection with avian influenza A (H5N8) – the Russian Federation. Available online at: https://www.who.int/csr/don/26-feb-2021-influenza-a-russian-federation/en/ (last accessed 18-03-2021).
WHO, 2021b. Human infection with avian influenza A (H5N8) – the Russian Federation. Available online at: https://www.who.int/csr/don/26-feb-2021-influenza-a-russian-federation/en/; last accessed: 27.02.2021, 21:32 Uhr).
WHO, 2021c. Human infection with avian influenza A(H5) viruses. Available online at: https://www.who.int/docs/default-source/wpro---documents/emergency/surveillance/avian-influenza/ai-20210219.pdf?sfvrsn=c0382d50_91 (last accessed: 19-03-2021).
Wise, H.M., Foeglein, A., Sun, J., Dalton, R.M., Patel, S., Howard, W., Anderson, E.C., Barclay, W.S., Digard, P., 2009. A complicated message: Identification of a novel PB1-related protein translated from influenza A virus segment 2 mRNA. J Virol 83, 8021-8031.
Wise, H.M., Hutchinson, E.C., Jagger, B.W., Stuart, A.D., Kang, Z.H., Robb, N., Schwartzman, L.M., Kash, J.C., Fodor, E., Firth, A.E., Gog, J.R., Taubenberger, J.K., Digard, P., 2012. Identification of a novel splice variant form of the influenza A virus M2 ion channel with an antigenically distinct ectodomain. PLoS Pathog 8, e1002998.
World Health Organization/World Organisation for Animal, H.F., Agriculture Organization, H.N.E.W.G., 2014. Revised and updated nomenclature for highly pathogenic avian influenza A (H5N1) viruses. Influenza Other Respir Viruses 8, 384-388.
Wrigley, N.G., Skehel, J.J., Charlwood, P.A., Brand, C.M., 1973. The size and shape of influenza virus neuraminidase. Virology 51, 525-529.
Wu, C.Y., Lin, C.W., Tsai, T.I., Lee, C.D., Chuang, H.Y., Chen, J.B., Tsai, M.H., Chen, B.R., Lo, P.W., Liu, C.P., Shivatare, V.S., Wong, C.H., 2017. Influenza A surface glycosylation and vaccine design. Proc Natl Acad Sci U S A 114, 280-285.

Wu, W.W., Sun, Y.H., Pante, N., 2007. Nuclear import of influenza A viral ribonucleoprotein complexes is mediated by two nuclear localization sequences on viral nucleoprotein. Virol J 4, 49.

Xu, L., Yu, D., Fan, Y., Peng, L., Wu, Y., Yao, Y.G., 2016. Loss of RIG-I leads to a functional replacement with MDA5 in the Chinese tree shrew. Proc Natl Acad Sci U S A 113, 10950-10955.

Yamada, S., Hatta, M., Staker, B.L., Watanabe, S., Imai, M., Shinya, K., Sakai-Tagawa, Y., Ito, M., Ozawa, M., Watanabe, T., Sakabe, S., Li, C., Kim, J.H., Myler, P.J., Phan, I., Raymond, A., Smith, E., Stacy, R., Nidom, C.A., Lank, S.M., Wiseman, R.W., Bimber, B.N., O'Connor, D.H., Neumann, G., Stewart, L.J., Kawaoka, Y., 2010. Biological and structural characterization of a host-adapting amino acid in influenza virus. PLoS Pathog 6, e1001034.

Yamaji, R., Saad, M.D., Davis, C.T., Swayne, D.E., Wang, D., Wong, F.Y.K., McCauley, J.W., Peiris, J.S.M., Webby, R.J., Fouchier, R.A.M., Kawaoka, Y., Zhang, W., 2020. Pandemic potential of highly pathogenic avian influenza clade 2.3.4.4 A(H5) viruses. Rev Med Virol 30, e2099.

Yamayoshi, S., Watanabe, M., Goto, H., Kawaoka, Y., 2016. Identification of a novel viral protein expressed from the PB2 segment of influenza A virus. J Virol 90, 444-456.

Yoshimura, A., Kuroda, K., Kawasaki, K., Yamashina, S., Maeda, T., Ohnishi, S., 1982. Infectious cell entry mechanism of influenza virus. J Virol 43, 284-293.

Yu, M., Liu, X., Cao, S., Zhao, Z., Zhang, K., Xie, Q., Chen, C., Gao, S., Bi, Y., Sun, L., Ye, X., Gao, G.F., Liu, W., 2012. Identification and characterization of three novel nuclear export signals in the influenza A virus nucleoprotein. J Virol 86, 4970-4980.

Zamarin, D., Ortigoza, M.B., Palese, P., 2006. Influenza A virus PB1-F2 protein contributes to viral pathogenesis in mice. J Virol 80, 7976-7983.

Zhang, X., Li, Y., Jin, S., Wang, T., Sun, W., Zhang, Y., Li, F., Zhao, M., Sun, L., Hu, X., Feng, N., Xie, Y., Zhao, Y., Yang, S., Xia, X., Gao, Y., 2021. H9N2 influenza virus spillover into wild birds from poultry in China bind to human-type receptors and transmit in mammals via respiratory droplets. Transbound Emerg Dis n/a, 1-16.

Zhirnov, O.P., Konakova, T.E., Wolff, T., Klenk, H.D., 2002. NS1 protein of influenza A virus down-regulates apoptosis. J Virol 76, 1617-1625.

Zhong, L., Zhao, Q., Zhao, K., Wang, X., Zhao, G., Li, Q., Gu, M., Peng, D., Liu, X., 2014. The antigenic drift molecular basis of the H5N1 influenza viruses in a novel branch of clade 2.3.4. Vet Microbiol 171, 23-30.

Zielecki, F., Semmler, I., Kalthoff, D., Voss, D., Mauel, S., Gruber, A.D., Beer, M., Wolff, T., 2010. Virulence determinants of avian H5N1 influenza A virus in mammalian and avian hosts: role of the C-terminal ESEV motif in the viral NS1 protein. J Virol 84, 10708-10718.

8 Appendix

8.1 Eigenständigkeitserklärung

Hiermit erkläre ich, dass diese Arbeit bisher von mir weder an der Mathematisch-Naturwissenschaftlichen Fakultät der Universität Greifswald noch einer anderen wissenschaftlichen Einrichtung zum Zwecke der Promotion eingereicht wurde.

Ferner erkläre ich, dass ich diese Arbeit selbstständig verfasst und keine anderen als die darin angegebenen Hilfsmittel und Hilfen benutzt und keine Textabschnitte eines Dritten ohne Kennzeichnung übernommen habe.

……

Claudia Blaurock

8.2 Curriculum vitae

8.3 Publications

Scheibner, D., **Blaurock, C.**, Mettenleiter, T.C., Abdelwhab, E.M., 2019. Virulence of three European highly pathogenic H7N1 and H7N7 avian influenza viruses in Pekin and Muscovy ducks. BMC Vet Res 15, 142.

Blaurock, C., Scheibner, D., Landmann, M., Vallbracht, M., Ulrich, R., Bottcher-Friebertshauser, E., Mettenleiter, T.C., Abdelwhab, E.M., 2020. Non-basic amino acids in the hemagglutinin proteolytic cleavage site of a European H9N2 avian influenza virus modulate virulence in turkeys. Sci Rep 10, 21226.

Mostafa, A., **Blaurock, C.**, Scheibner, D., Muller, C., Blohm, U., Schafer, A., Gischke, M., Salaheldin, A.H., Nooh, H.Z., Ali, M.A., Breithaupt, A., Mettenleiter, T.C., Pleschka, S., Abdelwhab, E.M., 2020. Genetic incompatibilities and reduced transmission in chickens may limit the evolution of reassortants between H9N2 and panzootic H5N8 clade 2.3.4.4 avian influenza virus showing high virulence for mammals. Virus Evol 6 (2), veaa077.

Gischke M., Bagato O., Breithaupt A., Scheibner D., **Blaurock C.**, Vallbracht M., Karger A., Crossley B., Veits J., Böttcher-Friebertshäuser E., Mettenleiter T.C., Abdelwhab E.M., 2021. The role of glycosylation in the N-terminus of the hemagglutinin of a unique H4N2 with a natural polybasic cleavage site in virus fitness *in vitro* and *in vivo*. Virulence. 2021 Dec;12(1):666-678.

Blaurock, C., Breithaupt, A., Scheibner, D., Bagato, O., Karger, A., Mettenleiter, T.C., Abdelwhab, E.M., 2021. Preferential selection and contribution of non-structural protein 1 (NS1) to the efficient transmission of the panzootic avian influenza H5N8 2.3.4.4 clades A and B viruses in chickens and ducks. Submitted to J Virol.

Blaurock, C., Blohm, U., Luttermann, C., Holzerland, J., Scheibner, D., Schäfer, A., Groseth, A., Mettenleiter, T.C., Abdelwhab, E.M., 2021. Deletion or extension in the C-terminus of non-structural protein 1 (NS1) in H5N8 Clade 2.3.4.4 highly pathogenic avian influenza virus modulates induction of interferon and apoptosis in human lung cells and virulence in mice. Submitted to Emerg Microb Infect.

8.4 Oral and poster presentations

24. - 26.09.2018: 7. FLI Junior Scientist Symposium, Insel Riems, Germany. Poster presentation with 3 min spotlight talk.
Polymorphism in the hemagglutinin proteolytic cleavage site of German H9N2 viruses: in vitro and in-vivo studies. Claudia Blaurock, Thomas C. Mettenleiter, El-Sayed M. Abdelwhab

20. - 23.03 2019: 29th Annual Meeting of the Society for Virology, Düsseldorf, Germany. Poster presentation.
Polymorphism in the hemagglutinin proteolytic cleavage site of H9N2 affected proteolytic activation and cell-to-cell-spread in cell culture and virus excretion in infected chickens. Claudia Blaurock, David Scheibner, Marcel Gischke, Thomas C. Mettenleiter, El-Sayed M. Abdelwhab

25. - 27.09.2019: 8. FLI Junior Scientist Symposium, Jena, Germany. Poster presentation.
Reassortment with H9N2 or NS1-mutations increased virulence of avian-influenza-H5N8 2.3.4.4 in mice but compromised virus transmission and replication in chickens. Claudia Blaurock, Thomas C. Mettenleiter, El-Sayed M. Abdelwhab

26. - 28.08.2019: 13th Annual Meeting EPIZONE, Berlin, Germany. Poster presentation.
Reassortment with H9N2 or NS1-mutations increased virulence of avian-influenza-H5N8 2.3.4.4 in mice but compromised virus transmission and replication in chickens. Claudia Blaurock, Thomas C. Mettenleiter, El-Sayed M. Abdelwhab

26. - 28.08.2019: 13th Annual Meeting EPIZONE, Berlin, Germany. Oral talk.
Polymorphism in the hemagglutinin proteolytic cleavage site of H9N2.
Claudia Blaurock, Thomas C. Mettenleiter, El-Sayed M. Abdelwhab

25. – 27.03.2020: 30th Annual Meeting of the Society of Virology, Berlin, Germany. Poster presentation.
Reassortment with H9N2 or NS1-mutations increased virulence of avian-influenza-H5N8 2.3.4.4 in mice but compromised virus transmission and replication in chickens. Claudia Blaurock, Thomas C. Mettenleiter, El-Sayed M. Abdelwhab (cancelled due to COVID-19 pandemic)

8.5 Acknowledgement

My special thanks goes to my supervisor **Prof. Dr. Dr. h.c. Thomas C. Mettenleiter**, President of the Friedrich-Loeffler-Institute (FLI), Federal Research Institute for Animal Health, Greifswald - Insel Riems, Germany, who gave me the opportunity to conduct my dissertation at the Institute of Molecular Virology and Cell Biology (IMVZ) at the FLI. Thank you for your support and kind supervision.

My deepest gratitude goes to **Dr. El-Sayed M. Abdelwhab**, Head of the Laboratory for Avian Influenza Virus, IMVZ, FLI. Thank you for introducing me to the world of avian influenza viruses and for supporting me during the last 3 years. Thank you for your patience, motivation and your always open door - this work would not have been possible without you.

Thank you to all current and former working group members who accompanied me during my time in the lab with many constructive discussions, but also with a lot of fun - especially I thank **Dajana Helke, Nadine Bock** and **Dr. David Scheibner**.

I would also like to thank the **animal caretakers** of the FLI for their help, as well as the pathologists **Prof. Dr. Reiner Ulrich** and **Dr. Angele Breithaupt**.

Moreover, I would like to thank **Prof. Dr. Timm C. Harder**, Head of the National Reference Laboratory for Avian Influenza Virus for providing the viruses used in this dissertation.

Furthermore, I would like to thank **Dr. Ulrike Blohm** and her team for introducing me to flow cytometry.

I thank the whole **IMVZ** for the nice time together and especially I would like to thank **Emmelie, Katrin, Magdalena, Felicitas, Juliane, Franziska** and **Julia** for the nice moments outside the lab.

My biggest thanks are reserved for **my family**, especially my parents and my brother. Thank you for always believing in me and supporting me in everything.